TECHNISCHE UNIVERSITÄT MÜNCHEN

Metabolomics investigations in body fluids of smokers and non-smokers

Daniel Christoph Müller

TECHNISCHE UNIVERSITÄT MÜNCHEN

FAKULTÄT FÜR CHEMIE

Metabolomics investigations in body fluids of smokers and non-smokers

Daniel Christoph Müller

Vollständiger Abdruck der von der Fakultät für Chemie der Technischen Universität München zur Erlangung des akademischen Grades eines
Doktors der Naturwissenschaften (Dr. rer. nat)
genehmigten Dissertation.

Vorsitzender: Univ.-Prof. Dr. M. Schuster

Prüfer der Dissertation: 1. Univ.-Prof. Dr. R. Niessner
                             2. apl. Prof. Dr. P. Schmitt-Kopplin

Die Dissertation wurde am 29.04.2014 bei der Technischen Universität München eingereicht und durch die Fakultät für Chemie am 04.07.2014 angenommen.

Publications

Mueller, D. C.; Piller, M.; Niessner, R.; Scherer, M.; Scherer, G*., Untargeted Metabolomic Profiling in Saliva of Smokers and Non-Smokers by a Validated GC-TOF-MS Method*. J. Proteome Res. **2014**, 13, 1602–1613

Mueller, D. C.; Degen, C.; Scherer, G.; Jahreis, G.; Niessner, R., *Metabolomics using GC-TOF-MS followed by subsequent GC-FID and HILIC-MS/MS analysis revealed significantly altered fatty acid and phospholipid species profiles in plasma of smokers.* J. Chromatogr. B, **2014**, in Press, DOI: 10.1016/j.jchromb.2014.02.044

Danksagung

Zur Vollendung dieser Arbeit haben viele Personen beigetragen, ohne deren Hilfe und Unterstützung es nicht möglich gewesen wäre dieses Projekt zu bearbeiten.

Ganz besonders möchte ich mich bei Herrn Prof. Dr. Gerhard Scherer, CEO des ABF, bedanken, der mir sein Vertrauen und die Möglichkeit gegeben hat dieses sehr spannende Thema zu bearbeiten. Die wissenschaftliche Betreuung und die zahlreichen Diskussionen haben mir sehr geholfen diese Arbeit anzufertigen.

Besonderer Dank gilt meinem Doktorvater Herrn Prof. Dr. Reinhard Niessner für die Betreuung und für die anregenden Diskussionen.

Bei Herrn Dr. Max Scherer und Herrn Dr. Josef Ecker möchte ich mich ganz herzlich für die wissenschaftliche Betreuung und die tatkräftige Unterstützung in analytischen Fragen bedanken. Danke auch für zahlreiche Verbesserungsvorschläge beim Anfertigen diverser wissenschaftlicher Manuskripte und die Geduld dabei.

Ein sehr großes Dankeschön geht auch an Frau Dr. Wibke Peters, für die Einführung am GC-TOF-MS-Gerät und die tatkräftige Unterstützung bei diversen Problemen mit dem TOF-MS-Instrument, das mich zeitweise zur Verzweiflung trieb.

Bei Markus Piller möchte ich mich ganz besonders für die Messungen von Nic+9 und Kreatinin im Urin sowie Cot und OH-Cot in Speichel und der Hilfe bei jeglicher Art von IT-Problemen bedanken. Besonderer Dank gilt auch Herrn Gerhard Gilch für die Messungen von Tyramin im Speichel der Zeitpunkte 3 – 5. Außerdem möchte ich mich herzlich bei den weiteren Kollegen des ABF, Dina Janket, Heinz Hagedorn, Kirsten Riedel, Kathi Sterz, Bernhard Ramsauer, Claudia Bernstein und Frau Marita Scherer bedanken. Danke, dass ihr mich so herzlich aufgenommen habt und immer bereit gewesen seid, mir mit eurem fundierten analytischen Wissen mit Rat und Tat zur Seite zu stehen. Ein großes Dankeschön geht auch an Herrn Dr. Degen für die Messungen der Fettsäuren im Plasma.

Catherine Sorbara bin ich sehr dankbar, dass Sie die Arbeit Korrektur gelesen hat.

Mein größter Dank gilt meiner Familie und meiner Freundin. Meine Eltern haben viele Entbehrungen hinnehmen müssen, um mir diese Chance zu ermöglichen.

Anja hat mir stets den Rücken frei gehalten, damit ich mich auf meine Forschung konzentrieren konnte. Danke auch, dass Du immer für mich dagewesen bist und mich unterstützt hast, vor allem während der sehr schwierigen Zeit meines Unfalls.

Schließlich möchte ich noch all meinen Freunden für Ihre Unterstützung danken.

ABSTRACT

Smoking is a major cause of several diseases. However, the underlying pathophysiological mechanisms are still not completely understood. To investigate endogenous alterations in the metabolome as a consequence of smoking, a gas chromatography hyphenated to time-of-flight mass spectrometry (GC-TOF-MS) method was developed and validated for analysis of the metabolic fingerprint in saliva, urine and plasma of smokers and non-smokers. The method was validated by spiking 37 (36 for plasma) different metabolites, covering a wide range of chemical classes, and 6 (3 for urine) internal standards to the respective matrices in concentrations between 0.1 µM and 2 mM. To evaluate the method, linearity, intra- and interday repeatability, stability and re-injection reproducibility were determined for all spiked metabolites. To obtain body fluids, a 24-hour nutrition-controlled study with 25 smokers and 25 non-smokers was planned and conducted. The GC-TOF-MS method was applied to the samples of urine, plasma and saliva of smokers and non-smokers. Uni- and multivariate statistical analyses (Mann-Whitney U test and partial least square discriminant analysis) were performed to discover metabolites which are significantly different in their levels between smokers and non-smokers. Beside nicotine and its metabolites, 18 metabolites in urine, 13 in saliva and 8 in plasma could be identified, which were significantly changed in their levels in smokers. Decreased levels of glucose-6-phosphate (saliva), alanine (urine, plasma), pyruvate (urine), 2-oxoglutaric acid (urine) and malic acid (saliva) indicate a shift from the glycolysis pathway towards the pentose pathway in smokers. Other metabolites from the metabolic fingerprinting are primarily involved in the amino acid metabolism as well as the lipid metabolism. Three monounsaturated fatty acids (MUFA) were found to be increased in plasma of smokers, namely oleic acid (FA 18:1 n-9), palmitoleic acid (FA 16:1 n-7) and presumably vaccenic acid (FA 18:1 n-7). A targeted analysis by gas chromatography coupled to flame ionization detection (GC-FID) of the total fatty acid content in plasma confirmed these results and revealed significantly increased proportions of other MUFA species, including FA 16:1 n-7, FA 17:1, FA 18:1 n-9, FA 18:1 n-7, FA 20:1 n-9 and FA 24:1 n-9 in smokers, whereas the saturated fatty acids FA 17:0 and FA 18:0 and the polyunsaturated fatty acid (PUFA) FA 22:6 n-3 showed a significant decrease ($p < 0.05$). The shift to MUFAs is presumably due to nicotine triggered activation of stearoyl-coenzyme A desaturase 1, which catalyzes the reaction from saturated to MUFAs. Since the main fraction of fatty acids in plasma is esterified to the phospholipids phosphatidylcholine (PC) and phosphatidylethanolamine (PE), the profiles of 39 PC and 40 PE species were analyzed with a newly developed and validated hydrophilic interaction liquid chromatography linked to electrospray ionization and triple quadruple mass spectrometry (HILIC-ESI-MS/MS) method. The phospholipids PC 36:1, PE 36:2 and PE 38:5

were found to be significantly increased, whereas PC 36:0, PC 38:7, PC 38:6, PE 36:3 and PE 38:4 were significantly decreased in smokers' plasma ($p < 0.05$). Altered phospholipid species profiles partly reflected the alterations in the fatty acid profile of smokers and indicate a perturbation of the lipid profile as a consequence of smoking.

The most pronounced difference between smokers and non-smokers was observed for salivary tyramine. To further elucidate this finding, a HILIC-MS/MS method was newly established, validated and for the first time, absolute tyramine concentrations were determined in human saliva samples. Median tyramine levels ranged from 5.7 nM to 4.3 µM. Tyramine concentrations in smokers' compared to non-smokers' saliva were 74 - 400-fold increased, depending on the point in time when the saliva samples were collected during the clinical study. It is hypothesized that the increased levels were either due to a smoking triggered inhibition of the enzyme monoamine oxidase (MAO) or resulted from differences in the oral flora between smokers and non-smokers.

In summary, for the first time a metabolic fingerprinting approach in saliva, urine and plasma of smokers and non-smokers has been developed and validated using GC-TOF-MS. The metabolic fingerprinting in the biofluids of smokers and non-smokers revealed several significant alterations, which could be interpreted to be linked to smoking related diseases. In particular, the alterations in the fatty acid and lipid metabolism are assumed to be linked to smoking related diseases, such as cardiovascular disease (CVD). Whether the significantly higher levels of tyramine in saliva of smokers play a role in smoking-related effects or addiction should be elucidated by further research.

Zusammenfassung

Rauchen ist als Auslöser verschiedener Krankheiten bekannt, allerdings sind die pathophysiologischen Mechanismen die zur Krankheitsentstehung führen wenig untersucht. Um einen Beitrag zur Aufklärung der zugrunde liegenden Mechanismen zu leisten, wurde der Einfluss des Rauchens auf das Metabolom untersucht. Um den Einfluss von Rauchen auf den Stoffwechsel zu untersuchen, wurde eine Methode zur metabolomischen Untersuchung von Speichel, Urin und Plasma bei Rauchern und Nichtrauchern aufgebaut und validiert. Die Methode basiert auf einer gaschromatographischen Trennung der Bestandteile der Proben und anschließender Messung mittels eines Flugzeitmassenspektrometers (GC-TOF-MS). Zur Validierung der Methoden wurden 37 endogene und exogene Analyten und 6 interne Standards (3 im Fall von Urin) verwendet. Diese wurden in einem Konzentrationsbereich zwischen 0.1 µM und 2 mM in entsprechende Pools der verschiedenen biologischen Matrizes pipettiert und deren analytische Kenndaten, wie Reproduzierbarkeit, Stabilität und Linearität, bestimmt.

Um für diese Untersuchungen geeignete Proben zu erhalten, wurde eine klinische Studie mit 25 Rauchern und 25 Nichtrauchern geplant und durchgeführt. Die Studie umfasste einen 24-stündigen Klinikaufenthalt, während dem die Probanden eine standardisierte Nahrung bekamen. Die Proben der klinischen Studie wurden im Anschluss mittels der neu entwickelten GC-TOF-MS-Methode analysiert und Unterschiede in den Metabolitenmustern der beiden Studiengruppen wurden mittels statistischer Methoden (uni- und multivariat) herausgearbeitet. Neben Nikotin und dessen Metaboliten trugen 18 Metabolite im Urin, 14 im Speichel und 8 im Plasma signifikant zur Unterscheidung der beiden Gruppen bei. Die Konzentrationen von Glucose-6-Phosphat (Speichel), Alanin (Urin und Plasma), Pyruvat (Urin), 2-Ketoglutarsäure (Urin) und Malat (Speichel) waren dabei signifikant niedriger in Rauchern. Dies lässt auf eine Änderung im Glykolyse-Stoffwechselweg in Richtung einer Erhöhung des Pentosephosphatweg schließen. Weitere Metabolite, deren Level in Rauchern signifikant verändert war, deuten auf eine Änderung im Aminosäure- und Lipidstoffwechsel hin. In den Plasmaproben der Raucher waren die 3 einfach ungesättigten Fettsäuren (FS), Ölsäure (FS 18:1 n-7), Palmitoleinsäure (FS 16:1 n-9) und vermutlich Vaccensäure (FS 18:1 n-7) signifikant erhöht. Daher wurde gezielt das gesamte Fettsäureprofil im Plasma analysiert. Dazu wurde ein Flammenionisationsdetektor (FID), der an einen GC gekoppelt war, verwendet. Die Ergebnisse der GC-TOF-MS-Untersuchungen konnten dabei bestätigt werden. Die einfach ungesättigten Fettsäuren FS 16:1 n-7, FS 17:1, FS 18:1 n-9, FS 18:1 n-7, FS 20:1 n-9 und FS 24:1 n-9 waren bei Rauchern signifikant erhöht, wohingegen die gesättigten Fettsäuren FS 17:0, FS 18:0 und die mehrfach ungesättigte Fettsäure FS 22:6 n-3 signifikant erniedrigt waren ($p < 0.05$).

Diese Veränderung kommt möglicherweise durch eine Nikotin-gesteuerte Aktivierung des Enzyms Stearoyl-Coenzym A Desaturase-1 (SCD 1) zustande. Dieses katalysiert die Desaturierung von gesättigten zu einfach ungesättigten Fettsäuren. Im Anschluss wurde untersucht, ob das veränderte Fettsäureprofil im Plasma Auswirkungen auf das Phosphatidylcholine (PC)- und Phosphatidylethanolamine (PE)-Profil hat. Dazu wurde eine neue Methode entwickelt und validiert, die es erlaubt, 39 PC und 40 PE Spezies in einem Analysenlauf zu quantifizieren. Nach einer Trennung der beiden Stoffklassen mittels hydrophiler Interaktionschromatographie (HILIC) wurden die gruppenspezifischen Übergänge mit einem Tandemmassenspektrometer (MS/MS) gemessen. Die Analyse der Plasmaproben ergab bei Rauchern eine signifikante Erhöhung der Lipid-Spezies PC 36:1, PE 36:2 und PE 38:5, wohingegen PC 36:0, PC 38:7, PC 38:6, PE 36:3 und PE 38:4 signifikant erniedrigt waren. Die Veränderung im Fettsäureprofil zeigte sich teilweise auch im Phospholipidprofil.

Von allen Metaboliten, die signifikant unterschiedliche Konzentrationen in den untersuchen Körperflüssigkeiten hatten, zeigte Tyramin im Speichel die stärkste Erhöhung bei Rauchern. Da Tyramin als indirektes Sympathomimetikum von physiologischer und toxikologischer Relevanz ist, wurde eine HILIC-MS/MS-Methode aufgebaut und validiert, um dieses in den Speichelproben der Raucher und Nichtraucher zu quantifizieren. Damit wurde zum ersten Mal das biogene Amin Tyramin in humanen Speichelproben gemessen. Die Mediane lagen zwischen 5.7 nM und 4.3 µM. Raucher hatten zu allen 5 Zeitpunkten, an denen Speichel gesammelt wurde, signifikant erhöhte Tyraminkonzentrationen, die zwischen 74- und 400-mal höher waren als im Speichel von Nichtrauchern. Es wird vermutet, dass diese extreme Erhöhung entweder durch eine Hemmung des Enzyms Monoaminoxidase zustande kommt, die bekanntermaßen durch das Rauchen ausgelöst wird oder auf eine bei Rauchern veränderte Mundflora zurückgeht.

Zum ersten Mal wird die Untersuchung des metabolischen Fingerabdrucks in Plasma, Urin und Speichel von Rauchern und Nichtrauchern mittels einer validierten GC-TOF-MS-Methode beschrieben. Die Untersuchungen in den Körperflüssigkeiten zeigten signifikante Änderungen im Metabolom von Rauchern. Einige dieser Unterschiede, wie zum Beispiel der veränderte Fettsäure- und Lipidstoffwechsel, stehen möglicherweise in Verbindung mit Krankheiten, die durch das Rauchen ausgelöst werden können, wie etwa Herzkreislauferkrankungen. Da Tyramin möglicherweise das Suchtpotenzial von Zigarettenrauch beeinflussen kann, können diese Untersuchungen einen wertvollen Beitrag leisten, um den Einfluss von Zigarettenrauch auf den Menschen besser zu verstehen. Die Aufklärung dieses Sachverhalts bedarf weiterer Untersuchungen.

Table of Content

I. Abbreviations

2-Me-hippuric acid	2-Methylhippuric acid
4-Me-hippuric acid	3-Methylhippuric acid
5-HIAA	5-Hydroxyindoleacetic acid
BMI	Body mass index
BSTFA	N,O-Bis-(trimethylsilyl)-trifluoroacetamide
$C_{16}H_{33}COOH$	Heptadecanoic acid
CID	Collision induced dissociation
COex	Carbon monoxide in exhaled breath
COPD	Chronic obstructive pulmonary disease
Cot	Cotinine
CV	Coefficient of variation
CVD	Cardiovascular diseases
EI	Electron impact ionization
ESI	Electrospray ionization
FA	Fatty acid
FDA	Food and Drug Administration
FID	Flame ionization detector
Gaba	γ-Aminobutyric acid
GAPDH	Glyceraldehyde-3-phosphate dehydrogenase
GC	Gas chromatography
Gluc	Glucuronide
Gly-Gly	Glycine-glycine
GP	Glycerophospholipid
GUI	Graphical user interface
HILIC	Hydrophilic interaction liquid chromatography
HPLC	High performance liquid chromatography
IS	Internal standard
KEGG	Kyoto Encyclopedia of Genes and Genomes
LC	Liquid chromatography
LLOQ	Lower limit of quantification
LOD	Limit of detection
LXR	Liver X receptor (transcription factor)
m/z	Mass to charge ratio
MRM	Multiple reaction monitoring
MS	Mass spectrometry

I. Abbreviations

MS/MS	Triple quadrupole mass spectrometry
MUFA	Monounsaturated fatty acid
MW	Molecular weight
NADPH	Nicotinamide adenine dinucleotide phosphate
Nic	Nicotine
Nic+9	Nicotine and its 9 most abundant metabolites
NP	Normal phase
NS	Non-smoker
PAH	Polycyclic aromatic hydrocarbon
PC	Phosphatidylcholine
PE	Phosphatidylethanolamine
PL	Phospholipid
PLS-DA	Partial least square discriminant analysis
p-OH-Ph-acetic acid	p-Hydroxyphenylacetic acid
PPAR	Peroxysome proliferator activated receptor
PUFA	Polyunsaturated fatty acid
ROS	Reactive oxygen species
RP	Reversed phase
S	Smoker
SCD1	Stearoyl Coenzyme desaturase 1
SD	Standard deviation
SEM	Standard error of the mean
SM	Sphingomyelin
SREBP-1c	Sterol regulatory element-binding protein 1c
TIC	Total ion current
TMCS	Trimethylsilyl chloride
TOF	Time-of-flight
TP	Time point
TSNA	Tobacco specific nitrosamine
ttMA	trans,trans-Muconic acid
UPLC	Ultra-performance liquid chromatography
VIP	Variable importance in projection
XIC	Extracted ion current

II. List of figures

III. List of tables

1   Introduction

1.1   Smoking and diseases

Worldwide, smoking causes about 5 to 6 million deaths per year and is responsible for 850.000 cancer deaths [1,2]. In fact, it is the most important risk factor for lung cancer, peripheral atherosclerosis and abdominal aortic aneurysm [3,4] in addition to cardiovascular diseases (CVD) and respiratory diseases such as chronic obstructive pulmonary disease (COPD) [5]. In the 20th century, approximately 100 million people died due to smoking, and as for the 21st century, almost 1 billion smoking-related death are predicted (Fig. 1) [6].
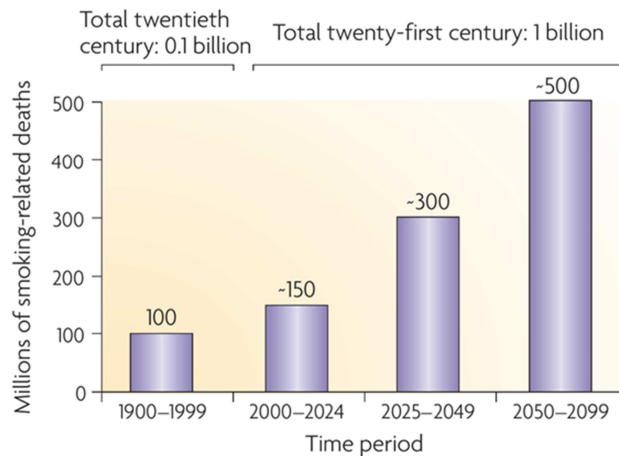
Fig. 1. Projected number of deaths due to tobacco smoke during the 21th century. Adapted from Jha [6].

In cigarette smoke, more than 5000 chemical compounds have been identified [7]. According to the International Agency for Research on Cancer (IARC) over 70 of them are established (Class 1), probable (Class 2A) or possible (Class 2B) human carcinogens, for example acetaldehyde, crotonaldehyde, formaldehyde or benzene [8]. Some mechanisms for disease induction and promotion by tobacco smoke are well investigated. For instance, the metabolic activation of polycyclic aromatic hydrocarbons (PAHs), during the detoxification process, can lead to DNA adducts. These adducts can cause gene mutations, protein miscoding, cellular degeneration and finally cancer, provided that these changes evade the body's own repair and defense systems [3]. This mechanism is also at play for the carcinogenic tobacco specific nitrosamines (TSNAs) NNK and NNN which are formed from

tobacco alkaloids such as nicotine (Nic) and nornicotine [9]. There are many biomarkers of exposure currently available for assessing the exposure to tobacco smoke (Table 1) [10]. These biomarkers are indicators for the exposure dose to tobacco related toxicants. On the other hand, biomarkers of effect are indicators of early changes in physiological pathways involved in the generation of chronic diseases.

1.2   Biomarkers

Biomarkers can help to investigate the exposure to disease pathway in all species, including humans. In general, there are three types of biomarkers. For smoking, quite a number of biomarkers of exposure are available and commonly in use (Table 1). These biomarkers, measured in various body fluids, reflect the uptake of toxic constituents from smoke such as the mentioned PAHs or TSNAs. Carcinogens such as PAHs and TSNA can also form DNA adducts, which in turn can be used as biomarkers of exposure (in this case termed 'biomarkers of effective dose) [10].

Furthermore, there are biomarkers of susceptibility. These indicate how vulnerable an organism or organ is to effects of chemical compounds. Such susceptibility factors can alter the biomarkers of exposure levels and also lead to altered disease risks. For example age, gender, ethnic background or genetic polymorphisms are susceptibility factors. Pheno- and genotypes of enzymes, which are involved in the metabolic activation and detoxification of toxicants, can serve as biomarkers of susceptibility. For instance, there is an increased sensitivity to genotoxic compounds of tobacco smoke for humans who lack the enzyme glutathione S-transferase M1 [11,12]. Also smoking behavior and susceptibility to tobacco smoke addiction is affected by genetic factors, for example due to variants of the enzyme monoamine oxidase (MAO) [13].

Biomarkers of effect are alterations in the endogenous metabolite levels caused by various factors including exposure to xenobiotics. Metabolites as intermediates and end products of all cellular processes are most predictable for the phenotype of an organism [14]. Therefore, they can serve as biomarkers of effect to characterize the physiological status, especially to determine perturbations in the organism at an early stage, which possibly lead to a disease at a later point in time [15]. Up to now, endogenous alterations and mechanisms of most smoking associated chronic diseases are still not well understood [16]. Biomarkers of effect, that reflect early physiological perturbations, have been less well investigated and less frequently applied for smoking research. For example, such biomarkers show the effects of oxidative stress, inflammation, lipid oxidation or mutations [10,17]. The identification of endogenous metabolites, which differ in their levels as a result of tobacco smoke exposures, might be promising for utilization as biomarkers of effect to decipher

1. Introduction

smoking-related diseases. Nevertheless, such endogenous metabolites are present both in healthy and diseased people and levels underlie normal inter-individual variations, making their discovery challenging. For instance, 8-hydroxy-2'-deoxyguanosine, an endogenous biomarker for oxidative stress and DNA damage, is significantly increased in smokers' urine [18].

Furthermore, to decipher alterations at the metabolite level induced by smoking is a challenging task, since there is an extensive amount of metabolites, which are very diverse in their physico-chemical properties as well as their biochemical functionality such as amino acids, sugars, lipids or fatty acids (FA). Furthermore, endogenous metabolites differ in their concentrations from very highly abundant (millimole range) to trace levels (picomole), causing their analytical quantification to become extremely challenging. Further, the complexity of the biological differences, such as inter-individual changes and circadian fluctuations or spatial variability, makes comprehensive investigations challenging [19]. In addition, the occurrence and levels in body-fluids of some metabolites are strongly dependent on nutrition [20].

1. Introduction

Table 1. Properties of some commonly used, smoking-related biomarkers

Analyzed biomarker or set of biomarkers	Parent compounds (examples)	Matrix	Implication of parent compound in disease or biological effect	Type of biomarker	Literature
Nic metabolites	Nic	P,SE,S,U	Addiction	Exposure	
Aromatic amines	4-Aminobiphenyl	U	Cancer	Exposure	[21]
Hemoglobine adducts	Acrylamide	B	Cancer	Exposure	[22,23]
Mercapturic acids	1,3-Butadiene	U	Cancer	Exposure	[24-30]
Acetonitrile	Acetonitrile	P, S		Exposure	
Benzene	Benzene	B	Cancer	Exposure	[31]
trans-trans-Muconic acid (ttMA)	Benzene	U	Cancer	Exposure	[32]
COex	CO	EB	Cardiopulmonary disease	Exposure	[33]
PAH	Naphthalene, pyrene	U	Cancer, mutagenic	Exposure	[34]
Thiocyanate	HCN	U, P, SE, S	Cytotoxic	Exposure	[35]
DNA adducts	TSNA, PAHs	U	Cancer, oxidative stress	Exposure	[35,36]
Cysteinylglycine Adducts	Acetaldehyde, formaldehyde	U	Cancer	Exposure	
Amino Acids	Homocysteine	P	Cardiovascular diseases	Effect	
Mercapturic acids	4-Hydroxy-2-nonenal	U	Lipid peroxidation	Effect	
β-Carotene		P, S	Oxidative stress	Effect	[37]
Vitamins (e. g. A, E)		P, S	Oxidative stress	Effect	
8-Hydroxy-2-deoxyguanosine		U	Oxidative stress	Effect	[38]
4-Hydroxy-2-nonenale		U	Lipid peroxidation, oxidative stress	Effect	
Malondialdehyde		U	Lipid peroxidation, oxidative stress	Effect	
Eicosanoides		U	Inflammation, oxidative stress, cardiovascular disease	Effect	[39]

EBC: exhaled breath condensate, EB: exhaled breath, PL: plasma, SE: serum, S: saliva, U: urine, B: blood. Not a complete list of all tobacco smoke-related biomarkers.

1.3   Metabolomics

Metabolomics is the fourth research field in a cascade of 'omics' following downstream genomics, transcriptomics and proteomics (Fig. 2) [15]. The metabolome, which represents the entity of all 'small' molecules (< 1500 Dalton), is most predictive for the phenotype of an organism [40]. Metabolomics is the research of all small molecules in an organism at a given state and defined time point. While the genome determines *"what can happen"* in an organism, the transcriptome determines *"what appears to be happening"* by translation of the genome. The *proteome makes alterations in the organism happen* and the metabolome indicates *"what has happened and is happening in the organism"* and can therefore be used to investigate the phenotype affected by environmental influences, changes in the genotype or affected by disease (Dettmer 2007) [19]. In the whole human organism (tissue and biofluids), there have been quantified at least 5,000 metabolites (endogenous and exogenous) (status 2013) [41]. The 'Human Metabolome Project' started to "identify, quantify, catalogue and store all metabolites that can potentially be found in human tissues and biofluids" in January 2004 [42]. This demonstrates the interest that this emerging research area has attracted in the past years. Nevertheless, quite recently, metabolomics has drawn less attention as compared to the other 'omics' sciences. A major reason is because of the technical challenges accompanied with metabolomics, since measuring the entire metabolome in a biological system requires sensitive and robust analytical methods and cannot be performed by a single platform alone. Improvements in analytical science and chemometrics have brought metabolomics to the focus of interest since the start of the 21st century. Mainly two different metabolomic approaches are described in the scientific literature [15].
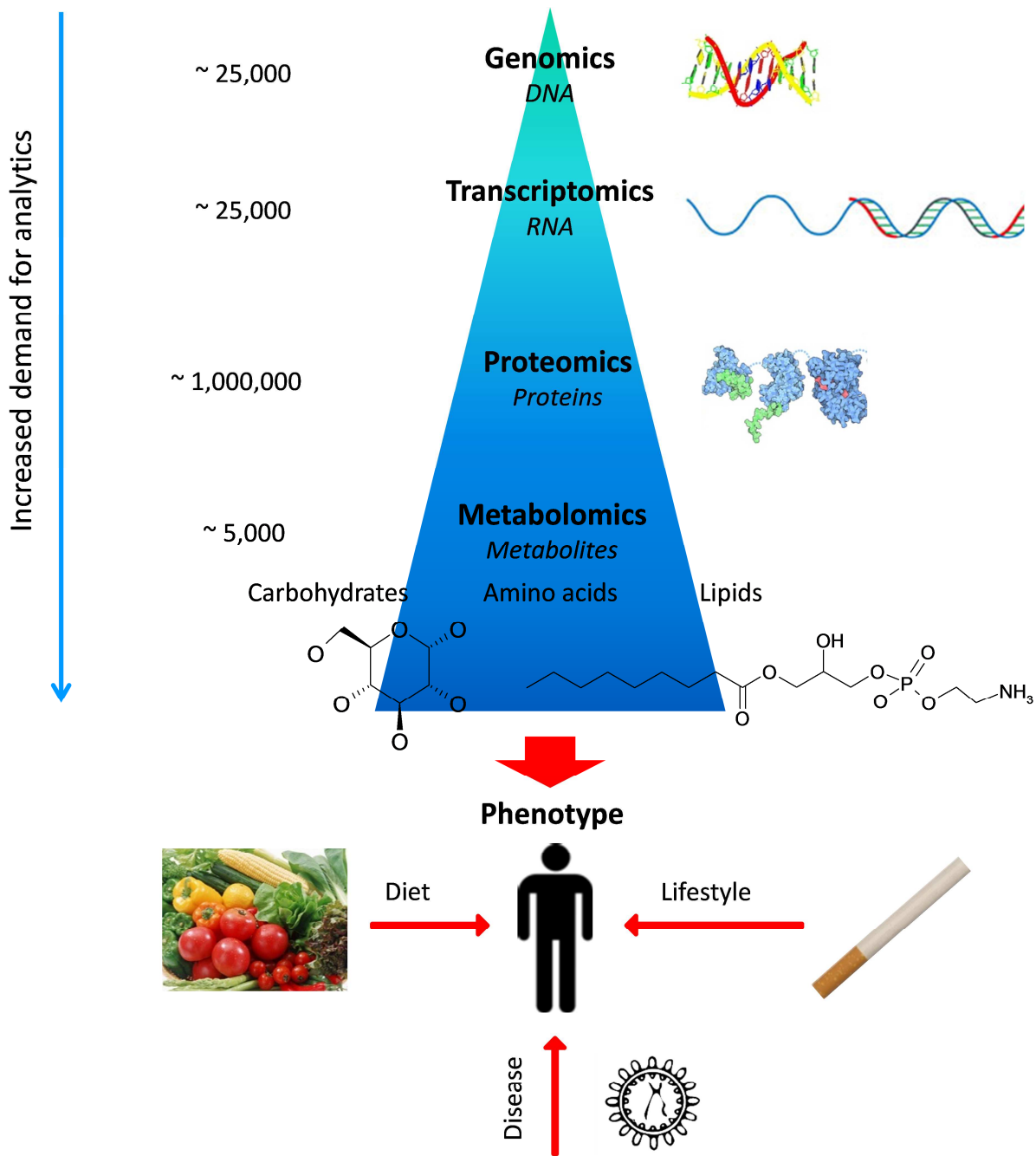
Fig. 2. Link between genomics and metabolomics. The phenotype of an organism is affected by genetic as well as environmental influences such as the lifestyle factor smoking. There is an increased analytical demand for metabolomics compared to genomics, transcriptomics and proteomics. The 5,000 metabolites are just a snapshot of how many have been quantified in human tissue and body fluids according to the Human Metabolome Database [41], so far. Parts of this pictures were taken and adapted from Drew et al. 1981 [43] and Rossmann et al. 1989 [44].

On the one hand, there is metabolic profiling which analyzes only a limited set of metabolites, like specific classes such as fatty acids, lipids or sugars. This approach is generally used, when there is already a hypothesis for altered metabolic pathways. Targeted

analysis of biomarkers is part of this analysis. Metabolic profiling, include a quantification of the compounds and is performed when there is already a hypothesis for changed metabolites. For that purpose, the analytical approach will be selected to meet the requirements for a given class of compounds within a given biological matrix.

On the other hand, there is metabolic fingerprinting, an untargeted approach that is used to simultaneously measure as many metabolites as possible, resulting in a metabolic fingerprint of an organism. This means, metabolites are not pre-selected (only by the analytical approach) and mostly unknown. The goal is to find metabolite patterns which are significantly altered between groups and therefore are well suited to separate between different phenotypes due to environmental or genetic differences. The identification of these patterns is the final step of a metabolic fingerprint (for definitions of terms used in metabolomics refer to Table 2). The final step consists of interpretation and subsequent hypothesis generation to put the different metabolic patterns into a biological context. A targeted approach capturing a dedicated metabolic pathway along with absolute metabolite concentrations is therefore a prerequisite to further strengthen and confirm such hypothesis.

Table 2. Definition of terms used in metabolomics.

Metabolite	Small molecules (< 1500 Da) that participate in general metabolic reactions in an organism
Metabolome	The complete set of metabolites in an organism
Metabolomics	Investigation of the metabolome, including identification and quantification of all metabolites in a biological system at a given status
Metabolic profiling	Quantitative analysis of set of metabolites in a selected biochemical pathway or a specific class of compounds. This includes target analysis, the analysis of a very limited number of metabolites, e.g. single analytes as precursors or products of biochemical reactions
Metabolic fingerprinting	Unbiased, global screening approach to classify samples based on metabolite patterns or "fingerprints" that change in response to disease, environmental or genetic perturbations with the goal to identify discriminating metabolites

Adapted from Dettmer et al. [19].

Using metabolomic approaches it is possible to measure simultaneously hundreds of metabolites in biofluids such as urine, plasma, serum, saliva, cerebrospinal fluid or different

tissue extracts [45]. The determination of a whole pattern of metabolites can be utilized to depict physiological changes that can occur in response to environmental changes such as lifestyle habits, nutrition, pathogens or due to mutations to genes or proteins. Such metabolite patterns can further improve monitoring of adverse drug reactions or detrimental health effects due to smoking and therefore improve personalized medication [46].

Metabolic fingerprinting can be used as a diagnostic tool by comparing the fingerprints of healthy with those of diseased subjects. However, quantitative information of metabolites provides more information of the phenotype of a disease for an organism. Therefore, metabolites which are responsible for a group separation in the fingerprint should be subsequently identified and quantified by targeted metabolic profiling method.

1.4   Lipidomics

Lipidomics can be seen as subcategory of metabolomics and delivers qualitative and quantitative information about lipids and their biochemical pathways, as well as lipid-lipid or lipid-protein interactions [47]. Lipidomic investigations provide data on, for example, different combinations of fatty acids with backbone structures such as glycerol or sphingoid bases (Fig. 3). They serve as precursors for signaling molecules and are of toxicological interest [47,48].
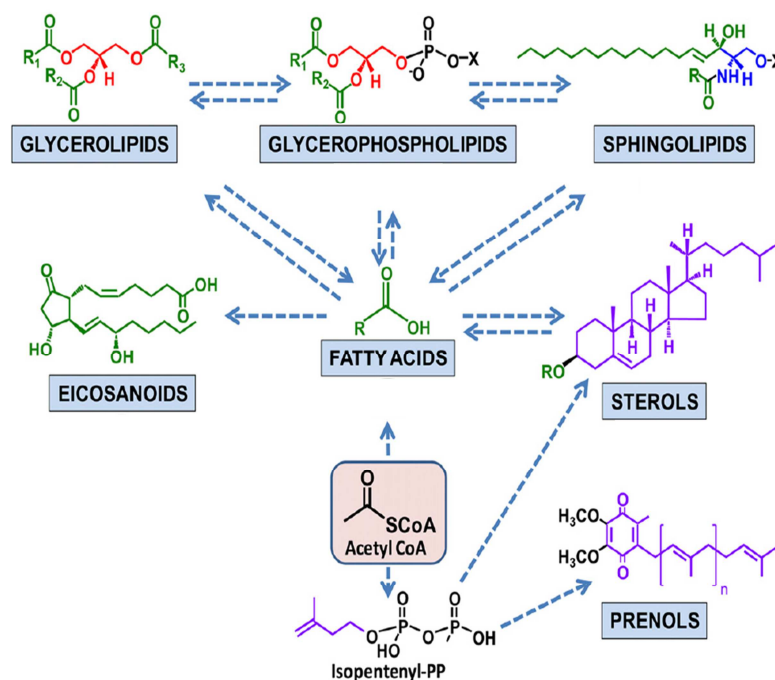
Fig. 3. Origin of fatty acids in plasma. The bulk amounts of FA in plasma are bound in the lipid class of glycerophospholipids (~93%). Adapted from Quehenberger et al. 2010 [49].

Up to now about 1000 lipid species can be quantified from the postulated 10,000 – 100,000 that may exist in mammalian systems [50]. These lipids take part in different metabolic and energy homeostasis. Glycerophospholipids, such as phosphatidylcholine (PC) and phosphatidylethanolamine (PE), are the major components of plasma membrane lipids and serve as substrates for the formation of bioactive lipids including diacylglycerol and phosphoinositides. Among all lipids occurring in human plasma, about 1/3 are glycerophospholipids and over 90% of them are PC and PE [49], which are the main building blocks of cell membranes. Others, like triacylglycerols, sphingolipids or sterols are responsible for the energy storage, signaling functions, cell membrane structure fluidity, hormone production or serve themselves as hormones [51-53]. Up to date, identification and quantification of the entire diversity of lipid species occurring in the human body still remains challenging mainly due to limitations in the available methodology and the lack of suitable extraction methods, especially for low abundant lipid species. Comprehensive data sets of alterations in the phospholipid and fatty acid profiles between smokers and non-smokers would give valuable clues about mechanisms involved in smoking-related diseases. For example, studies have shown that arachidonic acid can be released from phospholipids (PLs) by an activation of the phospholipase A2 (PLA2), which is the initial step in the formation of eicosanoids. These compounds are important mediators in inflammation processes [54], including chronic inflammation, which plays a major role in the smoking-related initiation of lung diseases [55].

1.5   Metabolomics by mass spectrometry

Mass spectrometry (MS) is an analytical technique that separates and quantifies ions according to their mass to charge ratio (*m/z*). MS instruments consist of an ion source followed by a mass analyzer that separates the ions by their *m/z* ratio and a detector, which measures the ion current. The detector can either be a photomultiplier, an electron multiplier tube, a Faraday Cup or a micro-channel plate [56]. Suitable ionization techniques and mass analyzers are discussed in the following sections.

In metabolomics, mainly two analytical approaches have been used, namely MS and NMR. However, the time-consuming analysis and interpretation of NMR spectra along with its slightly lower sensitivity compared to MS [57,58] makes this approach inferior to MS-based untargeted analysis of a large number of low-abundant metabolites [59].

1.5.1   Ionization techniques

ESI is a soft ionization technique which produces pseudo-molecular ions $[M+H]^+$ or $[M-H]^-$) and adduct ions with components of the eluent (e.g. Na^+, Li^+, NH_4^+, CH_3COO^-)

1. Introduction

during the ionization process. ESI is generally used in combination with liquid chromatography (LC). Under normal pressure conditions, the analyte containing fluid is pumped through a micro capillary with a metal tip. An electric field between the end of the capillary and a counter electrode in combination with a sheath gas flow leads to an ion spray that forms charged droplets. Depending on the polarity of the supplied voltage, the analytes (ions) carry a positive (ESI+) or negative (ESI-) charge. The desolvation process of these droplets leads to quasi-molecule ions which are transferred to the mass analyzer [56]. Only a low amount of in-source fragmentation occurs when ESI is applied [60]. Furthermore, ESI-MS is by two to three orders of magnitude more sensitive as compared to other ionization techniques such as fast atom bombardment [61]. Therefore, ESI is commonly used for the quantification of all kinds of lipids in body fluids, from high concentrated phospholipid species to very low abundant species [62]. The development and application of ESI-MS was originally developed for macromolecules [63]. This was a tremendous progress for the analysis of low abundant molecules, improving the limit of detection down to the femto molar range. For metabolomic approaches ESI is mostly hyphenated to high-performance liquid chromatography (HPLC).

Another ionization technique frequently used with LC is atmospheric pressure chemical ionization (APCI). The solution containing the analytes is introduced, through a capillary, into a pneumatic nebulizer using nitrogen as nebulizer gas. Subsequently, the droplets, containing the solvent and the analytes, are further evaporated in a heated quartz tube. The droplets and the nebulizer gas pass a corona discharge needle where ionization takes place [64]. The ionization can be carried out both in negative ionization (APCI-) mode which causes the loss of a proton or adduct formation. In positive ionization (APCI+) mode, ions are formed by proton transfer or adduct formation with molecules (cations) from the solvent [65]. The APCI technique is analogous to chemical ionization in GC, however, it takes place at atmospheric pressure. In the plasma at the corona discharge needle, the solvent is ionized and acts as ionization gas for the analytes. Normally, there are primary ions formed with molecules from the nebulizer gas (e. g. N_2^+) by electron ionization, which subsequently collide with the molecules from the solvent, to form the secondary reactant ions (e. g. $(H_2O)_2H^+$) that transfers the charge to the analyte [65]. The yielded analyte ions can subsequently be analyzed by mass spectrometry. Unlike ESI, the ionization of APCI takes place in the gas phase, thus the use of non-polar solvents as mobile phase is possible and the method can be used for analyzing preferably non-polar compounds.

Compared to ESI or APCI, electron impact ionization (EI) is a relatively harsh ionization technique. Thereby, energetic electrons (~70 eV) interact with neutral molecules in the gas phase to produce ions and fragments. EI leads to a vast number of fragment ions, due to cleavage and rearrangement reactions, which can be subsequently analyzed. This

ionization technique leads to complex mass spectra that are very specific for individual metabolites. For EI using 70eV there are several mass spectral libraries for the identification of respective analytes, such as the Golm Metabolome Database (GMD) [66]. EI is mostly used in combination to gas chromatography (GC) since analytes are already in the gaseous phase.

1.5.2   Mass analyzers

A suitable mass analyzer for metabolomics investigations is a time-of-flight mass spectrometer (TOF-MS). Ions from the ion source are accelerated in an electrical field and subsequent fly into an electrical field free cell with a high vacuum. The flight time of the ions to the detector is measured which is only dependent on the m/z ratio since all ions have the same kinetic energy. TOF-MS can be operated with very high data acquisition rates and, therefore, it is a very powerful tool for untargeted metabolomic investigations, allowing the analysis of many metabolites simultaneously.

For targeted metabolic profiling methods, where very low limits of detection are required, triple-quadrupole mass spectrometry (MS/MS) is the technique of choice. A MS/MS device consists of two quadrupoles, which are made of four parallel metal rods, and a collision cell (which actually is a third quadrupole) in between the two. The ions are accelerated in an electric field and fly in a vacuum through the quadrupoles, to which an oscillating electric field is applied. Depending on the electric field, only ions with defined *m/z* ratios yield stable trajectories and are able to pass the quadrupoles. In the collision cell, the ions can interact with neutral gaseous molecules such as nitrogen which lead to a fragmentation of the ions, termed collision induced dissociation (CID). For quantification purposes, multiple reaction monitoring (MRM) is predominantly used when applying MS/MS methodology. Thereby, the first quadrupole filters a precursor ion with a defined *m/z* ratio. CID leads then to characteristic product ion spectra that are subsequently analyzed with the third quadrupole by letting only the ion with a predefined *m/z* ratio pass. The use of MRMs enhances dramatically the specificity compared to single quadrupole techniques and also leads to a gain of sensitivity [60].

1.6   Chromatography in metabolomics

Prior to detection, chromatographic separation methods can be applied to improve sensitivity and overcome drawbacks of direct infusion methods, for example ion suppression due to co-eluting matrix components and isobaric overlaps.

The most commonly used separation techniques are LC and GC. The combination of GC with EI-MS provides high-chromatographic resolution, analyte-specific detection, as well

as identification capabilities of unknown metabolites followed by eventual quantification of these metabolites. GC separates the analytes due to their vapor pressure and interaction with a stationary phase. Therefore a prerequisite for using GC-MS is that the analytes have to be volatile and thermally stable. Since a vast number of metabolites have hydrophilic functional groups yielding low volatility, derivatization is needed to obtain volatile analytes. A very common derivatization technique is the conversion of the polar functional groups such as –COOH-, -SH, -OH or –NH$_2$/-NH- to silyl products (R–Si(CH$_3$)$_3$) which lead to thermally stable and volatile analytes. The active (acidic) hydrogen is replaced by a trimethylsilyl group, resulting in a higher volatility while maintaining stability. For example, *N,O-bis*-(trimethylsilyl)-trifluoroacetamide (BSTFA) is often used in metabolomics as silylation reagent [19]. For metabolic fingerprinting approaches one has to note that sugars can occur as different cyclic isomers which will appear as several peaks in the chromatogram. To overcome this problem and reduce the complexity of data evaluation, sugars can be derivatized with alkoxyamines prior to silylation, which stabilizes ketoacids in their open-ring conformation. This approach leads to only two different isomers (cis, trans) of the derivatives, depending on the orientation at the carbon-nitrogen (Fig. 4).
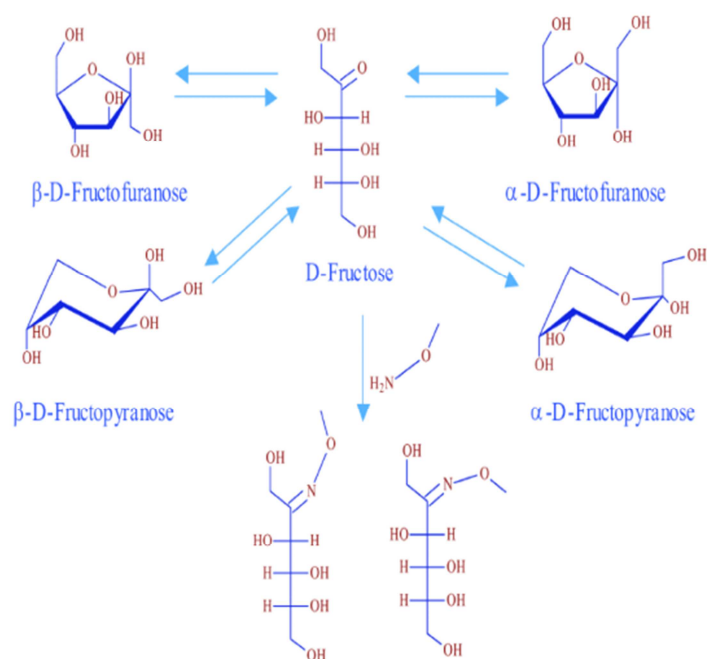
Fig. 4. Oximation of sugars during sample preparation. This leads to decreased numbers of isomers and thus to a reduction of complexity in metabolic fingerprinting methods. Taken from Strelkov 2004 [67].

Liquid chromatography (LC) in contrast to GC is not restricted to the analysis of thermally stable and small volatile metabolites. LC is a very efficient separation technique for both hydrophilic as well as hydrophobic compounds, acids, bases, aromatics, lipids and others. This methodology uses the solubility in a mobile phase and stationary phase and the interaction with the stationary phase for separation. There are different modes used in LC methodology, namely reversed phase (RP), normal phase (NP), ion exchange (IE), chiral, size exclusion (SEC) and hydrophilic interaction chromatography (HILIC). Utilization of these various modes depends on the physico-chemical properties of the metabolites to be analyzed [68]. Liquid chromatography coupled to ESI-MS is frequently used in lipidomics and metabolomics.

Generally, the selection of an appropriate chromatographic strategy and method is a major challenge in metabolomics. For example, the ionization efficiency in LC-ESI-MS approaches depends on the eluent composition in the ionization source. Therefore, to compensate such matrix effects in the ionization source, a co-elution of internal standards and analytes is required.

1.7 Chemometrics in metabolomics

Metabolic fingerprinting approaches using GC-TOF-MS lead to a vast number of raw data, consisting of a peak area/height or concentration, retention time and m/z value of each metabolite. This results in high-dimension data matrices, with up to millions of traits within one data set, that are difficult to summarize and usually contain considerably more variables than samples [69]. The adoption of chemometric methodologies for 'omics'-sciences improved the interpretation and handling of data sets, by robust modeling and production of highly reliable models containing collinear structures, leading to smaller assessable data sets. In particular, the assessment of multivariate statistical tools that can emphasize such collinear structures, can lead to metabolic patterns that can be used for a unambiguous group separation and therefore may serve as a set of biomarkers for investigation of disease development [70]. These methods are for example principal component analysis (PCA) and partial least square discriminant analysis (PLS-DA) [71]. PLS-DA is a supervised clustering and classification method, trying to separate two or more classes (e. g. smokers vs. non-smokers), by searching co-linearity within the metabolites. Therefore, the known class assignment (healthy vs. diseased, smokers vs. non-smokers etc.) is used for calculation of a new model. Thereby, the original data are projected into a low-dimensional space (Fig. 5). The dimensions of this new space are called latent variables (expressed by principal components, PCs) which are uncorrelated and capture the majority of the variance from the original data. These few PCs are ranked by the amount of explained variance between the

two original classes (smokers vs. non-smokers) [69,72]. Therefore, samples can be classified by specific patterns of endogenous compounds that are most important and possibly serve as biomarkers for an early biological effect evoked by tobacco smoke uptake [20,40]. It is important to select the optimal number of latent variables used in the PLS-DA model. For this purpose, cross-validation strategies can be used. A common approach is k-fold cross-validation, where the data set is divided into 1/k parts. The k-th part is used to build a model and the remaining k-1 parts are used to calculate the prediction errors for this model. This is done for all k parts and the prediction errors are used for model prediction for different numbers of latent variables [73,74].

	Sample	Peak area				
	Label	1 non-smoker	2 non-smoker	3 smoker	4 smoker	...N
m/z / RT						
254.07/12.021		8097	35829	11722	22493	
239.06/12.021		9786	38546	13777	20203	
189.05/16.178		24172	25403	18893	21363	
143.05/8.3		73304	129747	84919	78977	
		...M (> 7000)				

M dimensional space (original data)

PLS-DA

few dimensions after elucidation of co-linearity in original data
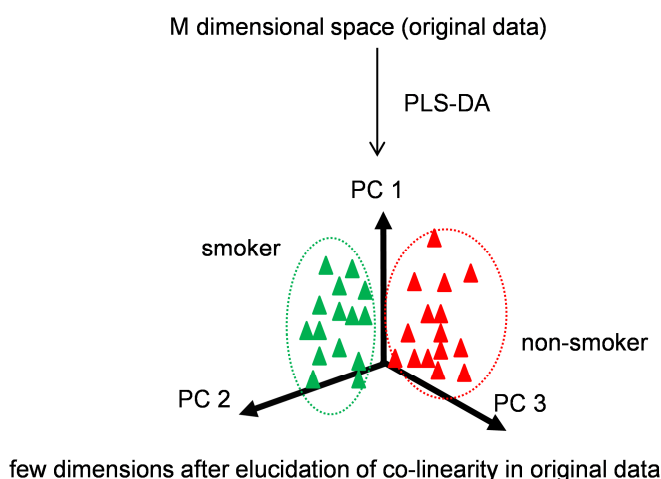
Fig. 5. PLS-DA calculation using metabolomics data. A PLS-DA reduces the high dimensional data to yield low number of new dimension called latent variables, depicted by principal components (PC), by detection of co-linearity in the original data structure. The principal components (axes of the new coordinate system) are in the direction of most explained variances between the groups based on the variation of the metabolites that are analyzed. The principal component 1 carrying most of the variation between the groups, the component 2 explains second most variation and so on.

1.8   Metabolomics in smokers

Knowledge of endogenous metabolic changes caused by cigarette smoking is, up to now, limited. Hsu and coworkers [75] investigated the plasma of smokers and non-smokers using a platform consisting of ultra-performance liquid chromatography coupled to a quadrupole time-of-flight MS (UPLC-QTOF-MS). In addition to the identification of Nic metabolites, as expected, a characteristic profile of metabolites distinguishing smokers from non-smokers was observed. Similar studies were published by Wang-Sattler et al. [76] and Xu et al. [77]. These groups used targeted metabolic profiling to demonstrate the impact of cigarette smoking on phospholipids such as PC. A significant alteration of these compounds in serum of smokers was observed. Other studies revealed significant changes in the fatty acid levels of FA 16:1 (palmitoleic acid) and FA 18:1 (oleic acid) in plasma or serum of smokers as compared to non-smokers, using a targeted metabolomic approach [78-81]. Hsu [75] and co-workers used UPLC coupled to quadrupole time-of-flight mass spectrometry (UPLC-QTOF-MS) for a metabolomics approach of smokers' plasma, however they reported mainly (exogenous) metabolites, which are known as constituents of tobacco smoke.

A major disadvantage of these studies was the lack of a strictly controlled study design with respect to diet and smoking behavior. Since metabolites are influenced by the genetic background as well as environmental factors, standardization for nutrition as well as ethno-demographic factors is crucial in order to obtain results, which can reliably be attributed to solely one factor, namely smoking in our case [82-84].

1.9   Scope and objectives of this thesis

Up to now, only little is known about the effects of smoking on the human metabolome. Metabolomic studies on the influence of smoking on metabolic pathways with samples from nutritional controlled clinical studies are scarce. To the best of the author's knowledge, studies applying validated metabolic fingerprinting methods to saliva or urine are completely missing. The investigation of smoking-related physiological perturbations on the human metabolome would be useful for the discovery of biomarkers of effect indicating pathophysiological alterations at an early and reversible state.

The aim of the current work was to investigate the human metabolome in urine, saliva and plasma of smokers and non-smokers to find significant smoking associated changes in the levels of endogenous metabolites. The identified metabolites should then be linked to involved metabolic pathways, which can give valuable clues about the genesis of smoking-related diseases.

The first working-step was to plan a controlled clinical study with smokers and non-smokers for collecting body fluids (blood, urine, saliva) suitable for metabolomics analysis. A

main goal of this clinical study was to standardize other factors such as diet, gender, age and ethnic origin in order to relate the observed changes to smoking as the sole cause.

In a second working-step, the collected samples ought to be analyzed by a metabolic fingerprinting approach. For this purpose, a suitable and robust GC-TOF-MS method had be developed and validated for capturing as many metabolites as possible in the body fluids saliva, urine and plasma. This step also included the subsequent normalization of the detected mass fragments to appropriate standards, to yield data that are comparable across all samples and which are useful for statistical evaluation.

In the third working-step, the normalized data were analyzed by uni- and multivariate statistical tools to find significant differences between smokers and non-smokers at the metabolic level. Potential hits, that are responsible for the difference between the two groups, were attempted to be identified using mass spectral libraries as well as authentic reference compounds. Subsequently, the identified metabolites were mapped into biochemical pathways that could be affected by smoking.

In a final working-step, the implicated biochemical pathways were further investigated by targeted approaches to confirm and substantiate the findings from the untargeted metabolic fingerprinting. The ultimate aim of these studies was to decipher the underlying pathophysiological and toxicological mechanisms of tobacco smoking. Fig. 6 depicts an overview of the applied work-flow in this thesis.
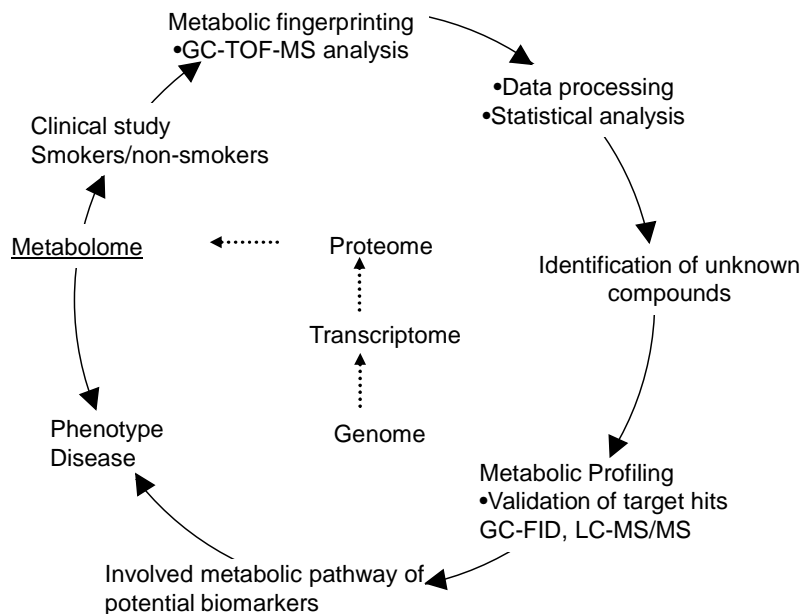
Fig. 6. Flowchart of the applied metabolomic approach used for this thesis.

2 Material and Methods

2.1 Software

In this work, the following software packages and databases were used: *QtiPlot 0.8.9* (http://soft.proindependent.com/qtiplot.html), *MZmine* 2.10 [85], *AMDIS* Version 2.71 (Automated Mass Spectral Deconvolution and Identification System) [86,87] equipped with the NIST *MS Search Program 2.0* (National Institute of Standards and Technology, Gaithersburg USA) and the mass spectral databases NIST 05 (replib, mainlib) and Golm Metabolome Database GMD 201032 [66], the online platform *Metaboanalyst* [88], Chemstation 2.0 (Agilent, Santa Clara, USA), *ProtoTOF* (Almsco, Llantrisant, United Kingdom), *Office 2007* (Microsoft, Redmond, USA), the statistic program *PSPP* Version 0.8.1.1 [89], MassLynx (Waters Corporation, Milford, USA), *Analyst Software 1.5.2* (AB Sciex, Darmstadt, Germany), *Maple 12.0* (Waterloo Maple Inc., Waterloo, Canada).and Endnote X7 (Thomson Reuters, New York City, USA).

2.2 Chemicals and standard solutions

Calibration standards, pyridine (anhydrous, 99.8%), N,O-Bis(trimethylsilyl)trifluoroacetamide containing trimethylsilyl chloride (BSTFA+1% TMCS, 99%), methoxyamine·HCl (MOX, 98%), C_7 - C_{30} saturated alkane standard mix (each at 1 mg/mL in hexane, analytical grade), formic acid (puriss), ammonium formate (MicroSelect ≥ 99%), acetonitrile containing 0.1% formic acid (LC-MS grade), methanol containing 0.1% ammonium acetate (LC-MS grade), potassium carbonate (Reagent Plus®), methanolic acetlychloride (≥ 99%), tyramine HCl (99%), urease from Canavalia ensiformis (Jack bean) and cotinine (Cot, ≥ 98%) were supplied by Sigma-Aldrich/Fluka (Taufkirchen, Germany). L-Proline, ttMA, pyruvate and water were purchased from Merck (Darmstadt, Germany). Thymidine was obtained from Roth (Karlsruhe, Germany). $^{13}C,^{15}N_2$-urea was supplied by Cambridge Isotopic Laboratories (Tewksbury, USA). $^{13}C_6$-glucose was purchased from Cortecnet (Voisins-Le-Bretonneux, France). The compounds d_4-ttMA, trans-3-OH-Cot (OH-Cot), trans-3-OH-Cot-methyl-d_3 (OH-Cot-d_3) and Cot-methyl-d_3 (Cot-d_3) were obtained from Toronto Research Chemicals (Toronto, Canada). 2-(4-Hydroxyphenyl)-ethyl-1,1,2,2-d_4-amine·HCl (d_4-tyramine, 98%) was purchased from C/D/N Isotopes Inc (Quebec, Canada). Methanol (UPLC grade) was purchased from Promochem (Wesel, Germany). Chloroform, methanol and water (all picograde) were purchased from LGC Standards (Wesel, Germany). VWR (Darmstadt, Germany) supplied n-hexane (HiPerSolv 95%). CPS Chemie (Aachen, Germany), Nu-Chek Prep (Elysian, USA), Sigma (Steinheim, Germany) and Supelco

2. Material and Methods

(Taufkirchen, Germany) supplied the fatty acid methyl ester standards for GC analysis. The phospholipid standards 1,2-dimyristoyl-sn-glycero-3-phosphocholine (PC 28:0), 1-palmitoyl-2-oleoyl-sn-glycero-3-phosphocholine (PC 34:1), 1-octadecanoyl-2-(9Z,12Z-octadecadienoyl)-sn-glycero-3-phosphocholine (PC 36:2), 1-stearoyl-2-arachidonoyl-sn-glycero-3-phosphocholine (PC 38:4), 1,2-dieicosanoyl-sn-glycero-3-phosphocholine (PC 40:0), 1,2-diphytanoyl-sn-glycero-3-phosphoethanolamine (PE 32:0 8 Me), 1,2-ditetradecanoyl-sn-glycero-3-phosphoethanolamine (PE 28:0), 1-palmitoyl-2-oleoyl-sn-glycero-3-phosphoethanolamine (PE 34:1), 1,2-dioleoyl-sn-glycero-3-phosphoethanolamine (PE 36:2), 1,2-dilinoleoyl-sn-glycero-3-phosphoethanolamine (PE 36:4), 1-stearoyl-2-docosahexaenoyl-sn-glycero-3-phosphoethanolamine (PE 40:6), 1-(1Z-octadecenyl)-2-arachidonoyl-sn-glycero-3-phosphoethanolamine (PE P-38:4), 1,2-dibehenoyl-sn-glycero-3-phosphocholine (PC 44:0) and 1-O-hexadecyl-2-arachidonoyl-sn-glycero-3-phosphocholine (PC O-36:4) were purchased from Avanti Polar Lipids Inc. (Alabaster, USA).

The derivatization solvent MOX was dissolved in pyridine, yielding a final concentration of 20 mg/mL. A surrogate stock solution containing the 37 standard metabolites was prepared at a concentration of 2 mM in water for each analyte, respectively.

Two internal standard (IS) solutions for the metabolomic fingerprinting were prepared separately by dissolving $^{13}C_9,^{15}N$-L-Tyr, $^{13}C,^{15}N_2$-urea, d_4-ttMA, d_4-succinic acid, $^{13}C_6$-glucose at a concentration of 1 mM in water (IS 1) and 2 mM heptadecanoic acid in methanol (IS 2). All solutions were stored at -20°C prior to use (for up to 3 months).

For Cot and OH-Cot analysis in saliva the respective labelled internal standards were dissolved and diluted in water, to obtain a final concentration of 5.2 mM for OH-Cot-d_3 and 5.7 mM for Cot-d_3.

Stock solutions of all lipid standards were prepared in chloroform except for PE 28:0, which was diluted in chloroform:methanol:water 65:30:5 (v:v:v). Working solutions were obtained by diluting the stock solution with methanol and were stored at -20°C.

Urease was diluted in a 0.2 M sodium phosphate buffer pH 7.0 to a final concentration of 1 unit/µL.

Stock solutions for tyramine and d_4-tyramine were prepared by dilution with methanol to a concentration of 200 mM. Working solutions were obtained by dilution of the stock solution with methanol and were stored for up to 3 month at -20°C.

2.3 Clinical study and sample collection

2.3.1 Design of the clinical study

A clinical study was conducted with 50 healthy male caucasian subjects at the "CRS Clinical Research Services Mönchengladbach GmbH". The study was performed according to the Helsinki declaration and was approved by the ethic commission of the Medical Chamber of Nordrhein-Westfalen, Germany. Table 3 shows the criteria for inclusion. The participants were separated into two groups comprising of 25 smokers and 25 non-smokers (never-smokers). All subjects had to have a body mass index (BMI) between 19 and 30 and were matched to have similar distributions in both groups. At baseline, a standard medical examination proved that none of the subjects showed any kind of disease traits. Smokers were defined to have a cigarette consumption of at least 5 cigarettes per day over a period of at least 1 year. During study entrance screening, subjects underwent a standard medical examination, where the COex levels were also measured to verify their smoking status. The cut-off for COex between smokers and non-smokers was defined at 5 ppm. Each individual completed a questionnaire providing different lifestyle parameters such as leisure time activities, sporting activities, dietary habits and smoking history. To obtain similar distribution in both groups, the participants were matched in 5-year age groups ranging from 20 to 50 years.

Table 3. Inclusion criteria for subjects in the metabolomic study.

General requirements	– Male
	– Caucasian
	– Healthy
	– 20 - 50 years
	– No drug abuse
	– 19 < BMI < 30
Non-smokers	– Never smokers (not having smoked more than 10 cigarettes during their life-time)
	– COex level at the study entrance screening < 5 ppm
	– No use of any other tobacco products
Smokers	– Smoking of 5 cigarettes for at least 1 year before the study
	– COex level > 5 ppm at the study entrance screening

Meals were served on Day 1 at 9 am, 12 noon and 7 pm (Fig. 7). All subjects were served the same food quantities normalized to their bodyweight (Table 4), by adjusting the quantities of the lunch while maintaining the same breakfast and dinner quantities for all participants. The caloric intake was estimated using the updated Harris-Benedict equation [90]. The calculated values were slightly changed in order to facilitate handling when serving meals at the clinical research organization. Caloric intake comprised of 72% carbohydrates, 14% fat and 14% proteins. Grilled, fried or otherwise extensively heated or smoked food was prohibited throughout the entire study, to avoid the dietary uptake of pyrolysis products, such as polycyclic aromatic hydrocarbons and nitrosamines, which might interfere with the uptake of these compounds by smoking. All participants had to drink 3 L of water during the stay in the clinic, no other beverages were allowed. The clinical study comprised a 24-hour stay of each subject in the clinic, starting on Day 1 at 8 am. No food consumption was allowed since 11 pm prior to Day 1. The smokers were allowed to smoke ad libitum prior and until 11 pm of Day 1. Each subject smoked their own cigarettes throughout the entire study. Manufactured as well as roll-your-own cigarettes were permitted for smoking. To avoid the exposure to environmental tobacco smoke of the non-smoking group, smoking took place in a designated room, where non-smokers were not permitted. From 11 pm (Day 1) to 8 am (Day 2) only drinking was allowed (no smoking or eating).

Table 4. Caloric intake during the clinical study, standardized to the weight of the participants. Caloric intake comprised 72% carbohydrates, 14% fat and 14% proteins.

Body weight range (kg)	< 65	65 - < 75	75 - < 85	85 - < 95	95 - < 105
Caloric intake (kcal)	1801	2036	2239	2436	2561

2.3.2 Saliva collection and COex determination

Saliva collection took place at five different time points: on Day 1 at 10 am, 2 pm, 6 pm, 10 pm and on Day 2 at 8 am (Fig. 7). To avoid systematic errors provoked by the collection method [91], saliva samples were collected by means of a modified unstimulated spitting method as described by Navazesh [92]. Briefly, subjects did not eat, smoke or tooth brush for at least 20 min before sampling. Five minutes prior to sampling the participants rinsed their mouth with water three times for 20 s. Saliva collection was conducted in sitting position. Saliva was allowed to accumulate on the floor of the mouth for 30 s and the subjects spitted it out into a 50 mL sterile polypropylene tube (Greiner Bio-One, Frickenhausen, Germany). This procedure was repeated until about 2 mL of saliva

accumulated. The sampling procedure took about 5 min and the samples were frozen at -20°C immediately after collection. Right after saliva collection, COex was measured using a Bedfont 'smoke analyser' (Harrietsham, England). COex measurements were conducted according the instructions of the manufacturer.

2.3.3 Blood sample collection

Blood samples (5 mL) were collected at 8 am on Day 2. At that time point, subjects were on a controlled diet for 24 hours and had fasted overnight for 9 hours (with only water allowed) (Fig. 7). To obtain EDTA plasma, blood was collected into cooled (4°C) Vacuettes® (Greiner Bio-One, Frickenhausen, Germany). Immediately after sampling and centrifugation at 2000 x g (10°C), obtained plasma samples were frozen at -20°C until analysis.

2.3.4 Urine sample Collection

Urine samples were collected in three different fractions. Fraction 1 represents a 24-hour urine pool without the two single spot urine fractions 2 and 3. fraction 2 was a spot urine, collected as the first urine after 6 pm on Day 1. Urine fraction 3 was the combined morning urine samples collected between 4 am and 8 am, which was usually a single spot urine (Fig. 7). After the sampling, the urine samples were immediately frozen on dry ice and stored at -20°C. Fraction 1 was stored at 4 - 8°C during the collection period. The 24-hour urine used for analysis was a pool of respective aliquots from fractions 1, 2 and 3.
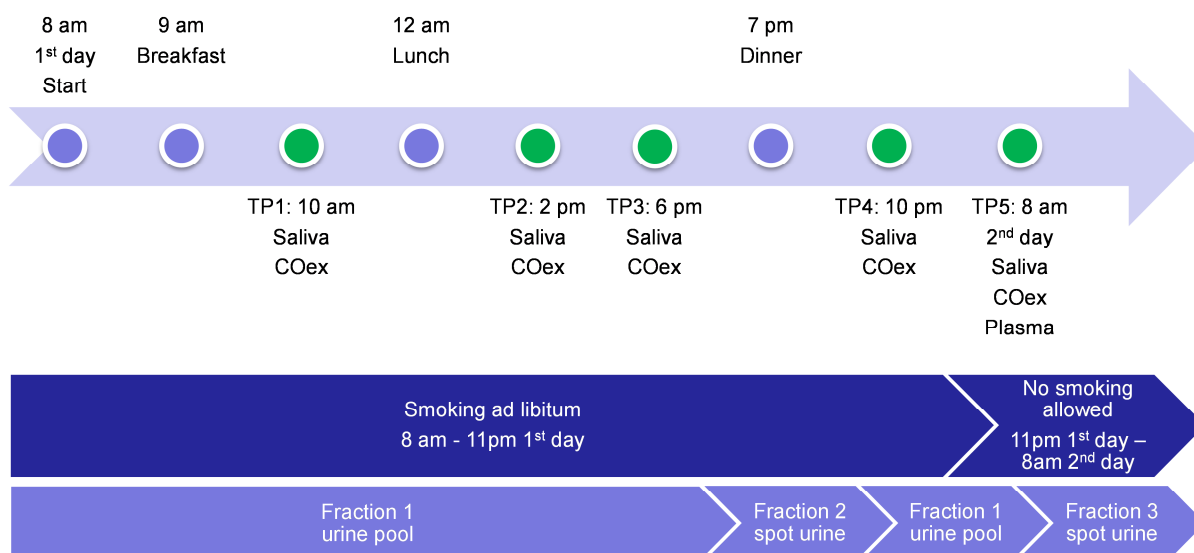
Fig. 7. Flowchart of the study timetable. Sample collection took place at different time points (TP) for saliva, plasma and urine. COex levels were measured at 5 time points and 3 meals were served. Smoking was allowed from wake up on Day 1 until 11 pm of Day 1. After dinner until blood sampling, only drinking was allowed.

2.4   Salivary Cot and OH-Cot

Sample preparation and measurements of salivary Cot and OH-Cot were conducted at the ABF Laboratory according to an accredited and validated LC-MS/MS method [93].

Briefly, 100 µL of saliva were spiked with 25 µL of an IS mix of deuterated analytes. Protein precipitation was conducted by adding 400 µL methanol followed by vortexing and freezing the mixture for 1 h at -20°C. The mixture was then vortexed for another 10 min, centrifuged at 15,330 x g and 200 µL of the supernatant was transferred into a glass vial. For analysis, 5 µL were injected in the HPLC-system (Agilent 1100 series, Waldbronn, Germany) equipped with a Synergi™ MAX-RP 80, (150 mm x 4.6 mm) column with 4 µm particles (Phenomenex, Torrance, USA). Column temperature was set to 45°C. Isocratic separation was performed using a mobile phase consisting of 20% water with 10 mM ammonium acetate and 80% methanol at a flow rate of 1 mL/min. MS/MS analysis was performed in positive ionization mode on a triple quadrupole MS (API 4000, AB Sciex, Darmstadt, Germany) equipped with an APCI ionization source (Turbo V™ Ion Source, AB Sciex, Darmstadt, Germany). Calibration was performed with the standard addition method by spiking increasing amounts of authentic standard compounds into matrix samples. The MRMs of m/z 177 to m/z 80 for Cot and m/z 193.1 to m/z 80 for OH-Cot were normalized to the areas of the corresponding deuterated internal standards (MRMs for Cot-d$_3$ 180 m/z to

80 *m/z* and for OH-Cot-d$_3$ 196 *m/z* to 80 *m/z*) and then divided by the calibration slope to get the absolute concentrations. The calibration ranged from 10 nM to 10 µM for both analytes.

2.5　　Determination of nicotine equivalents (Nic+9) in urine

Sample preparation and measurements of nicotine and nine of its metabolites (Nic+9) were conducted at the ABF laboratory according to an accredited and validated method using labeled internal standards for all analytes [94].

Nic, Cot, OH-Cot, nornicotine, norcotinine, Nic-N-oxide, Cot-N-oxide, Nic-glucuronide (Nic-gluc), Cot-gluc and OH-Cot-gluc (Nic+9) represent almost 90% of the absorbed nicotine dose [94]. The analysis was performed in two steps. Briefly, for the analysis of Nic, Cot, OH-Cot, Nic-gluc, Cot-gluc and OH-Cot-gluc, 100 µL of urine were added with 25 µL of labeled internal standard mixture (containing the respective labeled reference compounds). For protein precipitation, 400 µL of methanol was added, vortexed and the mixture was placed at -20°C for 1 hour. After centrifugation at 15,330 x g for 10 min, 1 µL of the supernatant was analyzed by means of HPLC-APCI-MS/MS method. In a second step the analytes nornicotine, norcotinine, Nic-N-oxide and Cot-N-oxide were analyzed. For that purpose, 200 µL of urine were centrifuged at 1000 x g for 10 min and 100 µL of the supernatant was transferred to a glass vial. Then 25 µL of an IS solution (containing the respective labeled reference compounds) was added, the mixture was vortexed and analyzed by means of a HPLC-ESI-MS/MS method. For detailed analytical settings refer to the Appendix "7.1 Nic+9 determination in 24-hour urine".

2.6　　Creatinine determination

Sample preparation and measurements of creatinine was conducted at the ABF laboratory according to an official photometric method from the DFG-method [95].

Urinary levels of metabolites were commonly normalized to creatinine concentrations in order to consider variations in urinary dilutions. Determination of creatinine in urine was conducted on a 96 well microplate (Greiner bio-one, Frickenhausen, Deutschland) using a GENios Microplate Reader (Tecan, Krailsheim, Deutschland).

2.7 Metabolic fingerprinting

2.7.1 Sample preparation for GC-TOF-MS analysis

For validation, saliva, plasma or urine samples were thawed at room temperature, 10 µL of the IS 1 solution and 5 µL of the IS 2 solution were added to 100 µL of urine and saliva (30 µL for plasma). IS 1 solution contained $^{13}C,^{15}N_2$-urea, d_4-succinic acid, d_4-ttMA, $^{13}C_9,^{15}N$-Tyr, $^{13}C_6$-glucose for saliva and plasma samples and d_4-ttMA and $^{13}C_6$-glucose for urine samples. IS 2 solution contained $C_{16}H_{33}COOH$ in methanol. 40 units of urease were added to urine prior to incubation for 45 min at 37°C to digest the excessive amount of urea in the matrix [96]. Protein precipitations and metabolite extraction was conducted by adding 500 µL of MeOH/ACN (70/30, v/v) to urine and saliva samples and 150 µL MeOH to plasma samples. The samples were thoroughly vortexed, kept at -20°C for 1 hour and subsequently centrifuged with 15,330 x g at 4°C for 15 min. The supernatant was transferred to a glass vial. A second extraction was conducted by adding 100 µL methanol/water (8:1 v/v) to the residue. The mixtures were vortexed, kept for 20 min at -20°C and then centrifuged for 15 min at 15,330 x g (4°C). The supernatants were combined and evaporated in a SpeedVac (RC10.22, Thermo Scientific, Dreieich, Germany) to near dryness. Then, 50 µL of pyridine was added and the mixture was dried under a gentle stream of nitrogen which leads to a homogenously distributed residue, thus enhancing the derivatization efficacy. For derivatization purposes, 60 µL the MOX solution in pyridine was added to plasma and saliva (70 µL for urine), sonicated for 3 min and incubated for 30 min at 60°C. Afterwards, 60 µL of BSTFA containing 1% TMCS was added (70 µL for urine), sonicated for 3 min, and incubated for further 30 min at 60°C, followed by addition of 2 µL of a saturated alkane standard solution. Finally, the mixture was centrifuged for 15 min at 3,300 x g (10°C) and the supernatants were transferred to GC vials and placed in an autosampler (MPS2, Gerstel, Mülheim an der Ruhr, Germany) at 10°C until analysis.

2.7.2 GC-TOF-MS analysis of the study samples

Analysis of the samples was performed by injection of 1 µL of the derivatized samples into the GC system (GC 6980, Agilent Technologies, Santa Clara, USA) coupled to a time of flight mass spectrometer (BenchTOF-dx™, Almsco, LLantrisant, United Kingdom). Split ratio was set to 1:5 in case of saliva samples, 1:20 for urine samples and 1:15 for plasma samples. A Rxi®-1ms 30 m x 250 µm ID fused silica column (Restek, Bad Homburg, Germany) with dimethyl polysiloxane as stationary phase (0.25 µm film thickness) was used for separation. Helium served as carrier gas at a flow rate of 1.1 mL/min. A CAS 4 (Gerstel, Mülheim an der Ruhr, Germany) was used for injection, equipped with a Siltek deactivated

baffled glass liner (Gerstel, Mülheim an der Ruhr, Germany). The injector temperature was set to 50 °C for 1 s followed by a linear increase to 300°C with 12°C/s and a hold step for 6 min at 300°C. The oven temperature was kept at 50°C for 1 min, increased to 300°C with 10°C/min and held at 300°C for 10 min. The transfer line between GC and MS was kept at 250°C. Ion source temperature was set to 240°C. The mass spectrometer was operated in electron ionization mode at 70 eV. The filament delay was set to 5.6 min. Data acquisition was performed in the full scan mode from *m/z* 40 to 650 with a sampling rate of 5 Hz.

2.7.3   Validation of the GC-TOF-MS Method

Calibration curves were obtained by plotting the response (peak area analyte / peak area corresponding IS) using the peak area of the most intense fragment of a spiked standard against the concentration of the spiked amount. In case of analyte co-elution with interfering peaks, differentiation was achieved by using different fragments for quantification. The linear range of the calibration curve was defined for the spiked concentrations showing an accuracy of 80 to 120% to the calibration curve. A linear calibration curve was only calculated if at least 4 concentration levels were within this linear range. A detailed analytical evaluation of the GC-TOF-MS method was conducted by determining the analytical performance including reproducibility, linearity, detection limits, re-injection, repeatability and stability across 37 reference compounds (Table 5). These compounds covered a broad range of chemical classes and metabolic pathways, potentially occurring in saliva, urine and plasma, representing both exogenous and endogenous metabolites.

Table 5. Reference (standard) compounds (N = 37) and 6 internal standards, used for validation of the metabolic fingerprinting method in urine, plasma and saliva.

Amino acids	L-Gly, L-Pro, L-4-Hyp, L-Leu, L-Val, L-Ala, γ-aminobutyric acid (gaba), L-Trp, L-Tyr, L-glutamine
Vitamin	nicotinic acid
Carboxylic acids	2-oxoglutaric acid, oxalic acid, succinic acid, mandelic acid, pyruvate, citric acid, ttMA, p-hydroxyphenylacetic acid (p-OH-Ph-acetic acid)
Carbohydrates	D-(+)-glucose, glucuronic acid, β-lactose, glucose-6-phosphate (G6P)
Nucleic acids, purine	thymine, thymidine, adenosine, uric acid
Indole/amine	5-hydroxyindoleacetic acid (5-HIAA)
Phenol/amine	Dopamine
Dipeptide	glycine-glycine (Gly-Gly)
Alcohols	glycerol, homovanillic acid, sorbitol
Ketones/Aldehydes	Cot, creatinine
Others	4-methylhippuric acid (4-Me-hippuric acid), 2-methylhippuric acid (2-Me-hippuric acid)
Internal standards	$^{13}C_6$-glucose, d_4-ttMA, d_4-succinic acid, $^{13}C_9$ ^{15}N-L-Tyr, $^{13}C,^{15}N_2$-urea, heptadecanoic acid ($C_{16}H_{33}COOH$)

2.7.3.1   Linear range

Calibration was performed by the standard addition method in a respective matrix pool samples. For this purpose, increasing amounts of the 37 authentic standard compounds were spiked at different concentration levels into saliva, plasma or urine pool samples, covering a calibration range from 0.1 µM to 2 mM. Calibration curves were determined by plotting the response (peak area analyte / peak area of corresponding IS) of the most characteristic fragment ion against the spiked concentrations. According to the Food and Drug Administration (FDA) guidelines "Guidance for Industry - Bioanalytical Method Validation*"* from 2001 [97], the linear range was defined for concentrations showing a deviation from the nominal concentrations of less than 20%.

2.7.3.2 Precision and accuracy

To assess the precision and accuracy of the analytical methods, the respective pools of each matrix were spiked at different concentrations using the 37 reference compounds. The samples were analyzed five times in a row and on 5 consecutive days to determine intraday and interday variations, respectively. The different levels were prepared by spiking the 37 standard compounds to saliva, at concentrations of 25 µM, 50 µM and 200 µM, and urine at the concentrations of 50 µM and 500 µM. Thirty six standard compounds (glucose omitted) were spiked to plasma at concentrations of 25 µM, 50 µM and 500 µM. To obtain instrument precision, re-injection analyses were performed. For this purpose, three saliva samples spiked with 25 µM, 50 µM and 200 µM (25 µM, 50 µM and 500 µM for plasma) of the standard compounds were injected 5 times and the respective CV of the calculated concentrations were used to determine the instrument precision.

2.7.3.3 Stability of derivatives

One GC run of the described method takes about 40 min (including cool down time of the GC). Therefore, the analysis time for a batch of 60 samples (25 smokers, 25 non-smokers, 6 quality control samples and 4 blanks) lasts about 40 hours. For this reason, the stability of the derivatized samples were tested by injecting 2 saliva samples spiked with 25 µM and 200 µM of the surrogate solution at 0, 1, 2, 3 and 5 days after derivatization. Between the measurements the samples were stored at 10°C (autosampler conditions). The deviation of the analytes on day 5 from the reference values measured on day 0 was determined. Since the conditions are assumed to be similar for all matrices after the sample preparation, the stability measurements were only performed for saliva.

2.7.4 Quality control samples

The reproducibility of the metabolic fingerprinting method was controlled during the analysis of the study samples to assure comparability of the results. For this purpose, 6 quality control (QC) samples were randomly placed in the batch. The QCs were prepared by pooling aliquots of all 50 samples of every matrix and spiking the pools with 50 µM from each of the 37 reference components used for the validation measurements. For each analyte, the CV was calculated from the respective chromatographic peak areas.

2.7.5 Data processing for metabolomic investigations

Data processing and background compensation of MS spectra were carried out by using the *ProtoTOF* software package. For the validation experiments, the raw data were

exported to *Chemstation 2.0* followed by manual integration of all analyte peaks. Internal standard (IS) selection for each standard analyte considered the chemical structure and/or the retention times. For the metabolic fingerprinting, the raw data were background corrected by means of the *ProtoTOF software.* The obtained files were converted to Common Data Format (CDF) files. Next, automated peak picking, integration, retention time adjustment by alkane standards and alignment were conducted with the open source software package *MZmine*. Refer to Fig. 8 for a detailed workflow of the metabolic fingerprinting methodology. The peak list generated by *MZmine* contains all features, representing signals, characterized by their *m/z* values, retention times and the peak areas. Then, the peak list was exported to *Excel*, and normalized to the fragment *m/z* 275 of the IS d_4-ttMA. To account for dilution differences, urine samples were further normalized to creatinine concentrations determined in the corresponding 24-hour urine samples. Next, known signals derived from the IS or alkane standards were removed and univariate analysis to find differences between the two groups (smokers and non-smokers) was performed by applying the Mann-Whitney U test using the *PSPP* software package. Signals with $p > 0.05$ and signals derived from tobacco specific biomarkers such as nicotine and its metabolites were manually removed, since the main interests were on endogenous metabolites significantly discriminating smokers from non-smokers. Subsequently, the peak list was uploaded to *Metaboanalyst*. The occupational degree was set to 50%. That means, each fragment at a given retention time had to be found in at least 25 samples. Afterward, missing peaks were replaced by half of the minimum of the respective feature measured in the respective sample series. Notably, the reason for variations within a metabolomic data set has different sources. Besides the relevant smoking induced biological variation, there are also environmental (e.g. diet), biological (e.g. genetic variation) and technical variations. There is a vast difference in variation of levels of the metabolites in the raw data. Without further data processing, PLS-DA would focus on a small number of metabolites present at high levels. However, in an organism, metabolites at low concentration levels are not automatically less important than high abundant metabolites. A data pretreatment can highlight the biologically relevant information from the clean data. For this reason, all features were autoscaled to get a zero mean and a unit variance, to have the same influence on the PLS-DA model [98]. With the autoscaled data, a PLS-DA was performed. The PLS-DA model calculates a so-called variable importance in projection (VIP). Therefore, a weighted sum of squares is calculated for each PLS loading that explains the variance of each component. Each fragment gets a value for every used principal component. The higher the value, the more influence the fragment has on the model and the more this fragment is responsible for a group separation. Model performance was evaluated by 10-fold cross validation using the R^2 and Q^2 parameters. R^2 provides a measure of how much variation is accounted for by the model.

How accurate the data are classified in the model is predicted by the Q^2 value. Both values are between 0 and 1 and are commonly represented as percentages [99]. Admittedly, PLS-DA is a supervised method that is prone to over-fit the data set. Particularly, the algorithm of the PLS-DA sometimes performs a group separation just by chance due to random noise instead of real biological differences. Applying cross validation often leads to too optimistic classifications and will not always reveal such random separations. Therefore a permutation test was performed additionally [74]. A permutation test re-designates the class labels of the samples (smoker / non-smoker) and repeats the PLS-DA with the new labeled data. This can be done up to 2000 times using *Metaboanalyst*. The Re-designated models and the original model are plotted in a histogram, which indicates whether the original model is a part of the re-designated models or significantly different from this distribution. Further, an empirical p-value is calculated that determines how often a better class separation was yielded [100,101].

Finally, significant hits obtained from the PLS-DA and Mann-Whitney U test (VIP > 0.8 and p < 0.05) were further processed for identification of underlying metabolites, using the NIST MS Search Program 2.0, mass spectral databases and the deconvolution software *AMDIS 2.71*. Further identification and confirmation of the results was performed with authentic reference compounds, if available.
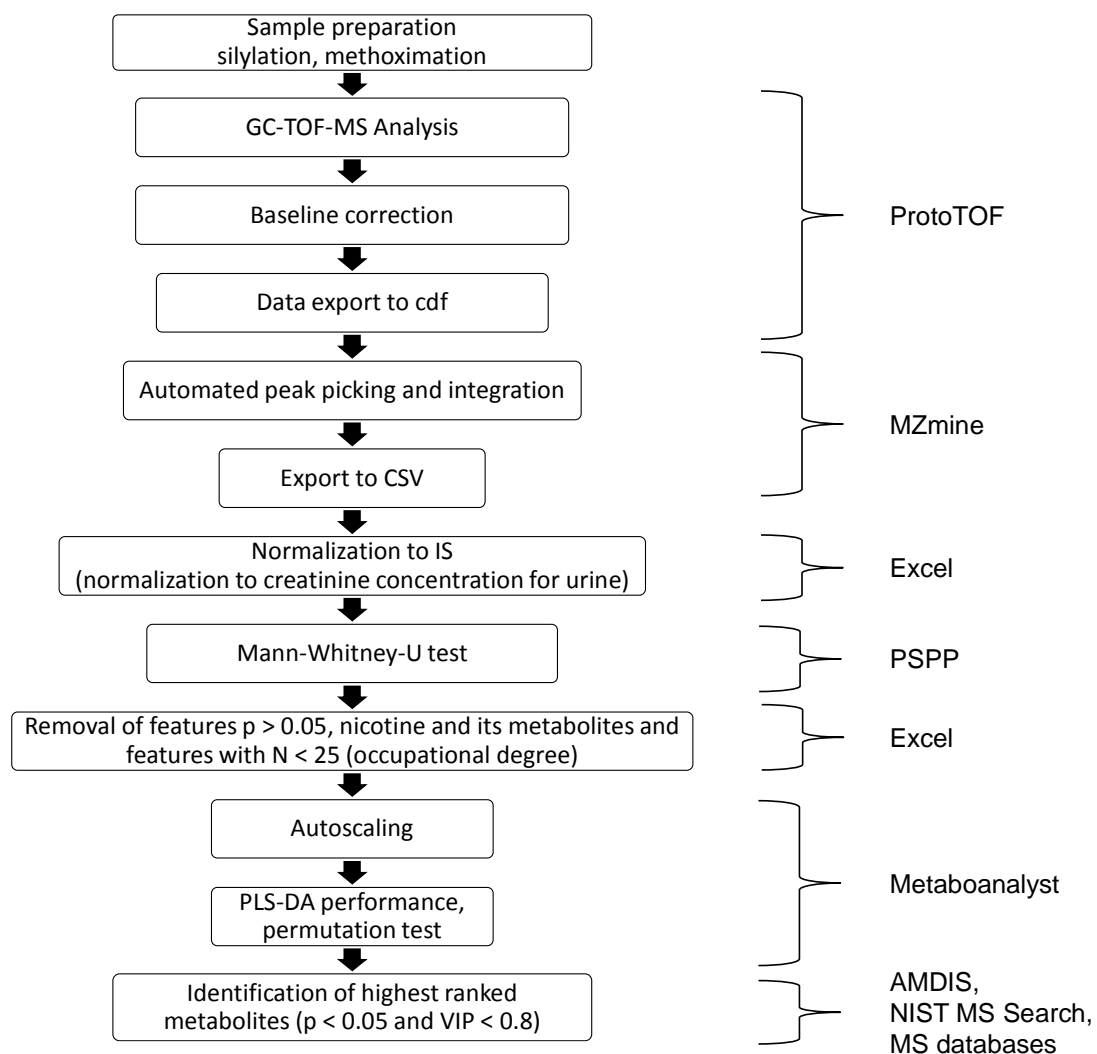
Fig. 8. Flowchart of the data-processing procedure applied for the metabolic fingerprinting.

2.7.6 Automated peak picking

Automated peak picking and integration for the metabolic fingerprinting experiments was conducted by the software package *MZmine 2.10*. The settings were as shown in Table 6.

Table 6. *MZmine* settings for the metabolic fingerprinting.

Raw data import	background compensated, .cdf-file format
Data set filtering - crop filter	5.7 min – 28 min
Mass detection - centroid	noise level 100
Chromatogram builder	minimum time span 0.020 min, minimum height 1e3, *m/z* tolerance 0.05
Peak detection - chromatogram deconvolution	local minimum search, chromatographic threshold 0.001%, search minimum in RT range (min) 0.020, minimum relative height 0%, minimum absolute height 1e3 (3e3 for urine), minimum ratio of peak top/edge 1, peak duration time (min) 0.020 to 0.300
Normalization - retention time normalizer	*m/z* tolerance 0.01, retention time tolerance 0.02 min, minimum standard intensity $1 \cdot 10^5$
Alignment – join aligner	*m/z* tolerance 0.05, weight for *m/z* 10, weight for RT 10, Retention time tolerance 0.03
Gap filling – peak finder	intensity tolerance 90%, *m/z* tolerance 0.05, retention time tolerance (min) 0.03
Filtering – duplicate peak filter	*m/z* tolerance 0.02, RT tolerance (min) 0.01
– peak list rows filter	minimum peaks in a row 15, minimum peaks in an isotopic pattern 1, *m/z* and RT auto range, peak duration range 0.020 – 0.300
export to csf-files	ID (*m/z*-value/RT), peak area, sample name

2.8　　Target hit identification

For identification of the target hits, the raw data of all samples were converted to the chemstation file format and imported in *AMDIS*, equipped with the *NIST MS-Search Program 2.0* and the mass spectral databases *NIST 05, Golm Metabolome Database* (GMD) and own in-house (ABF) established databases. *AMDIS* deconvolutes all *m/z* values, which form a peak in the total ion current chromatogram (TIC). Therefore, it is possible to distinguish compounds which could not be baseline-separated by GC. Fig. 9 depicts the discrimination of two components (tyrosine with *m/z* 218 and glucose with *m/z* 319) which could not be separated by means of GC. The mass fragments which are assigned to glucose were

extracted by *AMDIS* (Fig. 9 B) and the extracted corresponding spectrum (Fig. 9 E) is compared to mass spectral libraries, containing also retention indices for some compounds, by means of the MS Search program (Fig. 10).

2. Material and Methods
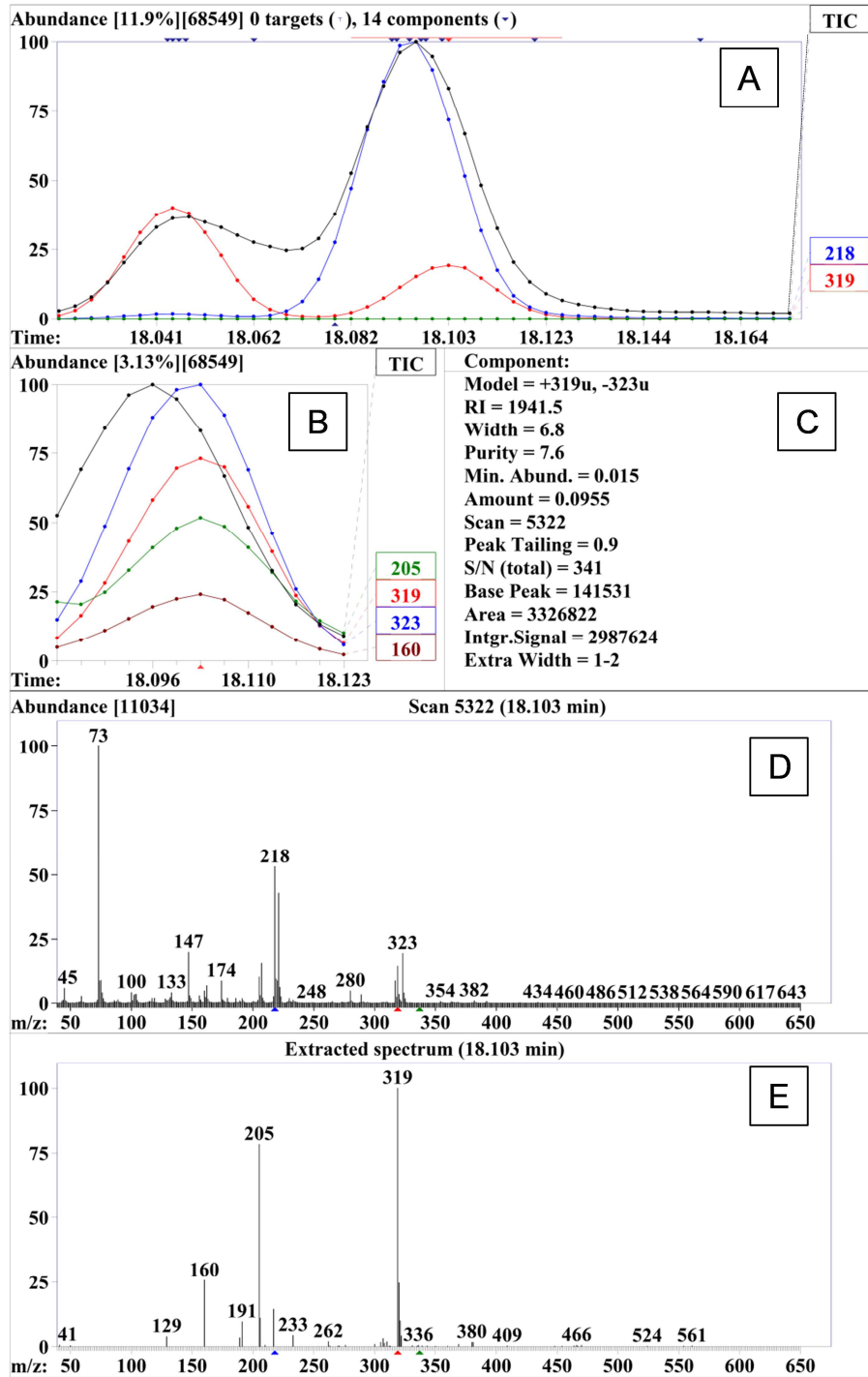
Fig. 9. Graphical user interface (GUI) of the software package *AMDIS*. A: Deconvoluted peaks showing two components which could not be properly separated by means of GC. The two *m/z* values 218 and 319 originate from tyrosine and glucose derivatives, respectively. B: *m/z* values which could be unambiguously assigned to glucose. C: Characteristics of the respective deconvoluted analyte (glucose derivate in this case). D: Total extracted fragments at 18.1 min. E: Extracted fragments which were assigned to glucose. The spectrum depicted in E is used for matching against mass spectral libraries.

2. Material and Methods

The extracted mass spectrum of glucose is shown in Fig. 10 A. The mass spectrum is matched against a spectral library (Fig. 10 B, C) resulting in a 'match factor' and a proposition for the name and structure (Fig. 10 D, E) of the compound. The match factor threshold for identification was set to 75%. Subsequently, the raw data for the identified compounds were verified for correct automated peak picking and integration.
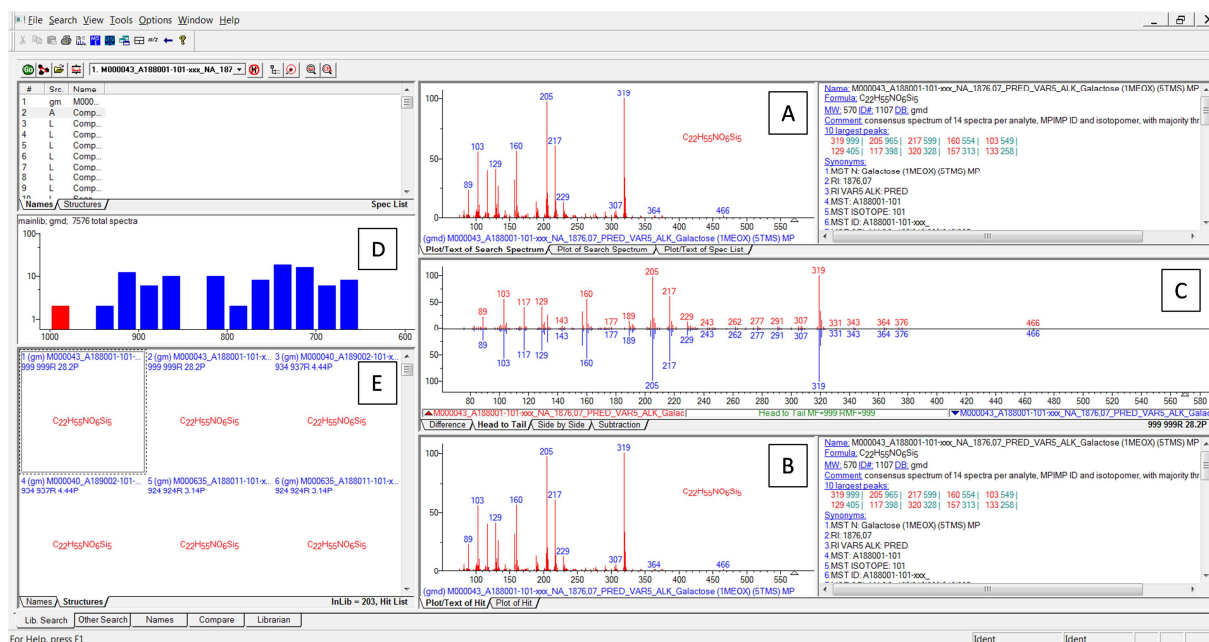
Fig. 10. GUI of the MS Search Program 2.0 used for the identification of metabolites by comparison to mass spectral libraries. Fragment spectra obtained from TOF-MS. A: Extracted spectra from *AMDIS*. B: Spectra of corresponding compound from the mass spectral library. C: Comparison of the both spectra from A and B (head to tail). D: Calculated match factor between the spectra extracted from *AMDIS* and the spectra in the database. E. Name of the compound in the database that is compared to the spectra of the analyte.

For visualization of identified metabolites that were significantly different between smokers and non-smokers, boxplots were used. All boxplots in this work are of the same format. Boxes represent the 25% and 75% percentiles. Whiskers represent the 5% and 95% percentiles. Crosses stand for single data. The middle line of the boxes indicates the median while the little squares show the arithmetic mean of the data.

2.9 Fatty acid profiling in plasma

Targeted fatty acid analysis was performed at the Institute of Nutrition, Dept. of Nutritional Physiology, Friedrich Schiller University, Jena. Further analyses such as statistical evaluations were done by the author.

The total relative fatty acid profiles (conjugated and free fatty acids) in plasma samples were analyzed as described previously [102,103]. Briefly, 20 µL of plasma were used for derivatization in PTFE screw capped Pyrex tubes. Total lipids were derivatized to fatty acid methyl esters using 2 mL of methanolic acetyl chloride (10%) and 400 µL n-hexane overnight at room temperature. After addition of 5 mL 6% potassium carbonate solution, 100 µL of the n-hexane top layer was transferred into a glass vial with micro insert. FAME analysis was conducted by GC on a GC-17 V3 (Shimadzu, Kyoto, Japan) using a fused-silica capillary column (DB-225 MS: 60 m × 0.25 mm ID with 0.25 µm film thickness; Agilent Technologies, USA) coupled to a FID (Shimadzu, Kyoto, Japan). Two microliters of the extract was injected applying a split of 1/20. The relative profile was calculated as area ratio of the respective single fatty acid to the sum of all fatty acids. The Mann-Whitney U test was applied for statistical analysis.

2.10 Phospholipid species determinations

2.10.1 Lipid annotation

Lipid species were annotated as recently described in a shorthand notation by Liebisch and colleagues [104]: ‹Lipid class abbreviation› ‹number of carbon atoms in the radyl side chains:number of double bonds in the radyl side chains›, meaning that PCs containing FA 16:1 and FA 18:1 or FA 16:0 and FA 18:2 or FA 14:0 and FA 20:2 are all annotated as 'PC 34:2' (Fig. 11). This annotation is also used for sphingomyelins (SM).

2.10.2 Phospholipid species quantification by HILIC-MS/MS

PE and PC species can be specifically measured by MRM using positive ESI coupled to triple mass spectrometry, since these lipids lose their headgroups (Fig. 11) during CID. For the PEs, the MRMs resulting from the neutral loss of the headgroup phospho-ethanolamine (141 Da) can be evaluated. The PC species can be quantified by measuring the positively charged phospho-choline headgroup (*m/z* 184) [105].
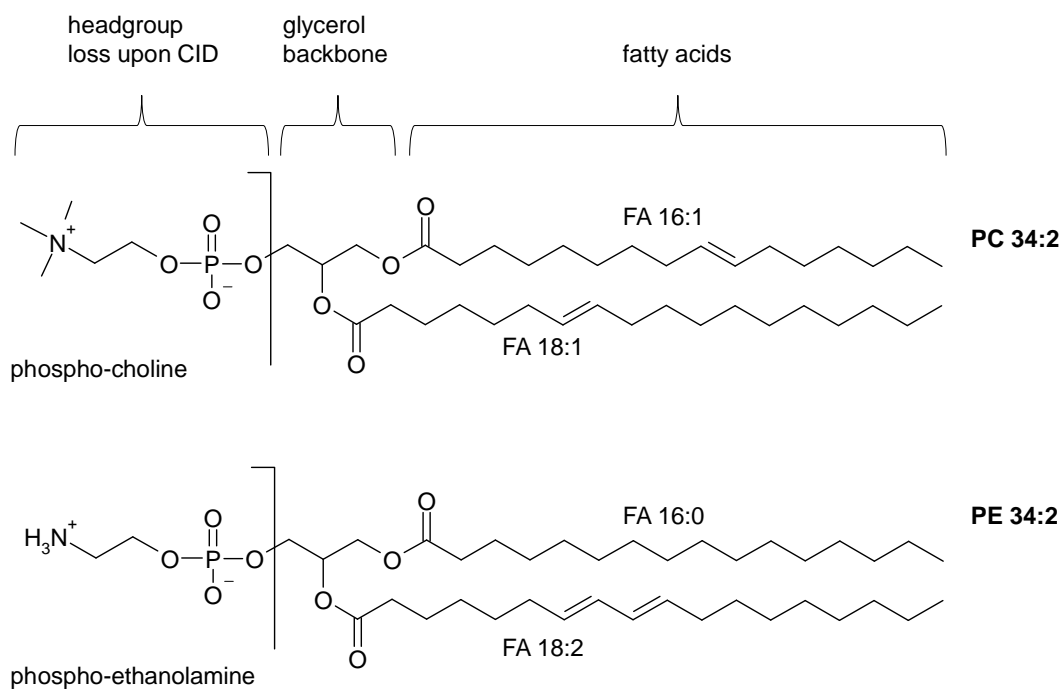
Fig. 11. Structure of the phospholipid classes PC and PE, illustrated by PC 34:2 and PE 34:2. PC and PE are comprised of a polar headgroup (phospho-choline for PC and phospho-ethanolamine for PE) and two fatty acids linked to glycerol.

For sample preparation, 20 μl of EDTA-plasma was spiked with 50 μL internal standard, containing 80 μM PC 28:0 and 4 μM PE 28:0 in methanol. These two lipids do not naturally occur, or occur at levels which are negligible. Lipid extraction was performed according to the method described by Bligh and Dyer [106]. Briefly, the samples were diluted with 750 μL water and 3 mL chloroform/methanol (2:1, v:v). After vortexing, the mixture was incubated for 1 h at room temperature. One milliliter water and 1 mL chloroform were added to allow phase separation. Samples were mixed and centrifuged at 1860 x g for 10 min at 10°C. The recovered chloroform phase was evaporated to dryness in a SpeedVac (Jouan RC10.22, Thermo Scientific, Dreieich, Germany). The dry residue was dissolved in 4 mL methanol containing 0.1% ammonium acetate. Phospholipid separation was performed by liquid chromatography using an Aquity UPLC® BEH HILIC column with 1.7 μM particle size (2.1 x 100 mm, Waters Corporation, Milford, USA), an Agilent 1100 series binary pump (G1312A), a degasser (G1379A) and a column oven (G1316A) (Agilent, Waldbronn, Germany) connected to an HTC-Pal autosampler (CTC Analytics, Zwingen, Switzerland). Samples were kept at 10°C until analysis. The injection volume was 2 μL. The column was maintained at 45°C. Gradient elution was performed with 5% eluent A (water + 13 mM ammonium formate + 1% formic acid, pH = 2.4) and 95% eluent B (ACN + 0.1% formic acid) for 1 min, a linear increase to 50% eluent A until 4 min, hold until 5 min and re-equilibration

from 5.1 min to 8 min with 5% eluent A. The flow rate was set to 550 µL/min. MS/MS analysis was performed in positive ionization (ESI+) mode on a triple quadrupole (API 4000, AB Sciex, Darmstadt, Germany) equipped with an electrospray ionization (ESI) source (Turbo V™ Ion Source, AB Sciex, Darmstadt, Germany). The ESI settings were as follows: Ion spray voltage = 5.0 kV, heater temperature = 600°C, source gas 1 = 30 psi, CAD gas = 4 psi, and curtain gas = 15 psi. Quadrupoles were working at unit resolution. Analytes were monitored in the scheduled MRM mode, applying a retention time window of 29 s. The specific headgroup product ion of *m/z* 184 (PC), and neutral loss of 141 Da (PE), were used for MRM-scanning, respectively. For LC-MS/MS settings refer to Appendix "7.2 HILIC-MS/MS settings for PC and PE species profiling". 39 PC and 40 PE species were selected based on previous findings, focusing particularly on MUFA species [107]. Although PC and PE peaks could not be attributed to a certain pair of fatty acids, the mass information allows the classification to a defined number of carbon atoms and double bounds. Raw data analysis and peak integration, after smoothing all peaks by the Savitzky-Golay filter, were performed with the software *Analyst 1.5.2*. Further data processing, including isotope correction, was performed with *Excel*.

2.10.3   Correction for isobaric overlap of isotopes

By using a triple quadrupole MS, it is not possible to unambiguously distinguish between isobaric species. Fig. 12 shows an example of an isotopic overlap among two isobaric PE species. The base peak of PE 40:5 is overlapping with the M+2 isotope of PE 40:6, which accounts for about 10% of the mono-isotopic peak. Therefore, the detected concentration levels for PE 40:5 would be overestimated by 10%. This has to be considered when calculating the concentrations of each lipid species. For this purpose, all raw data of co-eluting PE and PC species were corrected for an isotopic overlap of co-eluting isobaric species, before concentrations were calculated. Therefore, the isotopic distribution was calculated for all lipids omitting the headgroup fragment ion. For correction only the M+2 isotope was considered, since the M+4 isotope accounts for less than 0.4% of the molecular base peak ion (refer to Appendix "7.3 Isotopic distribution of PC and PE species").
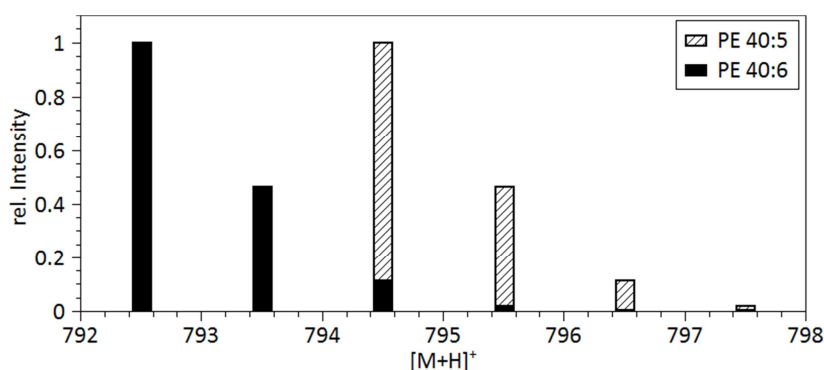
Fig. 12. Iotopic distribution of PE species. Overlap of MRMs due to isotopic distribution of the two PE species PE 40:5 and PE 40:6 differing in in the number of double bounds in the fatty acid side chains.

To confirm the results from the correction algorithm, 7 of the phospholipid standards were spiked to water in a concentration range between 5 and 2000 µM and the respective M+2 isotopes were measured. The concentrations of the isobaric phospholipids, which are not present in the water samples, were determined before and after the isotopic correction. Table 7 summarizes the isotope correction experiment.

Table 7. Phospholipid standards spiked to analyte free matrix (water) to observe the performance of the isotopic correction algorithm. The concentrations of the spiked phospholipids and the M+2 isotopes before and after the isotopic correction were determined.

PL standard	MW (Da)	M+2 isotope (Da) (rel. intensity of monoisotopic peak)	Lipid measured Isobaric to M+2 isotope of spiked lipid standard	MW measured lipid (DA)
PE 34:1	715.5	717.5 (9.3%)	PE 34:0	717.5
PE 36:2	743.6	745.6 (10.3%)	PE 36:1	745.6
PE 36:4	739.5	741.5 (10.3%)	PE 36:3	741.5
PE 40:6	791.5	793.5 (12.3%)	PE 40:5	793.5
PC 34:1	757.6	759.6 (9.3%)	PC 34:0	759.6
PC 36:2	785.6	787.6 (10.3%)	PC 36:1	787.6
PC 38:2	813.6	815.6 (11.3%)	PC 38:1	815.6

M+2 distribution of the spiked PL standard was calculated as relative intensity of base peak without the headgroup, MW: molecular weight.

2.10.4 Data analysis and quantification

Calibration was performed with the standard addition method by adding increasing amounts of the 4 PC standards (PC 34:1, PC 36:2, PC 38:4 and PC 40:0) and 4 PE standards (PE 34:1, PE 36:2, PE 36:4 and PE 40:6) to water. Since no analyte-free matrix was available for PC and PE species, calibration slopes were determined for plasma and water samples to assess, whether water is suitable as surrogate calibration matrix. Calibration curves were calculated by linear regression without weighting. The isotopically corrected areas of the PC and PE species were normalized to the corresponding internal standards (PC species normalized to PC 28:0 and PE species to PE 28:0) and the concentration was calculated by dividing the area ratio of analyte to internal standard by the corresponding slope of the calibration line.

2.11 Analysis of tyramine in saliva

Tyramine was analyzed in saliva of smokers and non-smokers by means of a LC-MS/MS method similar to the method described by Gosetti et al. 2013 for tyramine determination in urine [108]. The saliva samples were thawed at room temperature, vortexed and centrifuged at 3,300 x g to remove mucins. Fifty microliters of the supernatant was spiked with 10 µL the IS d_4-tyramine in methanol (500 nM). Afterward, 140 µL of methanol was added to get a volume of 200 µL and the mixture was vortexed and stored for one hour at -20°C to facilitate protein precipitation. Next, the samples were centrifuged at 15,330 x g, 150 µL of the supernatant was transferred to a glass vial and crimped. LC-MS/MS analysis was performed on the same HPLC-MS/MS system as described for the quantification of phospholipid species (refer to "2.10.2 Phospholipid species quantification by HILIC-MS/MS"). Until the analysis took place, samples were kept in the autosampler at 10°C. The injection volume was set to 2 µL. Separation was performed on an Atlantis® HILIC silica column with 3 µM particle size (2.1x150mm, Waters, Milford, USA) hyphenated to an Atlantis® HILIC guard column with 3 µM particle size (2.1x10mm, Waters, Milford, USA). The columns were maintained at 40°C. Gradient elution was performed with 5% eluent A (water + 20 mM ammonium formate + 0.05% formic acid) and 95% eluent B (ACN + 0.05% formic acid) for 1 min, a linear increase to 50% eluent A until 6 min, hold until 7 min and re-equilibration from 7.1 min to 10 min with 5% eluent A. The flow rate was set to 800 µL/min. MS/MS analysis was conducted in positive ionization mode. The ESI settings were as follows: Ion spray voltage = 5.0 kV, heater temperature = 550°C, source gas 1 = 25 psi, CAD gas = 4 psi, and curtain gas = 20 psi. Quadrupoles were working at unit resolution. Analytes were monitored by MRMs, applying a dwell time of 120 msec. For tyramine, the specific MRM of m/z 138 → m/z 121 was used as quantifier and m/z 138 → m/z 77 was used as qualifier. For

the labeled IS the MRMs of m/z 142 → m/z 125 and m/z of 142 → m/z 106 were used as quantifier and qualifier, respectively (Fig. 13). For detailed LC-MS/MS settings refer to Appendix "7.4 MS/MS settings for tyramine determination in saliva".
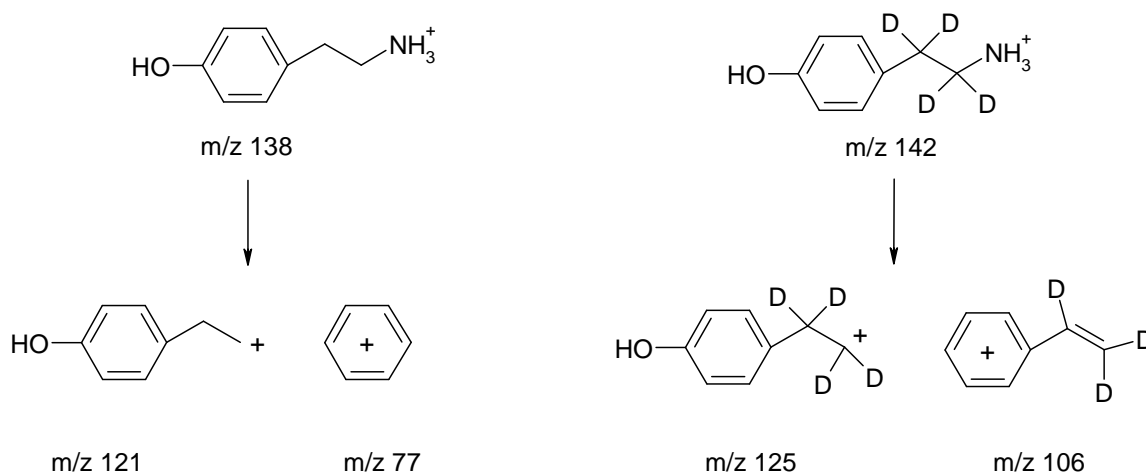
Fig. 13. Fragmentation of tyramine and d_4-tyramine during CID. Loss of ammonia leads to stable fragments of tyramine.

2.11.1 Calibration

Calibration was performed using the standard addition method. For this purpose, 50 µL of saliva was spiked with tyramine in methanol at concentrations of 10 nM, 20 nM, 50, 100 nM, 500 nM, 1 µM, 10 µM, 25 µM and 50 µM, prior to sample preparation and adjusted to a total volume of 200 µL. Calibration was performed in duplicates. Calibration curves were determined by plotting the response (peak area analyte / peak area of IS) of the quantifiers against the spiked concentrations. Linear range was defined for concentrations showing a deviation to the nominal concentrations of less than 15%.

2.11.2 Intraday accuracy and precision

Intraday accuracy and precision were determined for two concentration levels, by spiking saliva samples with 20 nM (N = 5) and 500 nM (N = 5) tyramine. For precision, a calculated CV < 15% and an accuracy of 85% to 115% was defined as acceptable, as recommended by the FDA [97].

3 Results

3.1 Clinical Study

The mean age (± standard deviation (SD)) of the participants was 36.5 ± 9.1 and 36.8 ± 9.7 years for smokers and non-smokers, respectively (Table 8). The BMI of the subjects were between 19.3 kg/cm^2 and 29.1 kg/cm^2 (non-smokers: 24.8 ± 2.8 kg/cm^2, smokers: 25.0 ± 2.7 kg/cm^2). All COex levels for non-smokers were lower than 5 ppm at most of the time points (Fig. 14), except on the time points 3 and 4 where two non-smokers showed COex levels of 6 ppm and 8 ppm, respectively. Increased COex levels can also be due to a prolonged stay in the garden of the clinic and therefore increased uptake from automobile exhausts from the street which was next to the clinic. COex can also be of exogenous origin, predominantly from the degradation of haemoglobin by the enzyme haem oxygenase [109], which might explain increased levels in some non-smokers. Nevertheless, the COex levels were significantly lower in non-smokers at all six time points. The concentrations measured during the screening phase (about 1 week before start of the study) also confirmed the self-reported smoking status (smoker or non-smoker) of the subjects. At the screening phase, COex levels of smokers and non-smokers were between 11 to 61 ppm and 0 to 3 ppm, respectively.

Table 8. Demographic characteristics of the participants and their smoking behavior.

Characteristics and nicotine equivalents	NS	S
	Mean ± SD	
Age (years)	36.5 ± 9.1	36.8 ± 9.7
BMI (kg/cm^2)	24.8 ± 2.8	25.0 ± 2.7
Cigarettes smoked	-	10.8 ± 2.3 (6 – 16)
Smoking years	-	17.4 ± 10 (2 – 35)
Nic+9 in 24-hour urine (µg/mg-creatinine)	-	10.8 ± 4.1
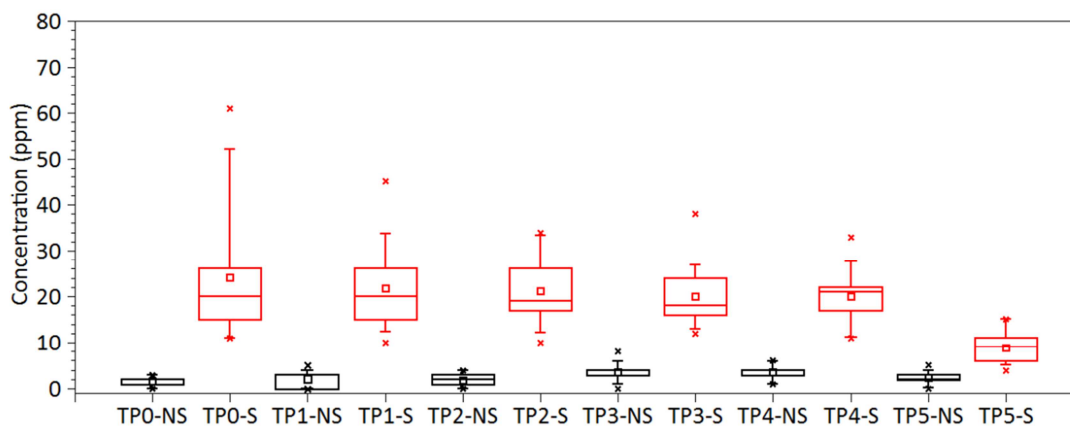
Fig. 14. Boxplot of COex levels measured in 25 smokers (S) and 25 non-smokers (NS). Levels were measured at 6 different time points (TP), including TP0 that was determined at the screening phase.

During the study, on average 11 cig (6 - 16 cig) were smoked, which was reflected by the smokers' COex levels on Day 2 (8.9 ± 3.4 ppm), the nicotine equivalents in urine (Nic+9 10.8 ± 2.3 µg/mg-creatinine), the salivary Cot (1.37 ± 0.50 µM, equating to 240.8 ± 88.3 ng/mL) and the salivary OH-Cot (0.28 ± 0.17 µM, 53.2 ± 32.2 ng/mL) levels on Day 2, which were in the common range of light to moderate cigarette smokers (Fig. 15) [22]. Non-smokers' Cot and OH-Cot levels in saliva were below the lower limit of quantification (LLOQ: Cot = 7 nM, OH-Cot = 10 nM), confirming that the non-smokers had not smoked, were not significantly exposed to environmental tobacco smoke (passive smoking) or used any other tobacco or nicotine containing products during and shortly before the clinical study.
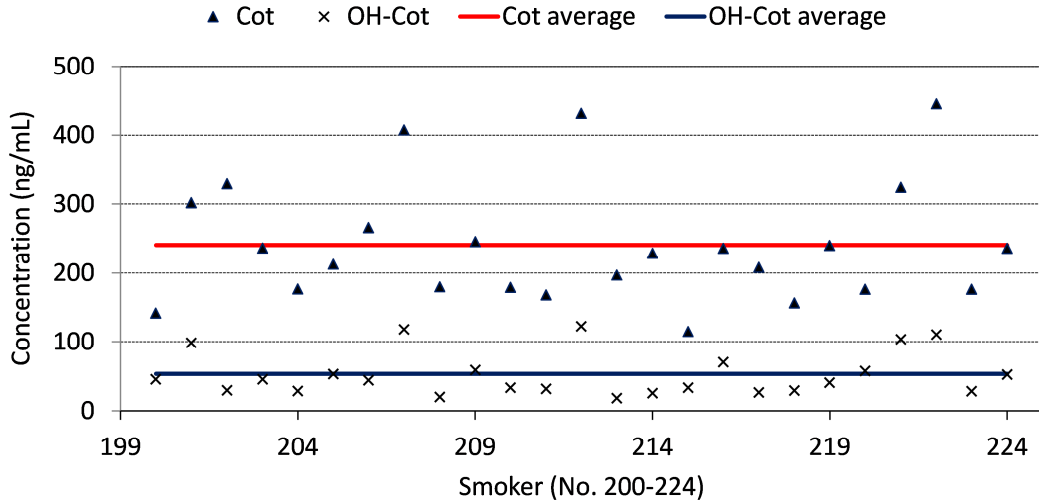
Fig. 15. Cot and OH-Cot measured in saliva samples of smokers and non-smokers. Date of analysis was the morning of the 2nd study day (TP5). Non-smokers were all below the LLOQ.

3.2 Metabolic fingerprinting results

3.2.1 Baseline correction of the metabolic fingerprinting method

The noise threshold was set to 80 counts and different retention time windows for the unspecific noise detection were tested. Optimal retention time setting was found to be 25 s (Fig. 16). Retention time windows larger than 25 s lead to falsely integrated matrix peaks during automated peak picking by *MZmine*. If the retention time window was set smaller than 25 s, the algorithm was unable to remove the noise level entirely from the chromatogram and thus, unspecific spikes remained in the chromatogram.
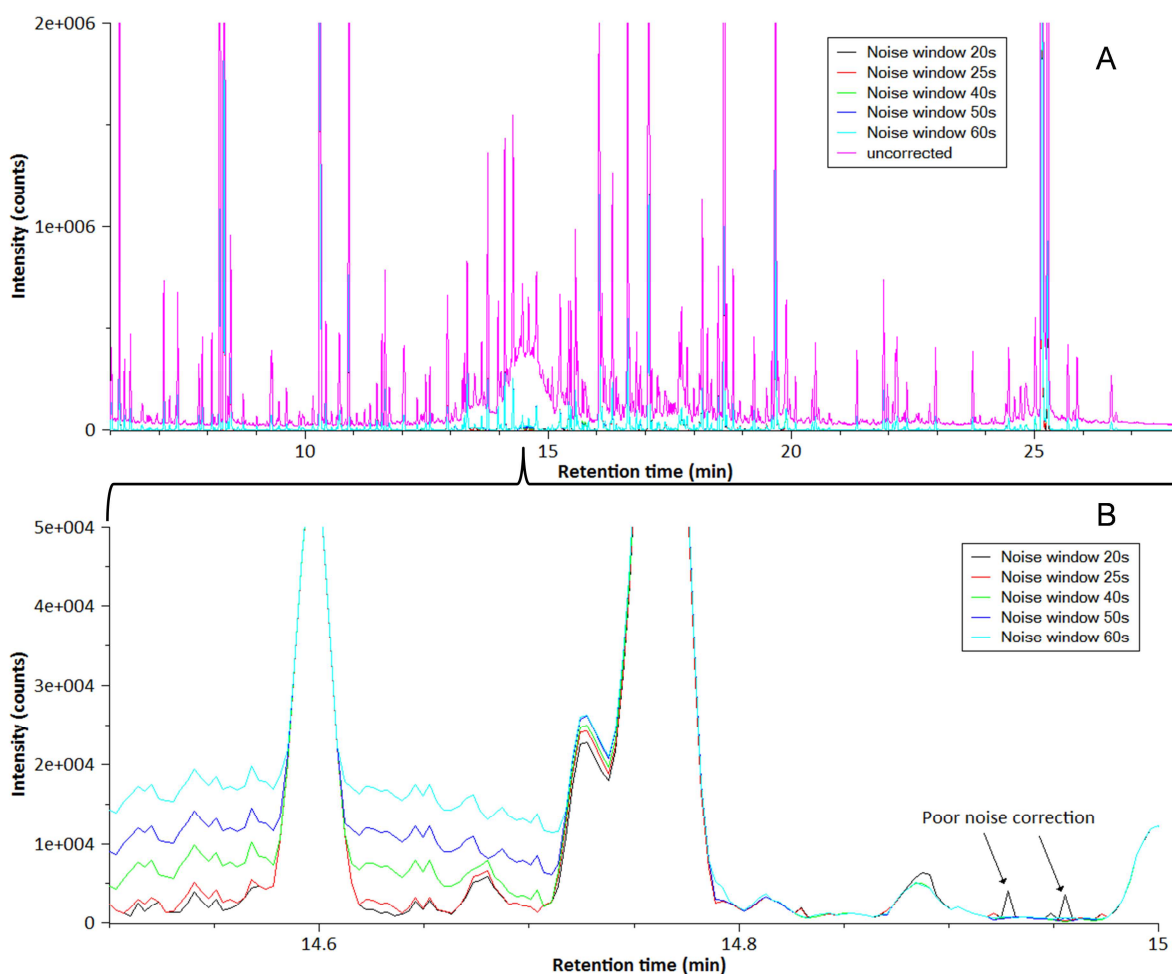
Fig. 16. TIC of a urine pool obtained from smoker and non-smoker samples. A. Removing noise by *ProtoTOF* led to a significant baseline reduction. B. Close up of the TIC showing in detail the influence time settings of the noise detection algorithm on the background signal. Time windows other than 25 s led to a poor noise reduction.

3.2.2   Urine

3.2.2.1   *Validation of the metabolic fingerprinting in urine*

A detailed analytical evaluation of the GC-TOF-MS method was conducted by examining the analytical performance (repeatability, reproducibility, linearity) of the method for different endogenous compounds covering a broad range of chemical classes in urine. For this purpose, 37 standard compounds at 13 levels (0, 0.1, 0.5, 1, 2.5, 5, 10, 25, 50, 100, 250, 500, 2000 μM) were spiked into 100 μL of a urine pool. A blank (water) and an un-spiked urine pool sample were also included (Fig. 17). Prior to digestion and derivatization, the three ISs (d_4-ttMA, $^{13}C_6$-glucose and $C_{16}H_{33}COOH$) were added. The double peak at 25.1 min is lactose that is present in the added urease solution in relatively large amounts.
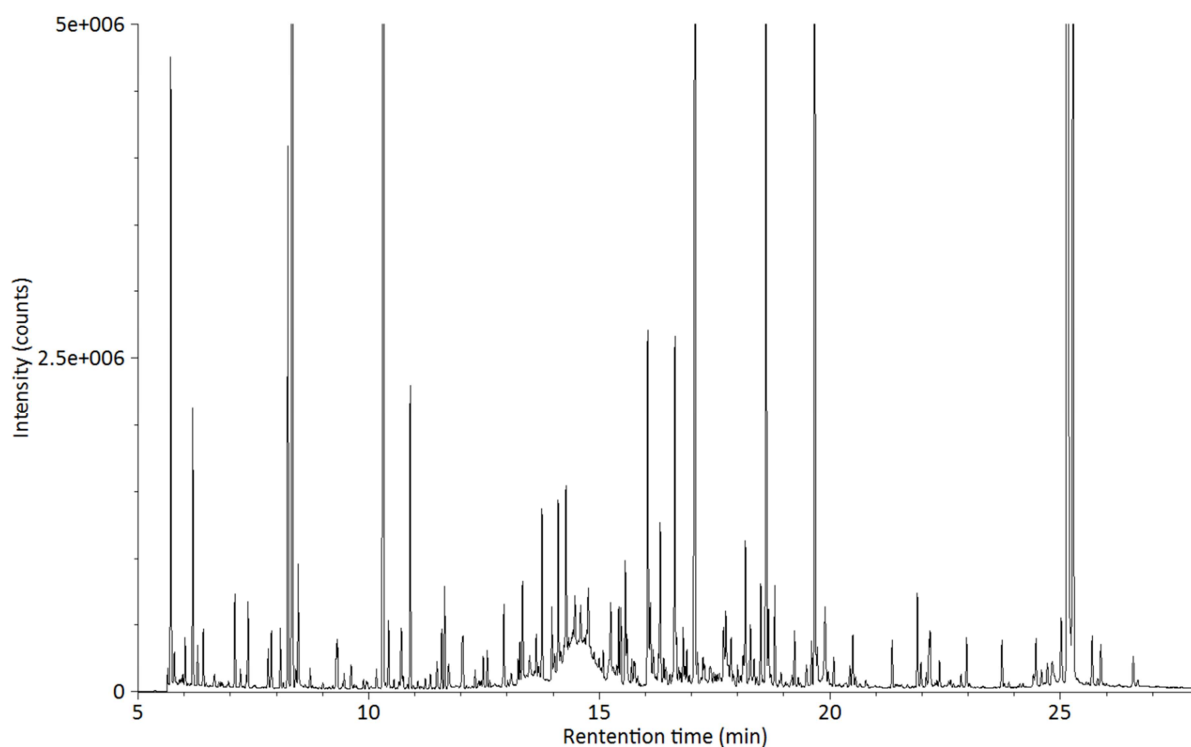
Fig. 17. TIC chromatogram of an unspiked urine pool sample. Measured by GC-TOF-MS in full scan mode (*m/z* 40 - 650). (Note that the double peak at 25.1 min is lactose originating from the urease preparation used for urine sample work-up procedure.)

Single measurements for each level were used for calibration without weighting. Linearity was found in the range between 5 µM to 2000 µM for all compounds. As indicated in Table 9, most of the coefficients of determination values and linear range were comparable to the reported literature [110]. For glycine, tryptophan, oxalic acid, citric acid, lactose and creatinine, no linearity was observed within the spiked concentration range. The reason for this is probably the high endogenous levels of these analytes in urine or in the digestion solution. This problem could be prevented by using synthetic urine as suggested by Tanaka et al. 1986 [111]. However this method is not applicable in general for all metabolites, since this surrogate urine matrix does not mimic real urine samples. For components such as creatinine, analysis should be carried out under highly selective GC conditions with an optimized derivatization or using LC-MS instead of GC-MS [95,112]. Moreover, application of more internal standards might lead to improvements in linearity [113].

To determine accuracies and precision of the method for all analytes, 50 µM and 500 µM of all compounds were spiked to a urine pool (Table 9). The intraday CV was on average 18.3% (29 compounds, N = 5) and 12.5% (26 compounds, N = 4) for 50 µM and 500 µM, respectively, with mean accuracies of 116.8% for 50 µM and 99.8% for 500µM. The

mean interday CVs were slightly higher with 21.1% for 50 µM (29 compounds, N = 5) and 17.0% for 500 µM (26 compounds, N = 5). However, the mean interday accuracies showed excellent results with 109.2% (50µM) and 101.8% (500µM).

For analytes, which showed no linearity, the precision was calculated from their background subtracted area ratio (analyte/internal standard) instead of their calculated concentrations, whenever possible. The CVs of these analytes, namely glycine, oxalic acid, tryptophan and citric acid were between 16.4% and 42.6%. Since it was impossible to find a linear range for these metabolites, these higher CVs were somehow expected as the analytical conditions were not optimal for these analytes. For creatinine and lactose it was impossible to calculate any validation data for the urinary profiling method. The extremely high deviation in intraday accuracy of 215% at 50 µM for glutamine is difficult to explain. In fact, it is well known that the treatment with urease can alter or diminish the levels of several metabolites [70].

Table 9. Analytical parameters and performance for the GC-TOF-MS method applied to urine.

Compound	Corresponding IS	m/z of considered ion	RT (min)	Linear range (µM)	R² N = 4-8	Spiked level (µM)	Intraday N = 5 Accuracy (%)	Intraday N = 5 CV (%)	Interday N = 5 Accuracy (%)	Interday N = 5 CV (%)
Amino acids										
L-Gly	$C_{16}H_{33}COOH$	174	11.06	-	-	500 / 50	- / -	23.4[a] / 37.2[a]	- / -	25.5[a,b] / 33.7[a,b]
L-Pro	d_4-ttMA	142	10.86	25-500	0.995	500 / 50	103.8 / 109.0	9.9 / 22.6	106.3 / 113.9	13.4 / 17.2
L-4-Hyp	d_4-ttMA	230	13.94	50-500	0.998	500 / 50	99.5 / 107.0	2.8 / 21.5	99.8 / 86.0	6.6 / 25.4
L-Leu	d_4-ttMA	158	10.60	10-500	0.997	500 / 50	98.4 / 99.9	14.8 / 43.5	102.9 / 111.9	23.3 / 32.8
L-Val	d_4-ttMA	144	9.80	10-500	0.998	500 / 50	98.3 / 109.5	11.4 / 35.8	101.2 / 113.4	15.3 / 23.5
L-Ala	d_4-ttMA	116	8.08	50-500	0.999	500 / 50	112.5 / 180.2	3.1 / 10.0	111.5 / 145.8	8.3 / 28.2
Gaba	d_4-ttMA	174	13.94	25-250	0.999	500 / 50	- / 10.3	- / 136.4	- / 127.0	- / 14.2
L-Trp	$^{13}C_6$-glucose	202	20.85	-	-	500 / 50	- / -	16.4[a] / -	- / -	28.6[a,b] / -
L-Tyr	d_4-ttMA	218	18.35	50-500	0.996	500 / 50	91.0 / 100.5	6.8 / 43.0	98.6 / 103.5	19.9 / 34.4
L-Glutamine	d_4-ttMA	156	13.54	50-500	0.997	500 / 50	110.4 / 215.0	20.1 / 39.8	96.6 / 149.6	12.1 / 26.4
Vitamin										
Nicotinic acid	d_4-ttMA	180	10.48	10-500	0.999	500 / 50	86.6 / 107.6	10.5 / 7.6	111.2[b] / 126.0[b]	32.4 / 30.0[b]
Carboxylic acids										
2-Oxoglutaric acid	d_4-ttMA	198	14.22	50-500	0.992	500 / 50	112.5 / 169.3	17.6 / 10.6	120.6 / 139.9	31.1 / 27.9
Oxalic acid	d_4-ttMA	190	8.27	-	-	500 / 50	- / -	25.9[a] / -	- / -	42.6[a] / -
Succinic acid	d_4-ttMA	247	10.94	50-500	0.992	500 / 50	122.4 / 116.1	16.7 / 24.3	115.1 / 107.7	21.5 / 26.4
Mandelic acid	d_4-ttMA	179	13.09	5-100	0.999	500 / 50	- / 119.0	- / 24.2	- / 117.0	- / 26.0
Pyruvate	d_4-ttMA	174	7.00	25-500	0.995	500 / 50	108.8 / 122.0	19.5 / 44.3	96.8 / 100.1	8.2 / 20.7
Citric acid	$C_{16}H_{33}COOH$	273	17.26	-	-	500 / 50	- / -	35.9[a] / -	- / -	39.1[a] / -
ttMA	d_4-ttMA	271	14.80	10-500	0.9998	500 / 50	99.1 / 95.8	2.0 / 1.7	100.6 / 3.0	4.7 / 95.6

Compound	IS		RT	Range	R²	Conc.				
p-OH-Ph-Acetic acid	d_4-ttMA	179	14.96	5-500	0.999	500	107.2	9.9	110.6	18.9
						50	116.0	21.9	124.5	27.2
Nucleic acids, purine										
Thymine	$C_{16}H_{33}COOH$	255	12.12	10-500	0.999	500	82.2	10.1	91.6	13.7
						50	174.5	6.2	98.8	20.2
Thymidine	$C_{16}H_{33}COOH$	103	22.21	50-500	0.994	500	80.5	9.8	87.5	19.1
						50	29.0	10.9	103.6	3.7
Adenosine	$C_{16}H_{33}COOH$	230	24.26	25-500	0.999	500	78.9	9.5	89.2	13.7
						50	69.5	4.9	75.7	20.5
Uric acid	$^{13}C_6$-Glucose	456	19.86	100-2000	0.998	500	126.7	16.1	127.4	23.8
						50	-	-	-	-
Carbohydrates										
Glucose	$^{13}C_6$-Glucose	319	18.35	10-500	0.9996	500	97.5	2.2	98.0	5.2
						50	99.5	1.8	101.6	6.8
Glucuronic acid	$^{13}C_6$-Glucose	333	18.68	50-500	0.979	500	132.5	25.5	95.3[b]	20.9[b]
						50	174.2	21.6	130.2	33.5
β-Lactose	$^{13}C_6$-Glucose	204	25.33	-	-	500	-	-	-	-
						50	-	-	-	-
G6P	$C_{17}H_{33}COOH$	299	22.61	25-250	0.987	500	-	-	-	-
						50	73.1	15.9	53.4[b]	57.1[b]
Alcohols										
Glycerol	$^{13}C_6$-Glucose	205	10.73	100-2000	0.997	500	99.9	17.4	101.0	24.9
						50	-	-	-	-
Homovanilic acid	$C_{16}H_{33}COOH$	326	16.40	10-500	0.998	500	82.0	9.7	93.9	16.3
						50	86.2	8.4	99.1	18.4
Sorbitol	$^{13}C_6$-Glucose	319	18.86	10-500	0.999	500	101.2	13.3	107.0	14.2
						50	124.3	27.0	125.1	15.0
Ketones/aldehydes										
Cot	$C_{16}H_{33}COOH$	98	15.18	10-100	0.990	500	-	-	-	-
						50	86.2	7.9	81.8[b]	12.5[b]
Creatinine	$C_{16}H_{33}COOH$	115	14.16	-	-	500	-	-	-	-
						50	-	-	-	-
Indole/amine										
5-HIAA	$C_{16}H_{33}COOH$	290	20.69	10-500	0.997	500	93.8	10.1	74.9	19.1
						50	118.1	8.9	83.3	22.3
Phenol/amine										
Dopamine	d_4-ttMA	174	19.82	10-250	0.9996	500	-	-	-	-
						50	124.6	29.1	124.9	29.3
Dipeptide										
Gly-Gly	d_4-ttMA	174	17.15	25-500	0.992	500	86.7	35.6	122.9	19.5
						50	136.5	3.6	125.7	11.7

Others

4-Me-Hippuric acid	$C_{16}H_{33}COOH$	119	17.36	25-500	0.997	500	87.2	12.4	97.9	21.4
						50	86.9	5.0	82.6	22.4
2-Me-Hippuric acid	$C_{16}H_{33}COOH$	119	18.11	50-500	0.993	500	93.9	9.2	96.5	13.4
						50	100.2	1.3	105.3	6.1

[a]. Calculated from area ratios (analyte/IS) instead of using absolute concentrations, not considered for the calculation of average CVs of the method. [b]: N = 4.

3.2.2.2   Metabolic fingerprinting of QC samples for urine

Since running one batch (25 S and 25 NS samples + Blanks + QCs) lasts more than 2 days, the instrumental and analytical stability had to be assured and controlled. For this purpose, 6 QCs were randomly analyzed within the batch. For this purpose, a urine pool was prepared from aliquots of all 50 subjects of the controlled clinical study. Subsequently, 6 aliquots (100 µL) were spiked with 50 µM of a standard mix containing the same 37 reference compounds as used for the validation experiments as well as with 100 µM each of the ISs d_4-ttMA and d_4-succinic acid. Data processing for the QC samples was performed similarly to the study samples using *MZmine* for automated peak detection and integration. Finally, CVs for each spiked analyte (based on the peak area) without IS correction was calculated using the same fragments as analyzed in the validation experiments, to assess the stability and reproducibility of the entire workflow. For all analytes the CV was below 20%, ranging from 1.6% to 18.9% with an average of 7.3% including the CV of the IS (Table 10). For evaluation of the CVs, similar fragments as for the validation experiments were used.

Table 10. QC samples for the metabolic fingerprinting analysis in urine. Samples (N = 6) were randomly distributed in the batch of the 50 study samples. CVs calculated for 37 compounds at 50 µM and the ISs d_4-ttMA and d_4-succinic acid at 100 µM spiked to a urine pool (spiked compounds are in alphabetic order).

Spiked compound	CV N = 6 (%)	Spiked compound	CV N = 6 (%)
Adenosine	5.1	Mandelic acid	6.1
L-Ala	5.5	2-Me-Hippuric acid	5.9
Citric acid	3.1	4-Me-Hippuric acid	6.2
Cot	6.0	Nicotinic acid	5.4
Creatinine	6.0	Oxalic acid	4.1
Dopamine	7.1	2-Oxoglutaric acid	8.0
G6P	12.2	L-Pro	14.3
Gaba	6.0	Pyruvate	3.2
Glucose	6.0	Sorbitol	8.9
Glucuronic acid	7.2	Succinic acid	8.8
Glutamine	5.3	d_4-Succinic acid	5.9
L-Gly	3.2	Thymidine	11.0
Glycerol	5.7	Thymine	5.9
Gly-Gly	6.5	L-Trp	18.9
5-HIAA	8.8	ttMA	7.2
p-OH-Ph-Acetic acid	5.6	d_4-ttMA	5.3
L-4-Hyp	11.5	L-Tyr	18.3
Homovanillic acid	7.3	Uric acid	7.5
β-Lactose	1.6	L-Val	8.5
L-Leu	5.2		

3.2.2.3 *Metabolic fingerprinting of study-derived urine samples*

The peak list for the 50 urine samples contained 7198 features, with 458 fragments that were significantly ($p < 0.05$) different in smokers as compared to non-smokers (Table 11).

3. Results

Table 11. Number of significant different features by p-value classes (Mann-Whitney U test) in urine of smokers (N = 25) as compared to non-smokers (N = 25). Peak list obtained from the metabolic fingerprinting approach obtained with the described workflow procedure.

Class by statistical significance level	Number of fragments in peak list
All	7198
$0.01 < p \leq 0.05$	27
$0.001 < p \leq 0.01$	121
$p \leq 0.001$	59

Expectedly, the identified tobacco-specific compounds nicotine, Cot, OH-Cot and Cot-gluc showed a highly significant increase in smokers' urine (Table 12). This result demonstrates the validity of the workflow (proof of concept) and confirms the applicability of the metabolic fingerprinting including sampling, sample preparation and data processing for the intended purpose.

Table 12. Nicotine metabolites significantly increased in smokers' (N = 25) urine samples as compared to non-smokers' (N = 25). Determined by means of the metabolic fingerprinting approach.

Compound	RT (min)	Considered ion (m/z)	p-value	Identification method
Nic	10.994	84.06	$9.5 \cdot 10^{-10}$	RF
Cot	14.907	98.03	$5.3 \cdot 10^{-10}$	RF
OH-Cot	17.114	249.06	$1.3 \cdot 10^{-09}$	RF
Cot-gluc	27.196	176.05	$9.1 \cdot 10^{-11}$	RF

RF: Authentic reference compound.

The four metabolites (Table 12) identified by the metabolic fingerprinting approach were also quantified in the 24 hour urine samples by means of a validated LC-MS/MS method (refer to "2.5 Determination of nicotine equivalents (Nic+9) in urine"). The results from this targeted and untargeted analysis were compared to assess performance of the untargeted approach, in particular the automated peak integration. To this end, the peak area ratios (Analyte/IS) of the metabolite fragments from Table 12 were plotted against the absolute concentrations for the smoking subjects (Fig. 18, raw data in Appendix "7.5 Nicotine and its metabolite levels in urine by metabolic fingerprinting and targeted analysis"). Nicotine, Cot and OH-Cot showed excellent correlation amongst both methodologies. The correlation

coefficients (Pearson) were between 0.858 and 0.993 with p-values between $4.1\cdot10^{-8}$ and $1.2\cdot10^{-22}$. The only exception is Cot-gluc, with r = 0.240, which showed no significant linear correlation (p = $2.5\cdot10^{-1}$) between both methods. From the targeted LC-MS/MS method it is known that Cot-gluc is not stable at high temperatures (> 200°C). In the untargeted GC-TOF-MS method, the sylilated Cot-gluc product eluted at temperatures over 200°C. Therefore, one can assume that the analyte was to a certain extent decomposed when reaching the detector and thus, lacking of correlation to the results of the targeted LC-MS/MS method.
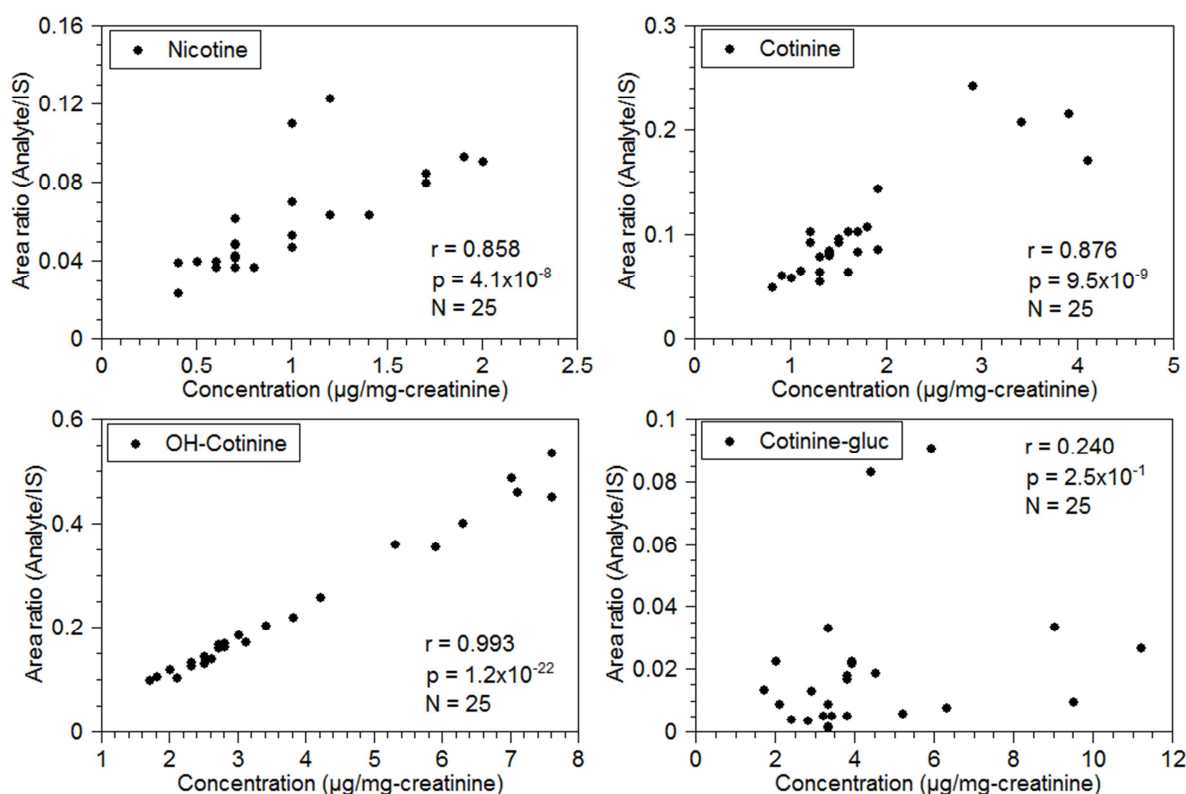
Fig. 18. Nic, Cot, OH-Cot and Cot-gluc detected in urine of 25 smokers, by different analytical approaches. Ordinate: Metabolic fingerprinting approach using GC-TOF-MS. Abscissa: Targeted LC-MS/MS method. r: Pearson's correlation coefficient.

Next, nicotine and its metabolites were removed from the peak list, since the focus was on endogenous metabolites which prove to be significantly different between smokers and non-smokers. The remaining peak list was uploaded to *Metaboanalyst*. With the autoscaled data, a PLS-DA was performed. Two principal components were selected based on 10-fold cross validation. The groups were separated in the PLS-DA score plot with Q^2 of 0.610 and a R^2 of 0.785 (Fig. 19). Permutation test statistics (p < $5\cdot10^{-4}$) validates the predictive ability of the PLS-DA model. 2000 Permutations denoted that none of the new models was better than the original (Fig. 20).
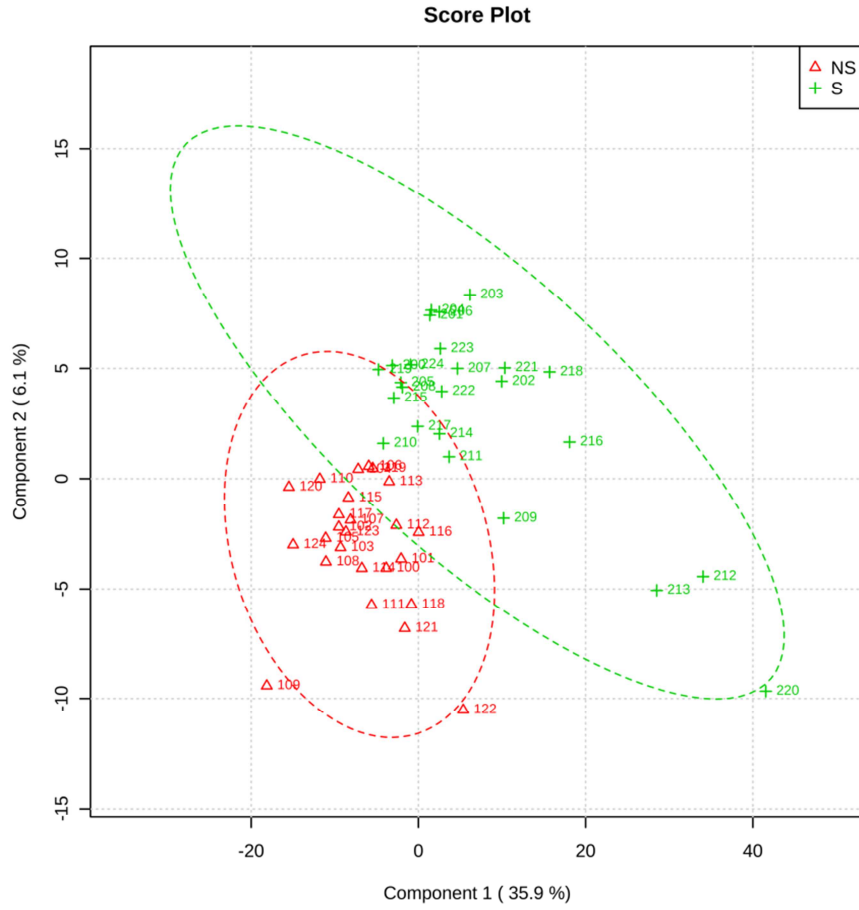
Score Plot

Fig. 19. PLS-DA score plot of the metabolic fingerprint in 25 smokers (S) and 25 non-smokers (NS) urine samples. $Q^2 = 0.610$, $R^2 = 0.785$. Circles depict the 99% confidence interval.
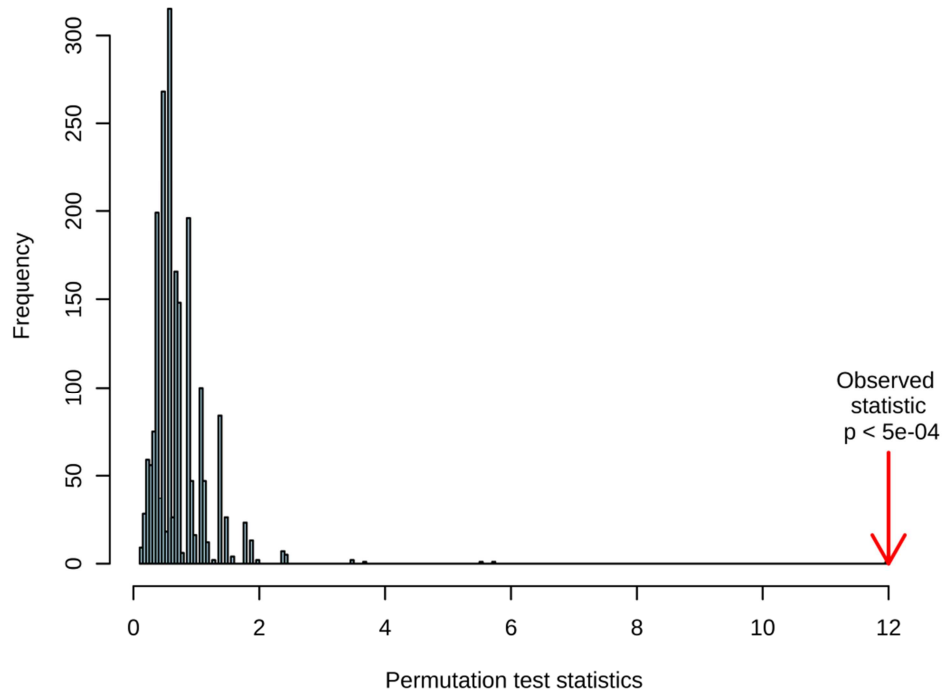
Fig. 20. Histogram for the permutation test of the PLS-DA model applied to the study-derived urine samples. Test statistics was calculated with 2000 permutations based on prediction accuracy by *Metaboanalyst*. The red arrow shows the performance of the model using original labels. The further the arrow is located to the right of the distribution, the better is the separation between the study groups (S and NS). As can be seen, the original model is highly significant (p-value $< 5\ 10^{-4}$) and not part of the obtained distribution of the permutation statistics.

Fragments with a VIP (average of two components) over 0.8 were further used for identification. A total of 334 fragment ions in the peak list exhibit p-values < 0.05 and a VIP-value > 0.8. These fragments could be assigned to about 78 metabolites based on their retention time and concentration increase or decrease compared to non-smokers (Table 13). Of these, 26 were significantly decreased and the other 52 significantly increased in the urine of smokers. A decrease is unlikely to occur from smoking-related exposure markers. Therefore, these metabolites are most likely of endogenous origin. In total, 18 metabolites could be identified by matching the mass spectra against MS libraries, 9 of them were also identified by authentic reference compounds (Fig. 21). Glycerol, 1,2-propanediol, 2-methoxyphenol and 4-oxopentanoic acid, which are known additives in cigarettes [7], were found to be increased in smokers. The increase for these metabolites can most probably be explained by a smoking-related uptake. On the other hand, the metabolites pyruvate, alanine, uracil and 2-oxoglutaric acid were found to be decreased in smokers' urine, and therefore, are most likely of endogenous origin. The significant decrease in smokers could result from a smoking-related perturbation of a metabolic pathway, in which these

metabolites are involved, for example detoxification and energy pathway. 3-OH-pyridine, 2-furoylglycine, quinic acid, 1,4-hydroxyquinone and 4-OH-cyclohexanecarboxylic acid were found to be elevated in urine of smokers as compared to non-smokers. The occurrence of precursors of these metabolites in tobacco smoke suggests that the likely explanation of these findings is a smoking-related uptake [7].

3. Results

Table 13. Significant different metabolites in urine of smokers (N = 25) as compared to non-smokers (N = 25). This list includes fragments found to be different between smokers and non-smokers (p < 0.05, Mann-Whitney U test) and having a VIP-value > 0.8 in PLS-DA model using 2 PCs. The table also shows which fragments were identified and indicates the method of identification.

No	RT (min)	S/NS	Compound	Ident.	No	RT (Min)	S/NS	Compound	Ident.
1	5.811	↓			40	16.171	↑		
2	6.409	↑	1,2-Propanediol	DB	41	16.405	↑		
3	6.767	↓			42	16.673	↓		
4	6.806	↓	Pyruvate	RF	43	17.082	↑		
5	7.899	↓	L-Ala	RF	44	17.132	↑		
6	8.094	↑	3-OH-Pyridine	RF	45	17.394	↑		
7	8.300	↑	4-Oxopentanoic acid	DB	46	17.431	↓		
8	8.862	↓			47	17.609	↑		
9	9.223	↓			48	17.630	↑		
10	9.442	↑	2-methoxyphenol	DB/RF	49	17.719	↑		
11	9.630	↓			50	17.743	↑	Quinic acid	RF
12	10.062	↑			51	17.899	↑		
13	10.556	↑	glycerol	RF	52	17.913	↓		
14	10.684	↑			53	18.086	↑		
15	10.748	↓			54	18.287	↓		
16	11.073	↓	uracil	DB	55	18.506	↑	Glucuronic acid	RF
17	11.906	↑			56	18.539	↑		
18	12.021	↑	1,4-Hydroxyquinone	RF	57	18.645	↑		
19	12.578	↑	3,4-Dihydroxybutanoic acid	DB	58	18.668	↑		
20	12.635	↑			59	18.950	↑	Gluconic acid	DB
21	12.903	↑	Mandelic acid	RF	60	19.026	↓		
22	13.022	↓			61	19.174	↓		
23	13.423	↑	4-OH-Cyclohexanecarboxylic acid	DB	62	19.248	↑		
24	13.497	↑			63	19.364	↓		
25	13.694	↑			64	19.682	↓		
26	13.785	↑			65	20.092	↑		
27	13.895	↑			66	20.335	↓		
28	14.003	↑			67	20.670	↓		
29	14.038	↓	2-Oxoglutaric acid	RF	68	21.430	↑		
30	14.235	↓			69	21.904	↑		
31	14.683	↑	2-Furoylglycine	RF	70	22.099	↑		
32	14.701	↓			71	22.166	↓		
33	14.741	↓			72	22.688	↑		
34	14.998	↑			73	22.853	↑		
35	15.008	↓			74	23.889	↑		
36	15.093	↑			75	24.196	↑		
37	15.312	↑	2,4,5-Trihydroxypentanoic acid	DB	76	24.423	↑		
38	15.473	↑			77	25.258	↓		
39	16.115	↑			78	25.884	↑		

Ident.: Identified. DB: Mass spectral database, RF: Reference compound. ↑: Increased in smokers.

↓: Decreased in smokers.
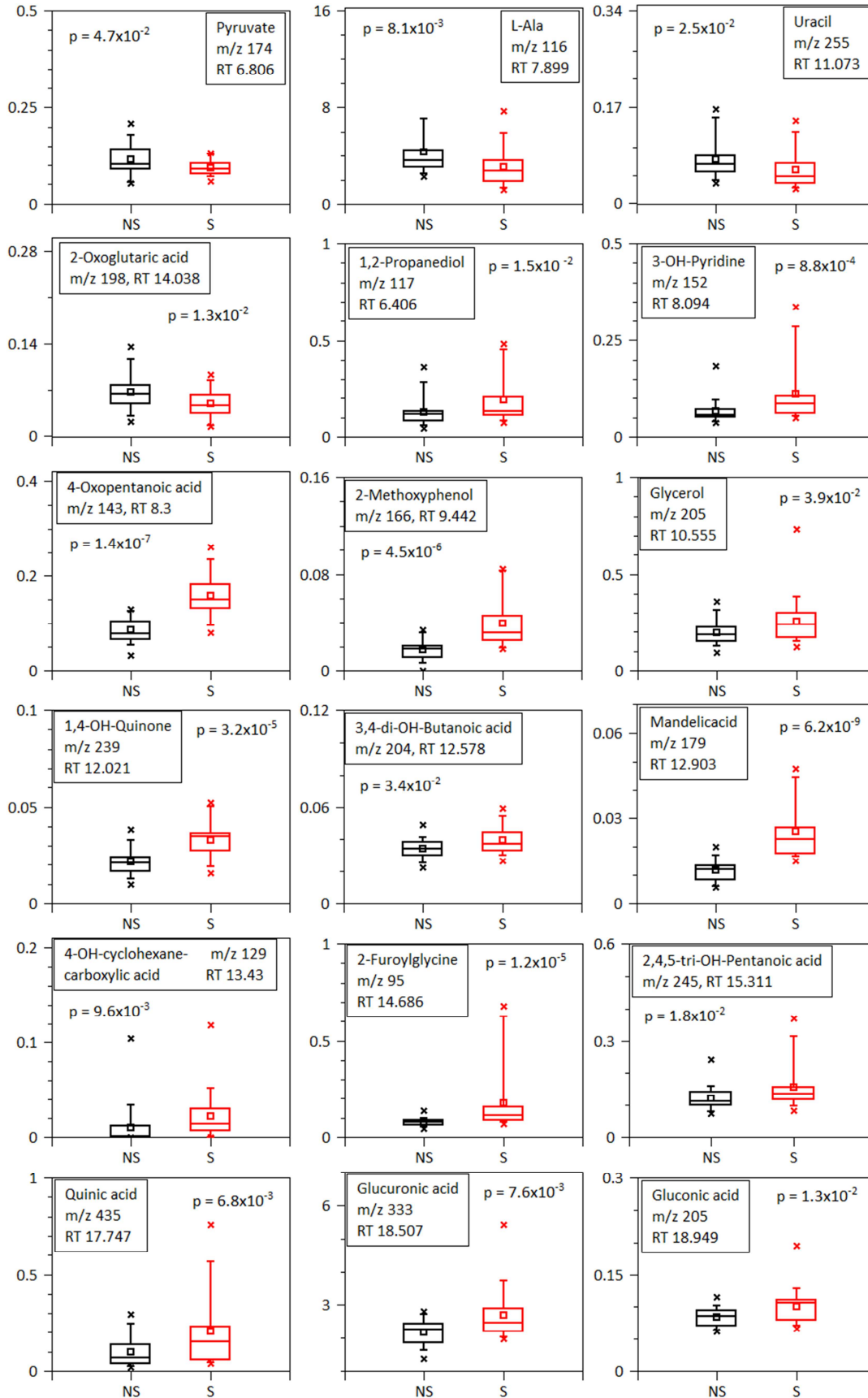
Fig. 21. Boxplots for the relative intensities of selected fragments derived from the 18 identified urinary metabolites found to be significantly different between 25 smokers (S, red) and 25 non-smokers (NS, black).

4-Oxopentanoic acid, a known cigarette additive that presumably reinforces the nicotine uptake, was present in all 50 subjects and showed a nearly 2-fold (1.9-fold for medians) increase in smokers. A moderate linear correlation ($r = 0.670$, $p = 2.5 \cdot 10^{-4}$, Pearson) between the peak area ratios (analyte/IS) and the Nic+9 concentration levels in urine were observed (Fig. 22, raw data in Appendix "7.1 Nic+9 determination in 24-hour urine").
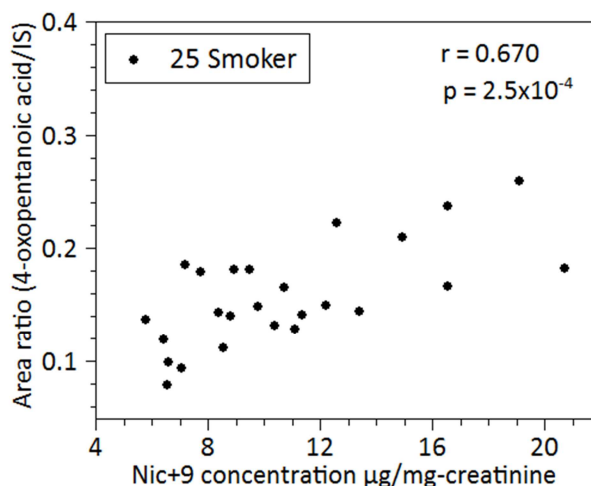
Fig. 22. Correlation between 4-oxopentanoic acid and Nic+9 in urine of smokers. Most abundant fragment of 4-oxopentanoic acid (m/z 143, RT = 8.3 min) detected by GC-TOF-MS plotted against the Nic+9 creatinine-standardized levels determined by LC-MS/MS. The observed moderate linear correlation between both variables indicates a dose-response relationship of this metabolite to smoking. Correlation coefficient (r) and and p-value according to Pearson.

3.2.3 Saliva

3.2.3.1 Validation of the metabolic fingerprinting in saliva

The GC-TOF-MS method produced very narrow peak shapes between 0.1 and 0.3 min also for saliva for almost all metabolites (Fig. 23). The chromatograms for saliva showed a lower baseline and significantly fewer peaks as compared to urine. Especially between 13 to 20 min, saliva chromatograms were much "cleaner" as compared to urine (see Fig. 17).
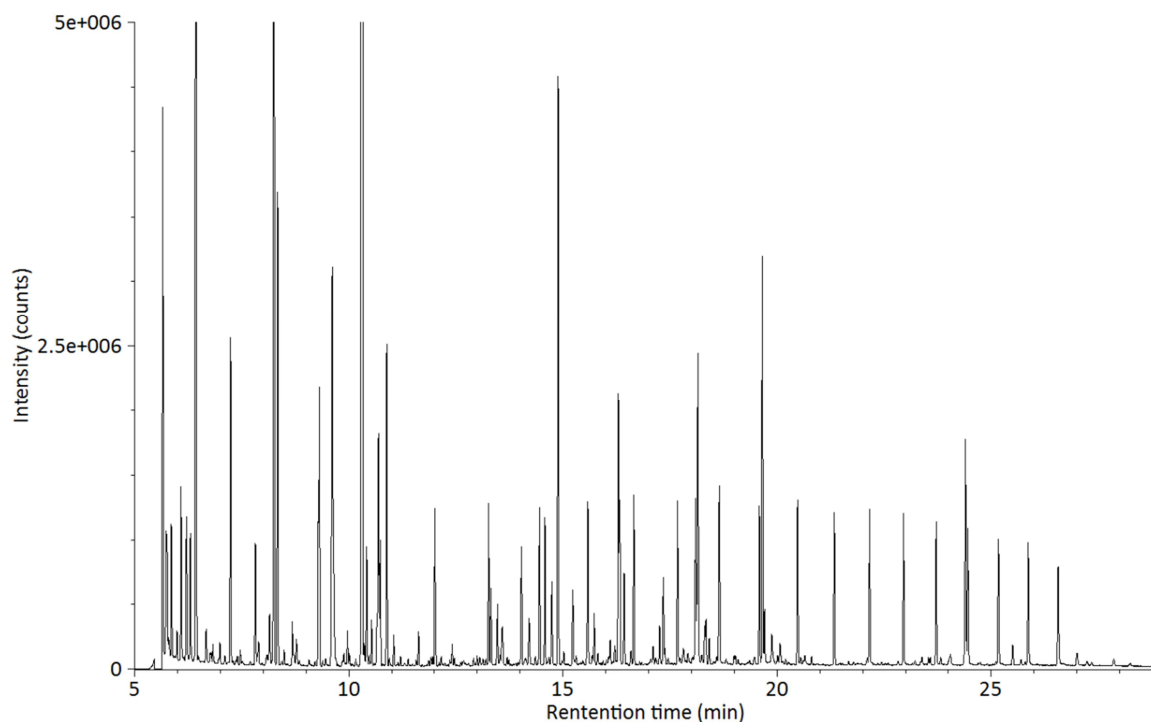
Fig. 23. TIC chromatogram of the saliva pool sample used for the validation experiments. Measured by GC-TOF-MS in full scan mode (m/z 40 - 650) after sample work-up.

As shown in Fig. 24 almost all reference compounds and internal standards, spiked to a saliva pool, were sufficiently separated and detectable by the developed GC-TOF-MS method. The co-eluting compounds gaba acid and L-Hyp as well as glucose and tyrosine could be unambiguously identified by analysing different fragment ions. The linear response of the detector signal ranged from 2.5 µM - 2 mM across all analytes (Table 14). Mean intraday precisions were 11.9%, 8.2% and 10.0% for spiked concentrations of 25 µM, 50 µM and 200 µM, respectively. The average accuracies were found to be 85.8% (25 µM), 88.9% (50 µM) and 106.7% (200 µM). The corresponding Interday accuracies (CV) were 97.0% (12.4%), 95.5% (18.8%), 105% (17.2%) over the entire calibration range. Although a quite simple and straightforward sample preparation (only derivatization) was performed with no further sample purification and only 6 IS were used for the quantification of 37 compounds, satisfactory validation results in terms of precision, accuracy and linearity were achieved with some exceptions. The high CVs and narrow linear ranges could be explained by the relatively high endogenous metabolite levels in saliva, limiting particularly the lower end of the calibration range. Additionally, accuracies at the lower end of the calibration range were of course affected by comparably high endogenous levels. For instance, the high background level of uric acid in saliva prevented the determination of the precision and accuracy for this metabolite. The accuracies and precisions were in general slightly better

60

compared to the corresponding data for urine. The main reasons for this are assumed to be the much simpler sample preparation procedure and the utilization of six internal standards instead of only three for urine.

The stabilities of the analytes, except for 2-Me-hippuric acid (50 µM), L-Leu (50 µM) and Gly-Gly (50 µM) showed excellent accuracies with deviations of < 30% (Table 14), taking into account that an untargeted approach is applied. There is no obvious reason for the remarkable deviation at the various concentrations investigated of these three mentioned analytes. Since the standard compounds covered a broad range of chemical classes, it can be assumed that most of the silylated products in the samples were stable over the time, which was required to measure the 50 study samples from smokers and non-smokers.
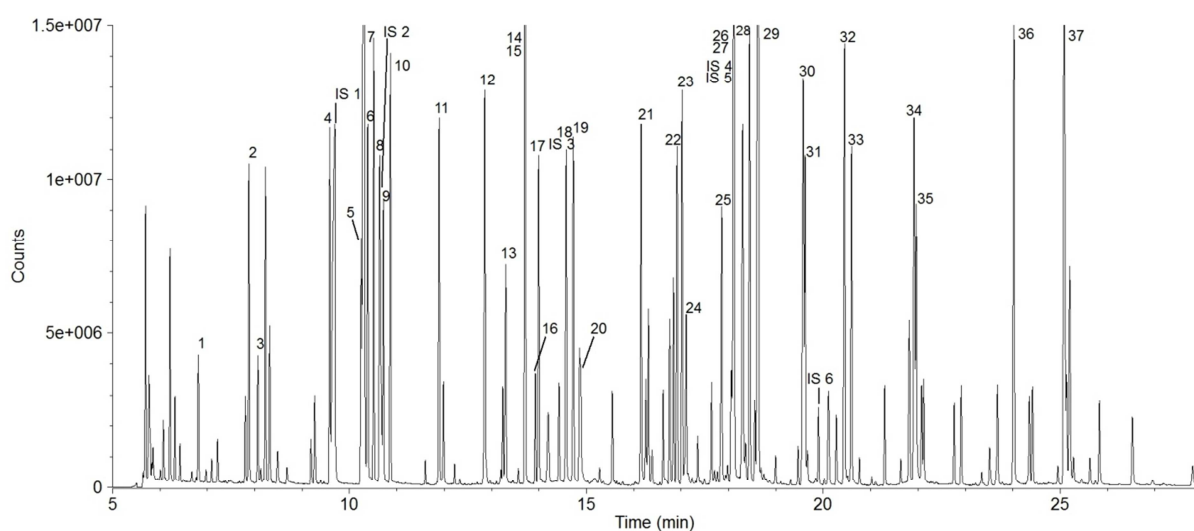
Fig. 24. TIC of saliva spiked with 750 µM of standard compounds. 1. Pyruvate, 2. L-Ala, 3. Oxalic acid, 4. L-Val, 5. Nicotinic acid, 6. L-Leu, 7. Glycerol, 8. L-Pro, 9. Succinic acid, 10. L-Gly, 11. Thymine, 12. Mandelic acid, 13. L-Glutamine, 14. Gaba, 15. L-4-Hyp, 16. Creatinine, 17. 2-Oxoglutaric acid, 18. ttMA, 19. p-OH-Ph-Aacetic acid, 20. Cot, 21. Homovanillic acid, 22. Gly-Gly, 23. Citric acid, 24. 2-Me-hippuric acid, 25. 4-Me-hippuric acid, 26. L-Tyr, 27. D-Glucose, 28. Glucuronic acid, 29. Sorbitol, 30. Dopamine, 31. Uric acid, 32. 5-HIAA, 33. L-Trp, 34. G6P, 35. Thymidine, 36. Adenosine, 37. β-Lactose, IS 1. $^{13}C,^{15}N_2$-Urea, IS 2. d_4-Succinic acid, IS 3. d_4-ttMA, IS 4. $^{13}C_9,^{15}N$-Tyr, IS 5. $^{13}C_6$-Glucose, IS 6. $C_{16}H_{33}COOH$.

Table 14. Analytical and performance parameters for the GC-TOF-MS method in saliva.

Compound	Corresponding IS	m/z considered ion	Retention time (min)	R²	Linear range N = 4-8* (µM)	Spiked level (µM)	Re-injection CV (%)	Intraday N = 5 Accuracy (%)	Intraday N = 5 CV (%)	Interday N = 5 Accuracy (%)	Interday N = 5 CV (%)	Stability D5/D1** (%)
Amino acids												
L-Gly	¹³C, ¹⁵N₂-Urea	174	11.86	0.9891	50-500	200	1.4	84.1	15.5	99.0	13.9	96
						50	2.4	81.6	20.3	105.3	34.0	101
						25	-	-	-	-	-	-
L-Pro	¹³C₉, ¹⁵N-L-Tyr	142	10.63	0.9948	75-750	200	1.2	104.1	8.1	123.6	23.2	124
						50	-	-	-	-	-	-
						25	-	-	-	-	-	-
L-4-Hyp	¹³C₉, ¹⁵N-L-Tyr	230	13.7	0.9992	7.5-100	200	-	-	-	-	-	-
						50	5.6	90.4	1.2	91.6	9.6	86
						25	9.0	78.3	11.2	91.5	5.2	92
L-Leu	¹³C₉, ¹⁵N-L-Tyr	158	10.38	0.9997	25-750	200	2.1	94.9	5.0	101.4	9.3	98
						50	10.4	89.1	1.8	96.3	19.5	60
						25	12.9	50.1	35.2	83.9	16.5	74
L-Val	¹³C, ¹⁵N₂-Urea	144	9.58	0.9996	5-200	200	1.4	91.5	6.3	98.9	7.6	102
						50	10.0	95.0	7.2	92.7	19.0	74
						25	9.5	69.1	20.3	86.8	16.1	83
L-Ala	¹³C, ¹⁵N₂-Urea	116	7.87	0.9944	5-200	200	2.2	92.0	8.8	102.3	9.7	103
						50	8.1	96.1	9.9	96.3	18.5	77
						25	7.4	63.3	31.9	99.1	16.4	94
Gaba	d₄-ttMA	174	13.7	0.9985	2.5-100	200	-	-	-	-	-	-
						50	0.2	93.2	2.2	98.7	9.4	102
						25	0.7	88.0	7.2	94.9	4.6	100
L-Trp	¹³C₉, ¹⁵N-L-Tyr	202	20.59	0.9956	5-100	200	-	-	-	-	-	-
						50	13.1	80.8	2.1	81.4	40.8	95
						25	10.9	73.8	11.5	74.1	31.7	82
L-Tyr	¹³C₉, ¹⁵N-L-Tyr	218	18.1	0.9985	50-1000	200	0.34	97.3	3.9	103.1	13.4	99
						50	0.6	66.6	4.7	74.8	18.4	100
						25	-	-	-	-	-	-
Glutamine	d₄-ttMA	156	13.29	0.9966	50-1000	200	1.9	84.4	11.2	102.8	24.2	108
						50	1.5	31.4	31.1	80.9	64.1	102
						25	-	-	-	-	-	-
Vitamin												
Nicotinic acid	d₄-Succinic acid	180	10.25	0.9989	10-750	200	1.3	93.9	8.8	97.3	10.1	100
						50	1.2	88.1	1.6	94.9	15.2	100
						25	1.5	88.6	6.9	92.6	4.9	97

Carboxylic acids

Compound	IS			R^2	Range	Level						
2-Oxoglutaric acid	d_4-ttMA	198	13.98	0.9995	25-1000	200	0.4	96.9	3.9	101.3	12.1	101
						50	1.2	100.1	2.8	103.0	4.0	101
						25	0.8	117.1	5.0	121.7	4.1	101
Oxalic acid	^{13}C,$^{15}N_2$-Urea	190	8.06	0.9989	2.5-200	200	1.7	100.8	14.3	112.2	21.6	105
						50	5.4	101.1	7.2	102.7	5.1	99
						25	3.5	90.6	14.0	102.1	7.1	99
Succinic acid	d_4-Succinic acid	247	10.71	0.9986	5-100	200	-	-	-	-	-	-
						50	0.4	87.0	2.7	103.9	16.1	101
						25	0.8	99.1	9.9	117.4	29.8	99
Mandelic acid	d_4-ttMA	179	12.85	0.9984	5-100	200	-	-	-	-	-	-
						50	0.7	88.0	3.4	94.6	14.5	102
						25	0.8	85.1	7.1	91.2	5.0	99
Pyruvate	d_4-Succinic acid	174	6.8	0.9945	5-100	200	-	-	-	-	-	-
						50	1.9	100.7	4.8	109.6	16.1	107
						25	3.1	105.1	11.1	118.5	27.8	105
Citric acid	d_4-Succinic acid	273	17.01	0.9985	5-100	200	-	-	-	-	-	-
						50	1.9	83.9	4.2	93.3	15.3	103
						25	1.5	88.7	8.8	100.7	15.3	104
ttMA	d_4-ttMA	271	14.56	0.9995	25-750	200	0.8	97.6	3.3	102.6	11.3	100
						50	0.6	90.8	3.1	93.0	7.8	100
						25	0.6	77.6	8.6	82.0	4.5	101
OH-Ph-Acetic acid	d_4-ttMA	179	14.71	0.9982	10-100	200	-	-	-	-	-	-
						50	0.2	84.9	1.5	93.6	14.9	102
						25	1.2	85.9	6.3	92.8	4.5	100

Nucleic acids, purine

Compound	IS			R^2	Range	Level						
Thymine	^{13}C,$^{15}N_2$-Urea	255	11.89	0.9988	7.5-75	200	-	-	-	-	-	-
						50	2.6	91.9	7.1	95.7	7.2	102
						25	2.1	89.1	7.5	96.1	3.5	102
Thymidine	$^{13}C_9$,^{15}N-L-Tyr	103	21.94	0.9983	50-750	200	2.2	95.7	6.6	103.8	22.0	105
						50	2.8	103.7	4.3	108.6	14.5	85
						25	-	-	-	-	-	-
Adenosine	$^{13}C_9$,^{15}N-L-Tyr	230	24.01	0.9996	10-1000	200	0.7	97.0	4.3	102.2	11.7	102
						50	2.1	91.7	1.7	100.2	8.8	85
						25	5.4	94.0	7.6	104.7	13.9	89
Uric acid	^{13}C,$^{15}N_2$-Urea	456	19.62	0.9950	500-2000	200	-	-	-	-	-	-
						50	-	-	-	-	-	-
						25	-	-	-	-	-	-

Carbohydrates

Analyte	IS		RT	R²	Range	Level						
Glucose	$^{13}C_6$-Glucose	319	18.11	0.9997	25-1000	200	0.20	94.7	3.8	102.2	14.6	92
						50	1.2	101.3	3.8	110.1	11.5	104
						25	3.6	93.4	4.8	124.5	29.8	98
Glucuronic acid	$^{13}C_6$-Glucose	333	18.44	0.9974	7.5-200	200	1.4	99.1	5.8	109.5	16.2	100
						50	0.5	94.5	5.4	94.8	4.8	103
						25	0.8	79.9	8.1	93.9	6.8	101
β-Lactose	$^{13}C_6$-glucose	204	25.08	0.9977	7.5-100	200	-	-	-	-	-	-
						50	0.7	110.1	6.5	109.0	21.1	103
						25	1.4	75.3	5.3	108.6	27.1	102
G6P	$C_{16}H_{33}COOH$	299	21.91	0.9993	50-750	200	1.4	80.3	14.3	100.4	6.8	100
						50	1.1	57.7	2.9	99.0	9.7	100
						25	3.8	86.0	8.9	165.5	9.2	100

Alcohols

Analyte	IS		RT	R²	Range	Level						
Glycerol	d_4-Succinic acid	205	10.5	0.9990	75-750	200	1.0	110.8	17.0	106.1	9.5	98
						50	-	-	-	-	-	
						25	-	-	-	-	-	
Homovanillic acid	d_4-ttMA	326	16.14	0.9976	50-1000	200	0.9	98.7	14.2	102.0	13.8	103
						50	0.8	63.2	5.4	72.9	23.8	102
						25	-	-	-	-	-	
Sorbitol	$^{13}C_6$-Glucose	319	18.61	0.9999	25-2000	200	0.7	98.6	7.2	101.8	7.5	99
						50	0.8	88.7	2.8	89.9	11.1	103
						25	0.9	107.5	8.7	100.3	12.1	101

Ketones/aldehydes

Analyte	IS		RT	R²	Range	Level						
Cot	$C_{16}H_{33}COOH$	98	14.9	0.9983	25-500	200	0.8	90.5	10.4	104.8	9.4	98
						50	1.0	88.0	12.6	84.3	8.7	98
						25	1.6	89.7	16.8	103.3	11.0	100
Creatinine	d_4-ttMA	115	13.92	0.9964	25-1000	200	1.0	71.6	28.1	89.9	24.0	98
						50	0.7	59.1	10.3	91.1	36.7	98
						25	0.9	52.8	15.3	87.7	20.5	90

Indole/amine

Analyte	IS		RT	R²	Range	Level						
5-HIAA	$^{13}C_9$ ^{15}N-L-Tyr	290	20.43	0.9993	5-200	200	0.9	100.2	5.0	108.0	15.0	106
						50	1.3	93.2	1.5	104.0	10.7	93
						25	6.0	89.0	9.7	103.8	22.2	108

Phenol/amine

Analyte	IS		RT	R²	Range	Level						
Dopamine	$^{13}C_9$ ^{15}N-L-Tyr	174	19.57	0.9988	5-100	200	-	-	-	-	-	-
						50	1.6	92.7	1.9	101.4	7.4	90
						25	5.5	95.1	8.6	105.1	18.8	102

Dipeptide

						Conc.						
Gly-Gly	$^{13}C_9,^{15}N$-L-Tyr	174	16.91	0.9992	2.5-50	200	-	-	-	-	-	227
						50	6.7	121.7	12.3	104.2	27.4	140
						25	9.1	97.3	26.7	99.0	14.5	
Others												
4-Me-Hippuric acid	$^{13}C_9,^{15}N$-L-Tyr	119	17.84	0.9997	10-200	200	1.3	99.1	4.4	107.9	14.4	101
						50	2.0	89.1	2.3	99.1	8.8	88
						25	6.6	92.9	7.3	103.2	16.3	98
2-Me-Hippuric acid	$^{13}C_9,^{15}N$-L-Tyr	119	17.10	0.9985	100-2000	200	4.0	100.9	10.5	101.7	24.5	99
						50	5.2	139.8	2.2	156.7	8.4	54
						25	-	-	-	-	-	

*: measured as duplicates, **: a: D5 (Day 5), D1 (Day 1).

3.2.3.2 Metabolic fingerprinting of saliva QC samples

The reproducibility of the method had to be assured and controlled during the metabolomic investigations of the study samples. For this purpose, 6 QC samples were randomly analyzed within the batch similar to the procedure described in Section "3.2.2.2 Metabolic fingerprinting of QC samples for urine". QC samples were prepared by pooling aliquots of the saliva collected at TP5 by the 50 subjects and spiking the pool with 50 µM from each of the 39 standards of the validation experiments, including the 37 reference compounds and the internal standards d_4-ttMA and d_4-succinic acid (Table 15). CVs, calculated from peak areas (without IS correction), were below 30% (range: 3.8 - 25.9%, average: 11.4%). Considering the fact that no IS correction has been applied in addition to automated peak picking and integration, this is a promising result, demonstrating good reproducibility also for saliva of the applied metabolomic GC-TOF-MS methodology. For evaluation of the CVs, similar fragments as for the validation experiments were used.

Table 15. Precisions for the saliva QC samples analyzed with the metabolic fingerprinting approach. Samples were randomly analyzed within the study samples. CVs calculated for 37 reference compounds spiked with 50 µM and the ISs d_4-ttMA and d_4-succinic acid spiked with 100 µM to the saliva pool (spiked compounds are in alphabetic order).

Spiked compound	CV N = 6 (%)	Spiked compound	CV N = 6 (%)
Adenosine	6.1	Mandelic acid	7.5
L-Ala	16.2	2-Me-Hippuric acid	6.2
Citric acid	9.3	4-Me-Hippuric acid	6.1
Cot	5.7	Nicotinic acid	6.7
Creatinine	19.3*	Oxalic acid	7.5
Dopamine	9.2**	2-Oxoglutaric acid	11.9
G6P	11.0	L-Pro	25.9*
Gaba	4.6**	Pyruvate	13.6
Glucose	7.6	Sorbitol	9.8
Glucuronic acid	9.4	Succinic acid	9.5
Glutamine	10.7	d_4-Succinic acid	11.0
L-Gly	3.8	Thymidine	15.0
Glycerol	19.7	Thymine	7.8
Gly-Gly	13.8	L-Trp	22.4
5-HIAA	25.1	ttMA	8.4
OH-Ph-Acetic acid	9.5	d_4-ttMA	9.3
L-4-Hyp	16.0	L-Tyr	6.2
Homovanillic acid	9.2	Uric acid	5.1
β-Lactose	8.4	L-Val	20.3
L-Leu	18.7		

*N = 5: Excluded one outlier at 95% significance level, **N = 5: excluded one outlier at the 99.9% significance level. Outlier detected using the Nalimov test [114].

3.2.3.3 *Metabolic fingerprinting of study saliva samples*

The peak list processed with *MZmine*, from the data analysis of the 25 smokers and 25 non-smokers samples, contained 14,896 features, of which over 1000 were significantly ($p < 0.05$) different in saliva of smokers and non-smokers (Table 16). The different features could be assigned to about 155 metabolites. The reason for twice as many features in the peak list as compared to urine is accounted to the fact that a lower threshold was selected in *MZmine* software for automated peak picking, because saliva contains less metabolites allowing a lower intensity threshold for peak picking of additionally low abundant fragments.

3. Results

Table 16. Number of significant different features by p-value classes (Mann-Whitney U test) in saliva of smokers (N = 25) as compared to non-smokers (N = 25). Peak list obtained from the metabolic fingerprinting approach obtained with the described workflow procedure.

Class by statistical significance level	Number of fragments in peak list
sum	14894
$0.01 < p \leq 0.05$	720
$0.001 < p \leq 0.01$	297
$p \leq 0.001$	58

Not unexpectedly, fragment ions resulting from Cot and OH-Cot were found to be significantly elevated (Table 17) in saliva of smokers compared to non-smokers, which again demonstrates the applicability of the metabolomic workflow used.

Table 17. Nicotine metabolites significantly increased in smokers' (N = 25) as compared to non-smokers' (N = 25) saliva samples. Data derived from the metabolic fingerprinting approach with saliva samples.

Compound	RT (min)	Considered ion (*m/z*)	p-value	Identification method
OH-Cot	17.091	249	$2.3 \cdot 10^{-10}$	RF
Cot	14.884	98	$6.2 \cdot 10^{-04}$	RF

RF: reference compound.

The relative salivary levels of Cot and OH-Cot determined with the metabolic fingerprinting approach were compared to the corresponding absolute saliva concentrations obtained with a validated (targeted) LC-MS/MS method, to investigate the performance of the automated peak picking of the metabolic fingerprinting method. For this purpose, the peak area ratio (Analyte/IS) of the metabolite fragments of Cot and OH-Cot (Table 17) were plotted against the absolute LC-MS/MS-derived concentrations for the smoking subjects (Fig. 25). OH-Cot showed a strong correlation between both methodologies (r = 0.970, p = $1.4 \cdot 10^{-14}$, Pearson), whereas Cot showed no significant linear correlation (r = 0.337, p = $1.0 \cdot 10^{-1}$, Pearson). A possible explanation for the lack of correlation could be due to co-elution of a metabolite yielding the same mass fragment of *m/z* 98 in the GC-TOF-MS chromatogram.
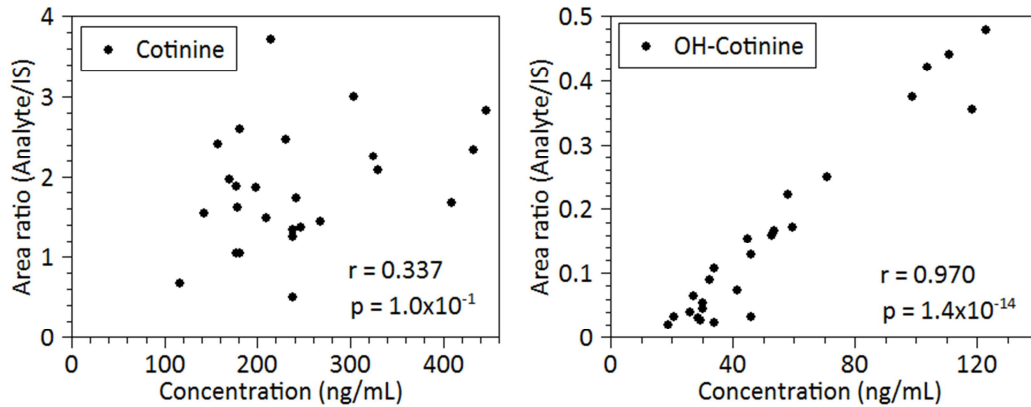
Fig. 25. Cot and OH-cot determined in saliva of 25 smokers, by different analytical approaches. Ordinate: Metabolic fingerprinting approach using GC-TOF-MS. Abscissa: Concentration levels by targeted LC-MS/MS analysis. r: Pearson's correlation coefficient.

Relatively high levels of the ion *m/z* 98 were found in the non-smokers' saliva (Fig. 26), resulting in a low average S/NS ratio of 1.6, which presumably hampers the correlation between the untargeted GC-TOF-MS and the targeted LC-MS/MS method. The usual S/NS ratio for cotinine in saliva is about 100 [115]. For OH-Cot, no or only very low signal intensities for *m/z* 249 were observed in saliva of non-smokers, yielding in a S/NS ratio of about 300. It has to be realized that in untargeted analytical approaches, such co-elution of isobaric fragments frequently occur and remain mostly undetected. This problem can only be avoided or reduced by applying more specific high-resolution techniques (both in terms of chromatographic separation and mass detection) as used on this approach.
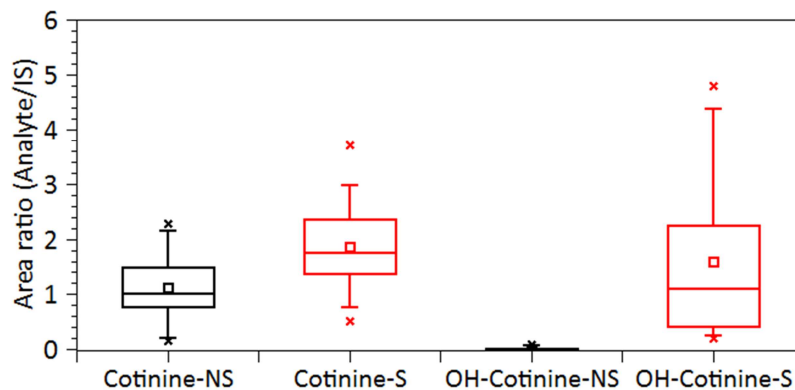
Fig. 26. Boxplot of relative Cot and OH-Cot levels measured in saliva of smokers (S) and non-smokers (NS) by the untargeted GC-TOF-MS method. For Cot the analyzed fragment *m/z* 98 was also present in significant levels in NS. The fragment *m/z* 249 analyzed for OH-Cot was barely detectable in non-smoking subjects. See text for further explanations.

3. Results

The tobacco-specific metabolite peaks from Cot and OH-Cot, as well as peaks showing no significant differences between the two groups (p > 0.05) and fragments derived from added compounds such as ISs, alkane standards and derivatisation agents were eliminated. The reduced peak list was uploaded to *Metaboanalyst*. With the remaining 1017 autoscaled fragments, a PLS-DA was performed. Using three principal components, the groups could be separated as shown in Fig. 27, with a Q^2 of 0.630 and a R^2 of 0.816. The statistics of a permutation test (p < $5 \cdot 10^{-4}$) approve the predictive ability of the PLS-DA model. None of the 2000 permutations denoted performed better than the original model (Fig. 28).
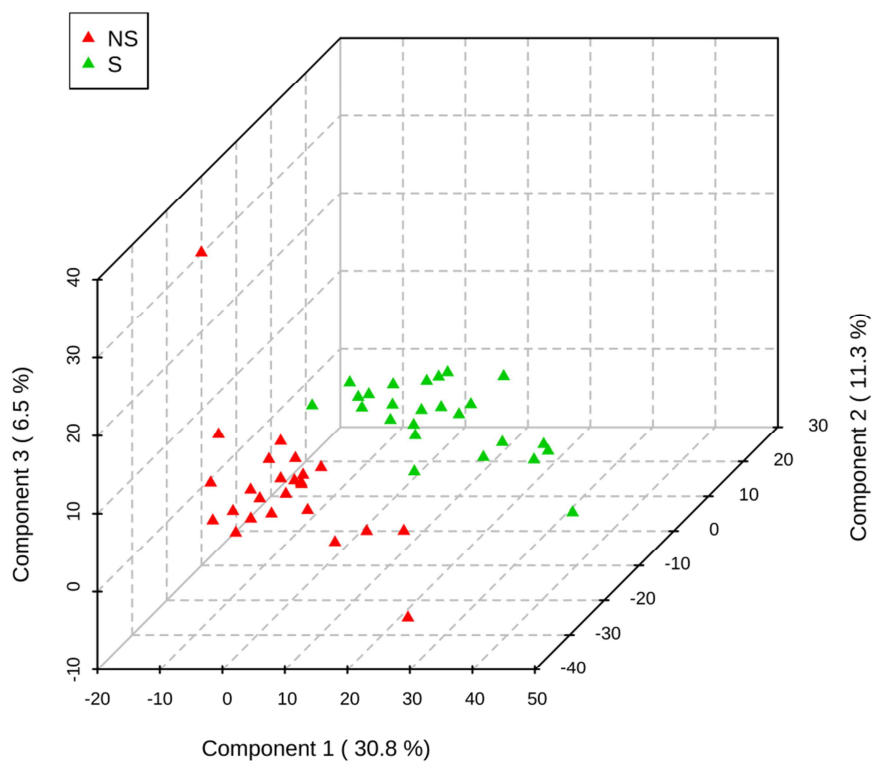
Fig. 27. Three-dimensional PLS-DA score plot for GC-TOF-MS analysis of saliva samples of 25 smokers (S) and 25 non-smokers (NS). Q^2 = 0.630. R^2 = 0.816.
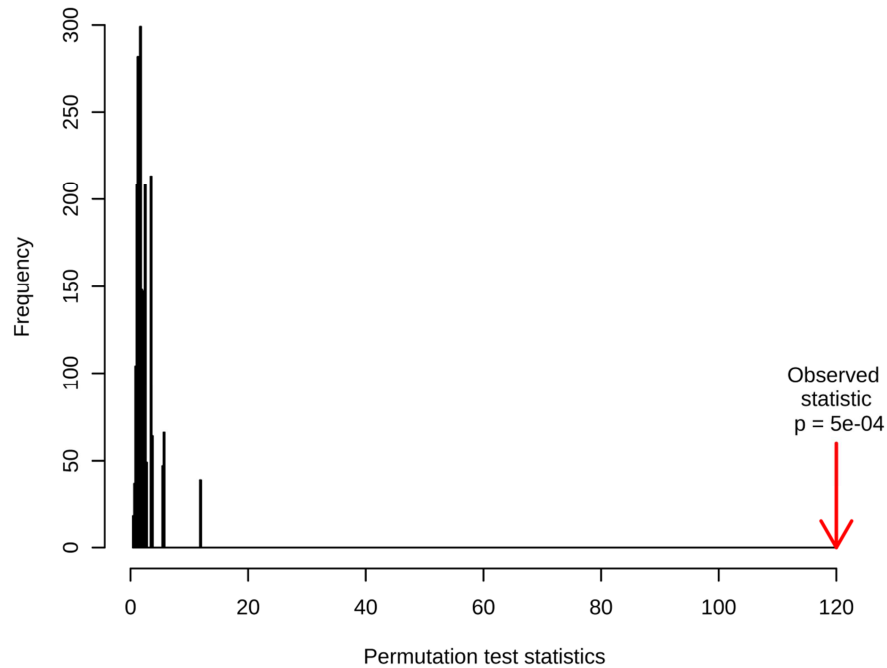
Fig. 28. Permutation test of PLS-DA model for saliva of 25 smokers and 25 non-smokers, based on 2000 permutations. Test statistics was calculated with 2000 permutations based on prediction accuracy by Metaboanalyst. The red arrow shows, the performance of the model using original labels. The further the arrow is to the right of the distribution, the more significant is the separation between the study groups (S and NS). As seen, the original model is very significant (p-value $< 5 \cdot 10^{-4}$) and not part of the obtained permutated distribution.

The univariate statistical test ($p < 0.05$, Mann-Whitney U test) and in the VIP measure derived from the PLS-DA (VIP > 0.8) resulted in 793 peaks (features) significantly different between the two groups. These signals originated from approximately 130 different compounds. Seventy-one of these compounds were decreased in smokers' saliva, while 59 were found to be increased when compared to non-smokers. Twelve of these metabolites could be identified using mass spectral libraries and authentic reference substances (Table 18). Four of the identified metabolites were significantly decreased in smokers' saliva and are most likely due to endogenous alterations of metabolic pathways. The most significantly increased metabolite was tyramine in the saliva of smokers (Fig. 29).
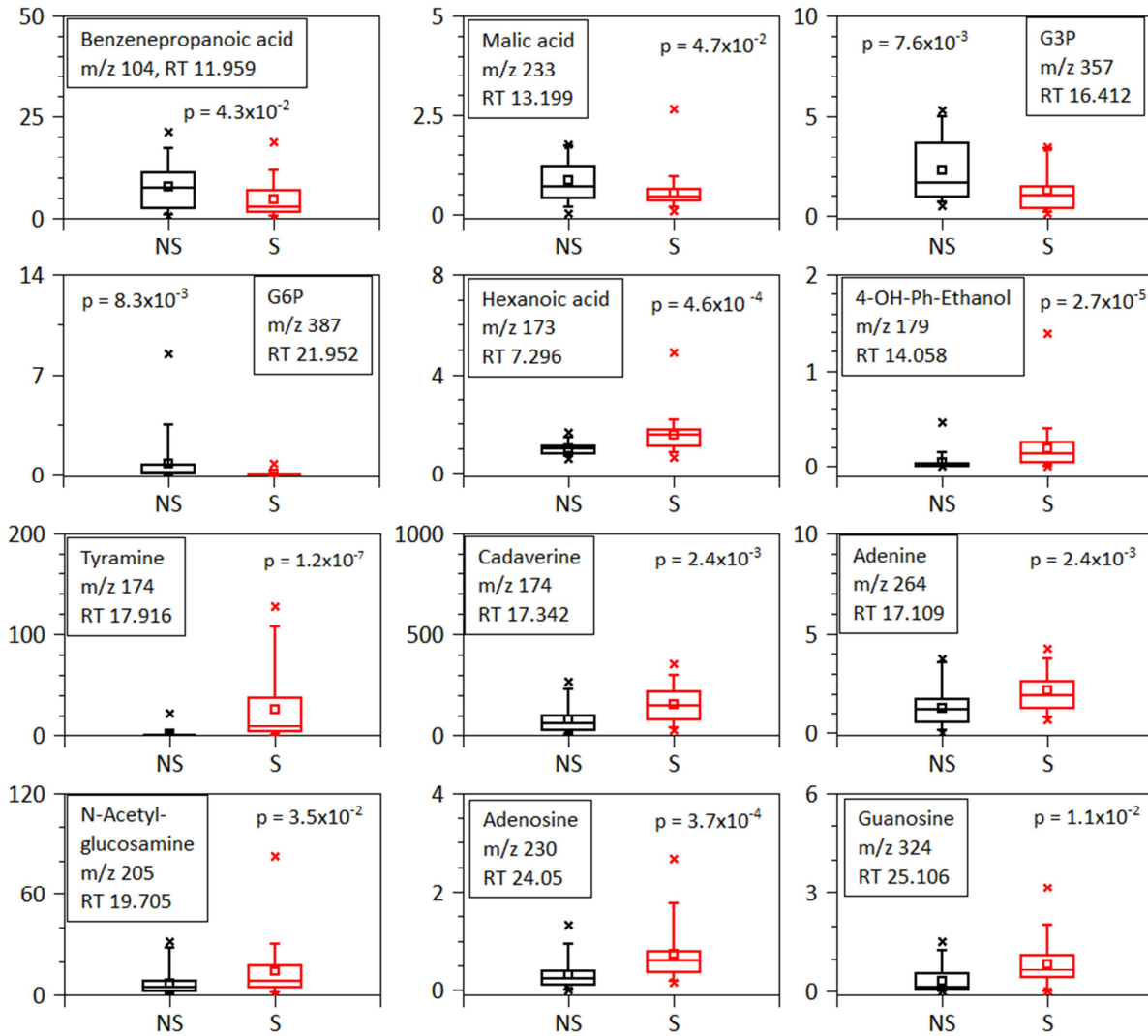
Fig. 29. Boxplots of peak intensities selected fragments derived from 12 identified salivary metabolites found to be significantly different between smokers (S) and non-smokers (NS).

Table 18. Significant different fragments and identified metabolites in saliva of smokers (N = 25) as compared to non-smokers (N = 25). All fragments found to be different in the univariate analysis (p < 0.05, Mann-Whitney U test) and in the multivariate analysis (VIP > 0.8 in PLS-DA model) were included. The PLS-DA model used 3 principal components.

No	RT (min)	S/NS	Compound	Ident.
1	5.74	←		
2	5.78	←		
3	5.80	←		
4	5.86	→		
5	6.09	←		
6	6.28	→		
7	6.35	←		
8	6.38	→		
9	6.43	→		
10	6.67	→		
11	6.77	→		
12	7.11	←		
13	7.18	→		
14	7.29	→	Hexanoic acid	DB
15	7.81	→		
16	7.85	→		
17	7.92	→		
18	8.09	←		
19	8.25	→		
20	8.58	←		
21	8.70	←		
22	9.13	→		
23	9.29	→		
24	9.46	←		
25	9.87	→		
26	10.07	→		
27	10.15	←		

No	RT (min)	S/NS	Compound	Ident.
45	12.68	←		
46	12.68	←		
47	12.69	→		
48	12.87	←		
49	12.90	→		
50	12.95	←		
51	13.20	→	Malic acid	DB
52	13.21	→		
53	13.26	→		
54	13.57	←		
55	13.90	→		
56	14.06	←	4-OH-Ph-Ethanol	DB
57	14.11	→		
58	14.36	→		
59	14.41	→		
60	14.45	→		
61	14.58	←		
62	14.58	→		
63	14.67	→		
64	14.74	←		
65	14.83	←		
66	14.88	←		
67	14.94	→		
68	15.20	←		
69	15.27	←		
70	15.30	→		
71	15.31	→		

No	RT (min)	S/NS	Compound	Ident.
88	17.44	→		
89	17.67	→		
90	17.75	←		
91	17.87	→		
92	17.91	←		
93	17.91	←	Tyramine	RF
94	18.09	←		
95	18.24	←		
96	18.41	←		
97	18.64	→		
98	18.74	←		
99	18.80	→		
100	18.90	→		
101	19.00	←		
102	19.17	←		
103	19.46	→		
104	19.72	←	N-Acetylglucosamine	DB
105	19.92	→		
106	20.02	→		
107	20.52	→		
108	20.73	←		
109	20.91	→		
110	21.45	→		
111	21.50	→		
112	21.51	→		
113	21.53	→		
114	21.77	←		

No.	RT	Identification	Ident.	Trend
28	10.31			↑
29	10.35			↑
30	10.47			↓
31	10.51			↓
32	10.59			↓
33	10.70			↓
34	10.72			↑
35	11.11			↓
36	11.30			↓
37	11.92			↑
38	11.96	Benzenepropanoic acid	DB	↓
39	12.01			↓
40	12.24			↑
41	12.36			↓
42	12.39			↑
43	12.41			↓
44	12.52			↓
72	15.48			↓
73	15.57			↓
74	15.57			↓
75	15.71			↓
76	16.29			↑
77	16.30			↓
78	16.32			↑
79	16.41	G3P	DB	↓
80	16.44			↑
81	16.56			↓
82	16.65			↓
83	16.67			↓
84	17.11	Adenine	DB	↑
85	17.29			↑
86	17.34	Cadaverine	DB	↑
87	17.36			↑
115	21.86			↓
116	21.95	G6P	RF	↓
117	21.96			↓
118	22.10			↓
119	22.42			↑
120	23.80			↑
121	23.91			↓
122	24.05	Adenosine	RF	↑
123	24.39			↑
124	24.74			↑
125	25.11	Guanosine	DB	↑
126	25.26			↓
127	25.88			↑
128	26.68			↑
129	27.00			↑
130	27.24			↑

Ident.: Identification method. DB: Database. RF: Standard reference compound. ↑: Increased in smokers. ↓: Decreased in smokers.

3.2.4 Plasma

3.2.4.1 Validation of the metabolic fingerprinting method for plasma

Due to limited availability for plasma, only 30 µL were used for analysis compared to the 100 µL used for urine and saliva. The chromatogram reflects these lower amounts utilized, by showing fewer, less intense peaks (Fig. 30) as compared the chromatograms obtained from saliva or urine. The plasma pool used for method validation showed high amounts of glucose, eluting at 18.1 min. (Fig. 30). Therefore, glucose was not used for the validation experiments. The residual 36 compounds and 6 internal standards were used as previously described in Section "2.7 Metabolic fingerprinting".
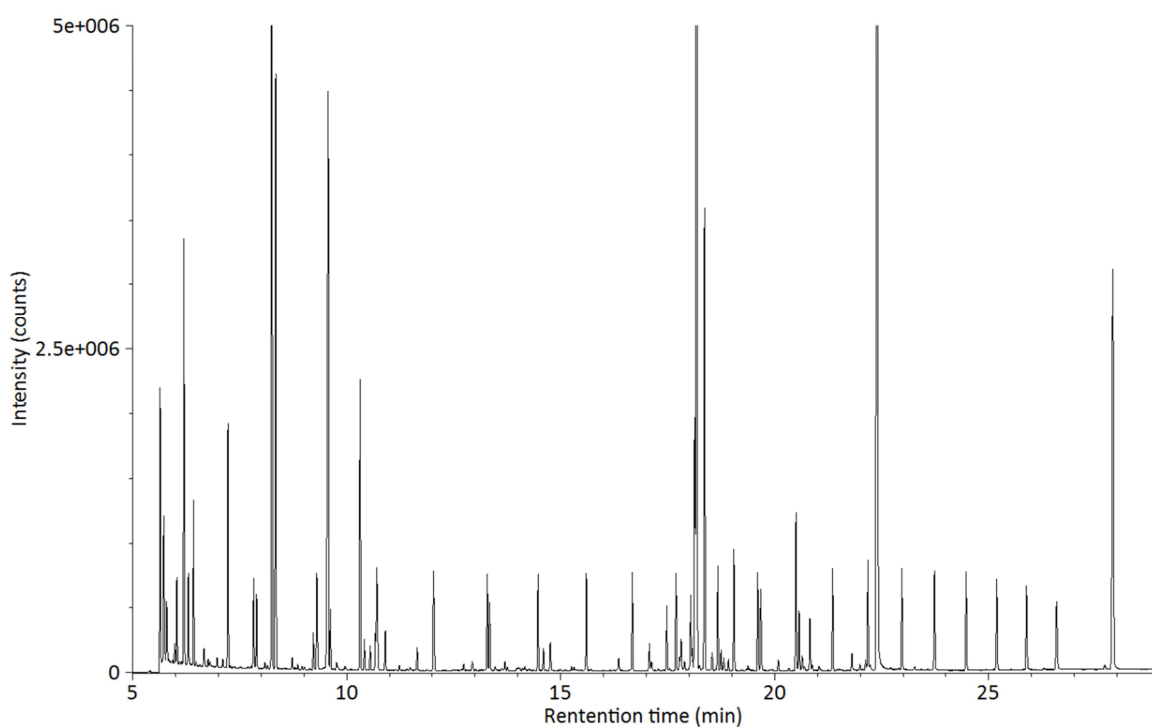
Fig. 30. TIC chromatogram of a plasma pool sample, generated by GC-TOF-MS in full scan mode (*m/z* 40 - 650).

Precisions and accuracies were determined from 5 samples at 3 different concentrations (25, 50 and 500 µM) (Table 19). Intraday accuracies were, on average, 93.5% (N = 19), 100.5% (N = 30) and 89.8% (N = 23) for the levels 25, 50 and 500 µM, respectively. The intraday CVs were, on average, 27.9% (25 µM), 5.7% (50 µM) and 6.9%

(500 µM). The remarkably high CV of 27.9% at 25 µM is mainly due to the very poor precision of the oxalic acid determination, yielding a CV greater than 55%. For the lowest level tested (25 µM), the interday CVs and accuracies were unexpectedly better than the intraday values, yielding 19.45% and 94.6%, respectively. The CVs for the levels 50 µM and 500 µM were 11.6% and 17.7% which is slightly higher as compared to the intraday values as expected. The corresponding interday accuracies amounted to 98.1% (50 µM) and 102.5% (500 µM) showed good precisions, comparable to the intraday results. For L-Gly it was not possible to calculate any inter- and intraday CV for 50 µM, since the concentration calculated was negative indicating problems with the calibration. Also the interday CV for 500 µM was extensively high for L-Gly. Therefore, the value was not considered for computing the average CV of the method. Possible reasons for the poor precision and accuracy could not be given. Re-injection analysis (N = 36) yielded mean CVs of 3.6%, 1.9% and 1.4% for 25, 50 and 500 µM, respectively (Table 19).

Table 19. Analytical performance parameters for the GC-TOF-MS method applied to plasma.

Compound	Corresponding IS	m/z considered ion	RT (min)	R^2	Linear range N = 4-8‡ (µM)	Spiked Level (µM)	Re-injection N=5 CV (%)	Intraday N = 5 Accuracy (%)	CV (%)	Interday N = 5 Accuracy (%)	CV (%)
Amino acids											
L-Gly	$^{13}C,^{15}N_2$-Urea	174	11.02	0.996	50-2000	500	1.1	65.8	13.4	110.1	45.1
						50	-	-	-	-	-
						25	-	-	-	-	-
L-Pro	$^{13}C_9,^{15}N$-L-Tyr	142	10.80	0.997	100-2000	500	0.9	72.9	5.2	97.8	19.3
						50	-	-	-	-	-
						25	-	-	-	-	-
L-4-Hyp	$^{13}C_9,^{15}N$-L-Tyr	230	13.88	0.992	1-75	500	-	-	-	-	-
						50	1.2	87.0	4.5	91.2	12.1
						25	5.3	121.1**	34.6**	84.9	13.4
L-Leu	$^{13}C_9,^{15}N$-L-Tyr	158	10.53	0.994	50-2000	500	0.8	82.7	3.7	99.8	21.1
						50	1.9	83.2	7.3	89.0	16.9
						25	3.2	-	-	-	-
L-Val	$^{13}C,^{15}N_2$-Urea	144	9.74	0.995	50-2000	500	2.2	93.9	5.2	94.4	11.0
						50	0.7	65.3	22.5	67.1	23.6
						25	-	-	-	-	-
L-Ala	$^{13}C,^{15}N_2$-Urea	116	8.02	0.996	100-2000	500	3.5	76.7	9.1	89.9	13.0
						50	-	-	-	-	-
						25	-	-	-	-	-
Gaba	d_4-ttMA	174	13.88	0.996	5-1000	500	0.8	98.1	5.0	79.4	23.3
						50	2.2	64.5	5.4	66.6	21.4
						25	2.3	69.9	32.2	64.2	33.7
L-Trp	$^{13}C_9,^{15}N$-L-Tyr	202	20.79	0.997	50-1000	500	0.7	87.4	3.0	100.6	20.8
						50	2.9	98.5	10.7	98.7	16.2
						25	-	-	-	-	-
L-Tyr	$^{13}C_9,^{15}N$-L-Tyr	218	18.29	0.9997	10-2000	500	0.5	105.6	3.3	109.2	12.5
						50	1.0	130.6	19.9	108.0	11.4
						25	2.7	96.0*	62.8*	92.6	35.6
Glutamine	d_4-ttMA	156	13.47	0.999	100-1000	500	1.7	97.8	11.1	122.3	15.4
						50	-	-	-	-	-
						25	-	-	-	-	-
Vitamin											
Nicotinic acid	d_4-Succinic acid	180	10.44	0.995	50-750	500	1.3	98.9	4.4	105.2	13.6
						50	1.2	127.6	2.2	120.0	7.4
						25	-	-	-	-	-

Carboxylic acids

Compound	Internal standard					Level					
α-Oxoglutaric acid	d₄-ttMA	198	14.16	0.9996	2.5-75	500	-	-	-	-	-
						50	1.1	123.9	3.7	102.5	10.8
						25	3.7	109.9	25.3	105.8	10.8
Oxalic acid	¹³C,¹⁵N₂-Urea	190	8.21	0.999	5-250	500	-	-	-	-	-
						50	3.1	74.1	16.6	74.1	36.0
						25	6.4	48.3*	26.6*	62.1	72.2
Succinic acid	d₄-Succinic acid	247	10.87	0.9996	5-500	500	1.5	98.2	2.6	106.2	8.2
						50	1.2	100.2	5.0	98.6	17.7
						25	3.6	96.5	21.5	100.3	27.1
Mandelic acid	d₄-ttMA	179	13.02	0.999	5-1000	500	2.1	100.3	3.2	105.2	11.3
						50	1.8	99.3	2.3	93.7	4.3
						25	1.4	99.0	23.0	91.3	8.0
Pyruvate	d₄-Succinic acid	174	6.95	0.999	7.5-75	500	-	-	-	-	-
						50	2.2	110.6	2.3	87.6	56.9
						25	2.7	100.6	21.6	11.7	13.4
Citric acid	d₄-Succinic acid	273	17.19	0.9996	10-750	500	1.7	103.8	3.3	108.6	10.6
						50	1.8	114.8	9.8	97.2	6.0
						25	1.7	91.9**	28.1**	95.2	34.4
ttMA	d₄-ttMA	271	14.74	0.99995	0.5-50	500	-	-	-	-	-
						50	2.8	113.4	2.1	105.2	9.6
						25	4.0	102.4	25.1	102.4	3.9
p-OH-Ph-Acetic acid	d₄-ttMA	179	14.90	0.998	1-75	500	0.5	-	-	-	-
						50	1.9	109.6	2.5	98.0	7.5
						25	3.8	102.3	25.7	97.3	6.8

Nucleic acids, purine

Compound	Internal standard					Level					
Thymine	¹³C,¹⁵N₂-Urea	255	12.06	0.9998	0.5-50	500	-	-	-	-	-
						50	2.0	110.9	2.1	107.7	8.8
						25	4.8	73.1*	29.6*	103.4	6.6
Thymidine	¹³C₉,¹⁵N-L-Tyr	103	22.15	0.9992	50-750	500	2.2	80.4	4.5	106.3	20.6
						50	3.1	115.6	2.7	109.2	7.7
						25	-	-	-	-	-
Adenosine	¹³C₉,¹⁵N-L-Tyr	230	24.21	0.9987	50-750	500	1.5	85.1	4.4	104.4	18.4
						50	1.7	106.5	3.1	101.2	7.6
						25	2.0	-	-	-	-
Uric acid	¹³C,¹⁵N₂-Urea	456	19.80	0.9886	500-2000	500	2.5	110.3	34.4	101.5*	30.0*
						50	-	-	-	-	-
						25	-	-	-	-	-

Carbohydrates

Compound	Internal standard					Level					
Glucuronic acid	¹³C₆-Glucose	333	18.62	0.9994	50-2000	500	0.9	77.5	2.8	97.6	20.8
						50	1.4	113.3	2.0	116.2	3.7
						25	-	-	-	-	-
β-Lactose	¹³C₆-Glucose	204	25.29	0.9994	25-2000	500	1.1	78.1	4.5	97.7	23.1
						50	1.9	81.9	2.9	89.9	4.8
						25	2.3	120.2	15.2	115.2	8.9

G6P	*$C_{16}H_{33}COOH$	299	22.1	0.9991	2.5-75	500	-	-	-	-	-
						50	2.0	107.0	6.7	98.5	8.6
						25	2.7	67.4	20.9	108.7	18.4
Alcohols											
Glycerol	d_4-Succinic acid	205	10.67	0.9991	250-2000	500	1.6	110.6	15.8	137.2	10.6
						50	-	-	-	-	-
						25	-	-	-	-	-
Homovanillic acid	d_4-ttMA	326	16.34	0.9999	2.5-50	500	-	-	-	-	-
						50	0.7	122.2	1.1	106.1	11.2
						25	3.5	103.6	21.6	100.8	3.9
Sorbitol	$^{13}C_6$-Glucose	319	18.80	0.9995	2.5-75	500	0.6	88.5	9.0	100.6	17.6
						50	0.14	105.3	14.6	90.1	21.3
						25	3.2	-	-	-	-
Ketones/Aldehydes											
Cot	$C_{16}H_{33}COOH$	98	15.12	0.9974	5-75	500	-	-	-	-	-
						50	2.0	97.7	2.0	88.5	6.6
						25	3.2	75.5	12.4	102.8	20.0
Creatinine	d_4-ttMA	115	14.10	0.9983	50-1000	500	1.0	88.5	10.8	114.7	13.5
						50	0.8	99.5	7.0	134.3	12.4
						25	3.9	-	-	-	-
Indole/amine											
5-HIAA	$^{13}C_9,^{15}N$-L-Tyr	290	20.63	0.9986	7.5-500	500	1.3	85.1	4.6	103.0	16.1
						50	1.4	89.2	2.8	87.8	6.0
						25	5.4	120.0	21.9	88.6	8.0
Phenol/amine											
Dopamine	$^{13}C_9,^{15}N$-L-Tyr	174	19.76	0.999	50-1000	500	1.4	84.8	6.8	73.3*	20.9*
						50	2.8	101.2	2.1	101.6	2.0
						25	8.0	-	-	-	-
Dipeptide											
Gly-Gly	$^{13}C_9,^{15}N$-L-Tyr	174	17.09	0.9998	2.5-50	500	-	-	-	-	-
						50	1.9	94.0	3.0	90.3	16.6
						25	3.9	73.0	67.5	82.2	25.8
Others											
4-Me-Hippuric acid	$^{13}C_9,^{15}N$-L-Tyr	119	17.32	0.9988	50-1000	500	3.4	74.7	8.0	105.9	29.9
						50	5.6	83.5	5.7	87.5	14.4
						25	-	-	-	-	-
2-Me-Hippuric acid	$^{13}C_9,^{15}N$-L-Tyr	119	17.02	0.9989	50-1000	500	0.6	74.5	3.1	96.5	22.7
						50	2.7	101.7	1.9	99.5	6.0
						25	-	-	-	-	-

‡: Measured as duplicates, * N=4, **N=3: Outlier detected using the Nalimov test [114].

3.2.4.2   Metabolic fingerprinting of plasma QC samples

For the QC samples of the metabolic fingerprinting in plasma, 6 aliquots (30 µL) of the plasma pool (comprising the 50 study samples) were spiked with 50 µM of the 36 reference compounds used for the validation experiments as well as 100 µM of the ISs d_4-ttMA and d_4-succinic acid. The samples were analyzed within the batch of the plasma study samples. Further processing was conducted as mentioned in Section "3.2.2.2 Metabolic fingerprinting of QC samples for urine". The average CV of the 38 spiked analytes was 8.8% ranging from 2.7% to 24.7% (Table 20). Except for Gly-Gly and 2-methylhippuric acid all CVs were below 20%, which proves the reproducibility of the entire analytical workflow. The results for 2-Me-hippuric acid showed no outlier using the Nalimov test [114] on the 99% level. For Gly-Gly, one outlier has been removed, since it significantly influenced the results, reflected in the CV of 24.7%. Since this is the only analyte above with a CV over 20% the results from the QC samples are acceptable with an overall deviation below 10%. For evaluation of the CVs, similar fragments as for the validation experiments were used.

Table 20. QC samples (N = 6) applied in the metabolic fingerprinting analysis of plasma. Samples were randomly analyzed within the batch of the study samples. CVs are shown for 36 compounds spiked at 50 µM as well as the ISs d_4-ttMA and d_4-succinic acid spiked at 100 µM to the plasma pool (spiked compounds are in alphabetic order).

Spiked compound	CV N = 6 (%)	Spiked compound	CV N = 6 (%)
Adenosine	16.7	Mandelic acid	6.3
L-Ala	2.7	2-Me-Hippuric acid	24.6
Citric acid	8.0	4-Me-Hippuric acid	8.0
Cot	6.7	Nicotinic acid	5.9
Creatinine	4.9	Oxalic acid	11.2
Dopamine	13.8	2-Oxoglutaric acid	8.3
G6P	7.1	L-Pro	4.4
Gaba	7.9	Pyruvate	5.1
Glucuronic acid	6.2	Sorbitol	7.6
Glutamine	5.3	Succinic acid	11.7
L-Gly	17.1	d_4-Succinic acid	4.1
Glycerol	8.7	Thymidine	8.5
Gly-Gly	24.7*	Thymine	7.2
Hydroxyindole5-HIAA	9.4	L-Trp	9.3*
p-OH-Ph-Acetic acid	5.3	ttMA	6.9
L-Hyp	5.5	d_4-ttMA	8.9
Homovanillic acid	5.0	L-Tyr	13.4
β-Lactose	6.4	Uric acid	13.8
L-Leu	6.3	L-Val	3.2

*N=5, excluded one outlier that was detected using the Nalimov test at a 99% significance level [114].

3.2.4.3   Metabolic fingerprinting of study plasma samples

For plasma series, the analysis and evaluation yielded a peak list containing 4261 features. The reasons for less features is mainly due to the lower sample volume used (30 µL) as compared to saliva and urine (100 µL). Two hundred sixty six features were significantly different between smokers and non-smokers (p < 0.05, Table 21). These features could be assigned to about 42 compounds. Fourteen of these compounds were significantly increased in smokers. From all matrices, plasma had the lowest amount of peaks in the peak list and therefore also the lowest amount of significantly different features.

3. Results

Table 21. Number of significant different features by p-value classes (Mann-Whitney U test) in plasma of smokers (N = 25) as compared to non-smokers (N = 25). Peak list obtained from the metabolic fingerprinting approach obtained with the described workflow procedure.

Class by statistical significance level	Number of peaks in peak list
All	4261
$0.01 < p \leq 0.05$	236
$0.001 < p \leq 0.01$	22
$p \leq 0.001$	8

Peaks showing no significant differences between the two groups ($p > 0.05$) were eliminated. The remaining peak list was uploaded to Metaboanalyst and missing peak intensity values were replaced by a value amounting to half of the minimum for this particular feature. The data were subsequently autoscaled and a PLS-DA was performed. The optimal number of principal components for a separation of the two study groups was four, selected by 10-fold cross validation. Fig. 31 shows the PLS-DA score plot of the two study groups. Using the four principal components for a group separation eventuated in a Q^2 of 0.601 and a R^2 of 0.852. The class separation was less pronounced in the score plot as compared to urine or saliva. The most likely explanation is that the low sample volume available for metabolomic analysis and the resulting fewer significantly different features in the plasma peak list lead to higher influence of technical variations, for example due to sampling, sample work-up and analytical variations. As a consequence, a lower separation power for plasma analysis is probably obtained.

The permutation test yielded a p-value of 0.0015, indicating that the PLS-DA model is significant, however with a higher influence of technical variations as compared to the model of urine and saliva. The application of 2000 permutations resulted in three PLS-DA models (p-value * number of permutations = 0.0015 x 2000 = 3) that are at least as good as the original model (Fig. 32).
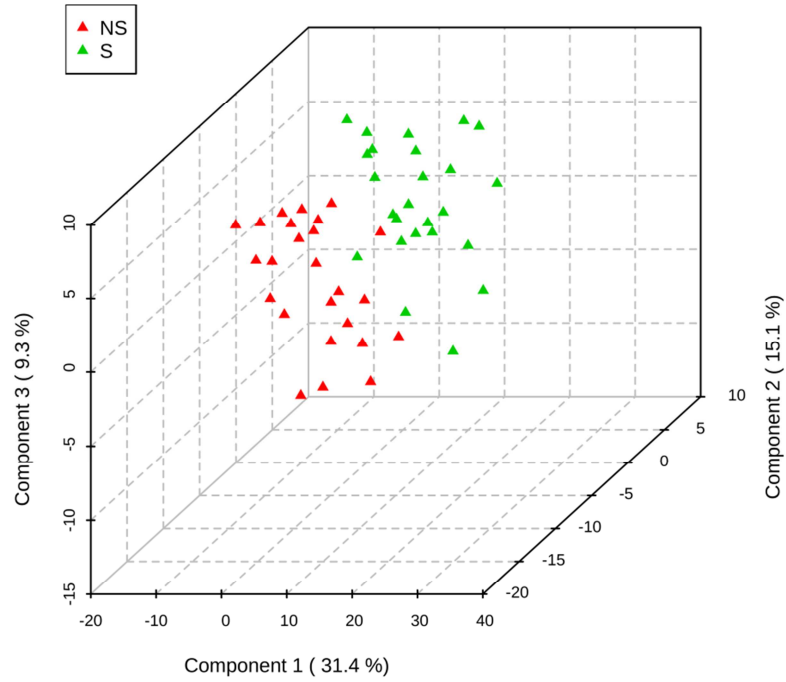
Fig. 31. Three-dimensional PLS-DA score plot for GC-TOF-MS analysis of plasma samples of 25 smokers (S) and 25 non-smokers (NS). Q^2=0.601, R^2 = 0.852.
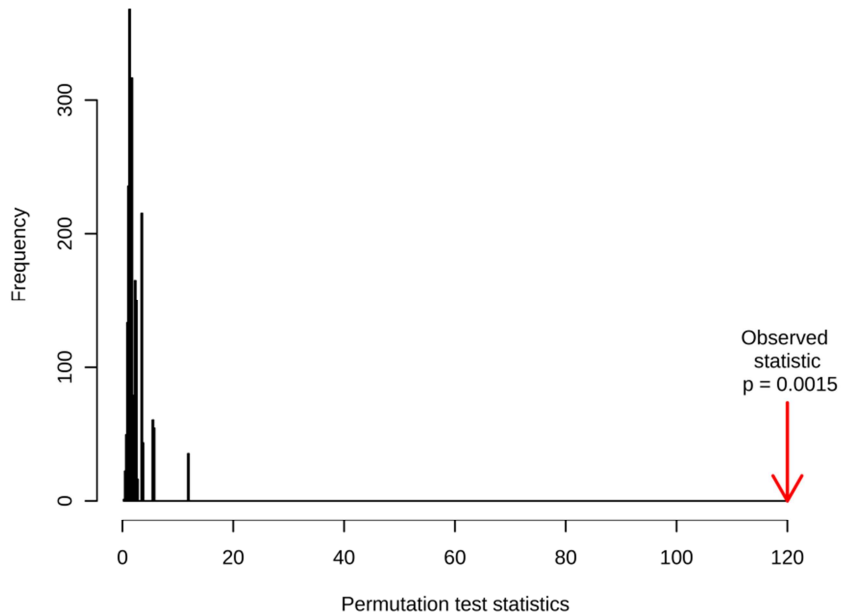
Fig. 32. Permutation test of PLS-DA model for plasma of 25 smokers and 25 non-smokers, based on 2000 permutations. Test statistics was calculated with 2000 permutations based on prediction accuracy by Metaboanalyst. The red arrow shows, the performance of the model using original labels. The further the arrow is to the right of the distribution, the more significant is the separation between the study groups (S and NS). As seen, the original model is very significant (p-value < $1.5 \cdot 10^{-3}$).

3. Results

The average VIPs for the features were calculated from the four principal components of the PLS-DA model. From the peak list, 225 fragments out of the 4261 showed a VIP over 0.8, which could be assigned to about 36 metabolites. From these 36 significant different metabolites were 14 decreased in smokers' plasma while the other 22 were increased as compared to non-smokers. Eight of these metabolites could be identified by matching the mass spectra against spectral databases. The identities of 3 of the 8 metabolites were confirmed by comparison to standard reference compounds (Table 22). Alanine and nonanoic acid were significantly decreased, while glutamic acid, ornithine, cholesterol and the MUFAs oleic acid (FA 18:1 n-9) palmitoleic acid (FA 16:1 n-9) and the FA 18:1 (presumably n-7) were significantly increased (Fig. 33).

3. Results

Table 22. Significantly different metabolites in plasma of smokers (N = 25) as compared to non-smokers (N = 25). Fragments found to be significantly different in univariate (p < 0.05, Mann-Whitney U test) and multivariate analysis (VIP > 0.8 in the PLS-DA model) were included. The PLS-DA model used 4 principal components.

No	RT (min)	S/NS	Compound	Identification method
1	5.845	↓		
2	5.925	↑		
3	6.144	↓		
4	7.877	↓		
5	7.895	↓	Ala	RF
6	8.252	↑		
7	9.620	↓		
8	9.891	↑		
9	10.093	↓		
10	10.717	↓		
11	11.157	↓		
12	11.410	↓	Nonanoic acid	DB
13	11.477	↑		
14	13.475	↓		
15	14.752	↓		
16	14.761	↑	Glutamic acid	RF
17	15.115	↑		
18	17.124	↑	Ornithine	DB
19	18.050	↑		
19	18.051	↑		
19	18.052	↑		
20	18.068	↑		
21	18.141	↓		
22	18.174	↑		
23	18.243	↑		
24	18.818	↑	Palmitoleic acid (FA 16:1 n-7)	DB
25	20.087	↓		
26	20.498	↑		
27	20.571	↑	Oleic acid (FA 18:1 n-9)	RF
28	20.630	↑	FA 18:1 (presumably n-7)	DB
29	20.823	↑		
30	21.353	↓		
31	22.394	↑		
32	22.460	↑		
32	22.463	↑		
33	22.696	↑		
34	23.581	↑		
35	23.794	↑		
36	27.897	↑	Cholesterol	DB

DB: Database. RF: Standard reference compound. ↑: Increased in smokers. ↓: Decreased in smokers.
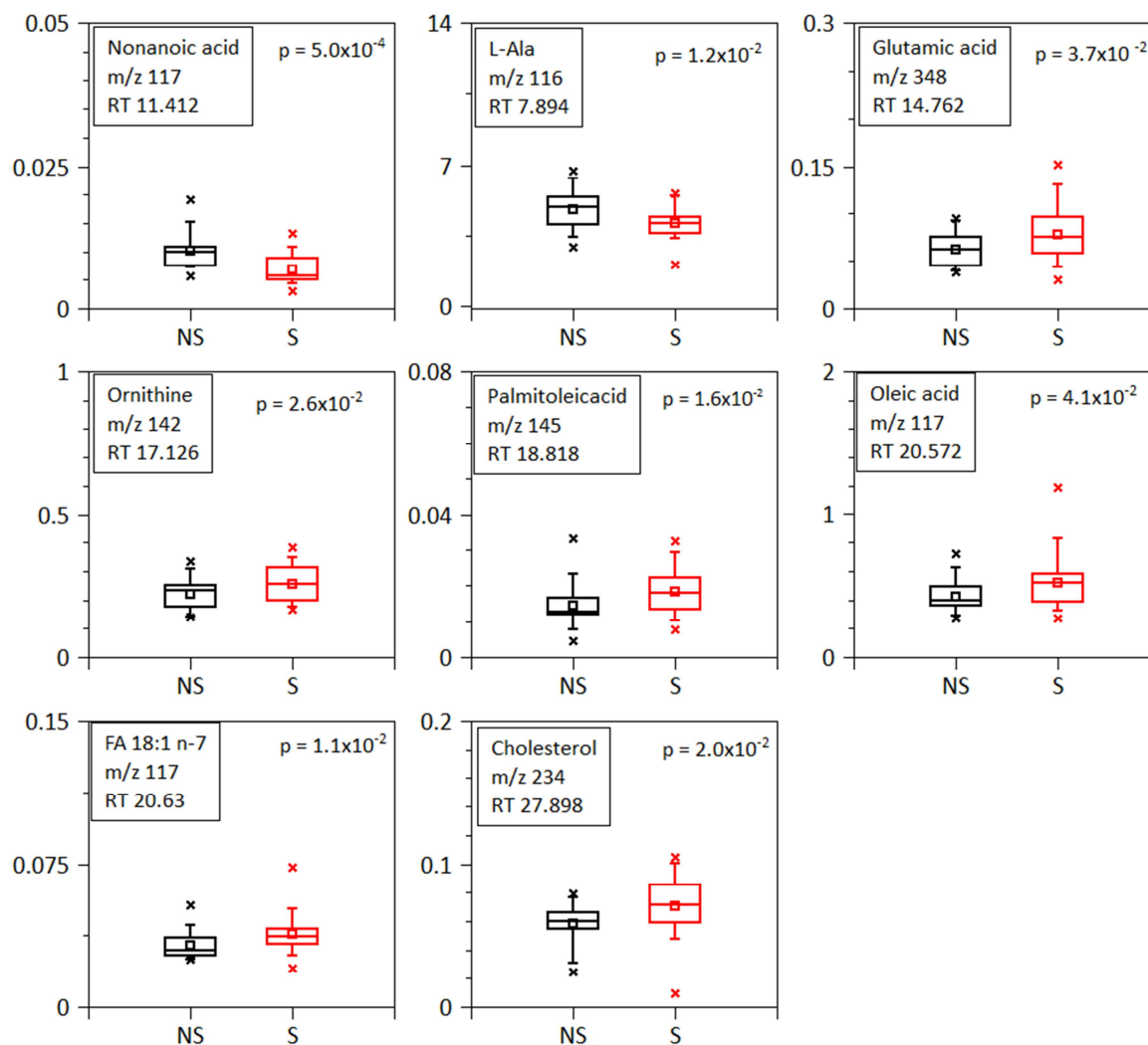
Fig. 33. Boxplots of selected fragments derived from metabolites in plasma found to be significantly different between 25 smokers (S) and 25 non-smokers (NS).

3.3   Targeted fatty acid profiling in plasma

Based on the findings of the metabolic fingerprinting in plasma, the total relative fatty acid profile was analyzed in the study plasma samples using GC-FID (refer to Section "2.9 Fatty acid profiling in plasma"). Since the metabolism of fatty acids is dependent on the relative cellular fatty acid composition, rather than the absolute concentrations [116], the fatty acid profiles in the two study groups were compared. The results obtained with the metabolomics approach could be verified by the targeted GC-FID analysis. The proportions of MUFA species, including FA 16:1 n-7, FA 17:1 c/t (cis or trans isomer), FA 18:1 n-9, FA 18:1 n-7, FA 20:1 n-9 and FA 24:1 n-9, were significantly increased in smokers compared to non-smokers ($p < 0.039$), whereas saturated fatty acids such as FA 17:0 and FA 18:0 and the polyunsaturated fatty acid (PUFA) FA 22:6 n-3 were significantly decreased

(p < 0.031, Table 23). Increased plasma levels from an exogenous uptake of FAs present in tobacco smoke is very unlikely. FA 16:0 and FA 18:3 are major fatty acids of tobacco smoke, which were found to be decreased rather than increased in smokers plasma samples [117,118] . Moreover, MUFA concentrations in tobacco smoke are too low for the observed FA increases in the plasma of smokers. The highest described concentration of FA 18:1 n-9 determined in non-filter cigarettes is 0.21 mg/g-tobacco smoked [117]. If one assumes that 1 g tobacco is smoked per cigarette and 20 cigarettes are smoked in 24 hours, the maximum amount of the adsorbed FA 18:1 n-9 would be 4.2 mg (14.9 µmol). Assuming a blood volume of 5 L, its concentration in blood would be 2.98 µM (14.9 µmol/5 L), which is less than 0.2% of the total FA 18:1 n-9 concentrations typically found in human plasma (1.89 mM) [103]. The relative amounts of FA 18:1 n-9 proportions in smokers were found to be 2.5% higher than in non-smokers. In addition, the estimated increase of 0.2% of FA 18:1 n-9 is certainly an overestimation considering the fact that all smokers in the study smoked less than 20 cigarettes per day (average number of cigarettes smoked was 13/d). Additionally, most of the subjects smoked filter-cigarettes, which should capture FAs partially from tobacco smoke. Furthermore, the assumption that the total amount of FA 18:1 n-9 will appear in blood is highly unlikely.

Table 23. Relative fatty acid profile in plasma of smokers and non-smokers obtained by means of GC-FID analysis, after hydrolyzation of the esterified fraction of fatty acids. The values represent the peak area ratios of the individual fatty acids to the sum of all measured fatty acids present in plasma with this methodology.

Fatty acid	Total relative FA profile (%, mean ± SEM)		S / NS	p-value
	NS[†]	S[†]		
FA 12:0	0.21 ± 0.0081	0.22 ± 0.011		0.84
FA 14:0	0.96 ± 0.042	0.90 ± 0.056		0.20
FA 14:1 n-5	0.039 ± 0.005	0.038 ± 0.01		0.68
FA 15:0	0.22 ± 0.0069	0.20 ± 0.0088		0.20
FA 16:0	22.7 ± 0.297	22.4 ± 0.29		0.59
FA 16:1 n-7	1.7 ± 0.11	1.9 ± 0.11	↑	0.031
FA 17:0	0.25 ± 0.0074	0.23 ± 0.0073	↓	0.029
FA 17:1 c/t	0.095 ± 0.0051	0.11 ± 0.0061	↑	0.039
FA 18:0	8.1 ± 0.17	7.4 ± 0.15	↓	0.0010
FA 18:1 n-9	21.3 ± 0.57	23.8 ± 0.47	↑	0.00088
FA 18:1 n-7	1.7 ± 0.037	1.9 ± 0.034	↑	0.021
FA 18:2 n-6	26.8 ± 0.56	26.5 ± 0.55		0.76
γ-FA 18:3 n-6	0.45 ± 0.027	0.44 ± 0.033		0.82
α-FA 18:3 n-3	0.95 ± 0.042	0.89 ± 0.055		0.30
FA 20:0	0.16 ± 0.014	0.14 ± 0.0095		0.18
FA 20:1 n-9	0.15 ± 0.0055	0.18 ± 0.0053	↑	0.0012
FA 20:2 n-6	0.19 ± 0.0073	0.19 ± 0.0054		0.58
FA 20:3 n-6	1.9 ± 0.081	1.7 ± 0.082		0.20
FA 20:4 n-6	7.7 ± 0.38	7.0 ± 0.28		0.37
FA 20:4 n-3	0.079 ± 0.012	0.076 ± 0.012		0.99
FA 20:5 n-3	0.66 ± 0.066	0.55 ± 0.046		0.39
FA 22:0	0.081 ± 0.0056	0.082 ± 0.0059		0.88
FA 22:4 n-6	0.23 ± 0.016	0.21 ± 0.010		0.65
FA 22:5 n-6	0.13 ± 0.013	0.13 ± 0.0081		0.28
FA 22:5 n-3	0.66 ± 0.027	0.63 ± 0.028		0.53
FA 22:6 n-3	1.7 ± 0.093	1.3 ± 0.053	↓	0.0017
FA 24:0	0.055 ± 0.0035	0.058 ± 0.0052		0.85
FA 24:1 n-9	0.063 ± 0.0057	0.079 ± 0.0061	↑	0.025
Others	0.77 ± 0.051	0.77 ± 0.051		-

c/t: cis or trans isomer not unambiguously identified. SEM: Standard error of the mean. [†]N = 25. P-value calculated by means of Mann-Whitney U test. ↑: Significantly increased in smokers. ↓: Significantly decreased in smokers.

3.4 Quantification of phospholipid species in plasma

The total fatty acid content that was measured in plasma of smokers and non-smokers consists of free fatty acids and fatty acids linked to lipids. In addition to triglycerides and

cholesterol esters, the major amounts of total fatty acids determined in plasma are bound to PC and PE species. To extend the findings from the untargeted screening and targeted fatty acid analysis, the impact of altered fatty acid profiles on the composition of the phospholipid species PC and PE was investigated.

In principle, different types of analytical strategies can be used for the analysis of PC and PE species: Flow injection analysis (FIA) bypasses the necessity of chromatographic separation [48] by normal phase (NP) LC-MS/MS [49], by HILIC-MS/MS or by reversed phase (RP) LC-MS/MS [119,120]. FIA might be hampered by matrix interferences and an overlap of isobaric compounds due to low mass resolution (e.g. PC species with isobaric +1 isotopes of SM species) when using a triple quadrupole instrument. Comparing the chromatographic approaches, HILIC provides several advantages over RP and NP chromatography [121]:

- Baseline separation of PC and PE by maintaining co-elution of individual molecular species within each lipid class [122-126].
- Co-elution of analytes, internal standards and calibrators, thus compensating for potential matrix effects and varying ionization efficiencies, which is of particular importance when gradient elution is applied.
- The use of polar solvent mixtures improves ionization conditions for ESI and chromatographic resolution. Classical NP chromatography may be impaired by limited reproducibility and insufficient peak shapes.
- Fast, robust and reliable quantification of various phospholipid species within the same run.

Moreover, in contrast to many previously published methods [122,124-133], an UPLC column containing sub-2-µm particles (100 x 2.1 mm, 1.7 µm particles) was used, leading to well defined peak shapes and shorter runtimes as compared to conventional LC particle sizes. As shown in Fig. 34 A and B, baseline separation for both lipid classes was achieved along with co-elution of the lipid species within the same class (Fig. 34 C, D). The peaks are characterized by a well-defined and narrow shape (peak width ~ 12 s), resulting in an improved signal to noise ratio and thus a gain of sensitivity. The total runtime of 8 min was acceptable and allows a throughput of about 160 samples per day. Furthermore, retention time shifts were below 5%. Most published methods using LC-MS/MS for phospholipid determination are limited by runtimes over 15 min, admittedly including additional lipid classes beside PC and PE [122-127,129,130,132,133]. Some of the measured MRMs of the PCs showed a second peak about 0.3 min after the actual analytes (Fig. 34 A). To investigate whether the method is able to separate diacyl from ether linked phospholipid species, two ether linked species (PC O-36:4 and PE P-38:4) were analyzed along with the corresponding diacyl phospholipid standards PC 34:1 and PE 40:6 (Fig. 34 E,F). The results

show that it was not possible to unambiguously differentiate between the diacyl species and co-eluting ether linked phospholipids. However, isobaric overlap occurs only with ether linked PC and PE species containing an odd-chain fatty acid, which represents only a minor fraction of the total phospholipids [134].
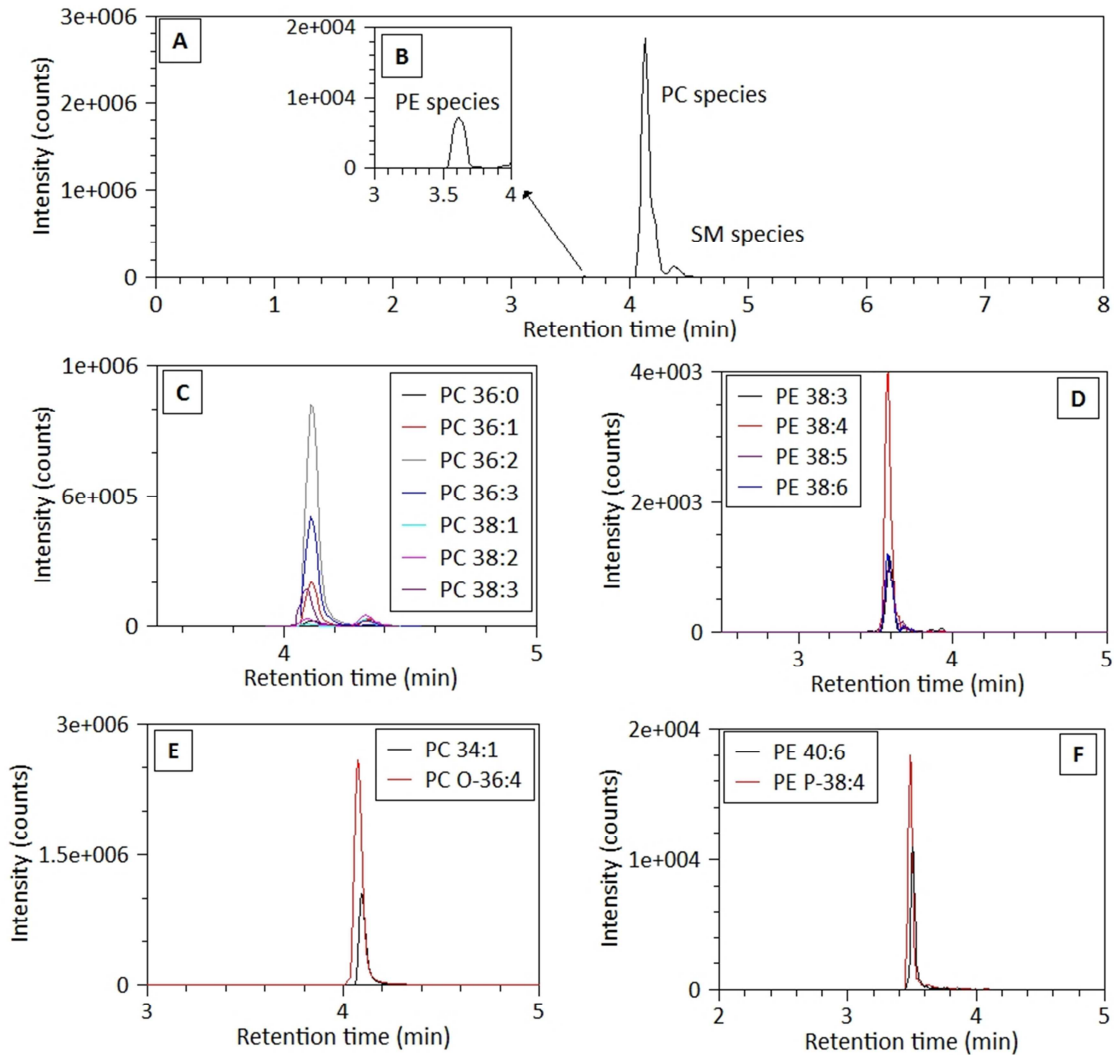
Fig. 34. Phospholipids separated by HILIC and detected by MS/MS in a plasma pool. A and B: TIC of PC and PE species which were baseline separated. It is assumed that the peak at 4.4 min is due to +1 isotopes of sphingomyelin (SM) species. C: Co-elution of PC species. D: Co-elution of PE species. E: The alkanyl/acyl species PC O-36:4 (MRM of m/z 768.6 → m/z 184) co-elutes with a diacyl species of PC (e.g. PC 34:1). F: Alkenyl/acyl (plasmalogen) species PE P-38:4 (MRM of m/z 752.6 → m/z 611.6) co-elutes with diacyl species of PE, indicating that the method is not capable of separating acyl from ether linked species.

3. Results

The +1 isotopes of sphingomyelin species as well as PCs lose their phospho-choline headgroup upon CID. In addition to the positively charged headgroup m/z 184, SM loses the sphingoid base which can be measured in positive ionization mode as m/z 264 [135]. To prove whether the peak at 4.4 min originates from SM species, the MRM trace of m/z 704.6 → m/z 184 (PC 30:1 or +1 isotope of SM 34:1) and the MRM trace of m/z 703.6 → m/z 184 (SM 34:1) were measured in a representative human plasma pool sample. Both peaks were only present at 4.4 min but did not appear at 4.1 min where the PC species elute (Fig. 35 A). Furthermore, the fact that the MRM trace of m/z 703.6 → m/z 264 was detectable, indicates the presence of SM 34:1 (Fig. 35 B) in the plasma pool. To determine the accurate mass, the method was transferred to a high resolution MS instrument (QTOF Xevo G2-S, Waters, Milford, USA) coupled to an UPLC (Acquity, Waters, Milford, USA). All chromatographic settings were kept the same as the initial HPLC method. The UPLC-QTOF settings are listed in the Appendix "7.6 UPLC-QTOF-MS settings for SM detection in plasma". The MS spectrum of the peak at 2.8 min showed that the intensity of 703.6 (45%) compared to the intensity of 704.6 (100%) yielded the same ratio as the theoretical isotopic distribution of the mono-isotopic SM 34:1 and the SM 34:1 +1 isotope (Fig. 35 C, D). Furthermore, excellent mass accuracy was achieved with a mass deviation of 1.4 ppm (theoretical m/z of $[M+H]^+$ 703.5754). These data provide strong evidence that the peak at 4.4 min originates from the sphingomyelin +1 isotope.
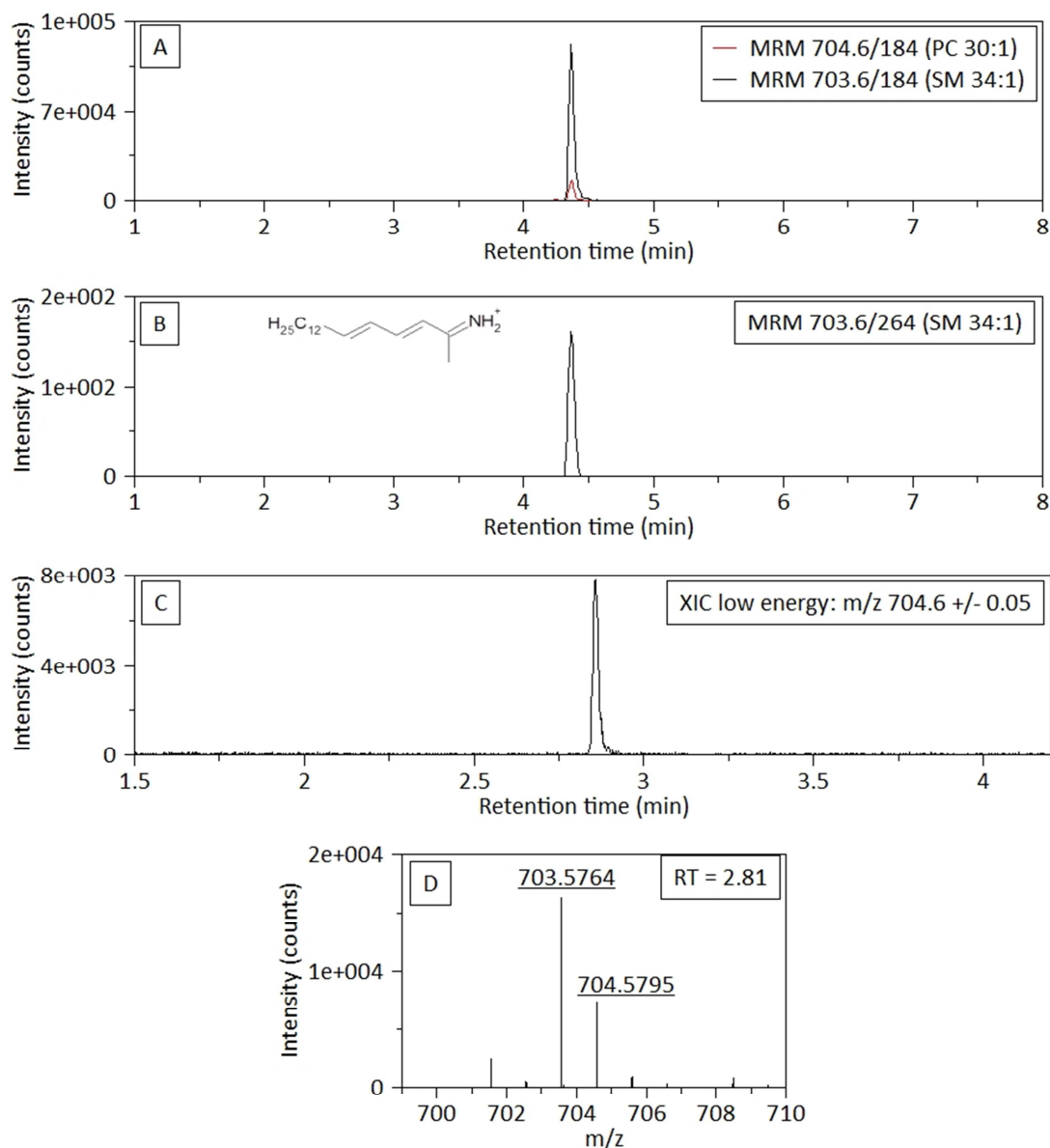
Fig. 35. Detection of PC and SM species in a human plasma pool. A: Analysis of the MRM of SM 34:1 and the +1 isotope of SM 34:1 which is quasi-isobaric to PC 30:1. B: Detection of the sphingoid base of SM 34:1 (A and B by HPLC-MS/MS). C: Extracted ion chromatogram (XIC) of the +1 isotope of SM 34:1 measured by means of UPLC-QTOF-MS. D: High–resolution mass spectrum showing the presence of [M+H]$^+$ and [M+H+1]$^+$ of SM 34:1 (C and D by UPLC-QTOF-MS).

3.4.1 Method development for quantification of PC and PE lipid species

Each lipid standard compound (applied for calibration) was used for several species. Selection was based on its ionization efficiency, which can depend on the fatty acid chain

length and the grade of saturation. For this purpose, 50 µM of each of the 8 phospholipid standards (PC 34:1, PC 36:2, PC, PC 38:4, PC 40:0, PE 34:1, PE 36:2, PE 36:4 and PE 40:6), PE as well as PC 44:0 and PE 32:0 8 Me were injected and the intensities were measured, to find ionization dependencies (Fig. 36). As shown in Fig. 36 A and B the ionization efficiency was only marginally influenced by the chain length and grade of saturation when low amounts of analyte was injected (< 2 pmol) as already reported by Ahn and co-workers [127]. Therefore, the standards used for calibrations were first selected on chain length and then on the grade of saturation, as shown in Table 26.
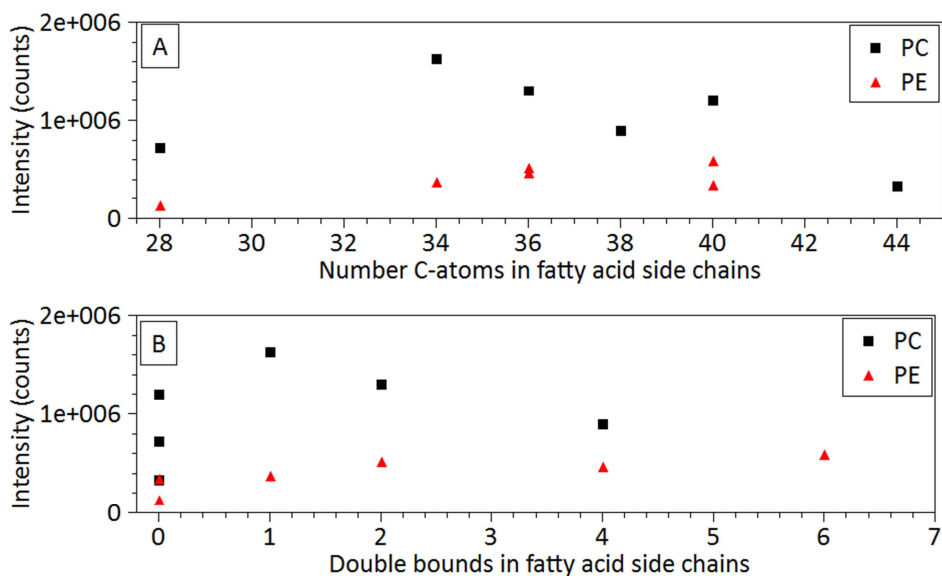
Fig. 36. Ionization efficiency of PC and PE species. 2 µL of each standard, dissolved in MeOH, was injected. A: Ionization efficiency in relation to fatty acid side chain. B: Ionization efficiency in relation to grade of saturation. There seems to be no association between the ionization efficiency and the length of the fatty acid properties.

3.4.2   Calibration of the phospholipids in water or matrix

The standard addition method for calibration in plasma poses the problem of relatively high endogenous analyte concentrations. For this reason, calibration in water was tested for suitability by comparing against a calibration performed in a plasma pool. The obtained calibration lines for the 8 phospholipid standards are shown in Fig. 37. All phospholipid standards revealed similar calibration slopes in plasma and water. For PE species, the concentration levels in plasma were low compared to the spiked levels so that the regression lines show almost identical intercepts. As a result of these experiments, it was decided to calibrate the PC and PE species in water.
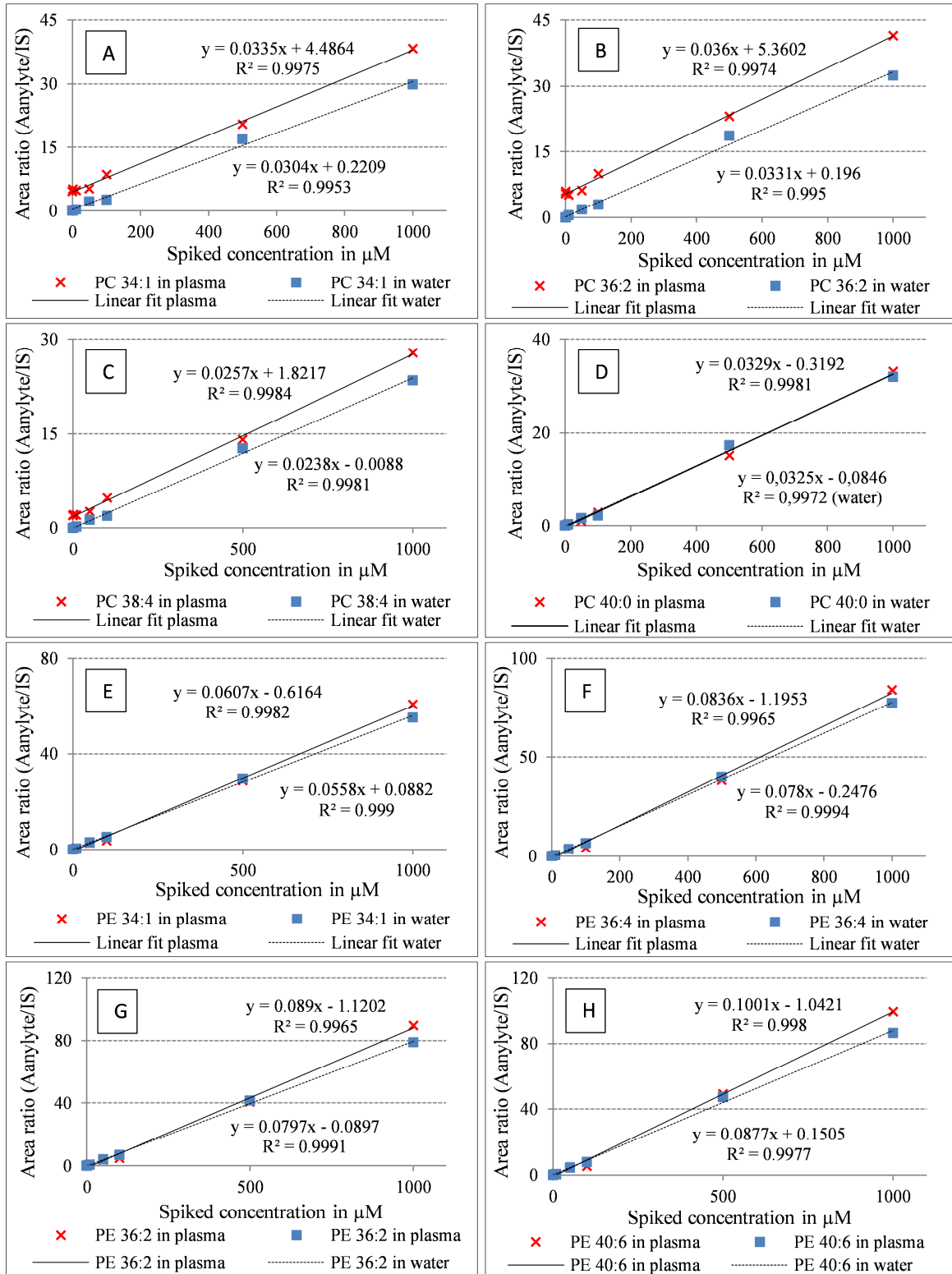
Fig. 37. Calibration of phospholipids (PC and PE species) in water and plasma. The spiking levels applied were below detector saturation. The calibration lines for all lipids show similar slopes in water and plasma. R^2: coefficient of determination. N = 7.

3.4.3 Isotope correction

The isotopic correction algorithm was tested by spiking 7 phospholipid standards to water and measuring the intensity of the M+2 isotope which is isobaric to the species containing one double bond (e. g. M+2 of PC 34:1 and PC 34:0 have the same mass of 761.6 Da). The concentrations of the phospholipids were calculated with and without isotopic correction. It is obvious that isotopic correction improves the results significantly as shown in Fig. 38 A-F.

3. Results
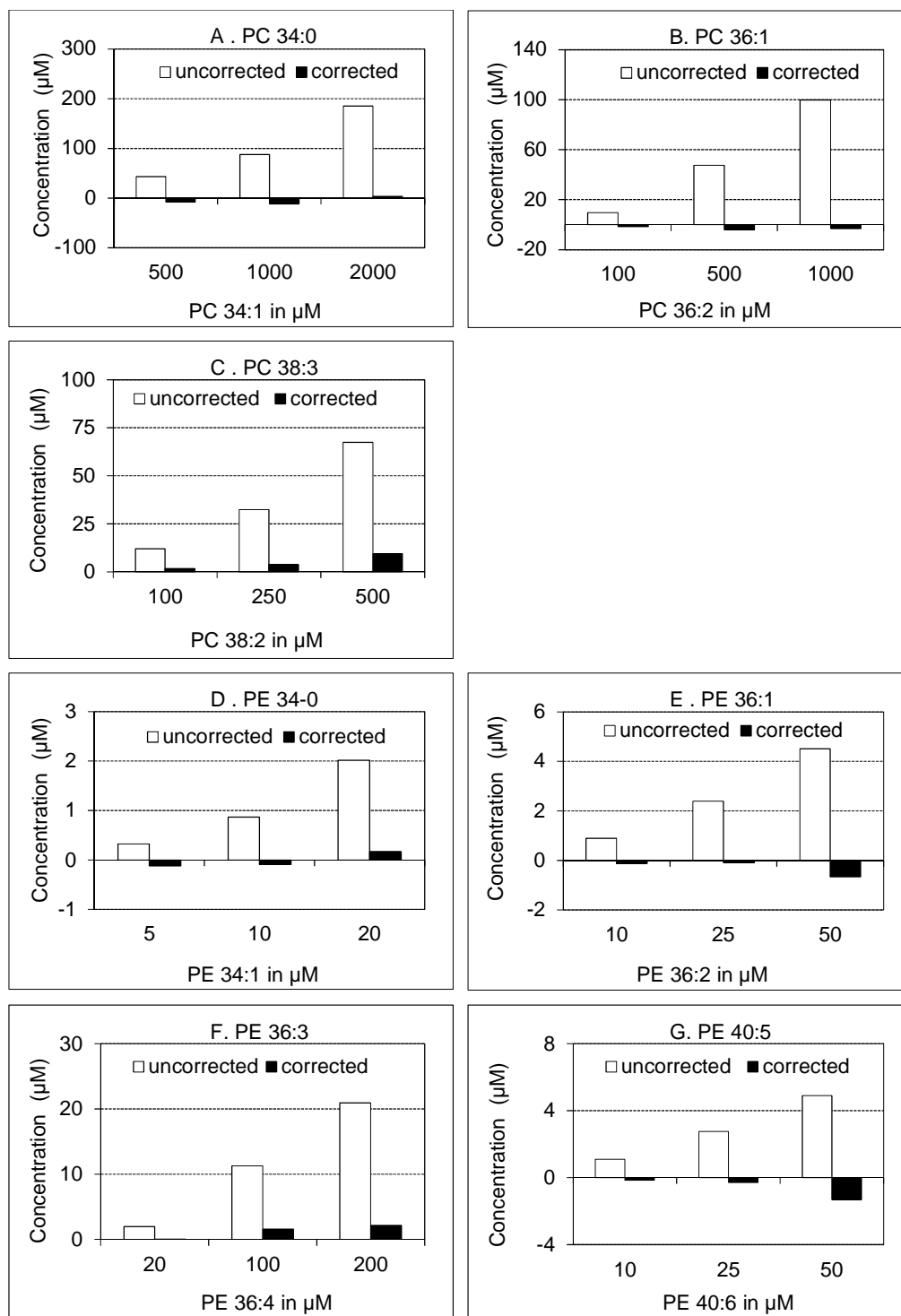
Fig. 38. Performance of the isotopic correction algorithm used for the quantification of phospholipid species. 7 phospholipid standards were spiked to water at three different concentration levels (abscissas). The concentration of the M+2 isotope that is overlapping with the spiked standard having one less double bond was determined, before (white) and after (black) isotopic correction (ordinates). A: Determined PC 34:0 when PC 34:1 was spiked. B: Determined PC 36:0 when PC 36:1 was spiked. C: Determined PC 38:3 when PC 38:4 was spiked. D: Determined PE 34:0 when PE 34:1 was spiked. E: Determined PE 36:1 when PE 36:0 was spiked. F: Determined PE 36:3 when PE 36:4 was spiked. G: Determined PE 40:5 when PE 40:6 was spiked. All concentrations were determined as duplicates.

96

3.4.4   Method validation

The validation of the PC/PE species method was conducted according to the FDA guidelines [97]. The validation procedure was adjusted for the profiling purposes, considering the fact that only one internal and four calibration standards were used for 40 compounds. In particular, a deviation of ± 20% from nominal values (e.g. for calibrators) and 20% variation (e.g. for precisions) were accepted, in contrast to usually 15% recommended by the FDA.

3.4.4.1   Carry-over effects

To exclude potential sample-to-sample carry-over of the lipids, a plasma pool sample containing high analyte concentrations was injected 5 times in a row, followed by a blank sample (MeOH). The entire procedure was repeated three times. No significant carry-over (< peak area at limit of detection) could be detected in the blank samples (refer to Appendix "7.7 Investigation of carry-over effects for PC and PE species").

3.4.4.2   Calibration and LLOQ

A 6 and 7 point calibration was performed for PE and PC species, respectively, using duplicates for each calibration level. The internal standards and phospholipid standards were added to water prior to sample extraction.

The obtained calibration curves were linear in the range of 0.5 µM up to 2000 µM (Table 24), with coefficients of determination (R^2) > 0.99. The achieved lower limits of quantification (LLOQ) of 0.5 µM were comparable or better than those reported in the literature [48,132,133]. The LLOQ was defined as the lowest concentration which could be robustly quantified (CV ≤ 20% in 6 different matrix samples).

3.4.4.3   Recoveries

Recoveries achieved with the modified Bligh and Dyer extraction method were determined for 8 representative phospholipid standards at 2 different concentration levels (medium, high). Recoveries were calculated as the area ratio of the analytes spiked to a plasma pool before and after extraction (N = 6). To account only for losses during plasma extraction, the internal standard mix was spiked to all samples prior to extraction. As expected, PC species were almost completely recovered (88% - 106%), whereas PE species showed slightly lower extraction yields, however still within an acceptable range of 73% - 89% (Table 24).

Table 24. Validation data of the HILIC-MS/MS method obtained for the 4 PC and 4 PE standard compounds. Observed recoveries determined by spiking a plasma pool at 2 different concentration levels. LLOQ for all phospholipids species was found to be 0.5 µM.

Lipid species	Level spiked	Recovery[p] N = 6	CV[w] at LLOQ N = 6	Linear range[w]	$R^{2\ w}$
	(µM)	(%)	(%)	(µM)	
PC 34:1	0.5	-	9.2	0.5 – 2000	0.9974[†]
	100	106.2	-		
	1000	96.2	-		
PC 36:2	0.5	-	8.7	0.5 – 1000	0.9999[†]
	50	88.9	-		
	500	94.4	-		
PC 38:4	0.5	-	9.8	0.5 – 500	0.9996[†]
	50	97.5	-		
	250	89.7	-		
PC 40:0	0.5	-	5.3	0.5 – 100	0.9995[†]
	10	87.8	-		
	50	101.7	-		
PE 34:1	0.5	-	8.8	0.5 – 20	0.9992[‡]
	2.5	78.8	-		
	10	89.1	-		
PE 36:2	0.5	-	7.4	0.5 – 50	0.9997[‡]
	5	79.0	-		
	25	72.9	-		
PE 36:4	0.5	-	14.0	0.5 – 200	0.9998[‡]
	5	77.5	-		
	100	73.7	-		
PE 40:6	0.5	-	13.2	0.5 – 50	0.9999[‡]
	5	76.5	-		
	25	73.3	-		

[p]: analysis performed in a plasma pool. [w]: analysis performed in water. [†]N = 7, [‡]N = 6. For linear range the concentration levels were analyzed as duplicates.

3.4.4.4 Precision and accuracy

Method accuracy was determined by spiking the 8 phospholipid standards (together with the ISs) into water at 3 different levels, covering the entire calibration range. Observed accuracies were between 90.3% and 111.7% for medium and high levels, and between 80.0% and 106.9% for levels at the LLOQ (Table 25). Precisions were determined by analyzing 3 different un-spiked plasma pools at three different concentration levels. The pools were obtained by diluting the unspiked plasma pool (high) 1:1 (v:v, medium) and 1:3 (v:v, low) with water. Intra- and interday imprecisions (defined as the CV of repeated

analyses) were below 20% for all analytes at levels above the LLOQ. For PCs, the average imprecision was 6.8% for intra- and 10.9% for interday analysis. For PEs, the average imprecision were 14.7% for intraday and 16.4% for interday analysis (Table 26). As expected, CVs tend to be higher at lower concentration levels. That might be the reason for the commonly higher CVs of PE species as compared to the PC species (Fig. 34 A, B).

Table 25. Intra- and interday accuracies for PC and PE standards spiked to water at 3 different concentrations.

PL standard	Level spiked (µM)	Accuracy (%)	
		Intraday[†]	Interday[‡]
PC 34:1	0.5	98.6	80.0
	1000	102.4	103.7
	2000	90.3	98.1
PC 36:2	0.5	105.4	100.4
	500	98.8	99.6
	1000	94.4	101.7
PC 38:4	0.5	89.7	97.4
	250	96.8	93.2
	500	96.6	99.6
PC 40:0	0.5	93.4	91.5
	50	94.7	97.3
	100	105.6	104.9
PE 34:1	0.5	103.2	91.9
	10	98.5	101.5
	20	106.9	111.7
PE 36:4	0.5	94.5	81.1
	100	95.7	91.4
	200	93.4	99.2
PE 36:2	0.5	87.1	87.7
	25	96.2	91.2
	50	101.7	107.0
PE 40:6	0.5	93.1	106.9
	25	98.2	94.7
	100	105.7	99.5

[†]N = 6 for 0.5 µM and N = 5 for all other concentrations. [‡]N = 6.

3.4.4.5 Post-preparative stability

Post-preparative sample stability was assessed by comparing the concentrations when analyzing the extracts immediately after sample work-up with those measured 5 days later.

3. Results

The extracts were stored at 10°C (auto-sampler conditions) and analyzed as triplicates. The accuracies were between 86.8% and 114.8% for PCs and between 86.3% and 119.6% for PEs. This finding proves post-preparative stability is sufficient for practical purposes (Table 26).

Table 26. Intra- and interday precisions as well as post-preparative stability of phospholipids determined in three different human plasma pools.

Lipid	Standard used for quantification	Intraday precision CV N = 5 (%)			Interday precision CV N = 6 (%)			Post-preparative stability* (expressed as accuracy) N=3 (%)
		Low	Medium	High	Low	Medium	High	High
PC 30:0	PC 34:1	< LLOQ	11.1	11.1	< LLOQ	13.5	11.2	98.5
PC 32:2	PC 34:1	< LLOQ	14.3	3.1	< LLOQ	14.1	7.6	111.6
PC 32:1	PC 34:1	6.1	12.3	9.1	5.8	8.2	9.7	95.0
PC 32:0	PC 34:1	4.0	7.2	7.2	12.9	7.5	9.7	105.7
PC 34:4	PC 34:1	< LLOQ	14.6	8.8	< LLOQ	13.1	14.0	86.8
PC 34:3	PC 34:1	14.0	10.3	10.2	11.3	11.6	4.1	96.6
PC 34:2	PC 34:1	8.4	11.8	5.4	14.0	7.2	6.5	101.8
PC 34:1	PC 34:1	5.9	5.5	6.8	8.3	5.0	8.2	105.3
PC 36:5	PC 36:2	9.2	7.6	4.8	14.4	10.9	7.6	100.1
PC 36:4	PC 36:2	5.3	5.3	4.6	14.1	7.0	13.3	102.0
PC 36:3	PC 36:2	8.1	6.4	7.9	10.1	8.6	6.4	107.1
PC 36:2	PC 36:2	8.6	4.1	5.0	11.3	10.3	6.4	107.9
PC 36:1	PC 36:2	13.6	6.7	6.4	12.9	13.2	10.0	100.1
PC 36:0	PC 36:2	< LLOQ	14.0	14.2	< LLOQ	19.3	7.1	96.7
PC 38:7	PC 38:4	11.2	10.1	10.5	6.5	9.4	13.4	101.5
PC 38:6	PC 38:4	8.0	7.4	4.2	14.5	5.4	8.1	102.4
PC 38:5	PC 38:4	11.9	6.3	6.8	7.0	6.3	10.9	106.6
PC 38:4	PC 38:4	8.6	8.6	4.0	12.0	9.9	6.3	103.7
PC 38:3	PC 38:4	9.3	6.7	4.1	14.0	7.7	8.7	108.5
PC 38:2	PC 38:4	< LLOQ	12.3	9.3	< LLOQ	14.3	13.4	97.5
PC 38:1	PC 38:4	< LLOQ	< LLOQ	8.5	< LLOQ	< LLOQ	18.6	107.2
PC 38:0	PC 38:4	13.2	14.7	8.5	12.4	14.8	11.6	100.6
PC 40:7	PC 40:0	10.4	5.1	9.5	12.0	13.4	9.7	105.1
PC 40:6	PC 40:0	9.3	5.5	7.9	8.7	14.3	7.5	106.4
PC 40:5	PC 40:0	7.8	4.3	3.8	14.4	11.1	11.1	114.6
PC 40:4	PC 40:0	13.0	6.6	11.7	12.4	14.8	11.0	107.7
PC 40:3	PC 40:0	< LLOQ	14.2	8.3	< LLOQ	16.1	6.8	114.8
PC 40:2	PC 40:0	< LLOQ	14.6	11.7	< LLOQ	18.0	8.7	107.9
PC 40:1	PC 40:0	< LLOQ	< LLOQ	15.1	< LLOQ	< LLOQ	13.8	96.1
PC 40:0	PC 40:0	< LLOQ	14.8	14.9	< LLOQ	17.4	13.4	100.4
PC 42:0	PC 40:0	< LLOQ	< LLOQ	14.6	< LLOQ	< LLOQ	15.6	110.2
PE 34:2	PE 34:1	< LLOQ	13.5	13.4	< LLOQ	19.5	17.5	106.2
PE 34:1	PE 34:1	< LLOQ	< LLOQ	19.5	< LLOQ	19.1	16.6	86.3
PE 36:4	PE 36:2	< LLOQ	12.8	11.0	< LLOQ	16.7	17.6	107.9
PE 36:3	PE 36:2	< LLOQ	8.3	11.0	< LLOQ	16.8	14.8	91.9
PE 36:2	PE 36:2	18.2	13.7	11.3	17.3	11.7	19.7	90.9
PE 38:6	PE 36:4	< LLOQ	19.9	16.6	< LLOQ	11.6	16.2	88.3
PE 38:5	PE 36:4	< LLOQ	< LLOQ	18.5	< LLOQ	< LLOQ	13.1	119.6
PE 38:4	PE 36:4	17.5	13.9	14.3	15.6	19.8	13.2	87.7
PE 40:6	PE 40:6	< LLOQ	< LLOQ	13.9	< LLOQ	< LLOQ	17.3	110.6

Unspiked plasma pool (high), pool diluted 1:1 (v:v) with water (medium) and 1:3 (v:v) with water (low). *Post-preparative stability was observed in the plasma samples after storage at 10°C for 5 days.

3.4.5   Phospholipid species profiles in the study plasma samples

The validated HILIC-MS/MS method was applied to the 50 plasma samples derived from smokers and non-smokers of the clinical study. The purpose of this investigation was to prove whether the observed altered total fatty acid profile in plasma is also reflected in the plasma PC and PE profiles.

For this investigation, 8 QC samples, obtained from a plasma pool (refer to Section "3.4.4.4 Precision and accuracy"), were prepared with the study samples and randomly measured within the batch. To ensure the reproducibility of the method, the CVs for all phospholipids that were used for the validation were calculated. The average CV was 12.8% for PCs (N = 31 different species) and 14.6% for PEs (N = 9 different species), which confirms the reproducibility of the method (Fig. 39). Only one PC (PC 36:4) shows a CV of 22.2%, which is acceptable for a profiling method. The accuracies of the QC samples were, on average, 109.6% for PCs and 87.3% for PEs (Fig. 40).
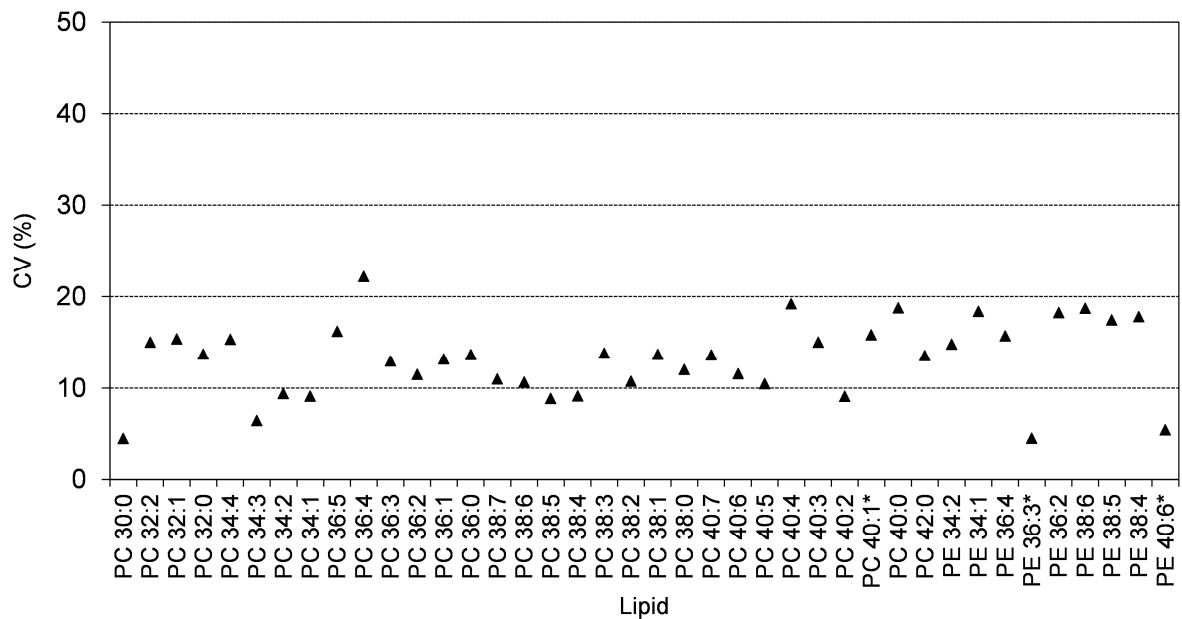
Fig. 39. Precision of PE and PC species determined with 8 plasma QC samples by the HILIC-MS/MS method. *N=7 after removal of an outlier according to the Nalimov test (find individual data in Appendix "7.8 QC samples for PC and PE profiling").
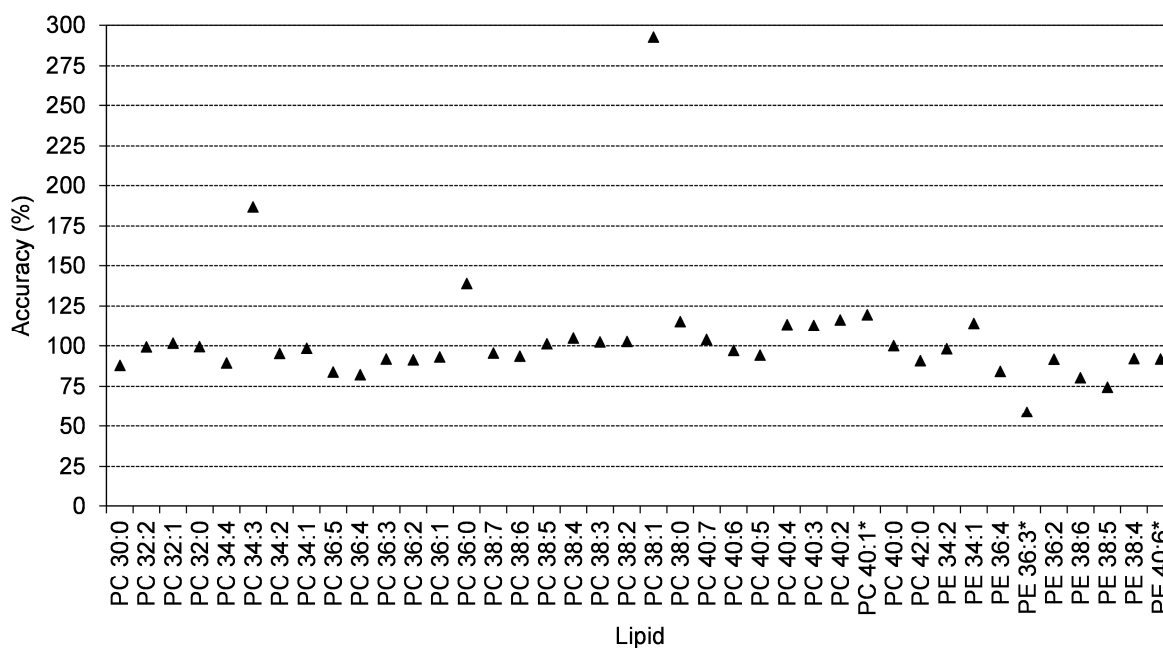
Fig. 40. Accuracy of PE and PC species determined in 8 plasma QC samples by the HILIC-MS/MS. *N=7 after removal of an outlier according to the Nalimov test (find individual data in Appendix "7.8 QC samples for PC and PE profiling").

From all measured molecular PC species, 33 were above the LLOQ (see Appendix "7.9 PC and PE species levels in plasma by HILIC-MS/MS"). Concentrations for the major PC species in the study plasma samples were, on average, monounsaturated PCs with 300.7 µM (comprising 18.3% of all PCs) and diunsaturated PCs with 657.5 µM (comprising 41.2% of all PCs). PC 34:2, PC 34:1 and PC 36:2 were the most abundant species measured in plasma exhibiting concentrations of 419.2 ± 113.5 µM, 258.8 ± 107.2 µM and 226.4 ± 71.2 µM, respectively. Twelve out of 40 analyzed PE species were above the LLOQ (0.5 µM). PE concentrations were about 100-fold lower than those of PC species. The major PE species contain higher unsaturated fatty acid side chains as compared to PC species. Particularly, major PE species had two (23.9%, 4.9 µM) and four double bonds (34.4%, 6.8 µM). PE 38:4 and PE 36:2 showed the highest concentrations of 5.4 ± 3.4 µM and 3.7 ± 2.7 µM, respectively.

Since relative phospholipid composition is more important for physiological effects such as membrane fluidity, the relative profiles were calculated for each lipid, by dividing the concentration of each phospholipid species to the total concentration of the respective phospholipid class. In smokers' plasma, PC 36:0, PC 38:7 and PC 38:6 were found to be significantly decreased (p < 0.039) whereas PC 36:1 was significantly increased (p < 0.034). Analysis of PE species profiles revealed significant increased percentages of PE 36:2 and PE 38:5 in smokers (p < 0.042), accompanied by a significant decrease of PE 36:3 and

PE 38:4 (p < 0.020) (Table 27). The latter is by far the most abundant PE species (27.9%) in human plasma and mainly composed of FA 18:0 and FA 20:4 [136]. Table 27 depicts the phospholipid profiles of PE and PC species in plasma of smokers and non-smokers from the clinical study. The most likely fatty acid composition is stated for the species found to be significant different between smokers and non-smokers.

Table 27. PE and PC species profiles in plasma of smokers and non-smokers.

Lipid species	PL composition (mole %, mean ± SEM)		S/NS	p-value	Most probable FA constituents in the lipids
	NS†	S†			
PC 30:0	0.13 ± 0.0097	0.11 ± 0.0068		0.24	
PC 32:2	0.19 ± 0.0095	0.17 ± 0.017		0.35	
PC 32:1	0.70 ± 0.083	0.71 ± 0.051		0.90	
PC 32:0	0.70 ± 0.029	0.70± 0.025		0.89	
PC 34:4	0.10 ± 0.0057	0.099 ± 0.0067		0.71	
PC 34:3	1.31 ± 0.054	1.25 ± 0.049		0.41	
PC 34:2	26.6 ± 0.71	26.0 ± 0.76		0.59	
PC 34:1	15.4 ± 0.60	16.1 ± 0.64		0.44	
PC 36:5	1.32 ± 0.068	1.21 ± 0.072		0.31	
PC 36:4	9.51 ± 0.37	9.16 ± 0.37		0.50	
PC 36:3	7.05 ± 0.23	7.21 ± 0.23		0.63	
PC 36:2	14.3 ± 0.60	14.1 ± 0.45		0.85	
PC 36:1	1.55 ± 0.12	1.87 ± 0.073	↑	0.034	PC 18:0/18:1 [137-139]
PC 36:0	0.24 ± 0.019	0.19 ± 0.012	↓	0.039	PC 18:0/18:0 [138]
PC 38:7	0.29 ± 0.017	0.24 ± 0.011	↓	0.020	PC 18:1/20:6 [136] or PC16:1/22:6 [139]
PC 38:6	4.49 ± 0.20	3.80 ± 0.20	↓	0.019	PC 16:0/22:6 [137-139]
PC 38:5	3.57 ± 0.15	3.68 ± 0.14		0.60	
PC 38:4	6.70 ± 0.35	7.31 ± 0.38		0.24	
PC 38:3	2.60 ± 0.13	2.93 ± 0.18		0.15	
PC 38:2	0.45 ± 0.046	0.41 ± 0.034		0.54	
PC 38:1	0.14 ± 0.013	0.12 ± 0.0089		0.33	
PC 38:0	0.19 ± 0.022	0.17 ± 0.012		0.42	
PC 40:7	0.29 ± 0.019	0.29 ± 0.018		0.97	
PC 40:6	1.09 ± 0.075	0.94 ± 0.076		0.15	
PC 40:5	0.50 ± 0. 038	0.58 ± 0.040		0.16	
PC 40:4	0.21 ± 0.020	0.21 ± 0.015		0.91	
PC 40:3	0.060 ± 0.0047	0.065 ± 0.0066		0.53	
PC 40:2	0.13 ± 0.012	0.12 ± 0.0083		0.67	
PC 40:1	0.055 ± 0.0040	0.052 ± 0.0037		0.66	
PC 40:0	0.11 ± 0.0076	0.10 ± 0.0048		0.32	
PC 42:5	0.035 ± 0.0021	0.036 ± 0.0020		0.75	
PC 42:4	0.036 ± 0.0036	0.033 ± 0.0029		0.58	
PC 42:0	0.059 ± 0.0047	0.052 ± 0.0031		0.24	
PE 34:2	5.29 ± 0.59	6.41 ± 0.69		0.23	
PE 34:1	4.82 ± 0.8	3.96 ± 0.44		0.34	
PE 36:4	5.97 ± 0.55	6.41 ± 0.69		0.63	
PE 36:3	5.79 ± 0.65	3.93 ± 0.41	↓	0.020	PE 18:1/18:2 [136]
PE 36:2	16.1 ± 1.26	20.1 ± 1.46	↑	0.042	PE 18:0/18:2 [136] or PE 18:1/18:1
PE 36:1	3.72 ± 0.52	3.4 ± 0.62		0.69	
PE 38:6	6.45 ± 0.55	8.13 ± 0.71		0.067	
PE 38:5	7.29 ± 0.66	9.49 ± 0.77	↑	0.035	PE 18:1/20:4 [136]
PE 38:4	32.1 ± 2.15	23.8 ± 1.9	↓	0.0060	PE 18:0/20:4 [136]
PE 38:3	2.57 ± 0.6	3.95 ± 0.54		0.096	
PE 40:6	6.44 ± 0.62	7.24 ± 0.84		0.45	
PE 40:5	3.46 ± 0.68	3.16 ± 0.52		0.73	

†N = 25. P-values calculated with Welch's t-test. ↑: Increased in smokers. ↓: Decreased in smokers.

3.5 Determination of tyramine in saliva

In the metabolic fingerprinting analysis of saliva, tyramine was found to be significantly increased in smokers compared to non-smokers. Since tyramine is a physiological and neurological active compound, this finding was further investigated. For this purpose, a targeted method was developed, for the quantification of tyramine using HILIC-MS/MS methodology. The method uses a simple sample preparation consisting of a precipitation of salivary mucins and proteins with methanol. Tyramine and d_4-tyramine (used as an IS for quantification) eluted at 4.1 min with a well-defined narrow peak shape and a peak width of 0.2 min (Fig. 41). Total chromatographic runtime of the method was 10 min. The retention time was stable during batch analysis consisting of 93 samples (study samples, calibrators, QC samples, blanks). The CV for the retention time was calculated to be 0.18%.
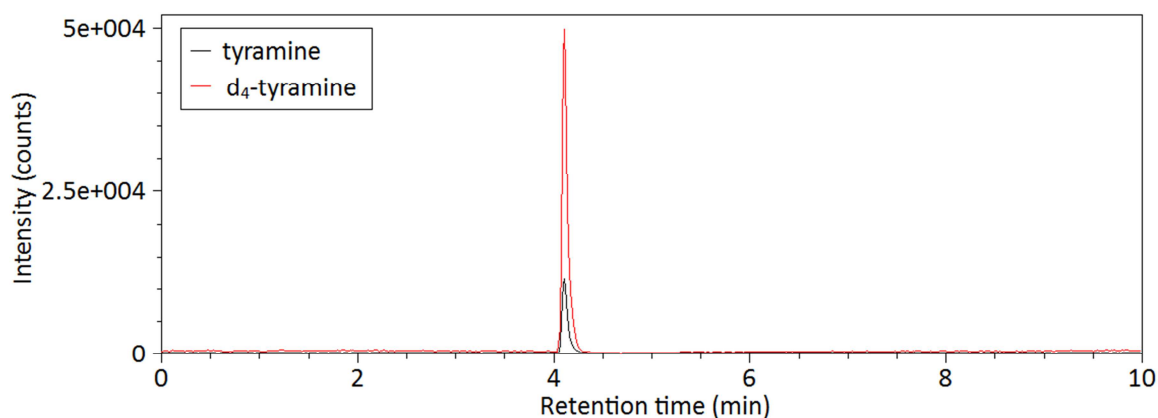
Fig. 41. Chromatogram of tyramine (MRM m/z 138 $\rightarrow$ m/z 121) and spiked d_4-tyramine (MRM m/z 142 $\rightarrow$ m/z 125) in saliva (spiking level was 500 nM). Analysis was performed by means of the described HILIC-MS/MS methodology.

3.5.1 Calibration

For calibration, nine concentration levels in the range of 10 nM and 50 μM were spiked into saliva and analyzed in duplicates. The method showed linearity after 1/y weighting over three orders of magnitude ranging from 10 nM to 50 μM with a coefficient of determination of 0.993 (Fig. 42).
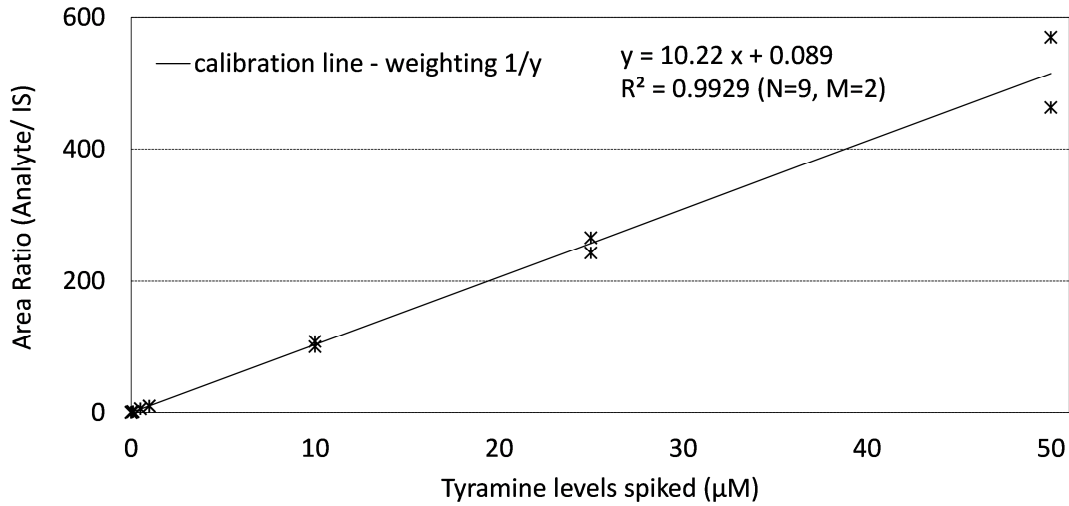
Fig. 42. Calibration line of tyramine in saliva weighted 1/y.

3.5.2   Intraday accuracy and precision

Intraday accuracies were determined at 20 nM (N = 5) and 500 nM (N = 5) with spiked saliva samples. Accuracies were found to be 100.4% at 20 nM and 98.0% at 500 nM. Intraday CVs were 10.8% and 4.7% for 20 nM and 500 nM, respectively (Fig. 43, raw data in Appendix "7.10 Validation and QC data for tyramine determination in saliva").
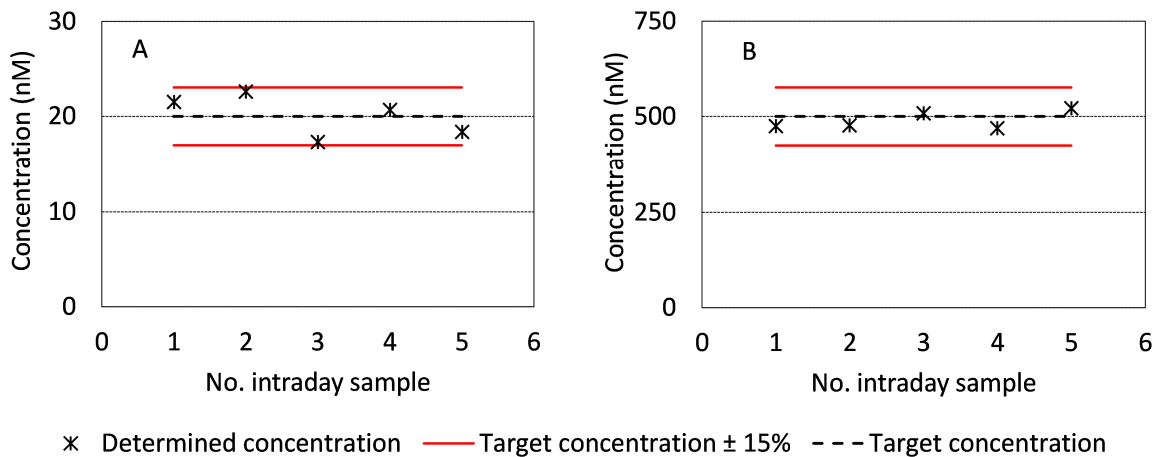
Fig. 43. Intraday precision of tyramine in saliva. A: 20 nM, CV = 10.8%, accuracy = 100.4%. B: 500 nM, CV = 4.7%, accuracy = 98.0%.

3.5.3   Tyramine in study saliva samples of smokers and non-smokers

To quantify the levels of tyramine in saliva of smokers and non-smokers, the saliva samples from TP1 to TP5 (collected on Day 1: 10 am, 2 pm, 6 pm, 10 pm and Day 2: 8 am) were analyzed by means of the HILIC-MS/MS method. All time points were measured in separate batches on different days. To prove reproducibility of the method, QC samples were analyzed within each batch. The CVs for the QC samples were below 15% and the accuracies were between 85% and 115% (Fig. 44 A and B), indicating that the requirements of the FDA [97] for method reproducibility are fulfilled (for raw data refer to Appendix "7.10 Validation and QC data for tyramine determination in saliva").
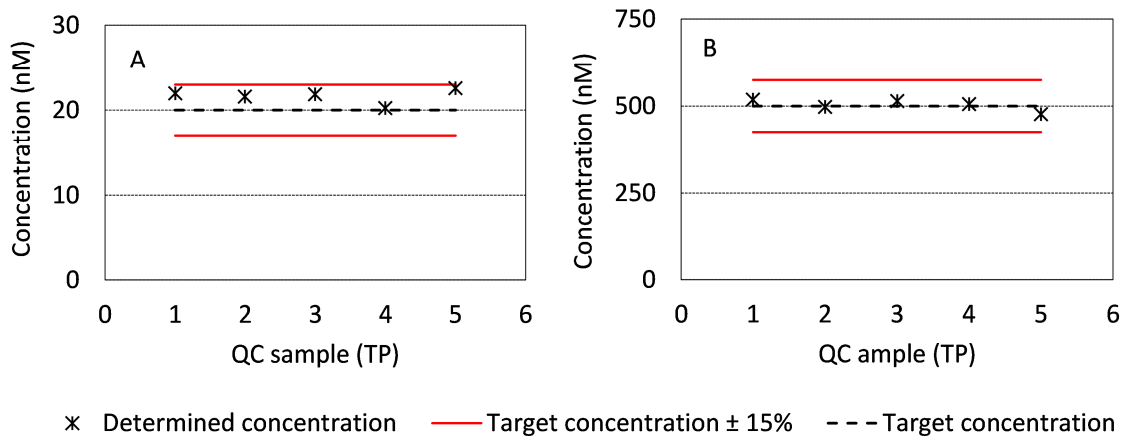
Fig. 44. Tyramine QC samples analyzed in the batch of saliva study samples using HILIC-MS/MS. A: 20 nM of tyramine spiked to saliva and measured within each batch of the respective time points. B: 500 nM of tyramine spiked to saliva and measured in the 5 batches (5 time points).

Evaluation of the study samples revealed that most of the smokers showed tyramine levels within the linear range of the method. Except for TP 1, 2 and 3, one smoker had levels below the LLOQ (10 nM). There were 11, 13, 13, 14 and 1 non-smoking subjects exhibiting below LLOQ tyramine levels in saliva for the TPs 1 to 5, respectively (Fig. 45, raw data in Appendix "7.11 Tyramine levels in saliva"). Levels < LLOQ were calculated by extrapolation. For both groups, the average concentrations were highest at TP 5. Median levels were 18.6 nM (TP1), 8.6 nM (TP2), 9.1 nM (TP3), 5.7 nM (TP4) and 57.8 nM (TP5) in saliva of non-smokers and 1.9 µM (TP1), 1.2 µM (TP2), 1.6 µM (TP3), 2.3 µM (TP4) and 4.3 µM (TP5) in saliva of smokers. Thus, at each time point, smokers' tyramine levels in saliva were multifold increased compared to non-smokers, in particular 104-fold (TP1), 141-fold (TP2), 173-fold (TP3), 402-fold (TP4) and 74.4-fold (TP5). This increase was highly significant, with

p-values between $1.0 \cdot 10^{-7}$ and $2.6 \cdot 10^{-7}$ (Mann-Whitney U test). The highest concentration of tyramine in the 250 (5 time points, 50 subjects) saliva samples of non-smokers was 7.8 µM. In 14 samples, no tyramine was detectable. Whereas, in all samples of the smokers (N = 250), tyramine was detectable. Smokers' tyramine levels ranged from 7.2 nM up to 41.5 µM.
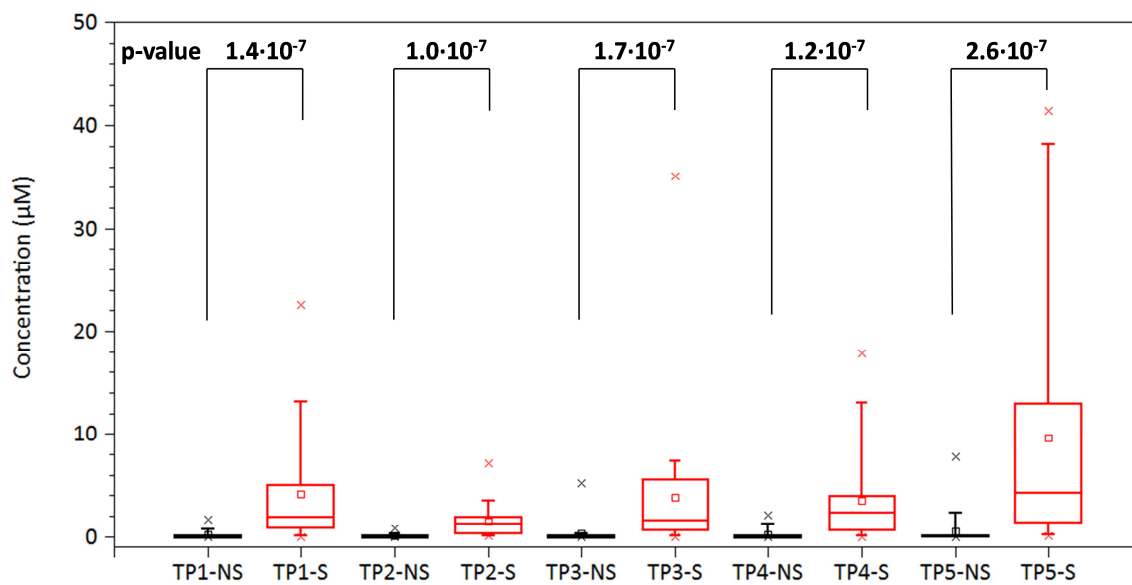
Fig. 45. Tyramine measured in saliva of 25 smokers (S) and 25 non-smokers (NS) at 5 different time points (TP). P-Values (p) were calculated with Mann-Whitney U test.

In order to check the validity of the results obtained with the metabolic fingerprinting method, the correlation between the tyramine concentrations obtained with the targeted LC-MS/MS method and the peak area ratios of the most abundant tyramine fragment (*m/z* 174, 17.9 min) to the IS d_4-ttMA from the untargeted GC-TOF-MS method was investigated. A strong correlation with a correlation coefficient of r = 0.990 (p = $6.9 \cdot 10^{-21}$, Pearson) was found (Fig. 46), providing further evidence for the validity of the metabolic fingerprinting methodology applied.
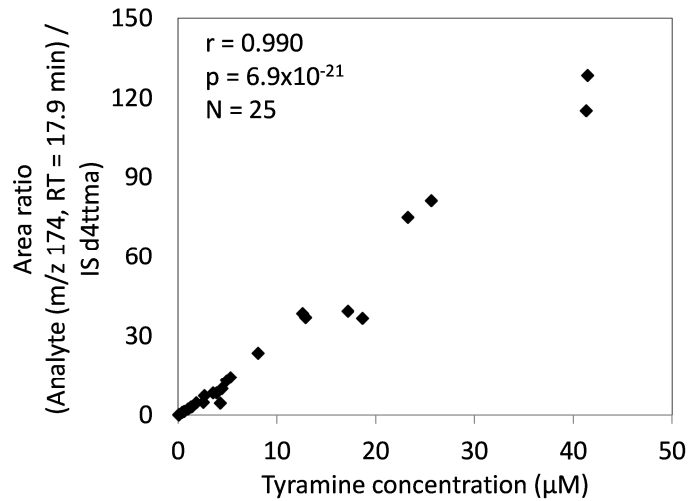
Fig. 46. Correlation of tyramine levels, determined with different methodologies. Ordinate: Metabolic fingerprinting approach using GC-TOF-MS. Abscissa: Quantified levels using a validated LC-MS/MS method. r: Pearson's correlation coefficient. The correlation was performed with the saliva samples of smokers from TP5.

Salivary tyramine concentrations in smokers correlated only weakly with nicotine uptake ($r = 0.415$, $p = 4.5 \cdot 10^{-2}$, Spearman) as determined by the nicotine equivalents in urine and did not significantly correlate with the number of cigarettes smoked during the clinical study ($r = 0.354$, $p = 8.9 \cdot 10^{-2}$)(Fig. 47), suggesting that there is no simple dose-response relationship between salivary tyramine levels and smoking, despite of the observed large difference between smokers and non-smokers in this metabolite.
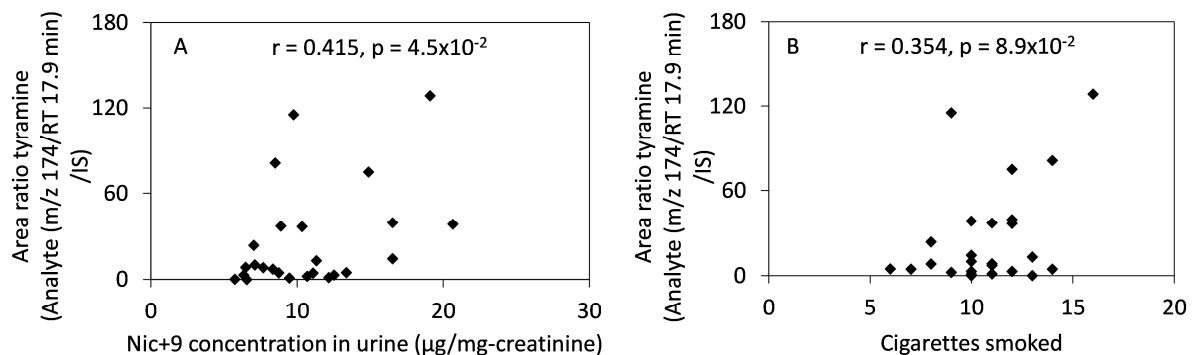
Fig. 47. Relationship between salivary tyramine and urinary nicotine equivalents (Nic+9) (A) as well as number of cigarettes smoked during study Day 1 (B). r: correlation coefficient according to Spearman. N = 25.

4 Discussion

4.1 Metabolic fingerprinting

4.1.1 Metabolic fingerprinting validation

There is a lack of knowledge about the underlying metabolic pathways as a consequence of smoking. Perturbations on metabolic levels will help to understand the pathogenesis of smoking related diseases. However, identification of such biomarkers is challenging. GC-TOF-MS can be applied for a metabolic fingerprinting in human body fluids to investigate significantly altered metabolic patterns due to smoking. These patterns can be used for a group separation and may identify physiological changes and affected metabolic pathways that may be linked to early biological effects possibly related to a disease occurring later in time. A GC-TOF-MS method was established and validated for metabolic fingerprinting in saliva, urine and plasma. For validation of the method, 36 or 37 reference compounds were spiked to respective sample pools in order to assess the method performance including repeatability, reproducibility, linearity and stability. To the best of the author's knowledge, up to now such a comprehensive validation of a metabolic fingerprinting method using GC-TOF-MS has not been applied to human plasma, saliva or urine. The method consists of a straight forward sample preparation, including protein precipitation, followed by a 2-step derivatization comprising of oximation and silylation and, in case of urine samples, urea digestion. This sample work-up procedure allows the analysis of the most important classes of metabolites in the body fluids of interest. Linear response ranges between 1 µM to 2 mM were obtained for most of the spiked reference compounds in the three different matrices which is slightly better than that reported for similar approaches [110,113]. For some spiked metabolites, for example citric acid and creatinine in urine or glucose in plasma, no linearity in the studied concentrations range was achieved. This could partly be caused by the fact that some metabolites are present at relatively high levels in the pool matrix, such as citric acid in urine and glucose in plasma. An unimpeded validation would only be possible by using an artificial, analyte-free matrix as described by Jacob et al. 2007 for urine [140]. However, the suitability of artificial matrices for these validation experiments is questionable for other reasons. Certainly, some metabolites without or with just a small linear range will benefit from the utilization of other calibration curves, for example a quadratic calibration line. In general, one has to consider that metabolic fingerprinting methods, which try to cover a variety of different chemical classes, must compromise different analytical parameters, for instance solubility, stability, influence of the

matrix, and derivatization, concentration ranges, amongst others. For metabolomic approaches, comprehensiveness and overall dynamic range for a large number of analytes and chemical classes, are considered more important than achieving very low detection limits or comprehensive linear calibration ranges for single metabolites [14].

There are no such unbiased metabolic fingerprinting approaches available, since a single analytical platform is only applicable for a subset of metabolites. The applied GC-TOF-MS method is only applicable to analytes which are volatile and thermic stable or can easily be converted (derivatized) to compounds with these properties. Organic acids and amino acids showed exceptionally good results in the validation experiments.

4.1.2 Metabolic fingerprinting in body fluids of smokers and non-smokers

In general, one has to consider that cigarette smoke contains more than 5000 compounds [7]. Hence, the differentiation between metabolites of exogenous and endogenous origin is challenging. In many cases, it must be assumed that the assessed metabolites can originate from both sources. The applied study design (standardization and control of all factors so that smoking is the 'only' difference between the two study groups) allows the simple assumption that metabolites found to be lower in body fluids of smokers compared to non-smokers are most likely of endogenous origin and smoking has probably affected the involved metabolic pathways. For metabolites which were found to be increased in smokers, the smoking-related uptake of the compound itself or a precursor in tobacco smoke must be considered as a possibility. In many cases, quantitative estimates including the possible amounts of uptake by smoking can be helpful in deciding whether smoke uptake or endogenous sources are more important for the observed difference. Some measurable metabolites can be assigned exclusively to tobacco smoke.. This was the case for nicotine and nicotine metabolites. These metabolites (and their assignable fragments) were excluded from further statistical evaluation.

4.1.2.1 Plasma

Under the assay conditions applied for the metabolic fingerprinting, plasma in comparison to urine and saliva showed the lowest number of metabolites valid for differentiating between smokers and non-smokers. As a consequence, the PLS-DA model exhibited the lowest group separation power when compared to the models of urine and saliva. A possible explanation for this finding is that significantly lower sample volume was used for analysis (30µl for plasma instead of 100µl for urine and saliva). Additionally, in terms of homeostasis, blood is certainly better controlled by regulatory mechanisms than

urine or saliva, thus leading to a leveling effect for endogenous metabolites, which may prevent differences between the groups from becoming statistically significant. Despite of that, some differences in metabolite levels were observed, which are presumably altered due to smoking and may indicate early biological effects. The presence of nonanoic acid was unexpected, since odd chain fatty acids are only present at very low concentrations in plasma. Decreased levels are even more remarkable, as they cannot be explained by an uptake from tobacco smoke. However, odd-chain fatty acids are used during gluconeogenesis to form glucose from non-carbohydrates [141], which is promoted by smoking [142]. Therefore, decreased levels of nonanoic acid may be induced by an increased appearance of glucose in the blood of smokers. An increased gluconeogenesis rate would also explain the observed decreased levels of alanine in plasma (Table 22) [143]. Interestingly, it was also found that non-smokers exhibit higher alanine levels in urine (Table 13), which would also be in agreement with an accelerating effect of smoking on gluconeogenesis. The observed increased levels of ornithine and glutamic acid (Table 22) are in agreement with results from Xu et al. 2013 [77].

Furthermore, the metabolic fingerprinting in plasma revealed significantly increased concentrations of MUFAs 16:1 n-7, 18:1 n-9 and most likely 18:1 n-7 and increased levels of cholesterol in smokers as compared to non-smokers. There were only healthy and non-obese subjects included in the clinical study and a standardized diet was served for 24 hours as suggested by Winnike et al. 2009 [83]. It is assumed that a prolonged standardized diet would not improve results by reducing variation of the metabolite levels [83]. Therefore one can assume that the alteration in the fatty acid metabolism is most likely an effect of smoking.

4.1.2.2 *Urine*

The observed strong correlation between nicotine and its metabolites (Cot, OH-Cot) obtained by the metabolic fingerprinting and a validated targeted LC-MS/MS method proves the suitability of the untargeted GC-TOF-MS method (Fig. 18). In particular, the applied sample preparation procedure as well as the adjusted settings for automated peak picking and integration in the *MZmine* software turned out to be suitable for the intended purpose. Prior digestion of urea (urease) was necessary because of the high levels of urea present in urine. However, the utilization of urease certainly alters other metabolite profiles [70].

4-Oxopentanoic acid was found to be significantly increased in smokers' compared to non-smokers' urine (Table 13). In addition, a correlation with the urinary Nic+9 levels in smokers was observed (Fig. 22), suggesting a dose-response relationship of this metabolite with smoking. 4-Oxopentanoic acid is used as flavorant additive in cigarettes. This additive is reported to reduce the pH of cigarette smoke and to desensitize the upper respiratory tract

[144]. Both properties of 4-oxopentanoic acid increased the inhalability of cigarette smoke deeper into the lungs. Furthermore, it also enhances binding of nicotine to neurons which can amplify the effects of nicotine [144]. Taken together, there is some evidence that the tobacco additive 4-oxopentanoic acid can lead to an increase in smoking intensity and may enhance the effect of nicotine. Further metabolites that were significantly decreased in smokers' urine are 2-oxoglutaric acid, pyruvate, uracil and alanine (Table 13). As discussed before, it is most probable that smoking affects metabolic pathways in which these metabolites are involved. Decreased levels of alanine were also found in plasma (Table 22) and strengthen the hypothesis of increased gluconeogenesis triggered by smoking (refer to discussion in Section "4.1.2.1 Plasma"). Possible smoking-affected metabolic pathways, where these metabolites take part, are discussed in the Section "4.1.2.4 Association to pathophysiological pathways".

The observed increases in the levels of 2-methoxyphenol, quinic acid, glycerol, 1,2-propanediol, 1,4-hydroxyquinone and 3-OH-pyridine are most likely an effect of tobacco smoke uptake. Above all, 1,4-hydroxyquinone is a known metabolite of tobacco smoke containing benzene. Quinic acid is presumably a pyrolysis product of chlorogenic acid contained in tobacco leaves [145].

4.1.2.3   Saliva

Saliva can be used as an alternative matrix for metabolic investigations [59,82,146,147], since it is easily and noninvasively accessible without any health risks and stress for the subjects. Up to now, NMR has been extensively used for metabolite profiling in smokers saliva samples, as it can uniquely identify and sometimes even simultaneously quantify a wide range of organic compounds. However, the time-consuming analysis and interpretation of NMR spectra along with its relatively poor sensitivity [57,58] has made this approach inappropriate for the analysis of a large number of low-abundant metabolites [59].

In this study using GC-TOF-MS, several compounds were found to be significantly increased in smokers' saliva compared to non-smokers. The observed strong correlation between salivary OH-Cot obtained by the metabolic fingerprinting and a validated targeted LC-MS/MS method proves the suitability of the untargeted GC-TOF-MS method.

The elevated levels of some salivary metabolites can be explained by an uptake from tobacco smoke, for example, hexanoic acid or 4-OH-Ph-ethanol. Other metabolites found to be different in smokers and non-smokers, such as adenine, adenosine, or cadaverine are constituents of tobacco leaves, however have not been reported as constituents of tobacco smoke thus far [7]. These metabolites are most likely of endogenous origin and a smoking-related alteration of the metabolism can be assumed. Cadaverine is a product of bacterial decarboxylation of lysine present in proteins. This reaction is reported to occur in the oral

cavity [148]. Results obtained on salivary levels of cadaverine and tyramine (a decarboxylation product of tyrosine) indicates that tobacco smoke exposure might alter the oral flora to the direction of increased protein degradation (Table 18). Further research is required to confirm and extend these observations.

Adenosine is increased in patients suffering from COPD [149], a disease which is causally linked to tobacco smoking. This metabolite is also released upon metabolic stress, cell damage, trauma, ischemia or hypoxia to modulate homeostasis [150]. Adenosine, although unspecific of the biological endpoint of disease, might be a promising effect biomarker candidate for early stage perturbations due to smoking. Further research is certainly required to elucidate the role of adenosine in saliva as a biomarker of smoking induced biological effects. Interestingly, the biogenic amine tyramine showed the highest significance in terms of differences between smokers and non-smokers in the analysis of saliva samples and was increased in smokers by 22-fold (Fig. 29). This metabolite was further investigated by a targeted approach which is discussed in Section "4.4.1 Tyramine in saliva determined by HILIC-MS/MS".

To remove residues from tobacco smoke constituents and nutrition in the oral cavity of smokers, a 9-hour interval of fasting and non-smoking along with an intense rinse technique prior to saliva sampling was conducted. Nicotine, the major constituent of tobacco smoke, was not significantly different between the two groups by the metabolic fingerprinting, which provides strong evidence of the effectiveness of the applied procedure.

As expected, Cot and OH-Cot were found to be significantly elevated in smokers' saliva (Fig. 25). Cot is the most frequently used biomarker for smoking and nicotine exposure. Its' levels in plasma and saliva are highly correlated [151]. Nicotine metabolism most likely takes place in the liver and the lungs. There is evidence that metabolites that are detectable and quantifiable in saliva likely originate from the blood stream from where it is transported by passive and active mechanisms. However, it is well known that the ratios of metabolite levels between blood and saliva can be highly variable and are determined by a number of factors including physico-chemical properties of the compounds, pH and flow rate of the saliva and possibly others [152,153]. Nevertheless, it was not possible to allocate with certainty in which organs or regions of the human body altered metabolism occurs. Admittedly, extensive metabolism takes place within the mouth, since there are over 700 bacterial species [154] and proteins in the oral cavity. It is well known that smoking causes various changes in the flora of the oral cavity [155]. Therefore, alterations from the cavity and a transition from metabolites to the blood and reuptake are theoretically possible, making a distinct assignment of the alterations in metabolite levels between smokers and non-smokers challenging.

4.1.2.4 Association to pathophysiological pathways

In total, 38 metabolites have been identified in all three matrices to be significantly different between smokers and non-smokers (Table 28). These 38 identified metabolites came from a total of 244 compounds, which turned out to be relevant for group separation in multivariate statistics (Table 13, Table 18 and Table 22). For the identified metabolites, the presumed exogenous and/or endogenous origin is outlined in Table 28. These metabolites can be involved in a number of pathways. Final assignment to the pathways, which are of biological/toxicological relevance for smoking-related effects and diseases, is complex and not possible using only the data measured in this thesis as the body fluids represent a cross-section of the metabolism in multiple organs. Nevertheless, the current work demonstrates that most of the smoking-induced biochemical pathway alterations involve the energy, amino acid, lipid and purine metabolism.

4. Discussion

Table 28. Identified metabolites found to be signifcantly changed in their levels in plasma, saliva and urine of smokers as compared to non-smokers.

S/NS	Metabolite	Matrix	Exogenous	Endogenous
↑	1,2-Propanediol	U	TSC [7]	Amino acid metabolism
↓	Pyruvate	U		Amino acid, energy metabolism
↓	L-Ala	U		Amino acid, energy metabolism
↑	3-OH-pyridine	U	TSC [7]	
↑	4-Oxopentanoic acid	U	TSC [7]	
↑	Glucuronic acid	U		Glucuronidation (detoxification)
↑	Methoxyphenol	U	TSC [7]	
↑	Quinic acid	U	TSC [7]	
↑	Gluconic acid	U		Energy metabolism, oxid. stress
↑	Glycerol	U	TSC [7]	
↓	Uracil	U		Detoxification
↑	1,4-Hydroxyquinone	U	TSC [7]	Tyrosine metabolism
↑	3,4-Dihydroxybutanoic acid	U		
↑	Mandelic acid	U	TSC [7]	
↑	4-OH-Cyclohexanecarboxylic acid	U		
↓	2-Oxoglutaric acid	U		Amino acid, energy metabolism
↑	2-Furoylglycine	U	TSC [7]	Lipid metabolism
↑	2,4,5-Trihydroxypentanoic acid	U		
↓	L-Ala	P		Amino acid metabolism
↓	Nonanoic acid	P		Energy metabolism
↑	Glutamic acid	P		Amino acid metabolism
↑	Ornithine	P		Amino acid metabolism
↑	FA 16:1 n-7	P		Lipid metabolism
↑	FA 18:1 n-9	P		Lipid metabolism
↑	FA 18:1 (presumably n-7)	P		Lipid metabolism
↑	Cholesterol	P		Lipid metabolism
↑	Tyramine	S		Tyrosine metabolism [156]
↑	4-OH-Ph-Ethanol	S	TSC [7]	Tyrosine metabolism
↑	Adenosine	S		Purine metabolism
↑	Hexanoic acid	S	TSC [7]	
↑	Adenine	S		Purine metabolism
↑	Cadaverine	S		Lysine metabolism [157]
↓	G6P	S		Energy metabolism
↓	G3P	S		Lipid/energy metabolism
↑	Guanosine	S		Purine metabolism
↑	N-Acetylglucosamine	S		Amino sugar metabolism
↓	Benzenepropanoic acid	S		Tyrosine metabolism
↓	Malic acid	S		Energy metabolism

U: urine, P: plasma, S: saliva. Potential pathways identified using Kegg [158]. TSC: Tobacco smoke constituent.

4. Discussion

In summary, there were several metabolites identified which are significantly different between smokers and non-smokers and part of the carbon metabolism, particularly in the citric and phosphate pentose pathway (Fig. 48). G6P, malic acid and G3P were significantly decreased in saliva of smokers. The latter compound is an intermediate metabolite in the glycolysis pathway and enzymatically converted to glyceraldehyde-3-phosphate. The enzyme which further degrades glyceraldehyde-3-phosphate, namely glyceraldehyde-3-phosphate dehydrogenase (GAPDH), has been shown to be up-regulated as a consequence of tobacco smoke exposure [159,160]. G3P might indicate an up-regulation of GAPDH. Another explanation for significantly decreased levels of G3P is its conversion to phospholipids or triglycerides by re-esterification with fatty acids. This pathway has been shown to be up-regulated in smokers [161]. Furthermore, malate dehydrogenase was found to be up-regulated in human cells, which might lead to enhanced decomposition of malic acid [160,162]. The finding of decreased salivary malic acid levels in this study is in agreement with this observation. G6P takes part in the glucose metabolism, which re-routes to the pentose phosphate pathway in smokers [159]. Therefore, the determined decreased levels of G6P in smokers might be an effect of activation and increased expression of the enzyme glucose-6-phosphate dehydrogenase which decomposes G6P in the pentose phosphate pathway [159]. This finding would explain the decreased levels of pyruvate in urine and alanine in urine and plasma of smokers. GAPDH and malic enzyme are involved in the carbon metabolism, producing nicotinamide adenine dinucleotide phosphate (NADPH). NADPH is an important reducing agent that counteracts reactive oxygen species (ROS) [159]. ROS are present in tobacco smoke and also generated in the organism after tobacco smoke exposure. ROS are most likely to be involved in smoking-related diseases such as cancer, diabetes, atherosclerosis and chronic inflammation [163,164]. The increased expenditure of NADPH, to prevent smokers from ROS, might explain such a shift in the energy metabolism triggered by tobacco smoke.

Increased levels of glutamate and ornithine in plasma of smokers as found in this study are in line with results reported by Xu et al. 2013 [77]. Glutamate concentrations are positively associated with smoking and the incidence of coronary artery disease [77,165]. Additionally, previous investigations indicated that the cysteine-glutamate transporter (antiporter) is activated leading to enhanced transfer of glutamate into the extracellular space and an subsequent increase of ornithine [77,166,167]. The activation of the cysteine-glutamate transporter and the subsequent increased levels of glutamate seem to be triggered by oxidative stress and appear to play an important role in the pathogenesis of atherosclerotic plagues and CVD [77,168-170].
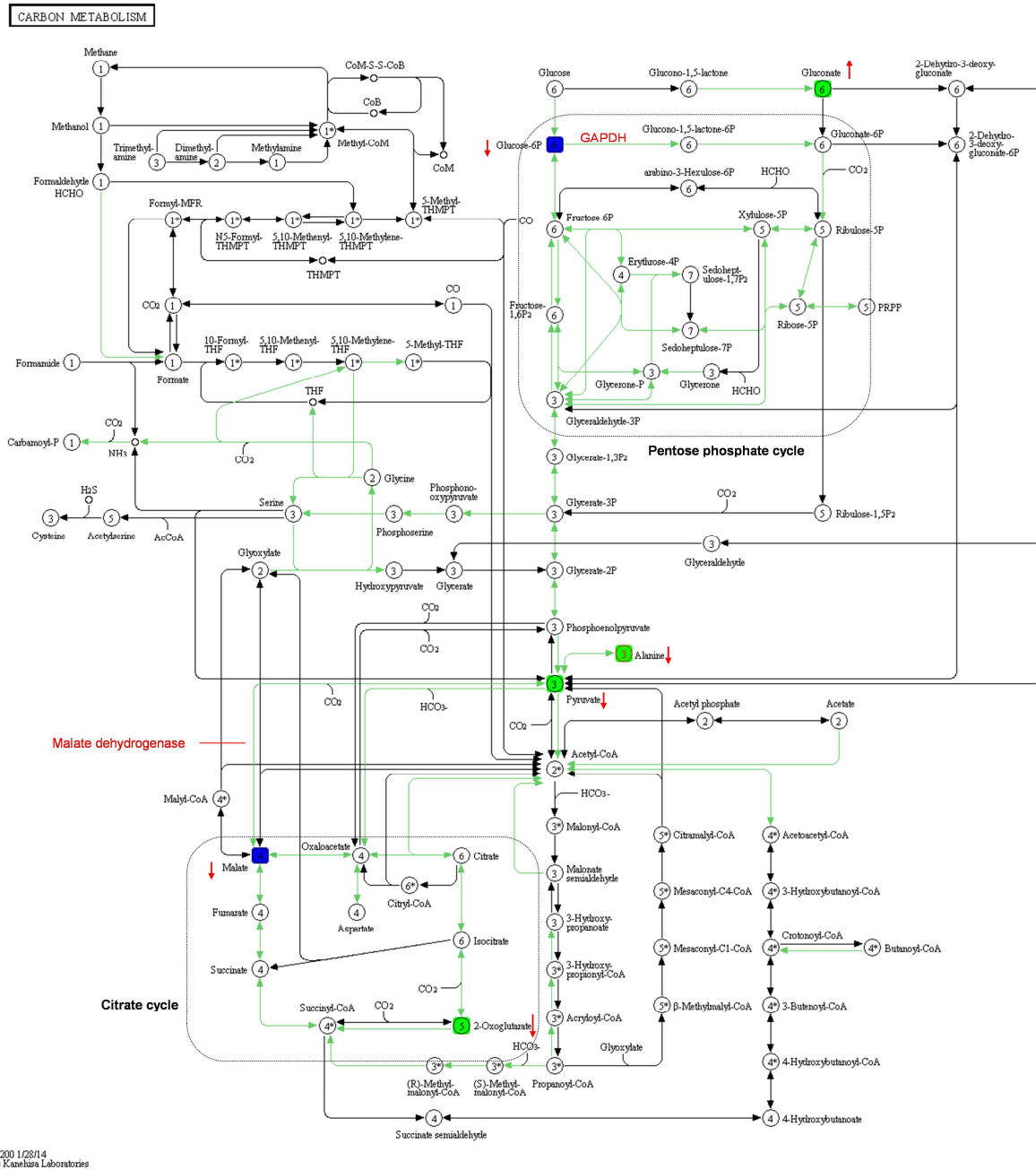
Fig. 48. A number of identified metabolites in this study are involved in the human carbon metabolism as shown in this graph. Green arrows depict homo sapiens-specific pathways/enzymes. Blue, green and red numbers are metabolites found to be significantly different between smokers and non-smokers in saliva, urine and plasma, respectively. Red arrows indicate increased or decreased levels in smokers. Taken and adapted from KEGG [158].

4.2   Metabolic profiling of fatty acids in plasma

The result of increased MUFAs revealed by the metabolic fingerprinting of plasma samples was confirmed by the total fatty acid profile analysis of the same set of samples by

means of a targeted GC-FID method. Beside the three MUFAs discovered in the metabolic approach (palmitoleic acid, oleic acid, FA 18:1 presumable n-7), further species of this class were found to be increased in smokers. Other fatty acids such as FA 17:0 (margaric acid), FA 18:0 (stearic acid) and the PUFA 22:6 n-3 were significantly decreased. Reduced PUFA 22:6 n-3 levels have been linked to the risk of developing COPD [78,171]. It is well established that smoking is causally related to COPD [5,16]. Metabolism-wise, omega-3 fatty acids such as FA 22:6 are precursors of the anti-inflammatory eicosanoids, including resolvins (D-series), protectins (D-series) and maresins, which are relevant for resolution of inflammatory reactions [172]. One likely explanation for the increased proportions of MUFAs in the total fatty acid profiles in smokers plasma could be a potentially altered endogenous fatty acid desaturation, caused by an up-regulation of stearoyl-Coenzyme A desaturase 1 (SCD1) (Fig. 49), as previously suggested by Hodson et al. [173], Yanagita et al. [174] and Amoruso et al. [175]. These groups of researchers showed that nicotine activates the transcription factor peroxisome proliferator activated receptor (PPAR), which in turn activates the transcription factor liver X receptor (*LXR*) and subsequently the sterol regulatory element binding protein-1c (SREBP-1c) [176,177]. It is also assumed that LXR plays a pivotal role in the up-regulation of SCD1 [178], which catalyzes the desaturation (Δ^9) of FA 16:0, FA 17:0 and FA 18:0 to form the MUFAs 16:1, 17:1 and 18:1, respectively [179]. The MUFAs were found to be significantly increased in plasma of smokers, whereas FA 17:0 and FA 18:0 were observed to be significantly decreased. The elevated levels of FA 20:1 n-9 might be explained by the formation from FA 18:1 n-9 by chain elongation. One can hypothesize that an activation of SREBP-1c could also lead to increased fatty acid turn-over and, as a result, to increased levels of 2-furoylglycine as products of increased FA β-oxidation. 2-Furoylglycine was found to be significantly increased in smokers' urine (Table 13). However, it appears more likely that the increase in 2-furoylglycine levels is due to an uptake and metabolism of the tobacco smoke constituent furfural [7,180].

4. Discussion
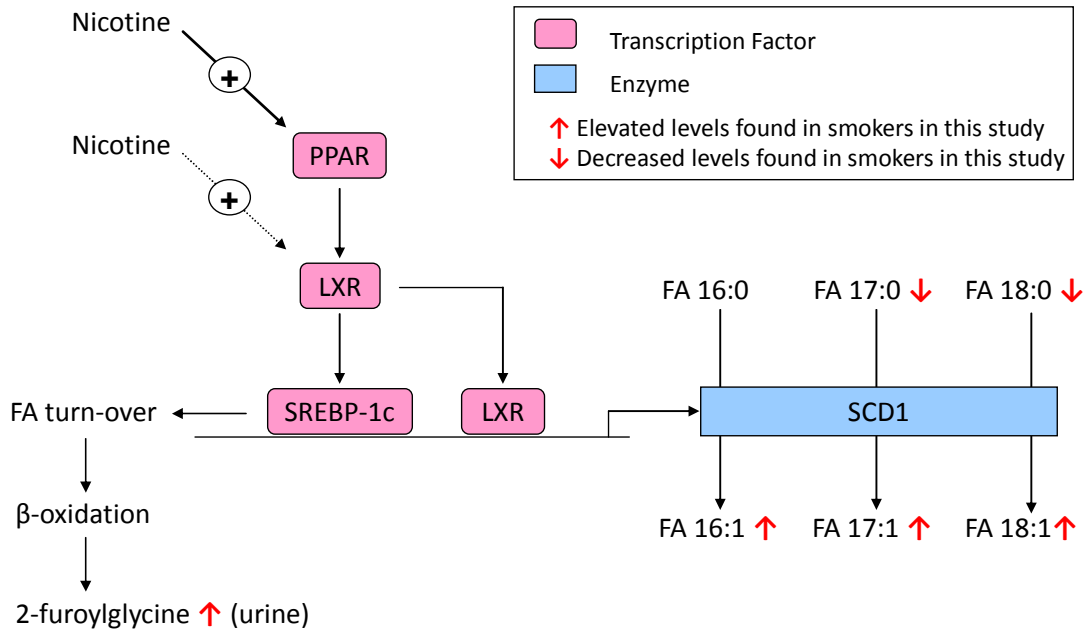
Fig. 49. Hypothesis for the emergence of increased levels of MUFAs in plasma of smokers. Nicotine leads to a transcription factor activated increase of the enzyme stearoyl Co-enzyme desaturase 1 (SCD1), which catalyzes the desaturation of saturated fatty acids to MUFAs. 2-Furoylglycine was found to be increased in smokers' urine and might be generated via a nicotine triggered activation of the transcription factor SREBP-1c, resulting in an elevated FA turn-over by β-oxidation. See text for further explanations. LXR: liver X receptor. Sterol regulatory element binding protein-1c: SREBP-1c.

High SCD1 expression is correlated with metabolic diseases such as obesity or insulin resistance [181]. The latter condition was also reported to be associated with smoking [182]. Furthermore, epidemiological studies have shown a significant positive association of FA 16:1 n-7 and FA 18:1 n-9 with smoking [78-81], which is in agreement with the results obtained from this study. It was also shown that FA 16:1 n-9 is correlated with hypertension [81,183]. Additionally, fatty acids play important physiological roles as precursors for eicosanoids, substrates for enzymes, determinants of cell membrane flexibility, in acylation of proteins and as transcription factors [39,184-187]. Since these physiological processes are involved in the generation of a number of diseases [17,188], one could assume that an altered fatty acid metabolism is an indicator for early biological effects of smoking in the development of diseases, such as atherosclerosis and COPD.

4.3 Targeted phospholipid species analysis

Free fatty acids in plasma are mainly stored in the form of the phospholipids PC and PE, which play a pivotal role in the pathogenesis of a number of diseases. The targeted analysis of lipids in samples derived from an appropriately designed study might, therefore, provide further biological insights into pathophysiological mechanisms with smoking as an isolated factor.

4.3.1 Method development and validation

A novel targeted HILIC-MS/MS method was established, validated and applied to the same set of plasma samples obtained from the clinical study, in order to determine levels of PC and PE. Using an HILIC-MS/MS method it was possible to quantify 39 PCs and 40 PEs by using only 2 internal standards and 8 reference compounds. Compared to direct infusion methods, which are frequently used for analysis of these classes of metabolites [48], the applied chromatographic separation leads to lower ion suppression by matrix effects. Importantly, the method allows baseline separation of assumed +1 isotope of sphingomyelin (SM) species, which lose similarly to PCs, their phospho-choline headgroup during CID. This is a main advantage when compared to direct infusion methods using triple quadrupole instruments. Due to the low mass resolution (typically in the range of 0.3 Da - 1 Da), these instruments cannot unambiguously distinguish between isobaric phospholipid species such as PC and co-eluting isotopes of SM. Considering the unavoidable isotopic overlap of PC species with SM+1 isotopes along with the relatively high concentrations of SM in plasma (around 100 µM) [134], a lack of separation would lead to erroneous quantifications.

4.3.2 Phospholipid profiles in plasma of smokers and non-smokers

The phospholipid levels in plasma of smokers and non-smokers determined with the novel HILIC-MS/MS method were in agreement with the concentration ranges and species profiles reported in the literature [48,134,137,138]. However, Quehenberger et al. [49] found up to 10 times higher or lower concentrations for some of the PC and PE species. This could be potentially explained by a different sample preparation procedure along with a different chromatographic separation strategy using normal phase instead of HILIC, leading to a lack of coelution of standards and analytes and therefore different ionization efficiencies. Further, this study mentioned that they could not differentiate between some coeluting molecular glycerophospholipids species leading to errors in the absolute quantification.

Phospholipids seem to play a crucial role in smoking-related diseases such as diabetes, obesity or atherosclerosis [189,190]. For instance, smoking is reported to increase

4. Discussion

the risk of developing type 2 diabetes [191]. Recent investigations revealed that alterations in phosphatidylcholine metabolism promote CVD, a disease to which smoking is also significantly related [192]. Results from this as well as other studies suggest that alterations in PC profiles might constitute a mechanistic link between smoking and cardiovascular disease [192]. The targeted PC and PE species determination in plasma of smokers and non-smokers revealed significant differences in the profiles of 8 phospholipids between the two groups (Table 27). The phospholipids (most likely containing the MUFAs 16:1 and 18:1) PC 36:1, PC 38:7, PE 36:2 and PE 38:5 were observed to be elevated in plasma of smokers when compared to non-smokers, which was predicted from the results of the total fatty acid profiles, that showed an increase of MUFAs in smokers (Table 23). As reported in the literature [137-139], PC 36:1 in human plasma mainly contains FA 18:1, which is in line with the results from the GC-FID analysis. Recently, Xu et al. [77] showed that PC 36:0 was decreased and PC 36:1 increased in the plasma of smokers, which is also in agreement with the results in this study. Additionally, no significant smoking-related alterations in PC 40:4 and PC 38:3 were observed, in contrast to findings by Xu et al. [77]. This discrepancy could be explained by completely different analytical strategies. Lipids in the Xu et al. study were analyzed by FIA using the AbsoluteIDQ P180 and P150 Kits provided by Biocrates Life Sciences AG (Innsbruck, Austria), bypassing chromatographic separation, which could, as a consequence, lead to strong matrix interferences and disturbance by unseparated isobaric compounds such as sphingomyelins.

Proportions of the PC species 36:0, (mainly PC 18:0/18:0 [138]), PC 38:7 (PC 16:1/22:6 [139]), PC 38:6 (PC 16:0/22:6 [137-139]) and PE (PE 18:0/20:4 [136]) were found to be significantly lower in smokers (Table 27), which is also in agreement with the targeted fatty acid analysis showing decreased levels of FA 18:0 and FA 22:6 in plasma of smokers (Table 23). Recently, Sterz et al. [39] showed that smoking leads to elevated levels of particular eicosanoids derived from arachidonic acid (FA 20:4). Therefore, one could hypothesize that plasma of smokers contains less arachidonic acid-containing phospholipids such as PE 38:4 (PE 18:0/20:4), as they might have been metabolized to eicosanoids. The observed patterns of phospholipids do not support this hypothesis. For example, the observed decrease of PC 38:7 in plasma of smokers, should actually show an increase as it is most likely comprised of FA 18:1 and FA 20:6. Obviously, there are also other sources for fatty acids like cholesterol, which contribute to the total fatty acids measured in plasma but are not considered in the determined PC and PE profiles (see Section "1.4 Lipidomics").

4.4 Tyramine analysis in saliva by HILIC-MS/MS

Salivary tyramine was determined at the five different time points where saliva collection took place with the newly developed and validated HILIC-MS/MS method. Up to now, tyramine has only been analyzed in urine and plasma of human subjects [108,193,194]. To the best of the author's knowledge, this is the first time that such a method has been applied for the quantification of tyramine in saliva. Gosetti et al. 2013 [108] and Yonekura et al. 1988 [193] analyzed tyramine in urine and plasma respectively, however, both used a more time consuming and complex sample preparation procedure. Both methods had a narrower linear range (2 – 80 µM for plasma and 18 – 15 µM for urine) as compared to the achieved range of 10 nM to 50 µM in saliva in this study. Admittedly, this comparison is, to a certain extent, in-appropriate, since urine and plasma matrices might be interfered by stronger matrix effects. The LLOQ can possibly be improved, if a more sophisticated sample preparation is applied, for example: evaporation and reuptake in less solvent.

4.4.1 Tyramine in saliva determined by HILIC-MS/MS

Smokers' saliva showed a pronounced elevation of tyramine (74 to 402-fold) when compared to their non-smoking counterparts. Concentrations for all non-smoking subjects were ≤ 7.8 µM, while the levels for smokers ranged from 7 nM to 42 µM. These levels were in the same concentration range like urine (~5 - 6 µM) [108,194] and 4 orders of magnitudes higher than in plasma (~0.49 nM) [193]. Interestingly, the highest concentration levels were found in the morning of study Day 2 (TP5) for both, smokers and non-smokers.

To date studies about salivary tyramine are missing. However other biogenic amines, such as cadaverine, have been quantified in saliva [195]. The time profiles determined by Cooke and co-workers [195] of biogenic amines showed a similar increase in the morning as observed for tyramine in this study (Fig. 50 A-C) [195]. These data suggests that endogenous biogenic amines in saliva, including tyramine, are obviously subject to a circadian rhythm. Furthermore, it was found that the biogenic amines analyzed by Cooke et al. [195] were decreased after toothbrushing and lunch because of increased salivary flow and mechanical cleaning by mastication. However, during the day, a slight increase in the levels of the biogenic amines in saliva was reported [195]. This observation was confirmed with salivary tyramine in this study.
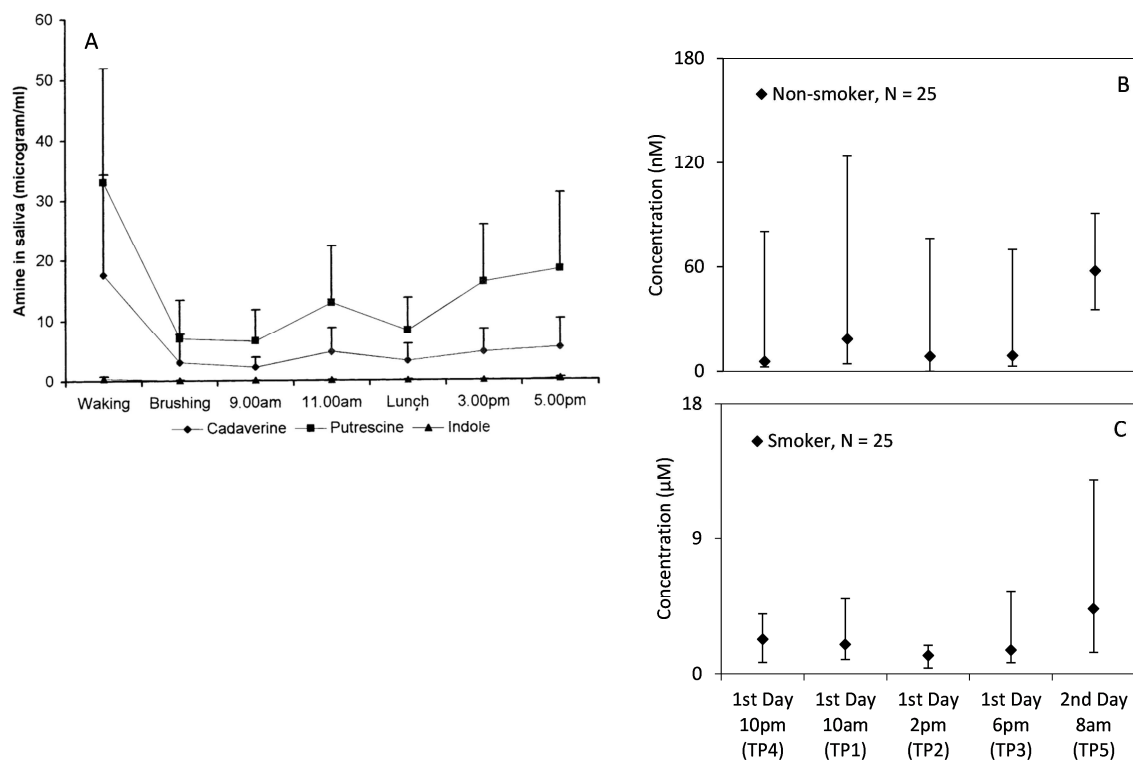
Fig. 50. Time profiles of biogenic amines determined in saliva of healthy human subjects. A: Biogenic amines in saliva of non-smokers showing the highest levels in the morning before toothbrushing (shown as mean ± SD, taken from Cooke et al. 2003 [195]). B and C: Tyramine in smokers and non-smokers showing the highest concentration in the morning of the 2nd study day before toothbrushing (shown as medians with error bars showing 25 and 75 percentile range). The saliva in the morning of the 1st study day (TP1) was collected after toothbrushing.

Amines in the oral cavity arise by the breakdown of proteins and peptides followed by a degradation of the resulting amino acids [195]. Tyramine is generated by endogenous decarboxylation of tyrosine [156]. This biogenic amine can also be taken up from the diet, particularly by consuming fermented food such as cheese [196]. Since this study was strictly diet controlled, the observed differences between smokers and non-smokers are most likely due to an altered endogenous metabolism or from an oral bacteria-mediated decarboxylation of tyrosine. In other words, smoking presumably shifts the oral flora activity to increased protein degradation leading to increased decarboxylation rate in smokers as compared to non-smokers. Tyramine was described as a constituent of tobacco and tobacco smoke [7,197], however, as yet no quantitative data were available. It appears unlikely that the hundred-fold increase of tyramine levels in smokers, at all time points, are caused by absorption of tyramine from tobacco smoke, as the smokers have not smoked for about 9 hours prior to saliva sampling at TP5. Metabolic degradation of tyramine in the human

4. Discussion

body is rather fast with an elimination half-life of about 0.5 hours after oral administration [198] so that no significant amounts of tyramine should be measurable 9 hours after food or smoking-related uptake of this biogenic amine. Another point which has to be considered when interpreting the tyramine results is the fact that smoking inhibits *in vivo* the enzyme MAO A and B by about 20 - 53% [199-203]. A number of tobacco smoke constituents including 2,3,6-trimethyl-benzochinone, 2-naphthylamine and ß-carbolines, [204,205] have been identified as potential MAO inhibitors.

Gilbert et al, 2003 [206] studied the platelet-derived MAO B activity in smokers who quit smoking and found increases from 22 to 50% after 3 and 10 d, respectively, of smoking abstinence. The enzyme activity remained at this level until 31 d after smoking cessation (end of the study). This observation suggests that the smoking-related effect on the MAO is partly, but not completely, reversible. More recently, Launay et al, 2009 [207] reported two opposite effects of smoking on the MAO: The first mode of action is the inhibition of the enzyme by smoke constituents such as harman and norharman; the second mechanism would work via the MAO promoter gene through a smoking-induced demethylation, resulting in an increase in the MAO protein concentration. The second mechanism can be regarded as a compensation effect for the MAO inhibition. Interestingly, the epigenetic effect was found to be irreversible, since increased MAO protein concentrations were observed also in former smokers, who quit smoking, on average, 13 years ago [207].

Nevertheless, the significantly higher tyramine levels in saliva of smokers as compared to non-smokers are not clearly understood. Further research is required in order to elucidate the origin of these high levels in smokers' saliva. There is evidence that bacterial decarboxylation in the oral cavity plays a major role in this process (see discussion in Section "4.1.2.3 Saliva"). The importance of this research field is emphasized by the fact that tyramine acts as an indirect sympathomimetic agent by inhibiting the neural cell uptake of catecholamines including dopamine, noradrenaline and adrenaline, thus prolonging the activity of these neurotransmitters (Fig. 51) [208]. These neuro-physiological properties of tyramine suggest that this biogenic amine is involved in the dependency and addiction issue of smoking and other tobacco- and nicotine-use habits.

Tyramine-related physiological effects include migraine, hypertension, increased heart rate or elevated blood sugar levels [198,208,209]. New studies have further indicated that altered vasoconstriction is mediated by trace amine-associated receptors [209,210]. Some of these physiological effects have been reported to be implicated with smoking [183,211]. Besides biogenic amines, such as tyramine, MAO A and B are also responsible for the metabolism of catecholamines. It has been hypothesized that the inhibition of MAO B plays an important role in the addictive potential of cigarette smoke, as an inhibition leads to increased synaptic availability of dopamine [212]. Additionally, nicotine triggers the release

4. Discussion

of such catecholamines which further increases the synaptic concentration of neurotransmitters [200,212,213]. The data from this study would strengthen this hypothesis, as increased levels of tyramine will reinforce the effects of the nicotine-triggered increase of neurotransmitters, as mentioned before. That might help to explain the tobacco addiction strength, which is hard to be explained solely by nicotine [214]. Inhibition of MAO activity seems to be part of the reinforcing properties of smoking addiction [215]. It is interesting to note that investigations are underway which test the use of reversible MAO B inhibitors in nicotine patches that will potentially help quit smoking.
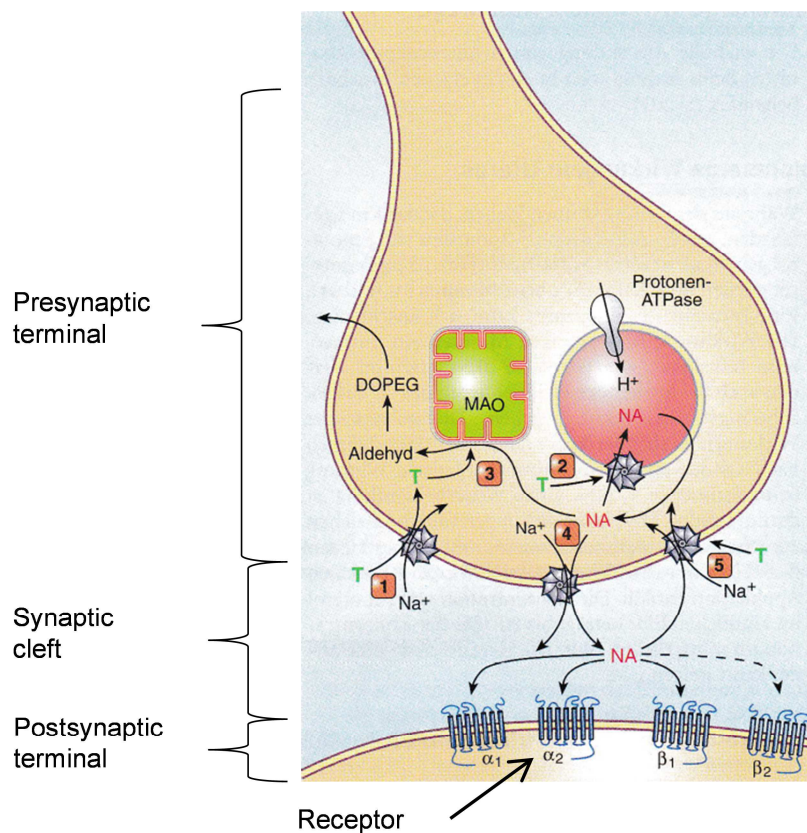
Fig. 51. Effect of tyramine on synaptic transduction. Tyramine (T) uptake along with Na^+ by the noradrenaline (NA)-carrier. 2. Tyramine increases the intracellular vesicular release of NA within the nerve terminal. 3. Tyramine competitively inhibits NA degradation by blocking monoamine oxidase (MAO) leading to increased NA concentration (weak effect). 4. NA is reversely released in the synaptic cleft by NA-carrier. 5. Tyramine competes with NA for reuptake, increasing the NA concentration in the synaptic cleft. DOPEG: Dihydroxyphenylethylene glycol. Adapted and modified from Aktories et al. 2005 [216].

4.5   Prospective investigations

Further studies are required to decipher the role of tyramine and smoking related induction of the aforementioned effects. Therefore, analyzing the urine and plasma samples of the study subjects will help to get a more detailed view on the metabolism of tyramine. This would require the development of a more sensitive method for tyramine determination in plasma. Further, it is of interest to get quantitative data for tyramine tobacco smoke itself. Since MAO A and B activity seem to increase after about one month after smoking cessation, it would be of interest to determine how tyramine levels would change within this period [213,217]. Further investigations are necessary to elucidate which tobacco smoke constituents are involved in MOA inhibition and what their mode of action is.

Some alterations of the total fatty acid profile in plasma are not reflected in the altered phospholipid species profiles. Lipidomic approaches would give a more detailed view of the changes of fatty acid profiles within lipids due to smoking. Further research, such as in-vitro experimentation, is required to confirm the hypothesized up-regulation of SCD1. In addition, the role of FA 17:0 and FA 17:1 in human plasma phospholipids is presently not well understood and requires further investigation. Therefore, applying a lipidomic approach to phospholipids containing odd chain fatty acids would provide a more detailed view about the contribution of these fatty acids in PC and PE species. A targeted analysis of the fatty acid side chains of the altered phospholipids could provide insight of how the altered fatty acid profiles influence the phospholipid profile. This could be achieved by analyzing the PC and PE species in negative ion mode using the same analytical approach, since diacyl phospholipids lose their fatty acid side chains during CID [61,218]). Further it would be of interest whether the altered fatty acid and phospholipid profiles are also reflected in the composition of the different lipoprotein fractions (LDL, HDL, VLDL) in human plasma samples, since changes in the lipid composition of lipoproteins play a key role in diseases such as Atherosclerosis [219].

As SCD1 is involved in smoking-related diseases and there is evidence that the activity of this enzyme might be altered in smokers, possibly by action of nicotine, cell-based applications might help to further elucidate the assumed mechanism.

Finally, it would be of interest to investigate, whether the observed alterations in this study disappear either completely or partly when subjects quit smoking and, if so, how long this vanishing process would take.

5   Conclusion

In summary, a metabolic fingerprinting method using GC-TOF-MS was developed, validated and applied to urine, plasma and saliva samples collected in a controlled clinical study. The aim of this investigation was to identify metabolic changes which are exclusively caused by smoking. The GC-TOF-MS method was validated with 36 (plasma) and 37 (urine, saliva) endogenous and exogenous metabolites. As part of the developed metabolomic platform, the open source software packages *MZmine*, *Metaboanalyst* and *PSPP* for an automated peak picking and integration as well as subsequent statistical analysis were applied. Increases in smoking-specific metabolites, such as nicotine and some of its metabolites, were identified to be highly significant in smokers' urine and saliva, providing evidence for the suitability of the developed metabolic fingerprinting approach. The relative levels for nicotine and its metabolites as determined by the untargeted GC-TOF-MS approach strongly correlated with the corresponding absolute concentrations determined with the validated, targeted LC-MS/MS method. This finding can be regarded as further evidence for the validity of the untargeted method. The statistical evaluation of the data obtained with the untargeted metabolic fingerprinting approach led to the discovery of about 240 metabolites in all three body fluids that are responsible for differences in the metabolome between the two groups (smoker and non-smokers). Thirty eight of these metabolites were identified by means of comparison to MS libraries and authentic reference compounds. The identified metabolites are mainly involved in the energy, detoxification and lipid metabolic pathways. Some of the findings, such as increased levels of glutamic acid, ornithine and oleic acid in plasma were also reported in previous studies which substantiates the reliability and performance of the analytical approach.

The finding of increased oleic acid and palmitoleic acid in plasma of smokers could be verified by applying a targeted fatty acid analysis using GC-FID, which revealed a significant altered fatty acid profile in smokers' plasma with an increased proportion of MUFAs. It is hypothesized that this effect is caused by a nicotine-triggered up-regulation of the SCD 1. To further investigate the substantially altered lipid metabolism induced by smoking, a HILIC-MS/MS was developed and validated. The novel method allows the robust and reliable quantification of PE and PC species in a single run. Smokers showed significant increases in some MUFA-containing lipid species, which are known to be involved in the generation of smoking-related diseases such as atherosclerosis.

Further, it could be demonstrated that saliva, as a non-invasive accessible body fluid, is a suitable biological matrix for investigating the human metabolome. The metabolomic approach revealed significantly increased tyramine levels in smokers' saliva as compared to non-smokers. This observation was confirmed by a targeted analysis of tyramine in saliva using a novel LC-MS/MS method. For the first time, tyramine has been quantified in human

5. Conclusion

saliva. Salivary tyramine levels in smokers were found to be remarkably increased compared to non-smokers at 5 different time points during the clinical study. The observed time pattern in salivary tyramine levels as well as similar finding reported in the literature for cadaverine, another biogenic amine, suggests that bacterial decarboxylation processes in the oral cavity play a major role in generating the observed levels of biogenic amines in saliva. Another aspect in interpreting the elevated salivary levels of tyramine in smokers is the well-known smoking-related inhibition of the MAO, which metabolizes tyramine. Whether and how the observed elevated levels of salivary tyramine, which acts as an indirect sympathomimetic drug, can influence smoking behaviour and addiction has yet to be elucidated. Therefore, it would be of interest whether the significantly increased tyramine concentrations are also reflected in urine and plasma of smokers[1].

The results of the presented metabolic fingerprinting created some new hypotheses related to the influence of smoking on the human organism. The findings may help to set up new experiments for a targeted analysis of metabolic pathways that might be perturbed by tobacco smoke and play a role in the pathogenesis of smoking-related diseases.

---

[1] Meanwhile, at ABF, tyramine was determined in all plasma and urine samples derived from the clinical study. The LC-MS/MS method as described above ("2.11 Analysis of tyramine in saliva") was applied for these analyses. Tyramine concentrations in plasma were found to be < LOD (0.5 nM) in all samples except one derived from a smoker (4.2 nM), Tyramine excretion rates in 24-h urine samples were in the range of 1.11 – 8.26 µmol/24h for all 50 subjects. No difference in tyramine excretion rates were observed between smokers (4.26 µmol/24h) and non-smokers (4.45 µmol/24h), Tyramine levels in the three urine fractions collected during the clinical study were also similar in smokers and non-smokers.

6   References

[1] Ezzati, M., Lopez, A. D.; *Regional, disease specific patterns of smoking-attributable mortality in 2000.* Tob. Control **2004**, 13, 388-395.

[2] Ezzati, M., Henley, S. J., Lopez, A. D., Thun, M. J.; *Role of smoking in global and regional cancer epidemiology: current patterns and data needs.* Int. J. Cancer **2005**, 116, 963-971.

[3] Hecht, S. S.; *Tobacco smoke carcinogens and lung cancer.* J. Natl. Cancer Inst. **1999**, 91, 1194-1210.

[4] Powell, J. T.; *Vascular damage from smoking: disease mechanisms at the arterial wall.* Vasc. Med. **1998**, 3, 21-28.

[5] Lindberg, A., Bjerg-Bäcklund, A., Rönmark, E., Larsson, L.-G., Lundbäck, B.; *Prevalence and underdiagnosis of COPD by disease severity and the attributable fraction of smoking: Report from the Obstructive Lung Disease in Northern Sweden Studies.* Respir. Med. **2006**, 100, 264-272.

[6] Jha, P.; *Avoidable global cancer deaths and total deaths from smoking.* Nat. Rev. Cancer **2009**, 9, 655-664.

[7] Rodgman, A., Perfetti, T. A.; *The chemical components of tobacco and tobacco smoke*, Boca Raton **2008.**

[8] International Agency for Research on Cancer (IARC), World Health Organisation; *IARC Monographs on the Evaluation of Carcinogenic Risks to Humans.* http://monographs.iarc.fr/ENG/Monographs/PDFs/index.php, Accessed 15.03.2014.

[9] Hecht, S. S., Hoffmann, D.; *Tobacco-specific nitrosamines, an important group of carcinogens in tobacco and tobacco smoke.* Carcinogenesis **1988**, 9, 875-884.

[10] Scherer, G.; *Biomonitoring of inhaled complex mixtures-ambient air, diesel exhaust and cigarette smoke.* Exp. Toxicol. Pathol. **2005**, 57 Suppl 1, 75-110.

[11] Scherer, G., Frank, S., Riedel, K., Meger-Kossien, I., Renner, T.; *Biomonitoring of Exposure to Polycyclic Aromatic Hydrocarbons of Nonoccupationally Exposed Persons.* Cancer Epidemiol. Biomarkers Prev. **2000**, 9, 373-380.

[12] Norppa, H.; *Cytogenetic biomarkers and genetic polymorphisms.* Toxicol. Lett. **2004**, 149, 309-334.

[13] Ito, H., Hamajima, N., Matsuo, K., Okuma, K., Sato, S., Ueda, R., Tajima, K.; *Monoamine oxidase polymorphisms and smoking behaviour in Japanese.* Pharmacogenetics **2003**, 13, 73-79.

[14] Fiehn, O.; *Metabolomics-the link between genotypes and phenotypes.* Plant Mol. Biol. **2002**, 48, 155-171.

[15] Dettmer, K., Hammock, B. D.; *Metabolomics-A new exciting field within the "omics" sciences.* Environ. Health Perspect. **2004**, 112, A396-397.

6. References

[16] US Department of Health and Human Services; *How Tobacco Smoke Causes Disease: The Biology and Behavioral Basis for Smoking-Attributable Disease- A Report of the Surgeon General*, Rockville, MD, USA **2010.**

[17] Calder, P. C.; *Polyunsaturated fatty acids and inflammatory processes: New twists in an old tale.* Biochimie **2009**, 91, 791-795.

[18] Loft, S., Vistisen, K., Ewertz, M., Tjonneland, A., Overvad, K., Poulsen, H. E.; *Oxidative DNA damage estimated by 8-hydroxydeoxyguanosine excretion in humans: influence of smoking, gender and body mass index.* Carcinogenesis **1992**, 13, 2241-2247.

[19] Dettmer, K., Aronov, P. A., Hammock, B. D.; *Mass spectrometry-based metabolomics.* Mass Spectrom. Rev. **2007**, 26, 51-78.

[20] Scalbert, A., Brennan, L., Fiehn, O., Hankemeier, T., Kristal, B., Ommen, B., Pujos-Guillot, E., Verheij, E., Wishart, D., Wopereis, S.; *Mass-spectrometry-based metabolomics: limitations and recommendations for future progress with particular focus on nutrition research.* Metabolomics **2009**, 5, 435-458.

[21] Riedel, K., Scherer, G., Engl, J., Hagedorn, H. W., Tricker, A. R.; *Determination of three carcinogenic aromatic amines in urine of smokers and nonsmokers.* J. Anal. Toxicol. **2006**, 30, 187-195.

[22] Scherer, G., Engl, J., Urban, M., Gilch, G., Janket, D., Riedel, K.; *Relationship between machine-derived smoke yields and biomarkers in cigarette smokers in Germany.* Regul. Toxicol. Pharm. **2007**, 47, 171-183.

[23] Richter, E., Rösler, S., Scherer, G., Gostomzyk, J. G., Grübl, A., Krämer, U., Behrendt, H.; *Haemoglobin adducts from aromatic amines in children in relation to area of residence and exposure to environmental tobacco smoke.* Int. Arch. Occup. Environ. Health **2001**, 74, 421-428.

[24] Urban, M., Gilch, G., Schepers, G., van Miert, E., Scherer, G.; *Determination of the major mercapturic acids of 1,3-butadiene in human and rat urine using liquid chromatography with tandem mass spectrometry.* J. Chromatogr. B **2003**, 796, 131-140.

[25] Minet, E., Cheung, F., Errington, G., Sterz, K., Scherer, G.; *Urinary excretion of the acrylonitrile metabolite 2-cyanoethylmercapturic acid is correlated with a variety of biomarkers of tobacco smoke exposure and consumption.* Biomarkers **2011**, 16, 89-96.

[26] Scherer, G., Urban, M., Hagedorn, H. W., Feng, S., Kinser, R. D., Sarkar, M., Liang, Q., Roethig, H. J.; *Determination of two mercapturic acids related to crotonaldehyde in human urine: influence of smoking.* Hum. Exp. Toxicol. **2007**, 26, 37-47.

[27] Urban, M., Kavvadias, D., Riedel, K., Scherer, G., Tricker, A. R.; *Urinary mercapturic acids and a hemoglobin adduct for the dosimetry of acrylamide exposure in smokers and nonsmokers.* Inhal. Toxicol. **2006**, 18, 831-839.

[28] Mascher, D. G., Mascher, H. J., Scherer, G., Schmid, E. R.; *High-performance liquid chromatographic-tandem mass spectrometric determination of 3-hydroxypropylmercapturic acid in human urine.* J. Chromatogr. B **2001**, 750, 163-169.

[29] Sterz, K., Scherer, G., Krumsiek, J., Theis, F. J., Ecker, J.; *Identification and quantification of 1-hydroxybutene-2-yl mercapturic acid in human urine by UPLC- HILIC-MS/MS as a novel biomarker for 1,3-butadiene exposure.* Chem. Res. Toxicol. **2012**, 25, 1565-1567.

6. References

[30] Sterz, K., Kohler, D., Schettgen, T., Scherer, G.; *Enrichment and properties of urinary pre-S-phenylmercapturic acid (pre-SPMA).* J. Chromatogr. B **2010**, 878, 2502-2505.

[31] Riedel, K., Ruppert, T., Conze, C., Scherer, G., Adlkofer, F.; *Determination of benzene and alkylated benzenes in ambient and exhaled air by microwave desorption coupled with gas chromatography-mass spectrometry.* J. Chromatogr. A **1996**, 719, 383-389.

[32] Scherer, G., Renner, T., Meger, M.; *Analysis and evaluation of trans,trans-muconic acid as a biomarker for benzene exposure.* J. Chromatogr. B **1998**, 717, 179-199.

[33] Raub, J. A., Mathieu-Nolf, M., Hampson, N. B., Thom, S. R.; *Carbon monoxide poisoning - a public health perspective.* Toxicology **2000**, 145, 1-14.

[34] Ramsauer, B., Sterz, K., Hagedorn, H. W., Engl, J., Scherer, G., McEwan, M., Errington, G., Shepperd, J., Cheung, F.; *A liquid chromatography/tandem mass spectrometry (LC-MS/MS) method for the determination of phenolic polycyclic aromatic hydrocarbons (OH-PAH) in urine of non-smokers and smokers.* Anal. Bioanal. Chem. **2011**, 399, 877-889.

[35] Scherer, G.; *Carboxyhemoglobin and thiocyanate as biomarkers of exposure to carbon monoxide and hydrogen cyanide in tobacco smoke.* Exp. Toxicol. Pathol. **2006**, 58, 101-124.

[36] Feng, S., Roethig, H. J., Liang, Q., Kinser, R., Jin, Y., Scherer, G., Urban, M., Engl, J., Riedel, K.; *Evaluation of urinary 1-hydroxypyrene, S-phenylmercapturic acid, trans,trans-muconic acid, 3-methyladenine, 3-ethyladenine, 8-hydroxy-2'-deoxyguanosine and thioethers as biomarkers of exposure to cigarette smoke.* Biomarkers **2006**, 11, 28-52.

[37] Tröbs, M., Renner, T., Scherer, G., Heller, W.-D., Geiß, H. C., Wolfram, G., Haas, G.-M., Schwandt, P.; *Nutrition, Antioxidants, and Risk Factor Profile of Nonsmokers, Passive Smokers and Smokers of the Prevention Education Program (PEP) in Nuremberg, Germany.* Prev. Med. **2002**, 34, 600-607.

[38] Renner, T., Fechner, T., Scherer, G.; *Fast quantification of the urinary marker of oxidative stress 8-hydroxy-2'-deoxyguanosine using solid-phase extraction and high-performance liquid chromatography with triple-stage quadrupole mass detection.* J. Chromatogr. B **2000**, 738, 311-317.

[39] Sterz, K., Scherer, G., Ecker, J.; *A simple and robust UPLC-SRM/MS method to quantify urinary eicosanoids.* J. Lipid Res. **2012**, 53, 1026-1036.

[40] Assfalg, M., Bertini, I., Colangiuli, D., Luchinat, C., Schäfer, H., Schütz, B., Spraul, M.; *Evidence of different metabolic phenotypes in humans.* Proc. Natl. Acad. Sci. U.S.A. **2008**, 105, 1420-1424.

[41] Wishart, D. S., Jewison, T., Guo, A. C., Wilson, M., Knox, C., Liu, Y., Djoumbou, Y., Mandal, R., Aziat, F., Dong, E., Bouatra, S., Sinelnikov, I., Arndt, D., Xia, J., Liu, P., Yallou, F., Bjorndahl, T., Perez-Pineiro, R., Eisner, R., Allen, F., Neveu, V., Greiner, R., Scalbert, A.; *HMDB 3.0--The Human Metabolome Database in 2013.* Nucleic Acids Res. **2013**, 41, D801-807.

[42] Wishart, D. S., Tzur, D., Knox, C., Eisner, R., Guo, A. C., Young, N., Cheng, D., Jewell, K., Arndt, D., Sawhney, S., Fung, C., Nikolai, L., Lewis, M., Coutouly, M. A., Forsythe, I., Tang, P., Shrivastava, S., Jeroncic, K., Stothard, P., Amegbey, G., Block, D., Hau, D. D., Wagner, J., Miniaci, J., Clements, M., Gebremedhin, M., Guo, N., Zhang, Y., Duggan, G. E., Macinnis, G. D., Weljie, A. M., Dowlatabadi, R., Bamforth, F., Clive, D., Greiner, R., Li, L., Marrie, T., Sykes, B. D., Vogel, H. J., Querengesser, L.; *HMDB: the Human Metabolome Database.* Nucleic Acids Res. **2007**, 35, D521-526.

6. References

[43] Drew, H. R., Wing, R. M., Takano, T., Broka, C., Tanaka, S., Itakura, K., Dickerson, R. E.; *Structure of a B-DNA dodecamer: conformation and dynamics.* Proc. Natl. Acad. Sci. U.S.A. **1981**, 78, 2179-2183.

[44] Rossmann, M. G., Johnson, J. E.; *Icosahedral RNA virus structure.* Annu. Rev. Biochem **1989**, 58, 533-573.

[45] Yuan, M., Breitkopf, S. B., Yang, X., Asara, J. M.; *A positive/negative ion-switching, targeted mass spectrometry-based metabolomics platform for bodily fluids, cells, and fresh and fixed tissue.* Nat. Protoc. **2012**, 7, 872-881.

[46] Baraldi, E., Carraro, S., Giordano, G., Reniero, F., Perilongo, G., Zacchello, F.; *Metabolomics: moving towards personalized medicine.* Ital. J. Pediatr. **2009**, 35, 30.

[47] Wenk, M. R.; *The emerging field of lipidomics.* Nat. Rev. Drug Discov. **2005**, 4, 594-610.

[48] Liebisch, G., Lieser, B., Rathenberg, J., Drobnik, W., Schmitz, G.; *High-throughput quantification of phosphatidylcholine and sphingomyelin by electrospray ionization tandem mass spectrometry coupled with isotope correction algorithm.* Biochim. Biophys. Acta **2004**, 1686, 108-117.

[49] Quehenberger, O., Armando, A. M., Brown, A. H., Milne, S. B., Myers, D. S., Merrill, A. H., Bandyopadhyay, S., Jones, K. N., Kelly, S., Shaner, R. L., Sullards, C. M., Wang, E., Murphy, R. C., Barkley, R. M., Leiker, T. J., Raetz, C. R., Guan, Z., Laird, G. M., Six, D. A., Russell, D. W., McDonald, J. G., Subramaniam, S., Fahy, E., Dennis, E. A.; *Lipidomics reveals a remarkable diversity of lipids in human plasma.* J. Lipid Res. **2010**, 51, 3299-3305.

[50] Wenk, M. R.; *Lipidomics: new tools and applications.* Cell **2010**, 143, 888-895.

[51] Shevchenko, A., Simons, K.; *Lipidomics: coming to grips with lipid diversity.* Nat. Rev. Mol. Cell Biol. **2010**, 11, 593-598.

[52] Cao, H., Gerhold, K., Mayers, J. R., Wiest, M. M., Watkins, S. M., Hotamisligil, G. S.; *Identification of a lipokine, a lipid hormone linking adipose tissue to systemic metabolism.* Cell **2008**, 134, 933-944.

[53] Casey, P. J.; *Protein lipidation in cell signaling.* Science **1995**, 268, 221-225.

[54] Lin, L. L., Lin, A. Y., Knopf, J. L.; *Cytosolic phospholipase A2 is coupled to hormonally regulated release of arachidonic acid.* Proc. Natl. Acad. Sci. U.S.A. **1992**, 89, 6147-6151.

[55] Chalmers, G. W., MacLeod, K. J., Thomson, L., Little, S. A., McSharry, C., Thomson, N. C.; *Smoking and airway inflammation in patients with mild asthma.* Chest **2001**, 120, 1917-1922.

[56] Budzikiewicz, H.; *Massenspektrometrie.: Eine Einführung*, Weinheim **1998.**

[57] Lenz, E. M., Bright, J., Knight, R., Wilson, I. D., Major, H.; *Cyclosporin A-induced changes in endogenous metabolites in rat urine: a metabonomic investigation using high field 1H NMR spectroscopy, HPLC-TOF/MS and chemometrics.* J. Pharm. Biomed. Anal. **2004**, 35, 599-608.

[58] Keun, H. C., Beckonert, O., Griffin, J. L., Richter, C., Moskau, D., Lindon, J. C., Nicholson, J. K.; *Cryogenic Probe 13C NMR Spectroscopy of Urine for Metabonomic Studies.* Anal. Chem. **2002**, 74, 4588-4593.

6. References

[59] Takeda, I., Stretch, C., Barnaby, P., Bhatnager, K., Rankin, K., Fu, H., Weljie, A., Jha, N., Slupsky, C.; *Understanding the human salivary metabolome.* NMR Biomed. **2009**, 22, 577-584.

[60] Blanksby, S. J., Mitchell, T. W.; *Advances in mass spectrometry for lipidomics.* Annu. Rev. Anal. Chem. (Palo Alto Calif.) **2010**, 3, 433-465.

[61] Han, X., Gross, R. W.; *Electrospray ionization mass spectroscopic analysis of human erythrocyte plasma membrane phospholipids.* Proc. Natl. Acad. Sci. U.S.A. **1994**, 91, 10635-10639.

[62] Han, X., Gross, R. W.; *Global analyses of cellular lipidomes directly from crude extracts of biological samples by ESI mass spectrometry: a bridge to lipidomics.* J. Lipid Res. **2003**, 44, 1071-1079.

[63] Fenn, J. B., Mann, M., Meng, C. K., Wong, S. F., Whitehouse, C. M.; *Electrospray ionization for mass spectrometry of large biomolecules.* Science **1989**, 246, 64-71.

[64] Bruins, A. P., Covey, T. R., Henion, J. D.; *Ion spray interface for combined liquid chromatography/atmospheric pressure ionization mass spectrometry.* Anal. Chem. **1987**, 59, 2642-2646.

[65] Bruins, A. P.; *Atmospheric-pressure-ionization mass spectrometry: II. Applications in pharmacy, biochemistry and general chemistry.* Trends Analyt. Chem. **1994**, 13, 81-90.

[66] Hummel, J., Strehmel, N., Selbig, J., Walther, D., Kopka, J.; *Decision tree supported substructure prediction of metabolites from GC-MS profiles.* Metabolomics **2010**, 6, 322-333.

[67] Strelkov, S.; *Entwicklung und Anwendung einer Methode zur Metabolomanalyse von Corynebacterium glutamicum.* Dissertation, University of Cologne, **2004**.

[68] Issaq, H. J., Abbott, E., Veenstra, T. D.; *Utility of separation science in metabolomic studies.* J. Sep. Sci. **2008**, 31, 1936-1947.

[69] Trygg, J., Holmes, E., Lundstedt, T.; *Chemometrics in metabonomics.* J. Proteome Res. **2007**, 6, 469-479.

[70] Kind, T., Tolstikov, V., Fiehn, O., Weiss, R. H.; *A comprehensive urinary metabolomic approach for identifying kidney cancer.* Anal. Biochem. **2007**, 363, 185-195.

[71] Barker, M., Rayens, W.; *Partial least squares for discrimination.* J. Chemom. **2003**, 17, 166-173.

[72] Xia, J., Psychogios, N., Young, N., Wishart, D. S.; *MetaboAnalyst: a web server for metabolomic data analysis and interpretation.* Nucleic Acids Res. **2009**, 37, W652-660.

[73] Hastie, T., Tibshirani, R., Friedman, J., Franklin, J.; *The elements of statistical learning: data mining, inference and prediction*, 2nd Edition, New York **2005.**

[74] Westerhuis, J., Hoefsloot, H. J., Smit, S., Vis, D., Smilde, A., Velzen, E. J., Duijnhoven, J. M., Dorsten, F.; *Assessment of PLSDA cross validation.* Metabolomics **2008**, 4, 81-89.

[75] Hsu, P. C., Zhou, B., Zhao, Y., Ressom, H. W., Cheema, A. K., Pickworth, W., Shields, P. G.; *Feasibility of Identifying the Tobacco-related Global Metabolome in Blood by UPLC–QTOF-MS.* J. Proteome Res. **2012**, 12, 679-691.

6. References

[76] Wang-Sattler, R., Yu, Y., Mittelstrass, K., Lattka, E., Altmaier, E., Gieger, C., Ladwig, K. H., Dahmen, N., Weinberger, K. M., Hao, P., Liu, L., Li, Y., Wichmann, H. E., Adamski, J., Suhre, K., Illig, T.; *Metabolic profiling reveals distinct variations linked to nicotine consumption in humans-first results from the KORA study.* PLoS One **2008**, 3, e3863.

[77] Xu, T., Holzapfel, C., Dong, X., Bader, E., Yu, Z., Prehn, C., Perstorfer, K., Jaremek, M., Roemisch-Margl, W., Rathmann, W., Li, Y., Wichmann, H. E., Wallaschofski, H., Ladwig, K. H., Theis, F., Suhre, K., Adamski, J., Illig, T., Peters, A., Wang-Sattler, R.; *Effects of smoking and smoking cessation on human serum metabolite profile: results from the KORA cohort study.* BMC Med. **2013**, 11, 60-73.

[78] Simon, J. A., Fong, J., Bemert, J. T., Browner, W. S.; *Relation of Smoking and Alcohol Consumption to Serum Fatty Acids.* Am. J. Epidemiol. **1996**, 144, 325-334.

[79] Leng, G. C., Smith, F. B., Fowkes, F. G. R., Horrobin, D. F., Ells, K., Morse-Fisher, N., Lowe, G. D. O.; *Relationship between plasma essential fatty acids and smoking, serum lipids, blood pressure and haemostatic and rheological factors.* Prostaglandins Leukot. Essent. Fatty Acids **1994**, 51, 101-108.

[80] Crowe, F. L., Skeaff, C. M., Green, T. J., Gray, A. R.; *Serum fatty acids as biomarkers of fat intake predict serum cholesterol concentrations in a population-based survey of New Zealand adolescents and adults.* Am. J. Clin. Nutr. **2006**, 83, 887-894.

[81] Cambien, F., Warnet, J. M., Vernier, V., Ducimetiere, P., Jacqueson, A., Flament, C., Orssaud, G., Richard, J. L., Claude, J. R.; *An epidemiologic appraisal of the associations between the fatty acids esterifying serum cholesterol and some cardiovascular risk factors in middle-aged men.* Am. J. Epidemiol. **1988**, 127, 75-86.

[82] Walsh, M. C., Brennan, L., Malthouse, J. P. G., Roche, H. M., Gibney, M. J.; *Effect of acute dietary standardization on the urinary, plasma, and salivary metabolomic profiles of healthy humans.* Am. J. Clin. Nutr. **2006**, 84, 531-539.

[83] Winnike, J. H., Busby, M. G., Watkins, P. B., O'Connell, T. M.; *Effects of a prolonged standardized diet on normalizing the human metabolome.* Am. J. Clin. Nutr. **2009**, 90, 1496-1501.

[84] Vigneau-Callahan, K. E., Shestopalov, A. I., Milbury, P. E., Matson, W. R., Kristal, B. S.; *Characterization of diet-dependent metabolic serotypes: analytical and biological variability issues in rats.* J. Nutr. **2001**, 131 Supplement, 924-932.

[85] Pluskal, T., Castillo, S., Villar-Briones, A., Oresic, M.; *MZmine 2: modular framework for processing, visualizing, and analyzing mass spectrometry-based molecular profile data.* BMC Bioinformatics **2010**, 11, 395-405.

[86] Stein, S. E.; *An integrated method for spectrum extraction and compound identification from gas chromatography/mass spectrometry data.* J. Am. Soc. Mass. Spectrom. **1999**, 10, 770-781.

[87] Halket, J. M., Przyborowska, A., Stein, S. E., Mallard, W. G., Down, S., Chalmers, R. A.; *Deconvolution gas chromatography/mass spectrometry of urinary organic acids – potential for pattern recognition and automated identification of metabolic disorders.* Rapid Commun. Mass Spectrom. **1999**, 13, 279-284.

[88] Xia, J., Mandal, R., Sinelnikov, I. V., Broadhurst, D., Wishart, D. S.; *MetaboAnalyst 2.0-a comprehensive server for metabolomic data analysis.* Nucleic Acids Res. **2012**, 40, 127-133.

6. References

[89] Pfaff, B., Darrington, J., Stover, J., Satman, M. H., Williams, J., Kiefte, M., Kobly, P., van Son, R.; GNU PSPP. [Version 0.8.1], **2013**, Available from: http://www.gnu.org/software/pspp/, Accessed 26.04.2014.

[90] Roza, A. M., Shizgal, H. M.; *The Harris Benedict equation reevaluated: resting energy requirements and the body cell mass.* Am. J. Clin. Nutr. **1984**, 40, 168-182.

[91] Shirtcliff, E. A., Granger, D. A., Schwartz, E., Curran, M. J.; *Use of salivary biomarkers in biobehavioral research: cotton-based sample collection methods can interfere with salivary immunoassay results.* Psychoneuroendocrinology **2001**, 26, 165-173.

[92] Navazesh, M.; *Methods for collecting saliva.* Ann. N. Y. Acad. Sci. **1993**, 694, 72-77.

[93] Mueller, D. C., Piller, M., Niessner, R., Scherer, M., Scherer, G.; *Untargeted Metabolomic Profiling in Saliva of Smokers and Nonsmokers by a Validated GC-TOF-MS Method.* J. Proteome Res. **2014**, 13, 1602–1613.

[94] Meger, M., Meger-Kossien, I., Schuler-Metz, A., Janket, D., Scherer, G.; *Simultaneous determination of nicotine and eight nicotine metabolites in urine of smokers using liquid chromatography–tandem mass spectrometry.* J. Chromatogr. B **2002**, 778, 251-261.

[95] Blaszkewicz, M., Liesenhoff-Henze, K.; *Creatinine in urine*, Volume 10, Weinheim **2010**, pp 169-184.

[96] Kuhara, T., Shinka, T., Inoue, Y., Ohse, M., Zhen-wei, X., Yoshida, I., Inokuchi, T., Yamaguchi, S., Takayanagi, M., Matsumoto, I.; *Pilot study of gas chromatographic–mass spectrometric screening of newborn urine for inborn errors of metabolism after treatment with urease.* J. Chromatogr. B **1999**, 731, 141-147.

[97] US Food and Drug Administration (FDA), Center for Drug Evaluation and Research (CDER), US Department of Health and Human Services, Ed.: Rockville, Maryland, **2001**, pp 1-22.

[98] van den Berg, R. A., Hoefsloot, H. C., Westerhuis, J. A., Smilde, A. K., van der Werf, M. J.; *Centering, scaling, and transformations: improving the biological information content of metabolomics data.* BMC Genomics **2006**, 7, 142.

[99] Pears, M. R., Cooper, J. D., Mitchison, H. M., Mortishire-Smith, R. J., Pearce, D. A., Griffin, J. L.; *High resolution 1H NMR-based metabolomics indicates a neurotransmitter cycling deficit in cerebral tissue from a mouse model of Batten disease.* J. Biol. Chem. **2005**, 280, 42508-42514.

[100] Bijlsma, S., Bobeldijk, I., Verheij, E. R., Ramaker, R., Kochhar, S., Macdonald, I. A., van Ommen, B., Smilde, A. K.; *Large-scale human metabolomics studies: a strategy for data (pre-) processing and validation.* Anal. Chem. **2006**, 78, 567-574.

[101] Xia, J., Wishart, D. S.; *Web-based inference of biological patterns, functions and pathways from metabolomic data using MetaboAnalyst.* Nat. Protoc. **2011**, 6, 743-760.

[102] Degen, C., Ecker, J., Piegholdt, S., Liebisch, G., Schmitz, G., Jahreis, G.; *Metabolic and growth inhibitory effects of conjugated fatty acids in the cell line HT-29 with special regard to the conversion of t11,t13-CLA.* Biochim. Biophys. Acta **2011**, 1811, 1070-1080.

[103] Ecker, J., Scherer, M., Schmitz, G., Liebisch, G.; *A rapid GC-MS method for quantification of positional and geometric isomers of fatty acid methyl esters.* J. Chromatogr. B **2012**, 897, 98-104.

6. References

[104] Liebisch, G., Vizcaino, J. A., Kofeler, H., Trotzmuller, M., Griffiths, W. J., Schmitz, G., Spener, F., Wakelam, M. J.; *Shorthand notation for lipid structures derived from mass spectrometry.* J. Lipid Res. **2013**, 54, 1523-1530.

[105] Brugger, B., Erben, G., Sandhoff, R., Wieland, F. T., Lehmann, W. D.; *Quantitative analysis of biological membrane lipids at the low picomole level by nano-electrospray ionization tandem mass spectrometry.* Proc. Natl. Acad. Sci. U.S.A. **1997**, 94, 2339-2344.

[106] Bligh, E. G., Dyer, W. J.; *A rapid method of total lipid extraction and purification.* Can. J. Biochem. Physiol. **1959**, 37, 911-917.

[107] Müller, D. C., Degen, C., Scherer, G., Jahreis, G., Niessner, R., Scherer, M.; *Metabolomics using GC–TOF–MS followed by subsequent GC–FID and HILIC–MS/MS analysis revealed significantly altered fatty acid and phospholipid species profiles in plasma of smokers.* J. Chromatogr. B **2014,** in Press**,** DOI: 10.1016/j.jchromb.2014.02.044.

[108] Gosetti, F., Mazzucco, E., Gennaro, M. C., Marengo, E.; *Simultaneous determination of sixteen underivatized biogenic amines in human urine by HPLC-MS/MS.* Anal. Bioanal. Chem. **2013**, 405, 907-916.

[109] Kharitonov, S. A., Barnes, P. J.; *Biomarkers of some pulmonary diseases in exhaled breath.* Biomarkers **2002**, 7, 1-32.

[110] Carrasco-Pancorbo, A., Nevedomskaya, E., Arthen-Engeland, T., Zey, T., Zurek, G., Baessmann, C., Deelder, A. M., Mayboroda, O. A.; *Gas chromatography/atmospheric pressure chemical ionization-time of flight mass spectrometry: analytical validation and applicability to metabolic profiling.* Anal. Chem. **2009**, 81, 10071-10079.

[111] Tanaka, T., Hayashi, Y.; *Determination of silicon, calcium, magnesium and phosphorus in urine using inductively-coupled plasma emission spectrometry and a matrix-matching technique.* Clin. Chim. Acta **1986**, 156, 109-113.

[112] Welch, M. J., Cohen, A., Hertz, H. S., Ng, K. J., Schaffer, R., Van der Lijn, P., White, E. T.; *Determination of serum creatinine by isotope dilution mass spectrometry as a candidate definitive method.* Anal. Chem. **1986**, 58, 1681-1685.

[113] Wachsmuth, C. J., Almstetter, M. F., Waldhier, M. C., Gruber, M. A., Nurnberger, N., Oefner, P. J., Dettmer, K.; *Performance evaluation of gas chromatography-atmospheric pressure chemical ionization-time-of-flight mass spectrometry for metabolic fingerprinting and profiling.* Anal. Chem. **2011**, 83, 7514-7522.

[114] Nalimov, V. V.; *The application of mathematical statistics to chemical analysis*, Oxford, **1963.**

[115] Etter, J.-F., Due, T. V., Perneger, T. V.; *Saliva Cotinine Levels in Smokers and Nonsmokers.* Am. J. Epidemiol. **2000**, 151, 251-258.

[116] Schmitz, G., Ecker, J.; *The opposing effects of n-3 and n-6 fatty acids.* Prog. Lipid Res. **2008**, 47, 147-155.

[117] Bellin, S. A., Snyder, G. A.; *Higher Fatty Acids in the Smoke Condensate of Burley and Flue-Cured Tobaccos. A Factorial Design Experiment Showing the Effect of Variation of Cigarette Moisture, Weight and Tobacco Type.* RJ Reynolds, **26.02.1961**, Bates No.: 504912499-504912524, http://tobaccodocuments.org/rjr/504912499-2524.html, Accessed 24.02.2014.

6. References

[118] Elmenhorst, H.; *Evaluation of Acids and Phenols in the Semi-Volatile Fraction of the Smoke of Blend Cigarettes and of Cigarettes Made from Virginia, Burley and Oriental Tobaccos.* Contribution to tobacco research **1972**, 6, 7.

[119] Brouwers, J. F.; *Liquid chromatographic-mass spectrometric analysis of phospholipids. Chromatography, ionization and quantification.* Biochim. Biophys. Acta **2011**, 1811, 763-775.

[120] Ecker, J.; *Profiling eicosanoids and phospholipids using LC-MS/MS: principles and recent applications.* J. Sep. Sci. **2012**, 35, 1227-1235.

[121] Scherer, M., Bottcher, A., Schmitz, G., Liebisch, G.; *Sphingolipid profiling of human plasma and FPLC-separated lipoprotein fractions by hydrophilic interaction chromatography tandem mass spectrometry.* Biochim. Biophys. Acta **2011**, 1811, 68-75.

[122] Schwalbe-Herrmann, M., Willmann, J., Leibfritz, D.; *Separation of phospholipid classes by hydrophilic interaction chromatography detected by electrospray ionization mass spectrometry.* J. Chromatogr. A **2010**, 1217, 5179-5183.

[123] Zhao, Y. Y., Xiong, Y., Curtis, J. M.; *Measurement of phospholipids by hydrophilic interaction liquid chromatography coupled to tandem mass spectrometry: the determination of choline containing compounds in foods.* J. Chromatogr. A **2011**, 1218, 5470-5479.

[124] Buré, C., Ayciriex, S., Testet, E., Schmitter, J.-M.; *A single run LC-MS/MS method for phospholipidomics.* Anal. Bioanal. Chem. **2013**, 405, 203-213.

[125] Zheng, L., T'Kind, R., Decuypere, S., von Freyend, S. J., Coombs, G. H., Watson, D. G.; *Profiling of lipids in Leishmania donovani using hydrophilic interaction chromatography in combination with Fourier transform mass spectrometry.* Rapid Commun. Mass Spectrom. **2010**, 24, 2074-2082.

[126] Rezanka, T., Kambourova, M., Derekova, A., Kolouchova, I., Sigler, K.; *LC-ESI-MS/MS identification of polar lipids of two thermophilic Anoxybacillus bacteria containing a unique lipid pattern.* Lipids **2012**, 47, 729-739.

[127] Ahn, E. J., Kim, H., Chung, B. C., Moon, M. H.; *Quantitative analysis of phosphatidylcholine in rat liver tissue by nanoflow liquid chromatography/tandem mass spectrometry.* J. Sep. Sci. **2007**, 30, 2598-2604.

[128] Dodbiba, E., Xu, C., Payagala, T., Wanigasekara, E., Moon, M. H., Armstrong, D. W.; *Use of ion pairing reagents for sensitive detection and separation of phospholipids in the positive ion mode LC-ESI-MS.* Analyst **2011**, 136, 1586-1593.

[129] Hermansson, M., Uphoff, A., Kakela, R., Somerharju, P.; *Automated quantitative analysis of complex lipidomes by liquid chromatography/mass spectrometry.* Anal. Chem. **2005**, 77, 2166-2175.

[130] Kim, H., Min, H. K., Kong, G., Moon, M. H.; *Quantitative analysis of phosphatidylcholines and phosphatidylethanolamines in urine of patients with breast cancer by nanoflow liquid chromatography/tandem mass spectrometry.* Anal. Bioanal. Chem. **2009**, 393, 1649-1656.

[131] Silversand, C., Haux, C.; *Improved high-performance liquid chromatographic method for the separation and quantification of lipid classes: application to fish lipids.* J. Chromatogr. B **1997**, 703, 7-14.

6. References

[132] Xiong, Y., Zhao, Y. Y., Goruk, S., Oilund, K., Field, C. J., Jacobs, R. L., Curtis, J. M.; *Validation of an LC-MS/MS method for the quantification of choline-related compounds and phospholipids in foods and tissues.* J. Chromatogr. B **2012**, 911, 170-179.

[133] Zhu, C., Dane, A., Spijksma, G., Wang, M., van der Greef, J., Luo, G., Hankemeier, T., Vreeken, R. J.; *An efficient hydrophilic interaction liquid chromatography separation of 7 phospholipid classes based on a diol column.* J. Chromatogr. A **2012**, 1220, 26-34.

[134] Schuhmann, K., Almeida, R., Baumert, M., Herzog, R., Bornstein, S. R., Shevchenko, A.; *Shotgun lipidomics on a LTQ Orbitrap mass spectrometer by successive switching between acquisition polarity modes.* J. Mass Spectrom. **2012**, 47, 96-104.

[135] Murphy, R. C., Axelsen, P. H.; *Mass spectrometric analysis of long-chain lipids.* Mass Spectrom. Rev. **2011**, 30, 579-599.

[136] Losito, I., Patruno, R., Conte, E., Cataldi, T. R., Megli, F. M., Palmisano, F.; *Phospholipidomics of human blood microparticles.* Anal. Chem. **2013**, 85, 6405-6413.

[137] Pynn, C. J., Henderson, N. G., Clark, H., Koster, G., Bernhard, W., Postle, A. D.; *Specificity and rate of human and mouse liver and plasma phosphatidylcholine synthesis analyzed in vivo.* J. Lipid Res. **2011**, 52, 399-407.

[138] Myher, J. J., Kuksis, A., Pind, S.; *Molecular species of glycerophospholipids and sphingomyelins of human plasma: comparison to red blood cells.* Lipids **1989**, 24, 408-418.

[139] Marai, L., Kuksis, A.; *Molecular species of lecithins from erythrocytes and plasma of man.* J. Lipid Res. **1969**, 10, 141-152.

[140] Jacob, P., 3rd, Wilson, M., Benowitz, N. L.; *Determination of phenolic metabolites of polycyclic aromatic hydrocarbons in human urine as their pentafluorobenzyl ether derivatives using liquid chromatography-tandem mass spectrometry.* Anal. Chem. **2007**, 79, 587-598.

[141] Beevers, H.; *Metabolic production of sucrose from fat.* Nature **1961**, 191, 433-436.

[142] Colberg, S. R., Casazza, G. A., Horning, M. A., Brooks, G. A.; *Increased dependence on blood glucose in smokers during rest and sustained exercise.* J. Appl. Physiol. **1994**, 76, 26-32.

[143] Felig, P., Pozefsk, T., Marlis, E., Cahill, G. F.; *Alanine: key role in gluconeogenesis.* Science **1970**, 167, 1003-1004.

[144] Keithly, L., Wayne, G. F., Cullen, D. M., Connolly, G. N.; *Industry Research on the Use and Effects of Levulinic Acid: A Case Study in Cigarette Additives.* Nicotine Tobacco Res. **2005**, 7, 761-771.

[145] Zucker, M., Ahrens, J. F.; *Quantitative Assay of Chlorogenic Acid and its Pattern of Distribution within Tobacco Leaves.* Plant Physiol. **1958**, 33, 246.

[146] Zhang, A., Sun, H., Wang, P., Han, Y., Wang, X.; *Recent and potential developments of biofluid analyses in metabolomics.* J. Proteomics **2012**, 75, 1079-1088.

[147] Zhang, A., Sun, H., Wang, X.; *Saliva metabolomics opens door to biomarker discovery, disease diagnosis, and treatment.* Appl. Biochem. Biotechnol. **2012**, 168, 1718-1727.

[148] Hayes, M. L., Hyatt, A. T.; *The decarboxylation of amino acids by bacteria derived from human dental plaque.* Arch. Oral Biol. **1974**, 19, 361-369.

6. References

[149] Mohsenin, A., Blackburn, M. R.; *Adenosine signaling in asthma and chronic obstructive pulmonary disease.* Curr. Opin. Pulm. Med. **2006**, 12, 54-59.

[150] Hasko, G., Linden, J., Cronstein, B., Pacher, P.; *Adenosine receptors: therapeutic aspects for inflammatory and immune diseases.* Nat. Rev. Drug Discov. **2008**, 7, 759-770.

[151] Benowitz, N. L.; *Cotinine as a biomarker of environmental tobacco smoke exposure.* Epidemiol. Rev. **1996**, 18, 188-204.

[152] Haeckel, R.; *Factors influencing the saliva/plasma ratio of drugs.* Ann.N.Y.Acad.Sci. **1993**, 694, 128-142.

[153] Schipper, R. G., Silletti, E., Vingerhoeds, M. H.; *Saliva as research material: biochemical, physicochemical and practical aspects.* Arch.Oral Biol. **2007**, 52, 1114-1135.

[154] Aas, J. A., Paster, B. J., Stokes, L. N., Olsen, I., Dewhirst, F. E.; *Defining the normal bacterial flora of the oral cavity.* J. Clin. Microbiol. **2005**, 43, 5721-5732.

[155] Soysa, N. S., Ellepola, A. N. B.; *The impact of cigarette/tobacco smoking on oral candidosis: an overview.* Oral Dis. **2005**, 11, 268-273.

[156] David, J. C., Dairman, W., Udenfriend, S.; *Decarboxylation to tyramine: a major route of tyrosine metabolism in mammals.* Proc. Natl. Acad. Sci. U.S.A. **1974**, 71, 1771-1775.

[157] McCabe-Sellers, B. J., Staggs, C. G., Bogle, M. L.; *Tyramine in foods and monoamine oxidase inhibitor drugs: A crossroad where medicine, nutrition, pharmacy, and food industry converge.* J. Food Comp. Anal. **2006**, 19 Supplement, 58-65.

[158] Kanehisa, M., Goto, S.; *KEGG: kyoto encyclopedia of genes and genomes.* Nucleic Acids Res. **2000**, 28, 27-30.

[159] Agarwal, A. R., Zhao, L., Sancheti, H., Sundar, I. K., Rahman, I., Cadenas, E.; *Short-term cigarette smoke exposure induces reversible changes in energy metabolism and cellular redox status independent of inflammatory responses in mouse lungs.* Am. J. Physiol. Lung Cell Mol. Physiol. **2012**, 303, L889-898.

[160] Kelsen, S. G., Duan, X., Ji, R., Perez, O., Liu, C., Merali, S.; *Cigarette smoke induces an unfolded protein response in the human lung: a proteomic approach.* Am. J. Respir. Cell Mol. Biol. **2008**, 38, 541-550.

[161] Hellerstein, M. K., Benowitz, N. L., Neese, R. A., Schwartz, J. M., Hoh, R., Jacob, P., 3rd, Hsieh, J., Faix, D.; *Effects of cigarette smoking and its cessation on lipid metabolism and energy expenditure in heavy smokers.* J. Clin. Invest. **1994**, 93, 265-272.

[162] Nagaraj, N. S., Beckers, S., Mensah, J. K., Waigel, S., Vigneswaran, N., Zacharias, W.; *Cigarette smoke condensate induces cytochromes P450 and aldo-keto reductases in oral cancer cells.* Toxicol. Lett. **2006**, 165, 182-194.

[163] Pryor, W. A., Prier, D. G., Church, D. F.; *Electron-spin resonance study of mainstream and sidestream cigarette smoke: nature of the free radicals in gas-phase smoke and in cigarette tar.* Environ. Health Perspect. **1983**, 47, 345.

[164] Waris, G., Ahsan, H.; *Reactive oxygen species: role in the development of cancer and various chronic conditions.* J. Carcinog. **2006**, 5, 14.

6. References

[165] Shah, S. H., Bain, J. R., Muehlbauer, M. J., Stevens, R. D., Crosslin, D. R., Haynes, C., Dungan, J., Newby, L. K., Hauser, E. R., Ginsburg, G. S., Newgard, C. B., Kraus, W. E.; *Association of a peripheral blood metabolic profile with coronary artery disease and risk of subsequent cardiovascular events.* Circ. Cardiovasc. Genet. **2010**, 3, 207-214.

[166] Bridges, C. C., Kekuda, R., Wang, H., Prasad, P. D., Mehta, P., Huang, W., Smith, S. B., Ganapathy, V.; *Structure, function, and regulation of human cystine/glutamate transporter in retinal pigment epithelial cells.* Invest. Ophthalmol. Vis. Sci. **2001**, 42, 47-54.

[167] Beane, J., Sebastiani, P., Liu, G., Brody, J. S., Lenburg, M. E., Spira, A.; *Reversible and permanent effects of tobacco smoke exposure on airway epithelial gene expression.* Genome Biol. **2007**, 8, R201.

[168] Harrison, D., Griendling, K. K., Landmesser, U., Hornig, B., Drexler, H.; *Role of oxidative stress in atherosclerosis.* Am. J. Cardiol. **2003**, 91, 7A-11A.

[169] Glass, C. K., Witztum, J. L.; *Atherosclerosis. the road ahead.* Cell **2001**, 104, 503-516.

[170] Shih, A. Y., Erb, H., Sun, X., Toda, S., Kalivas, P. W., Murphy, T. H.; *Cystine/glutamate exchange modulates glutathione supply for neuroprotection from oxidative stress and cell proliferation.* The Journal of neuroscience **2006**, 26, 10514-10523.

[171] Shahar, E., Boland, L. L., Folsom, A. R., Tockman, M. S., McGovern, P. G., Eckfeldt, J. H.; *Docosahexaenoic acid and smoking-related chronic obstructive pulmonary disease. The Atherosclerosis Risk in Communities Study Investigators.* Am. J. Respir. Crit. Care Med. **1999**, 159, 1780-1785.

[172] Spite, M., Serhan, C. N.; *Novel lipid mediators promote resolution of acute inflammation: impact of aspirin and statins.* Circ. Res. **2010**, 107, 1170-1184.

[173] Hodson, L., Fielding, B. A.; *Stearoyl-CoA desaturase: rogue or innocent bystander?* Prog. Lipid Res. **2013**, 52, 15-42.

[174] Yanagita, M., Kobayashi, R., Kojima, Y., Mori, K., Murakami, S.; *Nicotine modulates the immunological function of dendritic cells through peroxisome proliferator-activated receptor-gamma upregulation.* Cell. Immunol. **2012**, 274, 26-33.

[175] Amoruso, A., Bardelli, C., Gunella, G., Fresu, L. G., Ferrero, V., Brunelleschi, S.; *Quantification of PPAR-gamma protein in monocyte/macrophages from healthy smokers and non-smokers: a possible direct effect of nicotine.* Life Sci. **2007**, 81, 906-915.

[176] Sticozzi, C., Pecorelli, A., Belmonte, G., Valacchi, G.; *Cigarette Smoke Affects ABCAl Expression via Liver X Receptor Nuclear Translocation in Human Keratinocytes.* Int J Mol Sci **2010**, 11, 3375-3386.

[177] Chen, G., Liang, G., Ou, J., Goldstein, J. L., Brown, M. S.; *Central role for liver X receptor in insulin-mediated activation of Srebp-1c transcription and stimulation of fatty acid synthesis in liver.* Proc. Natl. Acad. Sci. U.S.A. **2004**, 101, 11245-11250.

[178] Chu, K., Miyazaki, M., Man, W. C., Ntambi, J. M.; *Stearoyl-coenzyme A desaturase 1 deficiency protects against hypertriglyceridemia and increases plasma high-density lipoprotein cholesterol induced by liver X receptor activation.* Mol. Cell. Biol. **2006**, 26, 6786-6798.

6. References

[179] Liu, G., Lynch, J. K., Freeman, J., Liu, B., Xin, Z., Zhao, H., Serby, M. D., Kym, P. R., Suhar, T. S., Smith, H. T., Cao, N., Yang, R., Janis, R. S., Krauser, J. A., Cepa, S. P., Beno, D. W., Sham, H. L., Collins, C. A., Surowy, T. K., Camp, H. S.; *Discovery of potent, selective, orally bioavailable stearoyl-CoA desaturase 1 inhibitors.* J. Med. Chem. **2007**, 50, 3086-3100.

[180] Pettersen, J. E., Jellum, E.; *The identification and metabolic origin of 2-furoylglycine and 2,5-furandicarboxylic acid in human urine.* Clin. Chim. Acta **1972**, 41, 199-207.

[181] Liu, X., Strable, M. S., Ntambi, J. M.; *Stearoyl CoA desaturase 1: role in cellular inflammation and stress.* Adv Nutr **2011**, 2, 15-22.

[182] Facchini, F. S., Hollenbeck, C. B., Jeppesen, J., Chen, Y. D., Reaven, G. M.; *Insulin resistance and cigarette smoking.* Lancet **1992**, 339, 1128-1130.

[183] Virdis, A., Giannarelli, C., Neves, M. F., Taddei, S., Ghiadoni, L.; *Cigarette smoking and hypertension.* Curr. Pharm. Des. **2010**, 16, 2518-2525.

[184] Wolfe, L. S.; *Eicosanoids: Prostaglandins, Thromboxanes, Leukotrienes, and Other Derivatives of Carbon-20 Unsaturated Fatty Acids.* J. Neurochem. **1982**, 38, 1-14.

[185] Jump, D. B.; *Fatty acid regulation of gene transcription.* Crit. Rev. Clin. Lab. Sci. **2004**, 41, 41-78.

[186] Duplus, E., Glorian, M., Forest, C.; *Fatty Acid Regulation of Gene Transcription.* J. Biol. Chem. **2000**, 275, 30749-30752.

[187] Resh, M. D.; *Fatty acylation of proteins: new insights into membrane targeting of myristoylated and palmitoylated proteins.* Biochim. Biophys. Acta **1999**, 1451, 1-16.

[188] Jump, D. B., Tripathy, S., Depner, C. M.; *Fatty Acid-regulated transcription factors in the liver.* Annu. Rev. Nutr. **2013**, 33, 249-269.

[189] Watson, A. D.; *Thematic review series: systems biology approaches to metabolic and cardiovascular disorders. Lipidomics: a global approach to lipid analysis in biological systems.* J. Lipid Res. **2006**, 47, 2101-2111.

[190] Kosicek, M., Hecimovic, S.; *Phospholipids and Alzheimer's disease: alterations, mechanisms and potential biomarkers.* Int J Mol Sci **2013**, 14, 1310-1322.

[191] Wannamethee, S. G., Shaper, A. G., Perry, I. J.; *Smoking as a Modifiable Risk Factor for Type 2 Diabetes in Middle-Aged Men.* Diabetes Care **2001**, 24, 1590-1595.

[192] Wang, Z., Klipfell, E., Bennett, B. J., Koeth, R., Levison, B. S., Dugar, B., Feldstein, A. E., Britt, E. B., Fu, X., Chung, Y. M., Wu, Y., Schauer, P., Smith, J. D., Allayee, H., Tang, W. H., DiDonato, J. A., Lusis, A. J., Hazen, S. L.; *Gut flora metabolism of phosphatidylcholine promotes cardiovascular disease.* Nature **2011**, 472, 57-63.

[193] Yonekura, T., Kamata, S., Wasa, M., Okada, A., Yamatodani, A., Watanabe, T., Wada, H.; *Simultaneous determination of plasma phenethylamine, phenylethanolamine, tyramine and octopamine by high-performance liquid chromatography using derivatization with fluorescamine.* J. Chromatogr. **1988**, 427, 320-325.

[194] Guo, K., Li, L.; *Differential 12C-/13C-Isotope Dansylation Labeling and Fast Liquid Chromatography/Mass Spectrometry for Absolute and Relative Quantification of the Metabolome.* Anal. Chem. **2009**, 81, 3919-3932.

6. References

[195] Cooke, M., Leeves, N., White, C.; *Time profile of putrescine, cadaverine, indole and skatole in human saliva.* Arch. Oral Biol. **2003**, 48, 323-327.

[196] Branchek, T. A., Blackburn, T. P.; *Trace amine receptors as targets for novel therapeutics: legend, myth and fact.* Curr. Opin. Pharmacol. **2003**, 3, 90-97.

[197] Schmeltz, I., Hoffmann, D.; *Nitrogen-containing compounds in tobacco and tobacco smoke.* Chem. Rev. **1977**, 77, 295-311.

[198] VanDenBerg, C. M., Blob, L. F., Kemper, E. M., Azzaro, A. J.; *Tyramine Pharmacokinetics and Reduced Bioavailability with Food.* J. Clin. Pharmacol. **2003**, 43, 604-609.

[199] Fowler, J. S., Volkow, N. D., Wang, G. J., Pappas, N., Logan, J., MacGregor, R., Alexoff, D., Shea, C., Schlyer, D., Wolf, A. P., Warner, D., Zezulkova, I., Cilento, R.; *Inhibition of monoamine oxidase B in the brains of smokers.* Nature **1996**, 379, 733-736.

[200] Fowler, J. S., Volkow, N. D., Wang, G. J., Pappas, N., Logan, J., Shea, C., Alexoff, D., MacGregor, R. R., Schlyer, D. J., Zezulkova, I., Wolf, A. P.; *Brain monoamine oxidase A inhibition in cigarette smokers.* Proc. Natl. Acad. Sci. U.S.A. **1996**, 93, 14065-14069.

[201] Fowler, J. S., Logan, J., Wang, G. J., Volkow, N. D., Telang, F., Zhu, W., Franceschi, D., Pappas, N., Ferrieri, R., Shea, C., Garza, V., Xu, Y., Schlyer, D., Gatley, S. J., Ding, Y. S., Alexoff, D., Warner, D., Netusil, N., Carter, P., Jayne, M., King, P., Vaska, P.; *Low monoamine oxidase B in peripheral organs in smokers.* Proc. Natl. Acad. Sci. U.S.A. **2003**, 100, 11600-11605.

[202] Fowler, J. S., Logan, J., Wang, G. J., Volkow, N. D., Telang, F., Zhu, W., Franceschi, D., Shea, C., Garza, V., Xu, Y., Ding, Y. S., Alexoff, D., Warner, D., Netusil, N., Carter, P., Jayne, M., King, P., Vaska, P.; *Comparison of monoamine oxidase a in peripheral organs in nonsmokers and smokers.* J. Nucl. Med. **2005**, 46, 1414-1420.

[203] Berlin, I., Said, S., Spreux-Varoquaux, O., Olivares, R., Launay, J. M., Puech, A. J.; *Monoamine oxidase A and B activities in heavy smokers.* Biol. Psychiatry **1995**, 38, 756-761.

[204] Fowler, J. S., Logan, J., Wang, G. J., Volkow, N. D.; *Monoamine oxidase and cigarette smoking.* Neurotoxicology **2003**, 24, 75-82.

[205] Herraiz, T., Chaparro, C.; *Human monoamine oxidase is inhibited by tobacco smoke: β-carboline alkaloids act as potent and reversible inhibitors.* Biochem. Biophys. Res. Commun. **2005**, 326, 378-386.

[206] Gilbert, D. G., Zuo, Y., Browning, R. A., Shaw, T. M., Rabinovich, N. E., Gilbert-Johnson, A. M., Plath, L.; *Platelet monoamine oxidase B activity changes across 31 days of smoking abstinence.* Nicotine & tobacco research : official journal of the Society for Research on Nicotine and Tobacco **2003**, 5, 813-819.

[207] Launay, J. M., Del Pino, M., Chironi, G., Callebert, J., Peoc'h, K., Megnien, J. L., Mallet, J., Simon, A., Rendu, F.; *Smoking induces long-lasting effects through a monoamine-oxidase epigenetic regulation.* PLoS One **2009**, 4, e7959.

[208] Strolin Benedetti, M., Tipton, K. F., Whomsley, R.; *Amine oxidases and monooxygenases in the in vivo metabolism of xenobiotic amines in humans: has the involvement of amine oxidases been neglected?* Fundam. Clin. Pharmacol. **2007**, 21, 467-479.

6. References

[209] Herbert, A. A., Kidd, E. J., Broadley, K. J.; *Dietary trace amine-dependent vasoconstriction in porcine coronary artery.* Br. J. Pharmacol. **2008**, 155, 525-534.

[210] Fehler, M., Broadley, K., Ford, W., Kidd, E.; *Identification of trace-amine-associated receptors (TAAR) in the rat aorta and their role in vasoconstriction by β-phenylethylamine.* Naunyn-Schmiedeberg's Arch. Pharmacol. **2010**, 382, 385-398.

[211] Barnes, P. J., Shapiro, S. D., Pauwels, R. A.; *Chronic obstructive pulmonary disease: molecular and cellular mechanisms.* Eur. Respir. J. **2003**, 22, 672-688.

[212] Berlin, I., Anthenelli, R. M.; *Monoamine oxidases and tobacco smoking.* Int. J. Neuropsychopharmacol. **2001**, 4, 33-42.

[213] Rose, J. E., Behm, F. M., Ramsey, C., Ritchie, J. C., Jr.; *Platelet monoamine oxidase, smoking cessation, and tobacco withdrawal symptoms.* Nicotine Tobacco Res. **2001**, 3, 383-390.

[214] Rose, J. E.; *Nicotine and nonnicotine factors in cigarette addiction.* Psychopharmacology **2006**, 184, 274-285.

[215] Guillem, K., Vouillac, C., Azar, M. R., Parsons, L. H., Koob, G. F., Cador, M., Stinus, L.; *Monoamine oxidase inhibition dramatically increases the motivation to self-administer nicotine in rats.* J. Neurosci. **2005**, 25, 8593-8600.

[216] Aktories, K., Hofmann, B., Förstermann, D., Starke, K.; 9. Auflage, München **2005**, p 186.

[217] Berlin, I., Said, S., Spreux-Varoquaux, O., Launay, J. M., Olivares, R., Millet, V., Lecrubier, Y., Puech, A. J.; *A reversible monoamine oxidase A inhibitor (moclobemide) facilitates smoking cessation and abstinence in heavy, dependent smokers.* Clin. Pharmacol. Ther. **1995**, 58, 444-452.

[218] Sommer, U., Herscovitz, H., Welty, F. K., Costello, C. E.; *LC-MS-based method for the qualitative and quantitative analysis of complex lipid mixtures.* J. Lipid Res. **2006**, 47, 804-814.

[219] Sharrett, A. R., Ballantyne, C. M., Coady, S. A., Heiss, G., Sorlie, P. D., Catellier, D., Patsch, W.; *Coronary Heart Disease Prediction From Lipoprotein Cholesterol Levels, Triglycerides, Lipoprotein(a), Apolipoproteins A-I and B, and HDL Density Subfractions: The Atherosclerosis Risk in Communities (ARIC) Study.* Circulation **2001**, 104, 1108-1113.

[220] Precht, M., Kraft, R.; *Bio-Statistik 2* 5. völlig überarbeitete Auflage, München Wien **1993.**

[221] Shapiro, S. S., Wilk, M. B.; *An analysis of variance test for normality (complete samples).* Biometrika **1965**, 52, 591-611.

7   Appendix

7.1   Nic+9 determination in 24-hour urine

Analytical settings for the analysis of nicotine and 9 of its metabolites in urine of smokers and non-smokers.

Analytes	Nic, Cot, OH-Cot, Nic-gluc, Cot-gluc and OH-Cot-gluc,	Nornicotine, norcotinine, Nic-N-oxide and Cot-N-oxide
HPLC-System	Binary pump 1100 series (G1312A), degasser (G1379A), column oven (G1316A), Agilent Technologies, Waldbronn, Germany	
MS-system	MS/MS-system, API 4000, AB Sciex, Darmstadt, Germany	
Autosampler (T = 10°C)	HTC-Pal, CTC Analytics, Zwingen, Switzerland	
Column (T = 45°C)	MAX RP 80, 4 µm particle size, 150 x 4.6 mm (Phenomenex, Aschaffenburg, Germany)	Kinetex PFP 2.6 µm particle size, 100 x 3.0 mm
Injection volume	1 µl	10 µL
Eluent	Isocratic: 50% A, 50% B, 1mL/min Eluent A: 40% 10 mM ammonium acetate, pH 6,8, 60% Methanol Eluent B: Methanol	Gradient Eluent A: Water + 0.1% ammonium acetate adjusted with trichloracetic acid to pH = 5.0 Eluent B: Acetonitrile Runtime (min) / Flow rate (µL/min) / Eluent A (%) 0 — 700 — 98 2.0 — 700 — 98 8.0 — 700 — 40 8.1 — 700 — 0 10.0 — 1500 — 0 15.0 — 1500 — 0 15.1 — 1500 — 98 16.0 — 700 — 98 18.0 — 700 — 98
Calibration Range	25-10,000 ng/mL	1.56 – 5,000 ng/mL

7. Appendix

Settings for the MS API 4000 for the determination of Nic, Cot, OH-Cot, Nic-gluc, Cot-gluc and OH-Cot-gluc in urine (MRM mode).

Analyte	Q1 (Da)	Q2 (Da)	DP (V)	CE (V)	CXP (V)
Nic(-gluc)	163,0	129,9	51	29	12
Nic(-gluc)-d_3	166,1	129,9	56	29	12
Cot(-gluc)	177,2	80,1	71	33	6
Cot(-gluc)-d_3	180,2	80,0	76	35	6
OH-Cot-gluc)	193,1	80,1	61	37	6
OH-Cot-gluc)-d_3	196,2	79,9	66	35	6
APCI positive, CUR=25; GS1=25; NC=3; TEM=500; CAD= 7; EP=10:					
APCI source: Turbo V™ Ion Source, AB Sciex, Darmstadt, German					

DP: Declustering potential. CE: Collision energy. RT: Retention time. CXP: collision cell exit potential. Settings for the respective glucuronides are same as for the aglycones.

Settings for the MS API 4000 for the determination of nornicotine, norcotinine, Nic-N-oxide and Cot-N-oxide in urine (MRM mode).

Analyte	Q1 (Da)	Q2 (Da)	DP (V)	CE (V)	CXP (V)
Nornicotine	149,3	129,9	106	23	24
Nornicotine-d_4	153,2	134,0	56	25	10
Norcotinine	163,1	79,9	91	35	14
Norcotinine-d_4	167,2	84,0	81	37	16
Nic-N-Oxide	179,1	129,9	101	33	12
Nic-N-Oxide-d_3	182,1	130,0	121	33	10
Cot-N-Oxide	193,1	96,1	66	31	18
Cot-N-Oxide-d_3	196,1	96,0	96	31	18
ESI positiv, CUR=45; GS1=25; GS2=40; IS=5500; TEM=500; CAD= 7; EP=10					

DP: Declustering potential. CE: Collision energy. RT: Retention time. CXP: collision cell exit potential.

7. Appendix

Nic+9 measured in 24 hour urine pool. Data were calculated from nicotine and 9 of its metabolites, namely: Cot, OH-Cot, Nic-gluc, Cot-gluc, OH-Cot-gluc, nornicotine, norcotinine, Nic-1-N-oxide, Cot-N-oxide. Non-smokers were all under the limit of quantification for all analytes. The Nic+9 results were divided by the creatinine concentration in the urine pool to remove dilution effects.

The analytes were measured by Markus Piller in the ABF by means of a validated LC-MS/MS method according to the in-house standard operating procedure.

Smoking subject	Creatinine mg/L	Nic+9 in 24-hour urine samples	
		mg/L	µg/mg creatinine
S 200	810.5	5.3	6.5
S 201	1014.4	12.3	12.2
S 202	610.2	10.1	16.5
S 203	674.3	6.6	9.7
S 204	662.7	4.7	7.1
S 205	641.0	5.7	8.9
S 206	910.7	9.7	10.7
S 207	1186.4	17.6	14.9
S 208	930.3	5.3	5.7
S 209	615.2	5.2	8.5
S 210	956.2	6.1	6.4
S 211	955.8	6.3	6.5
S 212	563.9	10.8	19.1
S 213	792.0	8.8	11.1
S 214	631.9	4.9	7.7
S 215	855.7	8.9	10.4
S 216	415.0	8.6	20.7
S 217	634.1	7.2	11.3
S 218	1024.5	8.6	8.4
S 219	803.8	7.0	8.7
S 220	806.7	10.8	13.4
S 221	1234.2	15.5	12.6
S 222	553.4	9.1	16.5
S 223	1501.6	10.6	7.0
S 224	829.9	7.9	9.5

7.2   HILIC-MS/MS settings for PC and PE species profiling

Settings for the MS API 4000 (ABsciex) used for the determination of phospholipid species in plasma by means of the novel HILIC-MS/MS method.

Actual Injection Volume (µL)	2.000
Source Temperature (at setpoint) (°C)	600.0
Left Heat Exchanger (°C)	45
Right Heat Exchanger (°C)	45
Scan Type	MRM
Polarity	Positive
MRM detection window (s)	29
Target Scan Time (s)	0.4000
Resolution Q1	Unit
Resolution Q3	Unit
MR Pause (ms)	3.0070

7. Appendix

Lipid	MW (Da)	MRM (m/z)	DP (V)	CE (V)	RT (min)	CXP (V)	Lipid	MW (Da)	MRM (m/z)	DP (V)	CE (V)	RT (min)	CXP (V)
PC 26:0	649.5	650.5 → 183.9	116	47	4.3	14	PE 24:0	579.5	580.5 → 439.5	100	30	3.7	15
PC 28:0	677.7	678.7 → 184.1	106	37	4.3	16	PE 26:0	607.5	608.5 → 467.5	100	30	3.7	15
PC 30:1	703.5	704.5 → 183.9	116	47	4.3	14	PE 28:0	635.6	636.6 → 495.4	86	27	3.7	14
PC 30:0	705.6	706.6 → 183.9	116	47	4.3	14	PE 30:3	657.5	658.5 → 517.5	100	30	3.7	15
PC 32:3	727.6	728.6 → 183.9	116	47	4.3	14	PE 30:2	659.5	660.5 → 519.5	100	30	3.7	15
PC 32:2	729.6	730.6 → 183.9	116	47	4.3	14	PE 30:1	661.5	662.5 → 521.5	100	30	3.7	15
PC 32:1	731.6	732.6 → 183.9	116	47	4.3	14	PE 30:0	663.5	664.5 → 523.5	100	30	3.7	15
PC 32:0	733.6	734.6 → 183.9	116	47	4.3	14	PE 32:3	685.5	686.5 → 545.5	100	30	3.7	15
PC 34:4	753.6	754.6 → 183.9	116	47	4.3	14	PE 32:2	687.5	688.5 → 547.5	100	30	3.7	15
PC 34:3	755.6	756.6 → 183.9	116	47	4.3	14	PE 32:1	689.5	690.5 → 549.5	100	30	3.7	15
PC 34:2	757.6	758.6 → 183.9	116	47	4.3	14	PE 32:0	691.5	692.5 → 551.5	100	30	3.7	15
PC 34:1	759.8	760.8 → 183.9	116	47	4.3	14	PE 34:4	711.5	712.5 → 571.5	100	30	3.7	15
PC 34:0	761.6	762.6 → 183.9	116	47	4.3	14	PE 34:3	713.5	714.5 → 573.5	100	30	3.7	15
PC 36:5	779.6	780.6 → 183.9	116	47	4.3	14	PE 34:2	715.5	716.5 → 575.5	100	30	3.7	15
PC 36:4	781.6	782.6 → 183.9	116	47	4.3	14	PE 34:1	717.6	718.6 → 577.4	101	31	3.7	16
PC 36:3	783.6	784.6 → 183.9	116	47	4.3	14	PE 34:0	719.5	720.5 → 579.5	100	30	3.7	15
PC 36:2	785.8	786.8 → 184	126	49	4.3	14	PE 36:6	735.5	736.5 → 595.5	100	30	3.7	15
PC 36:1	787.6	788.6 → 183.9	116	47	4.3	14	PE 36:5	737.5	738.5 → 597.5	100	30	3.7	15
PC 36:0	789.6	790.6 → 183.9	116	47	4.3	14	PE 36:4	739.7	740.7 → 599.3	61	33	3.7	16
PC 38:7	803.6	804.6 → 183.9	116	47	4.2	14	PE 36:3	741.5	742.5 → 601.5	100	30	3.7	15
PC 38:6	805.6	806.6 → 183.9	116	47	4.2	14	PE 36:2	743.6	744.6 → 603.4	101	31	3.7	16
PC 38:5	807.6	808.6 → 183.9	116	47	4.2	14	PE 36:1	745.6	746.6 → 605.6	100	30	3.7	15
PC 38:4	809.8	810.8 → 184.1	116	43	4.2	32	PE 36:0	727.6	728.6 → 607.6	100	30	3.7	15
PC 38:3	811.6	812.6 → 183.9	116	47	4.2	14	PE 38:7	761.5	762.5 → 621.5	100	30	3.7	15
PC 38:2	813.6	814.6 → 183.9	116	47	4.2	14	PE 38:6	763.5	764.5 → 623.5	100	30	3.7	15
PC 38:1	815.6	816.6 → 183.9	116	47	4.2	14	PE 38:5	765.5	766.5 → 625.5	100	30	3.7	15
PC 38:0	817.6	818.6 → 183.9	116	47	4.2	14	PE 38:4	767.5	768.5 → 627.5	100	30	3.7	15
PC 40:7	831.6	832.6 → 183.9	116	47	4.2	14	PE 38:3	769.6	770.6 → 629.6	100	30	3.7	15
PC 40:6	833.6	834.6 → 183.9	116	47	4.2	14	PE 38:2	771.6	772.6 → 631.6	100	30	3.7	15
PC 40:5	835.6	836.6 → 183.9	116	47	4.2	14	PE 38:1	773.6	774.6 → 633.6	100	30	3.7	15
PC 40:4	837.6	838.6 → 183.9	116	47	4.2	14	PE 38:0	775.6	776.6 → 635.6	100	30	3.7	15
PC 40:3	839.6	840.6 → 183.9	116	47	4.2	14	PE 40:6	791.7	792.7 → 651.4	86	33	3.7	18
PC 40:2	841.6	842.6 → 183.9	116	47	4.2	14	PE 40:5	793.6	794.6 → 653.6	100	30	3.7	15
PC 40:1	843.6	844.6 → 183.9	116	47	4.2	14	PE 40:4	795.6	796.6 → 655.6	100	30	3.7	15
PC 40:0	845.8	846.8 → 184.1	136	51	4.2	14	PE 40:3	797.6	798.6 → 657.6	100	30	3.7	15
PC 42:5	863.7	864.7 → 183.9	116	47	4.2	14	PE 40:2	799.5	800.5 → 659.5	100	30	3.7	15
PC 42:4	865.7	866.7 → 183.9	116	47	4.2	14	PE 40:1	801.5	802.5 → 661.5	100	30	3.7	15
PC 42:0	873.7	874.7 → 183.9	116	47	4.2	14	PE 40:0	803.5	804.5 → 663.5	100	30	3.7	15
PC 44:1	899.7	900.7 → 183.9	116	47	4.2	14	PE 42:7	817.5	818.5 → 677.5	100	30	3.7	15
PC 44:0	901.8	902.8 → 184	116	53	4.2	12	PE 42:6	819.5	820.5 → 679.5	100	30	3.7	15
							PE 42:5	821.5	822.5 → 681.5	100	30	3.7	15

DP: Declustering potential. CE: Collision energy. RT: Retention time. CXP: collision cell exit potential

7.3   Isotopic distribution of PC and PE species

Isotopic distribution calculated for PC and PE species that were determined with the novel HILIC-MS/MS method. Distribution calculated without the headgroup.

Lipid	Formula	Formula without headgroup	MW, (Da)	Isotopic distribution, (%)				
				Monoisotope	+1	+2	+3	+4
PC 30:1	C38H74NO8P	C33H59O4	519.4	100	37.4	7.6	1.1	0.1
PC 32:3	C40H74NO8P	C35H59O4	543.4	100	39.6	8.4	1.2	0.1
PC 32:2	C40H76NO8P	C35H61O4	545.5	100	39.6	8.4	1.2	0.1
PC 32:1	C40H78NO8P	C35H63O4	547.5	100	39.7	8.4	1.2	0.1
PC 34:4	C42H76NO8P	C37H61O4	569.5	100	41.9	9.3	1.4	0.1
PC 34:3	C42H78NO8P	C37H63O4	571.5	100	41.9	9.3	1.4	0.1
PC 34:2	C42H80NO8P	C37H65O4	573.5	100	41.9	9.3	1.4	0.1
PC 34:1	C42H82NO8P	C37H67O4	575.5	100	41.9	9.3	1.4	0.1
PC 36:5	C44H78NO8P	C39H63O4	595.5	100	44.1	10.3	1.6	0.2
PC 36:4	C44H80NO8P	C39H65O4	597.5	100	44.1	10.3	1.6	0.2
PC 36:3	C44H82NO8P	C39H67O4	599.5	100	44.2	10.3	1.6	0.2
PC 36:2	C44H84NO8P	C39H69O4	601.5	100	44.2	10.3	1.6	0.2
PC 36:1	C44H86NO8P	C39H71O4	603.5	100	44.2	10.3	1.6	0.2
PC 38:7	C46H78NO8P	C41H63O4	619.5	100	46.3	11.3	1.9	0.2
PC 38:6	C46H80NO8P	C41H65O4	621.5	100	46.4	11.3	1.9	0.2
PC 38:5	C46H82NO8P	C41H67O4	623.5	100	46.4	11.3	1.9	0.2
PC 38:4	C46H84NO8P	C41H69O4	625.5	100	46.4	11.3	1.9	0.2
PC 38:3	C46H86NO8P	C41H71O4	627.5	100	46.4	11.3	1.9	0.2
PC 38:2	C46H88NO8P	C41H73O4	629.5	100	46.4	11.3	1.9	0.2
PC 38:1	C46H90NO8P	C41H75O4	631.5	100	46.5	11.3	1.9	0.2
PC 40:7	C48H82NO8P	C43H67O4	647.5	100	48.6	12.3	2.1	0.2
PC 40:6	C48H84NO8P	C43H69O4	649.5	100	48.6	12.3	2.1	0.2
PC 40:5	C48H86NO8P	C43H71O4	651.5	100	48.6	12.3	2.1	0.2
PC 40:4	C48H88NO8P	C43H73O4	653.5	100	48.7	12.4	2.1	0.2
PC 40:3	C48H90NO8P	C43H75O4	655.6	100	48.7	12.4	2.1	0.3
PC 40:2	C48H92NO8P	C43H77O4	657.5	100	48.7	12.4	2.1	0.3
PC 40:1	C48H94NO8P	C43H79O4	659.5	100	48.7	12.4	2.1	0.3
PC 42:5	C50H90NO8P	C45H75O4	679.5	100	50.9	13.5	2.4	0.3
PC 44:1	C52H102NO8P	C47H87O4	715.7	100	53.3	14.7	2.7	0.4

Lipid	Formula	Formula without headgroup	MW, (Da)	Isotopic distribution, (%)				
				Monoisotopic	+1	+2	+3	+4
PE 30:3	C35H64NO8P	C33H56O4	516.4	100	37.4	7.6	1	0.1
PE 30:2	C35H66NO8P	C33H58O4	518.4	100	37.4	7.6	1.1	0.1
PE 30:1	C35H68NO8P	C33H60O4	520.4	100	37.4	7.6	1.1	0.1
PE 32:3	C37H68NO8P	C35H60O4	544.4	100	39.6	8.4	1.2	0.1
PE 32:2	C37H70NO8P	C35H62O4	546.5	100	39.7	8.4	1.2	0.1
PE 32:1	C37H72NO8P	C35H64O4	548.5	100	39.7	8.4	1.2	0.1
PE 34:4	C39H70NO8P	C37H62O4	570.4	100	41.9	9.3	1.4	0.1
PE 34:3	C39H72NO8P	C37H64O4	572.5	100	41.9	9.3	1.4	0.1
PE 34:2	C39H74NO8P	C37H66O4	574.5	100	41.9	9.3	1.4	0.1
PE 34:1	C39H76NO8P	C37H68O4	576.5	100	41.9	9.3	1.4	0.1
PE 36:6	C41H70NO8P	C39H62O4	594.5	100	44.1	10.3	1.6	0.2
PE 36:5	C41H72NO8P	C39H64O4	596.5	100	44.1	10.3	1.6	0.2
PE 36:4	C41H74NO8P	C39H66O4	598.5	100	44.1	10.3	1.6	0.2
PE 36:3	C41H76NO8P	C39H68O4	600.5	100	44.2	10.3	1.6	0.2
PE 36:2	C41H78NO8P	C39H70O4	602.5	100	44.2	10.3	1.6	0.2
PE 36:1	C41H80NO8P	C39H72O4	604.5	100	44.2	10.3	1.6	0.2
PE 38:7	C43H72NO8P	C41H64O4	620.5	100	46.4	11.3	1.9	0.2
PE 38:6	C43H74NO8P	C41H66O4	622.5	100	46.4	11.3	1.9	0.2
PE 38:5	C43H76NO8P	C41H68O4	624.5	100	46.4	11.3	1.9	0.2
PE 38:4	C43H78NO8P	C41H70O4	626.5	100	46.4	11.3	1.9	0.2
PE 38:3	C43H80NO8P	C41H72O4	628.5	100	46.4	11.3	1.9	0.2
PE 38:2	C43H82NO8P	C41H74O4	630.6	100	46.5	11.3	1.9	0.2
PE 38:1	C43H84NO8P	C41H76O4	632.6	100	46.5	11.3	1.9	0.2
PE 40:6	C45H78NO8P	C43H70O4	650.5	100	48.6	12.3	2.1	0.2
PE 40:5	C45H80NO8P	C43H72O4	652.5	100	48.7	12.3	2.1	0.2
PE 40:4	C45H82NO8P	C43H74O4	654.6	100	48.7	12.4	2.1	0.2
PE 40:3	C45H84NO8P	C43H76O4	656.6	100	48.7	12.4	2.1	0.3
PE 40:2	C45H86NO8P	C43H78O4	658.6	100	48.7	12.4	2.1	0.3
PE 40:1	C45H88NO8P	C43H80O4	660.6	100	48.7	12.4	2.1	0.3
PE 42:7	C47H80NO8P	C45H72O4	676.5	100	50.9	13.4	2.4	0.3
PE 42:6	C47H82NO8P	C45H74O4	678.6	100	50.9	13.5	2.4	0.3

Test of isotopic correction algorithm. For this purpose, 7 phospholipid standards were spiked to water and the MRMs of the +2 isotopes were measured before and after the isotopic correction. The +2 isotopes are isobaric to the phospholipids containing one less double bound and should not be present in the water samples after isotopic correction. Analysis was performed with duplicates.

Concentration (µM)

Sample	PE 34:1		PE 34:0		PE 36:2		PE 36:1		PE 36:4		PE 36:3		PE 40:6		PE 40:5	
	spiked	measured	uncor	cor	spiked	measured	uncor	cor	spiked	measured	uncor	cor	spiked	measured	uncor	cor
1	5.0	4.9	0.2	-0.2	10.0	9.9	1.0	-0.1	20.0	18.8	1.9	-0.1	10.0	10.0	0.9	-0.3
	10.0	10.4	0.8	-0.2	25.0	23.7	2.5	0.1	100.0	95.4	11.1	1.2	25.0	24.3	2.9	-0.1
	20.0	20.1	1.9	0.0	50.0	50.4	4.9	-0.3	200.0	181.6	21.1	2.4	50.0	49.5	4.7	-1.4
2	5.0	4.7	0.4	0.0	10.0	9.6	0.8	-0.2	20.0	18.7	2.0	0.1	10.0	10.2	1.3	0.0
	10.0	10.3	1.0	0.0	25.0	24.5	2.3	-0.3	100.0	92.5	11.4	1.9	25.0	25.2	2.6	-0.5
	20.0	19.7	2.1	0.3	50.0	50.0	4.2	-1.0	200.0	182.9	20.7	1.8	50.0	51.6	5.1	-1.2
average	5.0	4.8	0.3	-0.1	10.0	9.8	0.9	-0.1	20.0	18.8	1.9	0.0	10.0	10.1	1.1	-0.2
	10.0	10.3	0.9	-0.1	25.0	24.1	2.4	-0.1	100.0	94.0	11.2	1.6	25.0	24.7	2.8	-0.3
	20.0	19.9	2.0	0.2	50.0	50.2	4.5	-0.7	200.0	182.2	20.9	2.1	50.0	50.5	4.9	-1.3

uncor.: Concentration determined before isotopic correction. Cor.: concentration after isotopic correction

Concentration (µM)

Sample	PC 34:1		PC 34:0		PC 36:2		PC 36:1		PC 38:4		PC 38:3	
	spiked	measured	uncor	cor	spiked	measured	uncor	cor	spiked	measured	uncor	cor
1	500	547.5	45.0	-5.9	100.0	112.6	9.8	-1.8	100.0	103.1	11.6	-0.1
	1000	1057.5	86.6	-11.8	500.0	494.2	46.4	-4.5	250.0	228.7	30.1	4.3
	2000	1921.9	173.0	-5.8	1000.0	976.9	96.9	-3.7	500.0	496.5	64.1	8.0
2	500	552.9	41.8	-9.6	100.0	104.6	9.5	-1.3	100.0	91.8	12.0	1.7
	1000	1082.1	89.4	-11.3	500.0	507.9	48.6	-3.7	250.0	253.8	32.4	3.7
	2000	1981.3	197.4	13.1	1000.0	1019.7	102.6	-2.4	500.0	513.0	67.4	9.4
average	500	550.2	43.4	-7.7	100.0	108.6	9.6	-1.5	100.0	97.5	11.8	0.8
	1000	1069.8	88.0	-11.5	500.0	501.1	47.5	-4.1	250.0	241.3	31.3	4.0
	2000	1951.6	185.2	3.7	1000.0	998.3	99.8	-3.1	500.0	504.7	65.8	8.7

Uncor: Concentration determined before isotopic correction. Cor: concentration after isotopic correction

7.4   MS/MS settings for tyramine determination in saliva

Settings for the MS API 4000 (ABsciex) used for the determination of tyramine in saliva.

Analyte	MW (Da)	MRM (*m/z*)	Type	DP (V)	CE (V)	CXP (V)
Tyramine	137	138 → 121	Quantifier	21	13	8
		138 → 77	Qualifier	21	37	4
d_4-Tyramine	141	142 → 125	Quantifier	41	13	8
		142 → 106	Qualifier	41	31	6

DP: Declustering potential. CE: Collision energy. RT: Retention time. CXP: Collision cell exit potential

7.5   Nicotine and its metabolite levels in urine by metabolic fingerprinting and targeted analysis

Nic, Cot, OH-Cot and Cot-Gluc measured in the 24 hour urine pool samples of 25 smokers (S 200-224). Quantified by means of a targeted LC-MS/MS method and data obtained by the metabolic fingerprinting method using GC-TOF-MS. Data used for correlation amongst both methods.

Subject	Targeted				Metabolic fingerprinting			
	Nic	Cot	OH-Cot	Cot-Gluc	Nic 84.06/10.994*	Cot 98.03/14.907*	OH-Cot 249.06/17.114*	Cot-Gluc 176.05/27.196*
	mg/mg-creatinine				Area ratio (Analyte/IS)			
200	0.4	0.9	2.8	2.8	0.024	0.061	0.171	0.004
201	0.8	1.4	7.6	3.3	0.037	0.084	0.537	0.009
202	1.0	3.4	3.1	9.5	0.111	0.208	0.173	0.01
203	1.2	1.5	3.8	3.8	0.063	0.093	0.221	0.017
204	0.5	1.3	2.3	3.4	0.04	0.08	0.135	0.005
205	1.0	1.6	4.2	2.1	0.047	0.065	0.258	0.009
206	1.7	1.5	2.6	4.5	0.085	0.096	0.142	0.019
207	0.7	1.9	7.0	5.9	0.049	0.144	0.49	0.091
208	0.6	0.8	1.8	2.4	0.037	0.05	0.107	0.004
209	0.7	1.9	2.5	3.3	0.062	0.086	0.132	0.001
210	0.4	1.0	2.0	3.2	0.039	0.06	0.12	0.005
211	0.7	1.3	2.5	1.7	0.037	0.056	0.146	0.014
212	1.2	2.9	6.3	11.2	0.123	0.243	0.403	0.027
213	3.4	1.7	1.7	3.8	0.174	0.103	0.099	0.005
214	0.7	1.4	2.3	3.3	0.048	0.081	0.127	0.002
215	1.7	1.2	3.4	5.2	0.08	0.103	0.205	0.006
216	1.0	3.9	7.6	9.0	0.07	0.215	0.453	0.034
217	2.0	1.8	2.1	6.3	0.091	0.108	0.104	0.008
218	1.4	1.1	2.8	2.9	0.064	0.065	0.164	0.013
219	0.7	1.4	2.7	3.8	0.043	0.085	0.161	0.018
220	0.6	1.7	7.1	3.3	0.04	0.084	0.461	0.033
221	1.0	1.2	5.3	4.4	0.053	0.094	0.361	0.083
222	1.9	4.1	5.9	3.9	0.093	0.172	0.357	0.023
223	0.4	1.3	2.7	2.0	0.024	0.065	0.168	0.023
224	0.7	1.6	3.0	3.9	0.042	0.103	0.186	0.022

*m/z / retention time (min)

7.6 UPLC-QTOF-MS settings for SM detection in plasma

Settings of the UPLC-QTOF-MS method, used for the accurate mass detection of sphingomyelin species in plasma.

Instrument		XEVO-G2SQTOF	
Resolution		30000	
Polarity		ESI+	
Analyzer		Resolution Mode	
Capillary (kV)		1.2000	
Sampling Cone(V)		20.0000	
Source Temperature (°C)		140	
Desolvation Temperature (°C)		250	
Cone Gas Flow (L/hour)		0.0	
Desolvation Gas Flow (L/hour)		600.0	
Collision Energy (low) (eV)		6.0	
Ramp High Energy from (high) (eV)		20.0 to 35.0	
Acquisition mass range (*m/z*)		100.000 to 1000.000	
Experiment Reference Compound Name		Leu-enkephalin (Lock spray)	
Instrument:		Waters Acquity SDS	
Run Time: 8.00 min			
Time(min)	Flow Rate	Eluent A (%)	Eluent B (%)
Initial	0.550	5.0	95.0
1.00		5.0	95.0
4.00		50.0	50.0
5.00		50.0	50.0
5.10		5.0	95.0
8.00		5.0	95.0

7.7 Investigation of carry-over effects for PC and PE species

Validation data of sample-to-sample carry-over, determined for each phospholipid that was measured by the HILIC-MS/MS method. The LOD-area was defined as the area at the LOQ/3. The areas for the LOD were determined for the 8 phospholipid standards and used as representative for all other lipids detected by the method.

Lipid species	Standard for LOD calculation	Area LOD N = 2	Area measured N = 3	Lipid species	Standard for LOD calculation	Area LOD N = 2	Area measured N = 3
PC 26:0	PC 34:1	1787	33	PE 24:0	PE 34:1	407	0
PC 30:1	PC 34:1	1787	0	PE 26:0	PE 34:1	407	0
PC 30:0	PC 34:1	1787	0	PE 30:3	PE 34:1	407	0
PC 32:3	PC 34:1	1787	0	PE 30:2	PE 34:1	407	0
PC 32:2	PC 34:1	1787	33	PE 30:1	PE 34:1	407	0
PC 32:1	PC 34:1	1787	0	PE 30:0	PE 34:1	407	0
PC 32:0	PC 34:1	1787	0	PE 32:3	PE 34:1	407	0
PC 34:4	PC 34:1	1787	0	PE 32:2	PE 34:1	407	0
PC 34:3	PC 34:1	1787	0	PE 32:1	PE 34:1	407	0
PC 34:2	PC 34:1	1787	1764	PE 32:0	PE 34:1	407	0
PC 34:1	PC 34:1	1787	1434	PE 34:4	PE 34:1	407	0
PC 34:0	PC 34:1	1787	0	PE 34:3	PE 34:1	407	0
PC 36:5	PC 36:2	2280	0	PE 34:2	PE 34:1	407	0
PC 36:4	PC 36:2	2280	979	PE 34:1	PE 34:1	407	0
PC 36:3	PC 36:2	2280	886	PE 34:0	PE 34:1	407	0
PC 36:2	PC 36:2	2280	1454	PE 36:6	PE 36:2	440	0
PC 36:1	PC 36:2	2280	140	PE 36:5	PE 36:2	440	0
PC 36:0	PC 36:2	2280	1	PE 36:4	PE 36:2	440	0
PC 38:7	PC 38:4	1516	0	PE 36:3	PE 36:2	440	0
PC 38:6	PC 38:4	1516	302	PE 36:2	PE 36:2	440	0
PC 38:5	PC 38:4	1516	512	PE 36:1	PE 36:2	440	0
PC 38:4	PC 38:4	1516	714	PE 36:0	PE 36:2	440	0
PC 38:3	PC 38:4	1516	0	PE 38:7	PE 36:4	395	0
PC 38:2	PC 38:4	1516	9	PE 38:6	PE 36:4	395	0
PC 38:1	PC 38:4	1516	0	PE 38:5	PE 36:4	395	0
PC 38:0	PC 38:4	1516	0	PE 38:4	PE 36:4	395	0
PC 40:7	PC 40:0	1594	0	PE 38:3	PE 36:4	395	0
PC 40:6	PC 40:0	1594	0	PE 38:2	PE 36:4	395	0
PC 40:5	PC 40:0	1594	0	PE 38:1	PE 36:4	395	0
PC 40:4	PC 40:0	1594	0	PE 38:0	PE 36:4	395	0
PC 40:3	PC 40:0	1594	0	PE 40:6	PE 40:6	443	0
PC 40:2	PC 40:0	1594	0	PE 40:5	PE 40:6	443	0
PC 40:1	PC 40:0	1594	0	PE 40:4	PE 40:6	443	0
PC 40:0	PC 40:0	1594	0	PE 40:3	PE 40:6	443	0
PC 42:5	PC 40:0	1594	0	PE 40:2	PE 40:6	443	0
PC 42:4	PC 40:0	1594	0	PE 40:1	PE 40:6	443	0
PC 42:0	PC 40:0	1594	0	PE 40:0	PE 40:6	443	0
PC 44:1	PC 40:0	1594	0	PE 42:7	PE 40:6	443	0
PC 44:0	PC 40:0	1594	0	PE 42:6	PE 40:6	443	0
				PE 42:5	PE 40:6	443	0

7.8 QC samples for PC and PE profiling

Raw data of QC samples for PC and PE profiling in plasma by means of the HILIC-MS/MS method.

Lipid	Concentration (µM)								CV, (%)	Ref. conc. Interday (µM)	Accuracy (%)
	Q1	Q2	Q3	Q4	Q5	Q6	Q7	Q8			
PC 30:0	1.51	1.47	1.50	1.60	1.51	1.63	1.53	1.67	4.6	1.8	87.9
PC 32:2	2.13	2.10	2.18	2.63	2.23	2.37	3.15	2.18	15.0	2.4	99.3
PC 32:1	8.19	8.39	8.54	11.16	10.07	8.82	7.95	11.71	15.4	9.2	101.6
PC 32:0	8.82	8.98	9.39	12.14	12.31	9.98	9.42	9.44	13.7	10.1	99.4
PC 34:4	1.51	1.17	1.44	1.65	1.67	1.35	1.91	1.78	15.4	1.7	89.4
PC 34:3	18.63	21.23	20.58	22.35	21.12	19.30	18.89	19.64	6.5	10.8	186.8
PC 34:2	315.14	342.54	337.91	421.50	348.08	353.36	394.41	369.86	9.4	378.6	95.2
PC 34:1	151.82	158.81	157.76	185.86	179.62	170.31	168.07	197.78	9.1	174.0	98.4
PC 36:5	14.14	16.35	15.39	18.79	17.78	11.04	14.05	13.88	16.2	18.1	83.8
PC 36:4	110.08	115.40	115.91	129.53	114.06	67.00	112.68	68.77	22.2	126.9	82.1
PC 36:3	83.06	90.60	88.73	109.39	98.37	69.10	91.32	86.46	13.0	97.7	91.7
PC 36:2	183.39	194.00	198.03	243.27	207.91	171.78	182.26	218.42	11.5	218.9	91.3
PC 36:1	16.26	18.02	17.79	20.93	19.49	15.36	21.03	14.95	13.2	19.3	93.1
PC 36:0	2.79	2.77	2.51	3.65	3.50	2.80	2.71	3.21	13.7	2.2	139.0
PC 38:7	4.05	4.54	3.94	4.55	4.27	3.82	4.93	3.50	11.0	4.4	95.6
PC 38:6	34.59	39.71	37.15	41.05	46.21	40.29	34.45	44.28	10.7	42.4	93.6
PC 38:5	38.84	44.09	43.73	48.17	47.76	44.78	46.50	52.83	8.9	45.3	101.3
PC 38:4	90.49	100.91	94.46	116.26	105.54	100.69	117.47	106.37	9.1	99.3	104.8
PC 38:3	29.03	34.36	34.54	42.44	41.17	35.01	34.89	44.13	13.8	36.1	102.4
PC 38:2	6.14	6.13	4.71	6.41	5.63	6.05	6.62	5.28	10.8	5.7	102.6
PC 38:1	1.77	1.83	2.24	1.89	2.44	1.82	2.18	2.46	13.7	0.7	292.7
PC 38:0	2.21	2.83	2.68	3.25	2.99	2.83	2.81	3.31	12.0	2.5	115.5

Lipid	Concentration (µM)								CV (%)	Ref. conc. Interday (µM)	Accuracy (%)
	Q1	Q2	Q3	Q4	Q5	Q6	Q7	Q8			
PC 40:7	3.11	3.04	2.98	3.56	3.55	4.15	4.20	3.87	13.6	3.4	103.9
PC 40:6	9.87	13.86	10.97	11.71	13.21	11.46	10.68	12.84	11.6	12.2	97.1
PC 40:5	5.90	5.69	6.27	7.53	7.46	6.83	7.17	7.13	10.5	7.2	94.3
PC 40:4	2.22	2.60	2.74	3.77	3.24	3.01	4.03	3.26	19.2	2.7	113.5
PC 40:3	1.27	1.33	1.51	1.43	1.49	1.48	0.94	1.16	15.0	1.2	113.0
PC 40:2	1.59	1.95	1.60	1.98	1.75	1.93	2.00	1.88	9.1	1.6	116.5
PC 40:1	0.40[a]	0.72	0.75	1.02	0.79	0.78	0.71	0.62	15.8	0.6 Reference from Intraday	119.6
PC 40:0	1.46	1.55	0.85	1.16	1.15	1.24	1.00	1.17	18.8	1.2	100.1
PC 42:0	0.58	0.68	0.77	0.80	0.85	0.83	0.73	0.90	13.6	0.8	90.8
PE 34:2	1.49	1.20	1.35	1.46	1.20	1.05	1.17	0.98	14.8	1.3	98.2
PE 34:1	0.96	0.96	0.85	0.84	0.71	0.72	0.78	0.52	18.4	0.7	114.3
PE 36:4	1.29	1.10	0.89	1.23	1.33	1.16	0.84	1.12	15.7	1.3	84.2
PE 36:3	0.83	0.81	0.82	0.86	0.74	0.82	0.83	0.38[b]	4.6	1.4	58.9
PE 36:2	3.60	3.25	4.03	3.78	3.67	2.82	2.18	3.82	18.3	3.7	91.7
PE 38:6	0.93	0.82	1.14	1.09	1.24	0.87	1.03	0.69	18.7	1.2	80.2
PE 38:5	1.12	0.93	0.76	1.22	1.26	1.03	0.83	1.11	17.5	1.4	74.4
PE 38:4	3.70	3.13	3.84	5.20	4.21	3.34	3.19	4.18	17.8	4.2	92.1
PE 40:6	1.03	1.05	1.03	1.10	0.98	0.96	0.96	0.43[b]	5.5	1.0	91.8

Ref. conc.: Reference concentration, used for the calculation for the accuracy. [a]Outlier according to Nalimov on the 95% confidence interval, [b]Outlier according to Nalimov on the 95% confidence interval. Outlier not used for calculations.

7.9   PC and PE species levels in plasma by HILIC-MS/MS

Concentration levels of PE and PC species determined in 25 smokers (S 200-224) and 25 non-smokers (NS 100-124). Concentration of molecular phospholipid species measured by HILIC-MS/MS in plasma of smokers and non-smokers.

Lipid	Concentration (µM, mean ± SD)		
	NS + S (N = 50)	NS (N = 25)	S (N = 25)
PC 30:0	2.0 ± 1.0	2.0 ± 1.1	1.9 ± 0.9
PC 32:2	2.9 ± 1.5	3.1 ± 1.4	2.8 ± 1.7
PC 32:1	11.6 ± 7.6	11.3 ± 8.5	12 ± 6.6
PC 32:0	11.2 ± 3.3	11.1 ± 4	11.3 ± 2.5
PC 34:4	1.6 ± 0.8	1.6 ± 0.9	1.6 ± 0.7
PC 34:3	20.5 ± 6.4	20.8 ± 7.9	20.1 ± 4.5
PC 34:2	419.2 ± 113.5	416 ± 124.1	422.5 ± 104.3
PC 34:1	258.8 ± 107.2	253.3 ± 126.1	264.3 ± 86.7
PC 36:5	20.6 ± 9.7	21.6 ± 12.2	19.6 ± 6.5
PC 36:4	148.7 ± 45.5	147.7 ± 47.7	149.7 ± 44.1
PC 36:3	114.1 ± 34.4	111.2 ± 40.1	117 ± 28.2
PC 36:2	226.4 ± 71.2	221.4 ± 75.4	231.4 ± 68
PC 36:1	27.3 ± 10.8	24.4 ± 12.3	30.2 ± 8.3
PC 36:0	3.6 ± 1.8	3.9 ± 2.1	3.2 ± 1.4
PC 38:7	4.2 ± 1.4	4.5 ± 1.8	3.9 ± 0.9
PC 38:6	66.5 ± 25.6	70.4 ± 28.3	62.6 ± 22.4
PC 38:5	57.9 ± 19.5	56.1 ± 22.2	59.8 ± 16.6
PC 38:4	112.3 ± 42.3	103.2 ± 34.2	121.4 ± 48
PC 38:3	44.1 ± 15.4	40.6 ± 14.1	47.5 ± 16
PC 38:2	6.9 ± 3.4	6.9 ± 3.4	6.9 ± 3.5
PC 38:1	2.1 ± 1.0	2.2 ± 1.2	2.0 ± 0.9
PC 38:0	2.8 ± 1.2	2.9 ± 1.3	2.8 ± 1.0
PC 40:7	4.6 ± 1.8	4.5 ± 1.9	4.7 ± 1.7
PC 40:6	16.0 ± 7.0	16.9 ± 7.4	15.1 ± 6.5
PC 40:5	8.6 ± 3.8	7.6 ± 2.7	9.6 ± 4.5
PC 40:4	3.3 ± 1.4	3.2 ± 1.4	3.5 ± 1.4
PC 40:3	1.0 ± 0.6	1.0 ± 0.4	1.1 ± 0.7
PC 40:2	2.0 ± 0.8	2.0 ± 0.9	2.0 ± 0.8
PC 40:1	0.8 ± 0.4	0.9 ± 0.4	0.8 ± 0.3
PC 40:0	1.7 ± 0.5	1.7 ± 0.5	1.7 ± 0.5
PC 42:5	0.6 ± 0.2	0.5 ± 0.2	0.6 ± 0.2
PC 42:4	0.5 ± 0.3	0.6 ± 0.3	0.5 ± 0.3
PC 42:0	0.9 ± 0.3	0.9 ± 0.3	0.8 ± 0.3
PE 34:2	1.2 ± 0.9	1.1 ± 0.9	1.3 ± 1.0
PE 34:1	0.9 ± 0.8	1.0 ± 0.9	0.8 ± 0.6
PE 36:4	1.3 ± 1.4	1.5 ± 1.8	1.2 ± 0.7
PE 36:3	1.0 ± 0.8	1.1 ± 1.0	0.8 ± 0.5
PE 36:2	3.7 ± 2.7	3.2 ± 2.7	4.2 ± 2.7
PE 36:1	0.8 ± 0.8	0.8 ± 0.8	0.7 ± 0.8
PE 38:6	1.5 ± 1.2	1.4 ± 1.3	1.6 ± 1.0
PE 38:5	1.7 ± 1.1	1.5 ± 1.1	1.9 ± 1.1
PE 38:4	5.4 ± 3.4	6.1 ± 4.0	4.7 ± 2.5
PE 38:3	0.7 ± 0.7	0.5 ± 0.7	0.8 ± 0.7
PE 40:6	1.4 ± 1.2	1.3 ± 1.1	1.6 ± 1.3
PE 40:5	0.7 ± 0.8	0.7 ± 0.8	0.7 ± 0.8

7.10 Validation and QC data for tyramine determination in saliva

Intraday accuracy and precision raw data for tyramine measured by means of a HILIC-MS/MS method. Therefore, a saliva sample, spiked with 20 nM (N = 5) and 500 nM (N = 5) tyramine was analyzed.

Level spiked (nM)	Concentration determined (nM)				
	1	**2**	**3**	**4**	**5**
20	21.5	22.6	17.3	20.7	18.4
500	475.1	476.6	508.1	469.3	521.09

Raw data of the QC samples (tyramine spiked to saliva) for tyramine measured in saliva of 25 smokers and 25 non-smokers. One QC sample for the level 20 nM and for the level 500 nM was analyzed within each batch of the different time points, where saliva was collected (TP1 – TP5).

Level spiked (nM)	Concentration determined (nM)				
	TP1	**TP2**	**TP3**	**TP4**	**TP5**
20	22.0	21.6	21.9	20.2	22.6
500	518.1	497.5	513.8	505.1	476.6

7.11   Tyramine levels in saliva

Tyramine concentrations determined in saliva of 25 non-smokers (NS 100 – 124) and 25 smokers (S 200 – 224) by means of a HILIC-MS/MS method. The concentration levels were determined for all of the 5 time points (TP1 – TP5) where saliva was collected. Samples of TP3 – TP5 were measured by Gerhard Gilch in the ABF.

Subject	Concentration (µM)				
	TP1	TP2	TP3	TP4	TP5
NS 100	1710.3	833.3	5260.7	2160.2	7803.0
NS 101	797.7	277.7	322.0	313.4	2796.1
NS 102	34.1	76.4	55.8	40.8	90.8
NS 103	22.8	17.6	11.7	9.3	27.6
NS 104	125.4	45.9	70.0	100.7	58.7
NS 105	0.0	0.0	8.2	5.7	7.3
NS 106	409.5	126.5	96.0	87.5	100.0
NS 107	0.0	4.9	2.9	1.3	32.8
NS 108	0.0	0.0	0.0	3.5	72.2
NS 109	3.6	0.0	4.9	2.8	597.1
NS 110	40.2	51.5	36.2	42.6	55.5
NS 111	133.1	104.5	251.7	1542.7	68.0
NS 112	5.2	4.0	0.0	1.4	35.3
NS 113	12.4	22.1	9.1	10.8	48.9
NS 114	6.9	8.3	7.0	3.3	34.0
NS 115	20.2	8.6	0.0	3.1	42.2
NS 116	0.0	0.0	3.0	0.7	50.2
NS 117	4.4	0.0	0.0	2.5	64.3
NS 118	6.0	6.5	6.8	3.8	179.5
NS 119	4.3	0.0	0.0	1.1	35.6
NS 120	29.7	8.1	11.9	1.2	38.9
NS 121	328.7	195.4	180.0	130.1	57.8
NS 122	124.2	91.4	76.9	80.4	98.1
NS 123	18.6	13.6	39.1	51.0	60.3
NS 124	0.0	0.0	0.0	1.2	29.1
S 200	8270.2	1375.2	2499.5	2806.6	3531.1
S 201	228.6	107.1	319.1	950.8	637.4
S 202	1374.2	610.7	1403.0	1835.8	17185.4
S 203	11983.4	1888.3	5498.6	8226.3	41329.7
S 204	1003.3	291.2	1290.1	3578.3	4432.4
S 205	13390.9	3568.5	6621.8	4261.2	12906.4
S 206	1047.1	346.2	440.8	559.2	1020.4
S 207	2991.6	1006.5	5536.2	14212.0	23249.3
S 208	163.4	31.1	79.5	120.1	57.5
S 209	10853.2	7094.2	35078.4	17843.5	25656.5
S 210	1871.7	1652.9	4472.2	3933.5	1414.7
S 211	8.0	21.5	7.2	9.9	59.1
S 212	22529.2	2252.7	2172.1	7156.5	41461.9
S 213	632.7	372.5	507.0	234.2	4297.2
S 214	6287.9	1217.8	1047.1	2289.0	3887.2
S 215	2710.6	1696.3	6450.1	4167.3	18719.5
S 216	2098.5	1218.4	1565.0	3525.4	12632.7
S 217	570.5	2692.1	7558.5	3974.0	4892.9
S 218	2960.6	3128.3	936.6	1652.8	2656.2
S 219	942.4	654.5	763.6	658.8	1855.1
S 220	2960.1	781.5	738.9	757.1	2556.6
S 221	1001.4	1477.3	2027.1	1202.1	1262.8
S 222	1942.9	1808.8	2168.3	1814.5	5339.3
S 223	4973.5	2467.1	6700.7	2377.0	8139.8
S 224	26.7	28.6	55.1	41.4	415.7

7.12   Statistics

For univariate statistical analysis of the metabolomics data a Mann-Whitney U test was applied, since the criteria for Student's t-test (normal distribution, equal standard deviation) or Welch's test (normal distribution) were not fulfilled for 28 to 79% of the features (see the following table) [220]. The criteria for normal distribution and equal standard deviation were tested using Shapiro-Wilk and F-test, respectively.

Matrix	Number of features in peak list	Peaks with unequal SD [a] (Number / %)	Features that were not normal distributed (Number / %)[b]	
			NS	S
		$(N_i = 25)$	(N = 25)	(N = 25)
Urine	7,198	1,969 (27.4)	3,442 (47.8)	3,327 (46.2)
Plasma	4,261	1,199 (28.1)	1,347 (31.6)	1,609 (37.8)
Saliva	14,894	6,348 (42.6)	11,691 (78.5)	10,429 (70.0)

[a] $p < 0.05$, calculated using F-test [220].

[b] $p < 0.05$, calculated using Shapiro-Wilk test [221].

Curriculum Vitae

Daniel Christoph Müller

Personal information

Date/place of birth:	25.12.1985 in Weilheim

Study and work experience

Since 08/2011	PhD thesis at the Analytisch-Biologisches Forschungslabor GmbH (ABF) in Munich and the Technische Universität München at the Chair for Analytical Chemistry with Prof. Dr. Niessner Thesis: *"Metabolomics investigations in body fluids of smokers and non-smokers."*
11/2010 – 07/2011	Application engineer at *W. L. Gore & Associates*
07/2010	Diplom-Ingenieur (graduate engineer) Diploma thesis at Roche Diagnostics GmbH in Penzberg Thesis: "*Analysis of a Monoclonal Antibody with a Macro Ion Mobility Spectrometer.*"
10/2005 – 07/2010	Physical engineering with specialization in chemistry at the Munich University of Applied Sciences

Community service

09/2004 – 06/2005	Sozialstation in Peissenberg, Germany

Education

07/2004	Advanced technical certificate
09/2002 – 07/2004	Staatliche Fachoberschule Weilheim (technical secondary school)
09/1996 – 07/2002	Staatliche Realschule Weilheim (middle school)
09/1992 – 07/1996	Grundschule Wessobrunn (elementary school)